Uniting models and otoliths to explore migration, connectivity and space use in marine fishes

Jed I. Macdonald

Faculty of Life and Environmental Sciences
University of Iceland
2019

Uniting models and otoliths to explore migration, connectivity and space use in marine fishes

Jed I. Macdonald

Dissertation submitted in partial fulfillment of a
Philosophiae Doctor degree in Biology

PhD Committee
Professor Guðrún Marteinsdóttir
Mr. Þorsteinn Sigurðsson
Dr. Geir Huse

Opponents
Professor Audrey J. Geffen
Dr. Pierre Petitgas

Faculty of Life and Environmental Sciences
School of Engineering and Natural Sciences
University of Iceland
Reykjavík, May 2019

Uniting models and otoliths to explore migration, connectivity and space use in marine fishes

Short title: Models, otoliths and migration in marine fishes

Dissertation submitted in partial fulfillment of a *Philosophiae Doctor* degree in Biology

Faculty of Life and Environmental Sciences
School of Engineering and Natural Sciences
University of Iceland
Sturlugata 7
101, Reykjavík
Iceland

Telephone: (+354) 525 4000

Bibliographic information:
Jed I. Macdonald, 2019, *Uniting models and otoliths to explore migration, connectivity and space use in marine fishes*, PhD dissertation, Faculty of Life and Environmental Sciences, University of Iceland, 221 pp.

ISBN 978-9935-9473-7-6

Printing: Háskólaprent
Reykjavík, Iceland, October 2019

Abstract

Movements of animals en masse are impressive phenomena that continue to fascinate scientists of all persuasions. Fishes display some of the most striking examples, and an extensive literature has explored the subject in marine species with long histories of commercial harvest, and/or strong, enduring cultural values. Yet, as recognition of the cognitive capacity of fishes grows, and strong inter-individual variability in behavioural traits among sympatric conspecifics is revealed as the norm, fundamental questions on the drivers underpinning both large-scale migrations, and the spatial outcomes of such moves require reexamination. This thesis comprises five papers that focus broadly on understanding the factors that shape movement decisions, distribution patterns and connectivity in schooling marine fishes. Using Atlantic herring (*Clupea harengus* L.) in Iceland, and striped red mullet (*Mullus surmuletus* L.) in the North Sea and Eastern English Channel for illustration, the work combines new Bayesian modelling approaches with analyses of otolith (ear stone) chemistry to test the role of intrinsic (i.e. collective behaviour, demographic traits, ontogeny) and extrinsic (i.e. the environment, fishing pressure, prey availability) factors in influencing the spatial dynamics of these commercially-important species. The outcomes highlight the natural synergy between model-based and empirical approaches in addressing questions on the movements of group-living fishes, and demonstrate how these can be integrated to guide fishery-management decisions, both under present conditions, and under future scenarios of environmental change.

Útdráttur

Hreyfingar og hjarðhegðun dýra er heillandi og áhrifamikil sjónarspil sem hefur verið uppspretta ýmissa rannsókna. Fiskar eru meðal þeirra dýra sem sýna hvað mest sláandi dæmi um hjarðhegðun og margar heimildir eru til um slíkt atferli hjá nytjastofnum sem og öðrum lífverum sjávar. Eftir því sem meiri vitneskja safnast um vitsmunalega getu fiska, sem og um breytileika á meðal einstaklinga innan sömu tegundar, vakna spurningar um hvaða þættir hafa mest áhrif á hegðun þeirra. Þessi ritgerð samanstendur af fimm vísindagreinum þar sem notuð eru líkön til að lýsa útbreiðslu fiska í sjó með sérstakri áherslu á að skýra þætti sem hafa áhrif á úbreiðslu íslenskrar sumargotssíldar (*Clupea harengus* L.) við Ísland og rauðröndungs (*Mullus surmuletus* L.) í Norðursjó og Ermasundi. Notaðar eru nýjar Bayesian aðferðir í líkanagerð sem eru samtvinnaðar við greiningar á efnainnihaldi kvarna til að skoða innri þætti (s.s. samhæft atferli, lýðfræðilega eiginleika, einstaklingsþroska) og ytri þætti (s.s. umhverfisþætti, veiðiálag, fæðuframboð) sem áhrif hafa á dreifingu þessarra mikilvægu nytjastofna. Niðurstöðurnar sýna að með því að tengja saman innri og ytri þætti þá má betur lýsa göngum torfufiska. Þá er einnig sýnt fram á hvernig nýta má niðurstöðurnar við fiskveiðistjórnun, bæði við núverandi umhverfisaðstæður og einnig ef umhverfisaðstæður breytast.

For Mum and Dad

Table of Contents

Abstract ..... **iii**

Útdráttur ..... **iv**

List of Papers ..... **viii**

List of Figures ..... **x**

Acknowledgements ..... **xi**

1 Introduction and synthesis **1**

1.1 Movement and migration 1
1.2 Fishes as exemplars 2
1.3 Drivers of movement, migration and space use in fishes 3
1.3.1 Group-living and sociality 3
1.3.2 Disentangling sociality and extrinsic processes 4
1.3.3 Papers I and II 5
1.4 Connectivity among populations and stocks 9
1.4.1 Harnessing otoliths' true potential 11
1.4.2 Papers III and IV 12
1.5 Fishing- and climate-related distribution shifts 14
1.5.1 Paper V 15
1.6 Conclusions and further work 15
1.7 References 17

Paper I **29**

Paper II **89**

Paper III **117**

Paper IV **173**

Paper V **211**

List of Papers

This thesis comprises five papers, outlined below. These papers will be referred to in the text based on their respective numbers, as follows:-

- **Paper I:** Macdonald, J.I., Logemann, K., Krainski, E.T., Sigurðsson, Þ., Beale, C.M., Huse, G., Hjøllo, S.S. and Marteinsdóttir, G. 2018. Can collective memories shape fish distributions? A test, linking space-time occurrence models and population demographics. Ecography 41: 938–957.

- **Paper II:** Pinto, C., Travers-Trolet, M., Macdonald, J.I., Rivot, É. and Vermard, Y. 2019. Combining multiple data sets to unravel the spatiotemporal dynamics of a data-limited fish stock. Can. J. Fish. Aquat. Sci. 76: 1338–1349.

- **Paper III:** Macdonald, J.I., Drysdale, R.N., Witt, R., Cságoly, Z. and Marteinsdóttir, G. In review. Isolating the influence of ontogeny helps predict island-wide variability in chemical traits stored in fish otoliths. Rev. Fish Biol. Fisher.

- **Paper IV:** Macdonald, J.I., Jónsdóttir, I.G., Drysdale, R.N., Witt, R., Sigurðsson, Þ., Reynisson, P., Óskarsson, G.J., Cságoly, Z. and Marteinsdóttir, G. In review. Defining the scales of otolith chemical variability reveals long-term fidelity to nurseries and multiple origins in a fished herring population. Can. J. Fish. Aquat. Sci.

- **Paper V:** Macdonald, J.I. Otoliths as thermometers: reconstructing temperature histories of fish to predict range shifts under climate change. Manuscript.

Other papers published during the PhD, but not included in this thesis

Boonstra, W.J., Ottosen, K.M., Ferreira, A.S.A., Richter, A., Rogers, L., Pedersen, M.W., Kokkalis, A., Bárðarson, H., Bonanomi, S., Butler, W., Diekert, F.K., Fouzai, N., Holma, M., Holt, R.E., Kvile, K.Ø., Malanski, E., Macdonald, J.I., Nieminen, E., Romagnoni, G., Snickars, M., Törnroos, A., Weigel, B., Woods, P., Yletyinen, J. and Whittington, J.D. 2015. What are the major global threats and impacts in marine environments? Investigating the contours of a shared perception among marine scientists from the bottom-up. Mar. Policy 60: 197–201.

Crook, D.A., Macdonald, J.I., McNeil, D.G., Gilligan, D., Asmus, M., Mass, R. and Woodhead J. 2013. Recruitment sources and dispersal of an invasive fish in a large river system as revealed by otolith chemistry analysis. Can. J. Fish. Aquat. Sci. 70: 953–963.

Crook, D.A., Macdonald, J.I., Morrongiello, J.R., Belcher, C.A., Lovett, D., Walker, A. and Nicol, S.J. 2014. Environmental cues and extended estuarine residence in seaward migrating eels (*Anguilla australis*). Freshwater Biol. 59: 1710–1720.

Daewel, U., Schrum, C. and Macdonald, J.I. 2019. Towards end-2-end modelling in a consistent NPZD-F modelling framework (ECOSMO E2E_v1.0): application to the North Sea and Baltic Sea. Geosci. Model Dev. 12: 1765–1789.

Holt, R.E., Woods, P.J., Ferreira, A.S.A., Bárðarson, H, Bonanomi, S., Boonstra, W.J., Butler, W.E., Diekert, F.K., Fouzai, N., Holma, M., Kokkalis, A., Kvile, K.Ø., Macdonald, J.I., Malanski, E., Nieminen, E., Ottosen, K.M., Pedersen, M.W., Richter, A., Rogers, L., Romagnoni, G., Snickars, M., Törnroos, A., Weigel, B., Whittington, J.D. and Yletyinen, J. 2017. Avoiding pitfalls in interdisciplinary education. Clim. Res. 74: 121–129.

Huey, J.A., Crook, D.A., Macdonald, J.I., Schmidt, D.J., Marshall, J.C., Balcombe, S.R., Woods, R.J. and Hughes, J.M. 2014. Is variable connectivity among populations of a continental gobiid fish driven by local adaptation or passive dispersal? Freshwater Biol. 59: 1672–1686.

Hughes, J.M., Schmidt, D.J., Macdonald, J.I., Huey, J.A. and Crook, D.A. 2014. Low interbasin connectivity in a facultatively diadromous fish: evidence from genetics and otolith chemistry. Mol. Ecol. 23: 1000-1013.

Macdonald, J.I. and Crook, D.A. 2014. Nursery sources and cohort strength of young-of-the-year common carp (*Cyprinus carpio*) under differing flow regimes in a regulated floodplain river. Ecol. Freshw. Fish 23: 269–282.

Macdonald, J.I., Farley, J.H., Clear, N.P., Williams, A.J., Carter, T.H., Davies, C. and Nicol, S.J. 2013. Insights into mixing and movement of south Pacific albacore *Thunnus alalunga* derived from trace elements in otoliths. Fish. Res. 148: 56–63.

Schmidt, D.J., Crook, D.A., Macdonald, J.I., Huey, J.A., Zampatti, B.P., Chilcott, S., Raadik, T.A. and Hughes, J.M. 2014. Migration history and stock structure of two putatively diadromous teleost fishes, as determined by genetic and otolith chemistry analyses. Freshw. Sci. 33: 193–206.

Tonkin, Z.D., Ramsey, D.S.L., Macdonald, J.I., Kaus, A. Crook, D.A. and King, A.J. 2014. Does localised control of invasive eastern gambusia (*Gambusia holbrooki*) increase population growth of generalist wetland fishes? Austral Ecol. 39: 355–366.

List of Figures

Figure 1.1. Sketch of a mature herring (Clupea harengus). *(Jonathan Couch, 1862).* 6

Figure 1.2. An investigation by Huse et al. (2010) into the wintering dynamics of Norwegian spring spawning herring showed that the five major shifts in wintering distribution observed over ~60 years (vertical lines) coincided with years in which the ratio of first-year spawner abundance (i.e. age 4) to repeat spawner abundance (i.e. age 5+) was high. The authors suggested that when there is a numerical domination of naïve fish in the population, there are too few experienced teachers available to guide the younger fish to traditional wintering areas, and hence, new migration routes are forged. Figure redrawn from Huse et al. (2010). 7

Figure 1.3. Sketch of a mature striped red mullet (Mullus surmuletus). *(Jonathan Couch, 1862).* 8

Figure 1.4. A) Chasing juvenile ISS herring aboard w/w Dröfn RE-35. Ísafjarðardjúpi, November 2014. (Photo: Jed Macdonald). B) A selection of age 1 and age 2 ISS herring fresh from the trawl. C) Polished sagittal otoliths from age 2 ISS herring (viewed under reflected light) awaiting the MicroMill (see Papers III and IV for analytical details). 12

Acknowledgements

I am grateful to many fine folk who collectively made finishing this PhD possible. To those who inspired and funded me to dip the toe back into academia and pursue this project, those who shaped its direction through heated, late-night discussions on ecological and evolutionary theory, those who shared their hard-earned knowledge so generously, those who provided essential distractions of the wave, rock, fish, and hot and cold beverage variety, and those that showed me the light during some long, dark winters, I express my deepest thanks to you all. To some special mentions…

This work was supported by a grant from the Icelandic Association of Herring Fisheries under 'Rannsóknarsjóður síldarútvegsins 2013', and funding through Nordforsk via the Nordic Centre for Research on Marine Ecosystems and Resources Under Climate Change (NorMER). A big thanks to Valdi Ingi Gunnarsson for administering the former grant, and for his interest and efforts in promoting the project's results to the fishing industry. Thanks also to Jason Whittington for coordinating the NorMER initiative, and to my fellow NorMER PhDs and post-docs for a 'seriesly' good time.

To my supervisors Guðrún, Steini and Geir, thanks for the opportunity to undertake this PhD, and for granting me full creative license to take the project where I wished. I feel like my experience as a doctoral student was more closely aligned with the philosophical, rather than the biological aspects of the '*Philosophiae doctor* in Biology', harking back to the original tenets (and timeframe!) of the degree. I thank you all for encouraging me to pursue the questions that intrigued me.

Thanks also to my collaborators, both in Iceland and abroad, for your input into the papers that appear in the thesis and into others we worked on together over the past five years (see your names in the 'List of Papers'). Living in Iceland, in such close proximity to the UK and continental Europe, definitely showcased the beauty of the short, cheap flight in building friendships and collaborations across the North Atlantic and beyond. In Iceland, several colleagues at the Marine and Freshwater Research Institute (MFRI) collected samples, shared information on herring ecology and local oceanography and contributed to papers. In particular, thanks to Inga Jónsdóttir, Guðmundur Óskarsson, Magnus Danielsen, Páll Reynisson, Jónas Jónasson and Klara Jakobsdóttir. Gunnar Jóhannsson and the crew aboard w/w Dröfn RE-35 are thanked for their hospitality, for a hands-on introduction to preparing the delicious skata during a pre-Christmas cruise, and for sampling assistance on the juvenile herring surveys along Iceland's north coast.

Further afield, thanks to Geir Huse (IMR, Bergen, Norway) for his seminal work on herring that largely inspired the ideas behind **Paper I**, and for his hospitality during my stay in Bergen in 2014. Thanks to Elias Krainski and Håvard Rue for hosting me at NTNU in Trondheim, Norway, during 2015, and to Pierre Petitgas, Youen Vermard (Ifremer, Nantes, France) and Cecilia Pinto (Joint Research Centre, Ispra, Italy) for the opportunity to visit Ifremer in Nantes in 2016, and to work on the striped red mullet project. Geoff Heard (Arthur Rylah Institute, Melbourne, Australia), thanks for your insight and wisdom throughout mate, and for that invitation to visit the University of York (York, UK) in 2015. To Colin Beale and Chris Thomas (University of York), thanks both of you for your interest in the mysteries of the herring, and your input on the spatial models I used in an attempt to demystify them. Thank you Russ Drysdale, Roman Witt, Jon Woodhead and Alan Greig (University of

Melbourne, Australia) and Ian Williams (The Australian National University, Canberra, Australia) for your time and analytical prowess with regard to the otolith elemental and stable isotopic analyses. Thanks to Mick McCarthy and Jian Yen (University of Melbourne) for their advice on priors in mixed effects models, to Dave Ramsey and Mike Scroggie (Arthur Rylah Institute) for discussions on the modelling approach and to Dave Crook (La Trobe University, Albury, Australia) for planting the PhD seed, and for reviewing manuscript drafts. Thanks John Morrongiello, the Morrongiello Lab, and members of room 242: Ana, Karla, Henry, CJ, Qi and Katherine (University of Melbourne) for kindly providing me a work space, allowing me open access to the BioSciences 4 'brown doctor' supply, and for lending open ears and eyes to fishy monologues. And finally, to Zsófi, thanks for your enquiring mind, and for always posing the most interesting questions on the meaning of work, life, and the finer points of English breakfast tea brewing. You've taught me much, and I treasure the adventures we've had together, both in Dalí and more metaphysically. Thanks also for your help in the field and lab, and for your insightful contributions to the papers in this thesis.

To my friends in MARICE and Askja, I feel very lucky to have met, worked, and in several cases, lived with you over the past few years. Here, I express my thanks to people in line with the natural hierarchy of intelligence – from those studying fish and marine systems at the top, followed by the terrestrially-focused folk, with the devotees of inanimate objects, i.e. the earth scientists, geophysicists and volcanologists, placed on the lowest rung… To Will B, mate, what an epic we've had! Thanks for being such a cool cat and for always being there for a chinwag, quiet cuppa, or Gúll when needed (which as we both know, was fairly often). To the MARICE crew (and alumni): Hlynur, Kai, Pam, Fraser, Niall, Teresa, Cecilia, Caroline, Freydis, Lovisa, Hildur, Steve and Guðni, it was a pleasure to have shared the best lab in Askja with you. Thanks to you, and to David, Chloé, Olli B, Edwin, Hrönn, Kalina, Habba, Lísa Anne, Rannveig, Óli Patrick, Ehsan, Águsta, Will M, Hannah, Becca, Vincent, Joaquín, Dan J, Han, Mona and Eduardo for the chats and fun times.

I had the chance to live in many places during my tenure, and shared houses with lovely people from all corners of the globe. In particular, Martin, Julle, Óli B, Deirdre and Dato, thanks so much for the company, the parties, and the long breakfasts.

To BT, Sindri, Konni, Martin and Olli B, the fishing we shared was a true highlight of my time on the rock, and provided calmness during some rather icy storms. Thanks for wetting a line with me. To my surfing posse from Spout Creek to Grindavík: Niko, BT, Jamesy, Marcy, Zeb, Chris B, Fi, Timmy, Robster, Liam, Benno, Markús, Conor, Róbbi, Atli and Dana, folks, it has been a privilege to share many oceans with you through these years, and thanks so much for getting immersed. To Águst, Rob, Gro, Werner, Paavo, Martin, Dan, Sydney, Jakob, Óli Páll, Zsófi and Jay, I have fond memories of long KH sessions, unearthly boulder-strewn landscapes and run-out multi pitches. Thanks for the vertical times and for spotting me when falling was likely. To my mates in Oz, especially Moff, Ev, Sandy, Sonnie, Suz, Caz, Panda, Cookie, Kerryn, Mich and Renae, you made visits home to more temperate climates that much more enjoyable. Thanks for always being there and for making the time to hang out.

And finally, to Mum and Dad, words cannot describe your contribution to this project. Your wisdom, guidance, support and friendship allowed to complete this tome, so this is for you.

1 Introduction and synthesis

"Should I stay or should I go?", a question immortalised by The Clash, is one central to the lives and fates of migratory animals. Such decisions are often tricky to make, and can be strongly influenced by answers to other emergent questions, such as when, in which direction and how far should I move? Does the risk of predation associated with moving outweigh the benefits of productive foraging in distant areas? What are my neighbours, and older, experienced conspecifics doing, and what did I/we do in the past? In the case of marine fishes, movement decisions must also be reached under the highly dynamic environmental conditions typically encountered in the ocean; conditions that in themselves add uncertainties and often play a decisive role in the decision-making process.

These issues go to the heart of this thesis. In the five papers that comprise it, I unite spatiotemporal distribution models for two marine fishes of high commercial importance across the North Atlantic, chemical analyses of fish otoliths (ear stones) and output from ocean models, with an overarching objective of gaining new insight into the reasons behind, and consequences of, migration in fully marine species.

Specifically, I explore the importance of 'intrinsic' (i.e. behaviour, demographics, ontogeny) and 'extrinsic' (i.e. environment, fishing pressure, prey availability) factors in shaping movement and migratory decisions, and predict the spatial outcomes of these decisions, both in a contemporary context and under future scenarios of environmental change (**Papers I, II, V)**. Continuing this theme, I next develop models to test how, and at which scales, ontogenetic and environmental processes impact on individuals' expression of the chemical traits stored within their otoliths. This information is then used to chart connections among juvenile populations distributed across a large geographic domain, and between juvenile and fished adult populations (**Papers III, IV)**. The intention here was to provide a quantitative template upon which estimates of population linkages could be enhanced, with subsequent benefits for the spatial management and conservation of fished stocks.

The remainder of this chapter is structured as follows. I begin with some relevant background on movement and migration, highlighting fishes' capacity as model organisms for testing theories in this arena. Next, I set the scene for each paper in turn, delving deeper into the literature to provide context for the questions addressed, then summarising the main findings of each study and how these link with the other papers in the thesis. Finally, I conclude with some perspectives and potential future directions.

1.1 Movement and migration

The coordinated, collective movements of animals across land- and ocean-scapes are spectacular phenomena that continue to fascinate scientific boffins, weekend naturalists and couch-bound Attenborough fans alike. Celebrated examples include the long-distance,

seasonal migrations of large African herbivores (e.g. Talbot and Talbot 1963), annual transitions between high-latitude feeding grounds and low-latitude breeding and calving areas by baleen whales (Dawbin 1966; Rizzo and Schulte 2009; Mate et al. 2015) and the return of anadromous salmonid fishes to their natal rivers to spawn (Banks 1969; Jonsson and Jonsson 2011). Despite their often iconic status, populations of many migratory species have declined steeply (e.g. Dekker 2003; Sanderson et al. 2006), and indeed the act of migration itself is increasingly recognised as a threatened process (Wilcove and Wikelski 2008; Harris et al. 2009; Dybas 2014).

Human activities are considered largely responsible for many of these losses. Growth in urbanisation, expanding agriculture and the construction of barriers are fragmenting habitats and disrupting migratory traditions (see Harris et al. 2009; Løvchal et al. 2017), often with dramatic ecological, socio-economic and/or evolutionary consequences, though not all of them detrimental (see Flack et al. 2016). Overexploitation of commercially-targeted species can exacerbate these issues, as can climate change, which is redistributing species across jurisdictional boundaries and creating mismatches between the scales of management units and those at which population processes operate (e.g. Astthorsson et al. 2012; Jansen et al. 2016; Champion et al. 2018; Moore et al. 2018).

In devising strategies to minimise the negative impacts of our actions with a view to ensuring the long-term survival and sustainability of harvested migratory species, it is crucial that we seek to understand the complexities of their life histories (Brower and Malcolm 1991; Righton and Walker 2013). This is no easy feat, yet progress may lie in quantifying how individual-level variability in behavioural, physiological and genetic traits manifests at the population level, and assessing the ecological and evolutionary repercussions of such variability. Further, we require both new tools and the refinement of existing ones to explore the synergies between such ‘intrinsic’ processes and ‘extrinsic’ forces in shaping the movement decisions that ultimately define the distribution of populations and their structure in space and through time (Alerstam et al. 2003; Dingle and Drake 2007; Flack et al. 2016).

1.2 Fishes as exemplars

Fishes provide some of the most interesting and well-studied examples of migratory phenomena in animals. In many cases, this level of attention can be attributed to a long history of commercial harvest (e.g. Barrett et al. 2000), strong and enduring cultural values ascribed to a particular species (Smith and Steel 1997; Atlas et al. 2017), and/or its ongoing socio-economic importance for consumptive purposes (Jakobsson and Stefánsson 1999). In the North Atlantic, the commercial value of Atlantic salmon (*Salmo salar* L.), Atlantic cod (*Gadus morhua* L.) and Atlantic herring (*Clupea harengus* L., hereafter ‘herring’) to economies in Europe and North America inspired early theoretical and experimental work on migratory tendencies in these species (Schmidt 1907; Scheer 1939; Fridriksson and Aasen 1950; Jakobsson 1969). Such studies, in conjunction with more recent efforts (e.g. Iles and Sinclair 1982; Blaxter 1985; Corten 1993, 2002; Dragesund et al. 1997; McQuinn 1997; Nøttestad et al. 1999) have revealed remarkable complexity in schooling behaviours, movement patterns, migratory traditions and population dynamics – features that often differ among stocks of conspecifics, and the mechanics of which are still being explored (see section 1.3 below for details, and Huse et al. 2010; Grabowski et al. 2012; Libungan et al.

2015; Pampoulie et al. 2015; Huse 2016; Bárðarson et al. 2017; **Papers I**, **III**, **IV**, **V** for examples).

1.3 Drivers of movement, migration and space use in fishes

Numerous factors have been shown to influence the movement and migratory decisions of fishes, as well as the outcomes of these decisions – i.e. their resultant spatial distributions. For example, the use of visual stimuli and electroreception to locate landmarks is well known (Walton and Moller 2010; Silveira et al. 2015), whilst geomagnetic and imprinted olfactory cues provide compasses for returning anadromous salmon (Hasler and Scholz 1983; Lohmann et al. 2008; Putman et al. 2013). Moreover, environmental gradients, the distribution of predators (both human and aquatic), competitors and prey, density-dependent processes, demographic structure and social cues can also act strongly, and oftentimes interactively, in shaping occurrence and abundance patterns (Swain 1999; Fisher and Frank 2004; Spencer 2008; Loots et al. 2010; Planque et al. 2011; Ciannelli et al. 2012; Bartolino et al. 2014; **Papers I**, **II**).

1.3.1 Group-living and sociality

Of particular importance for fishes that school, or animals that live within groups or 'societies' more generally, are the realities and pressures enforced by group living itself. Individuals can gain much from this kind of lifestyle, often experiencing lower predation risk, improved foraging efficiency, enhanced navigational accuracy and heightened capacity to sense dynamic environmental gradients, among other benefits (Berdahl et al. 2013, 2016). These gains provide strong incentives to stick together, whilst also creating opportunities for movement decisions to be made collectively and optimised for maximum group benefit based on democratic consensus (Conradt and Roper 2005; Sumpter and Pratt 2009). Indeed, the spatial proximity, number and status of conspecifics within groups can strongly affect individuals' decisions about how, when and where to move; decisions simultaneously influenced by, and influencing, the behaviour of the collective around them (Conradt and Roper 2005; Sumpter and Pratt 2009; Strandburg-Peshkin et al. 2015; Berdahl et al. 2016). In exploring these ideas with shoals of three-spined sticklebacks (*Gasterosteus aculeatus*), Sumpter et al. (2008) and Ward et al. (2008) demonstrated that collective movement decisions can follow non-linear 'quorum' rules – the likelihood of a single stickleback choosing a certain route rising sharply beyond a threshold number of sticklebacks in the shoal that recently chose that same route. In subsequent experimental work (Ward et al. 2011), these authors also showed that quorum responses can improve decision accuracy, and that larger shoals often make better decisions, *sensu* 'the wisdom of crowds' (Surowiecki 2004).

Similar patterns seem to emerge across a wide range of taxa and ecological functions (see Sumpter and Pratt 2009), though comparable consensus might also be achieved through leadership by a minority of 'experienced' individuals, or those with strongly-held preferences (Reebs 2000; Huse et al. 2002). Usually, only a few well-informed leaders are

needed to produce highly accurate movement decisions (Reebs 2000; see also Berdahl et al. 2018); however, the complete absence of such leaders may lead to poor group navigation (Helfman and Schultz 1984). Such observations, in conjunction with growing recognition of the cognitive abilities of group-living fishes (Hotta et al. 2015) strengthens arguments for the existence of social and collective learning and tradition formation in some species (see Brown 2015; Berdahl et al. 2018 for reviews) in which information on previously-used migration routes is thought to be passed down from older, experienced fish to younger, naïve ones, communicated within cohorts and remembered (Corten 1993; McQuinn 1997). Further support for such ideas derives from evidence for time-place learning in fishes (e.g. Brännäs 2014), and experimental demonstrations of accurate short- and long-term memory (Brown 2001; Hotta et al. 2015).

So, although concepts of animal consciousness and sentience remain hotly debated (Dawkins 2001; Rose et al. 2014; Brown 2015), the aforementioned studies on fishes, and theoretical and empirical work on other taxa demonstrate that aspects of sociality, learning and memory can play important roles in determining migration patterns and space use in group-living animals (e.g. Couzin 2009; Guttal and Couzin 2010; Petit et al. 2013; Kao et al. 2014; Merkle et al. 2014; Andersson et al. 2015; Berdahl et al. 2018). Despite clear fitness advantages at ecological time scales, the mechanisms, ecological outcomes and evolutionary consequences of sociality remain unclear for many social animals. In light of such uncertainties, there have been recent calls for further work into how animal groups adapt their collective decisions dynamically, and how our observations of group-level actions (e.g. detection of realised spatial distributions) can be influenced by a collective's previous experiences, or memories of them (Biro et al. 2016).

1.3.2 Disentangling sociality and extrinsic processes

To progress on this front, we need to quantify the synergies between these socially-driven factors and other extrinsic processes in how movement decisions are reached and subsequent distribution patterns realised. This is a challenging task, particularly for wild, long-lived fishes that are rarely directly observable beyond the length of a survey cruise or a fishery trawl shot. Yet these data are crucial, especially for migratory, commercially-targeted stocks that straddle international and/or jurisdictional borders – stocks for which accurate, spatially-resolved predictions of occurrence and abundance patterns are needed to balance harvest and conservation goals.

When mechanistic information is scarce and observational data plentiful, a sensible first step might involve identifying the proximate processes acting on the level of biological organisation of interest (e.g. individual-, population-, species-level) based on available ecological knowledge and/or theory, then defining the spatial and temporal scales at which these processes operate (Levin 1992). As an example, coordinated movements of a hypothetical population might emerge as a result of 1) exposure to, and retention of specific cues experienced during early age (e.g. natal homing in salmon), 2) the social transmission of long-standing traditions among individuals and cohorts (e.g. 'The adopted migrant hypothesis' in herring – McQuinn 1997), or 3) the rapid spread of information within the school driven by school-wide responses to environmental gradients, prey resources or predation threats (e.g. Nøttestad et al. 1996), or combinations thereof. Capturing such processes effectively, and at scales appropriate to the question(s) at hand within spatially-

explicit, temporally-dynamic models, would provide a base for improving ecological knowledge, generating new hypotheses and providing reliable spatiotemporal predictions of occurrence and/or abundance patterns.

1.3.3 Papers I and II

In the first two papers in the thesis (i.e. **Papers I**, **II),** we develop these types of space-time distribution models for stocks of two long-lived, commercially-important fish species with vastly different life-history strategies and geographic distributions – Icelandic summer spawning (ISS) herring (*C. harengus*), and North Sea striped red mullet (*Mullus surmuletus* L.). We took an hypothesis-driven approach to model development for these stocks, with two main objectives: 1) to identify key processes shaping current and past distribution patterns and to define the scales at which these operate, and 2) to generate accurate predictions of distributional patterns that can help guide fishery-management directives.

Modelling shifting fish distributions

The models we built fall within the class of empirical statistical models, as defined by Levins (1966). These are in essence 'correlative', but draw on mechanistic underpinnings as related to concepts of Grinnellian and Eltonian niches (Hutchinson 1957; Soberón 2007) (see **Paper I** – Appendix 9 for a discussion).

Models were fitted in Bayesian framework, using integrated nested Laplace approximation (INLA) and the Stochastic Partial Differential Equations (SPDE) approach (Rue et al. 2009; Lindgren et al. 2011) to explicitly capture spatial and temporal dependencies in the data. The merits of the Bayesian approach for this type of hierarchical model are many (Gelfand et al. 2006; Gelman and Hill 2007; Royle et al. 2007). Without reviewing these exhaustively here (see Elderd and Miller 2016 for a comprehensive appraisal), we highlight the inherent way in which random effects are handled as parameters of interest, resulting in fully specified probability distributions from which information on the intensity and uncertainty of the effects can be drawn; the option to incorporate prior knowledge based on existing empirical data or theory; and the ability to robustly quantify and propagate uncertainty through all modelling stages.

Model fitting using INLA is computationally efficient, and provides accurate approximations of the posterior marginal distributions of model parameters that show high concordance with Markov Chain Monte Carlo simulations (Rue and Martino 2007; Rue et al. 2009; Held et al. 2010). Since Lindgren and colleagues proved that a continuously indexed Gaussian field described by a Matérn covariance function can be represented as a discretely indexed Gaussian Markov random field (GMRF) (Rue and Held 2005; Lindgren et al. 2011), rapid development of the SPDE approach within the 'R-INLA' package in R has facilitated fitting of an expanding suite of hierarchical spatial and spatiotemporal models to spatial point patterns (Krainski et al. 2016). This approach has recently proven useful in analyses of georeferenced fisheries datasets, which are often data- rich and where inference at the scale of point locations, rather than grids, is required (e.g. Cosandey-Godin et al. 2015; Ward et al. 2015; Ono et al. 2016).

Study species

Despite their many differences morphologically (see Figures 1.1, 1.3) and ecologically, both herring and striped red mullet share long histories of commercial exploitation, and have continuing high cultural and commercial significance across the North Atlantic and beyond (Reñones et al. 1995; Jakobsson and Stefánsson 1999; Geffen 2009; Mahé et al. 2014; Huse 2016). Importantly, key questions regarding the triggers and outcomes of migratory decisions remain unresolved for both species, for which answers are needed to inform spatial management actions for the fisheries targeting them. We profile both species now.

Atlantic herring

Herring, a pelagic, dense-schooling clupeid, is one of the most widely-distributed and heavily-fished species in the North Atlantic Ocean. 'Sild' as they are known in Icelandic, occupy a unique position in the history of the Nordic region in both socio-economic and ecological contexts. Indeed, herring fishing in Icelandic waters has often been called Iceland's first industry. Commercial fishing for the species began in earnest in the 1880s, with effort focussed initially on the east coast fjords. However, due to easier access to fishing grounds in the north, interest soon shifted to areas around Eyjafjörður and Siglufjörður. The herring industry, producing salt herring, fish-meal and oil, sometimes accounted for nearly half of Iceland's national income, and so herring came to be known as *the silver of the sea*, and *Iceland's gold* (Sigurðsson et al. 2007).

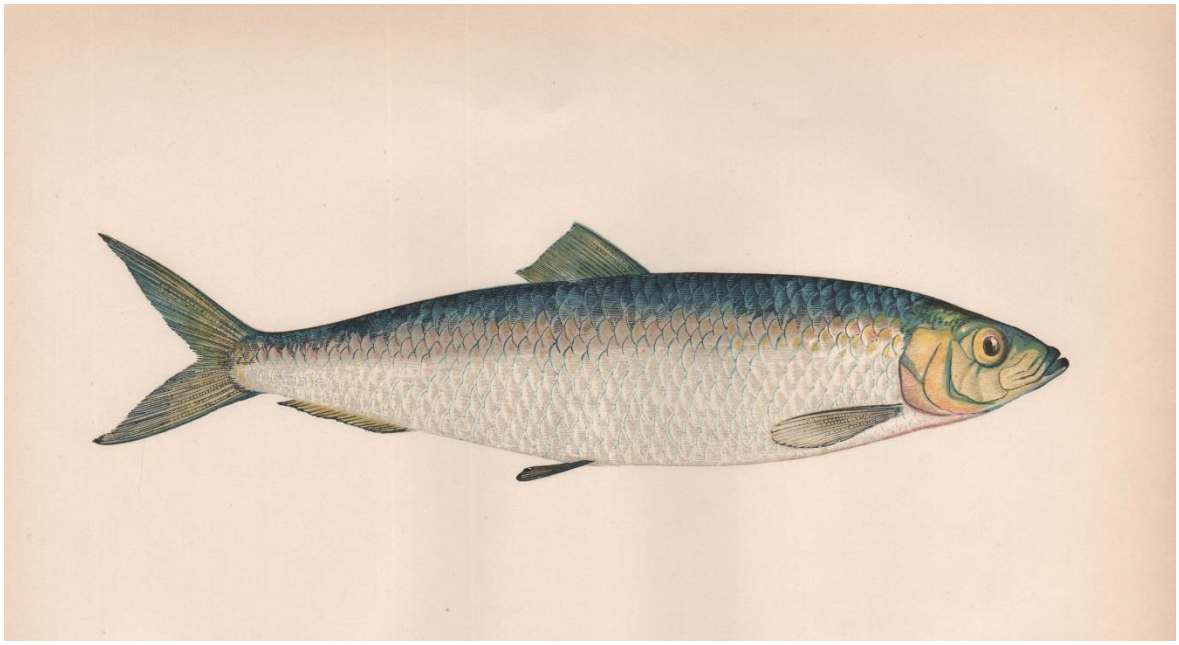

Figure 1.1. Sketch of a mature herring (Clupea harengus). *(Jonathan Couch, 1862).*

Notwithstanding its clear commercial appeal, aspects of the species' biology, schooling behaviour and rather unpredictable migration patterns have captured the imagination of fisheries researchers for centuries. In fact, several of the major theoretical advances in fisheries ecology have stemmed from early work on herring (see Geffen 2009 for a review). The species is characterised by complex population dynamics (Iles and Sinclair 1982; Libungan 2015; Huse 2016) perhaps best described by a metapopulation model (McQuinn

1997), with individuals within local populations forming dense schools for much of the year and undertaking large-scale migrations between spawning, feeding and overwintering areas for which strong fidelity is exhibited in most, but not all years (Fernö et al. 1998; Langård et al. 2014). Several hypotheses have been advanced to explain this fluctuating 'conservatism' in migratory strategies (Jakobsson 1969; Corten 2002), with a particular focus recently on the drivers of the striking shifts in winter distribution observed periodically (Óskarsson et al. 2009; Huse et al. 2010). Current thinking favours aspects of McQuinn's 'adopted migrant hypothesis' (McQuinn 1997), akin to Petitgas et al.'s 'entrainment hypothesis' (Petitgas et al. 2006), which both assert the importance of social and collective learning. When tuned to wintering herring, these hypotheses contend that naïve, first-time winterers (i.e. at age 3 in the ISS stock) learn the location of traditional wintering areas by schooling with older, experienced winterers (i.e. age 4+), typically returning to these same areas subsequently (Höglund 1955). However, when the learning process is disrupted in some way, dramatic shifts in winter distribution seem to occur, suggesting a break in tradition when teachers are few (Corten 1999, 2002; Huse et al. 2002, 2010) (Figure 1.2).

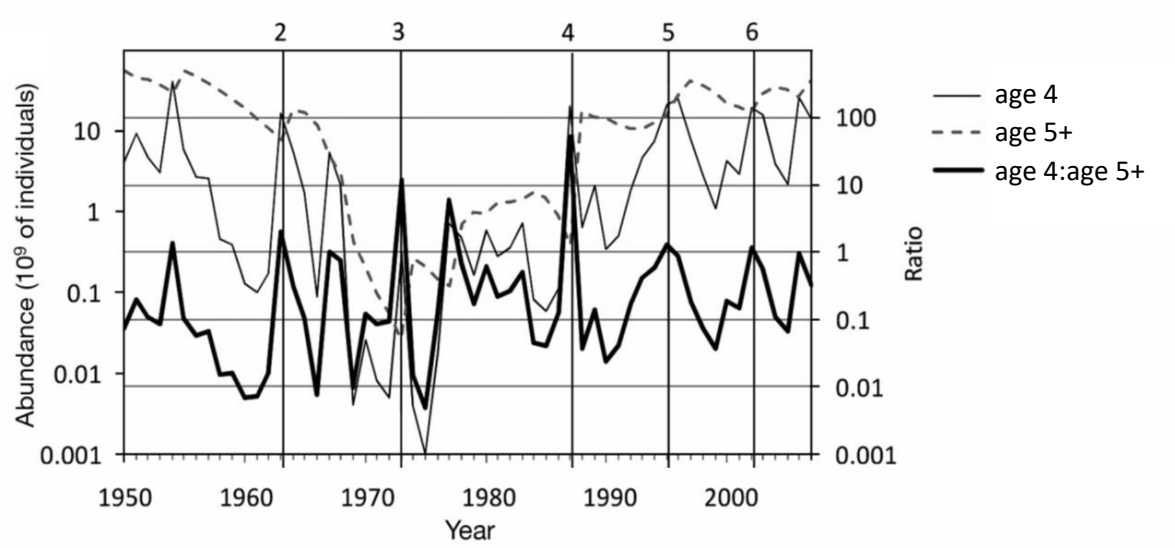

Figure 1.2. An investigation by Huse et al. (2010) into the wintering dynamics of Norwegian spring spawning herring showed that the five major shifts in wintering distribution observed over ~60 years (vertical lines) coincided with years in which the ratio of first-year spawner abundance (i.e. age 4) to repeat spawner abundance (i.e. age 5+) was high. The authors suggested that when there is a numerical domination of naïve fish in the population, there are too few experienced teachers available to guide the younger fish to traditional wintering areas, and hence, new migration routes are forged. Figure redrawn from Huse et al. (2010).

So, which factors emerge as key drivers of migratory decisions under these circumstances? A large body of work has demonstrated the importance of both bottom-up (e.g. climate, local-scale environment, zooplankton biomass) and top-down (i.e. fishing effort, predation and competition) processes in shaping the spatial distribution and biomass-at-age for several herring stocks (e.g. Glover 1955; Jakobsson 1969; Bainbridge and Forsyth 1972; Bainbridge et al. 1978; Huse and Ona 1996; Corten 2000; Maravelias and Reid 1995, 1997; Maravelias et al. 2000a, b; Kvamme et al. 2003; Óskarsson et al. 2009; Lindegren et al. 2011; Trenkel et al. 2014). However, spatially-resolved information on how migratory traditions are jointly influenced by collective learning or spatial 'memory', the demographics of the population and relevant extrinsic processes is currently lacking.

I address this issue in **Paper I**, in which we fit SPDE models to fishery and survey data for ISS herring to investigate wintering dynamics around Iceland across more than two decades (i.e. from 1991 to 2014). We included covariates reflecting dynamic (e.g. sea surface temperature) and static (e.g. bottom depth) environmental factors, the distribution of prey, and recent fishing pressure at scales matching the catch records, and through an index capturing distributional persistence over time, derived two proxies for spatial memory of past wintering sites. The winter occurrence pattern in one year was a key driver of the pattern in the next, its influence increasing when adult population size was large. Though the mechanisms remain uncertain, we suggest that a 'wisdom of the crowd' dynamic may be acting, by which directionality towards traditional wintering grounds improves in larger, better organised schools. Our results also exposed strong synergies among demographic processes and environmental effects in shaping winter distribution patterns, whilst recent fishing effort had little impact. Notably, we were able to accurately forecast winter distribution patterns one year in advance, highlighting how demographic inputs can improve predictions from dynamic models, and how such models might be useful for fishery-management applications.

Striped red mullet

In collaboration with colleagues at Ifremer in France, we applied similar, though less complex models to explore the movement patterns of striped red mullet (hereafter 'mullet') in the North Sea and Eastern English channel across 20 years (i.e. 1995 to 2015) (**Paper II**). Although relatively 'data-poor' when compared with the long-term datasets and rich literature devoted to herring (but see Heesen 1996), published accounts on the biology of this demersal mullid (see Figure 1.3) still span a century, beginning with the early work of Fage (1909) and Desbrosses (1933, 1995) (see N´Da and Déniel 1993; Mahé et al. 2013 for more recent studies on growth and reproductive biology).

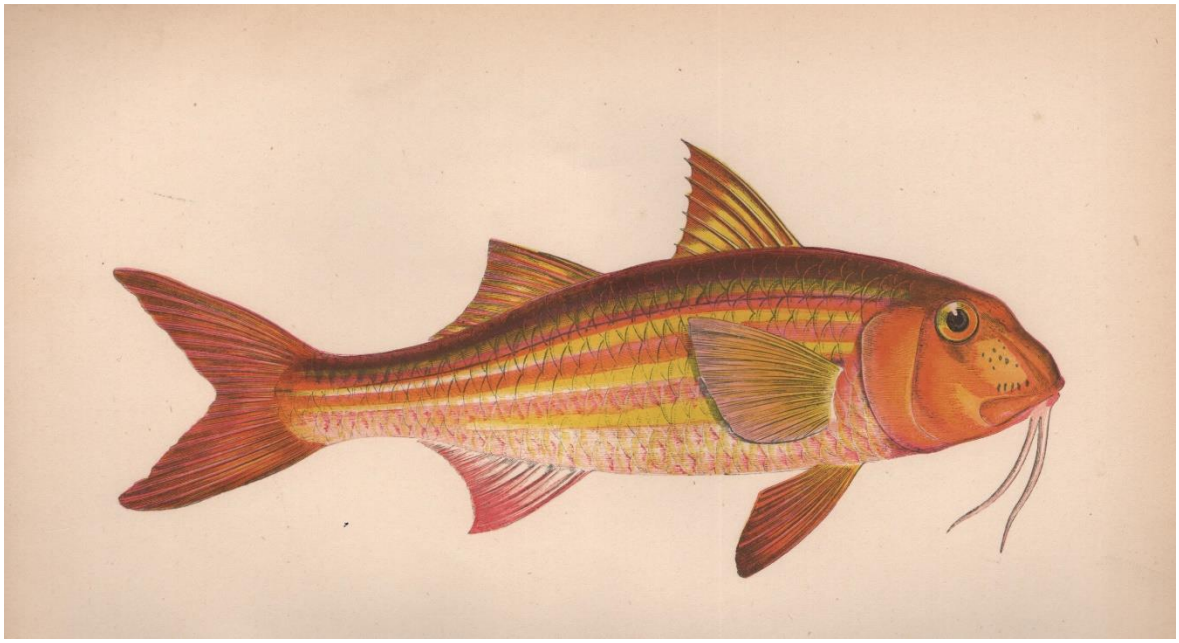

Figure 1.3. Sketch of a mature striped red mullet (Mullus surmuletus). *(Jonathan Couch, 1862).*

Initially treated as a valuable by-catch species, mullet is now fished extensively throughout the North Sea, the English Channel, the Bay of Biscay, off Spain and France, and the Mediterranean Sea (Reñones et al. 1995; Mahé et al. 2014). Indeed, abundances and catch rates have increased markedly over the past three decades in the Eastern English Channel and southern North Sea fishery that targets what is now recognised as the 'northern subpopulation' (Beare et al. 2005; ICES 2012; Mahé et al. 2014). In the Eastern English Channel for example, landings are now greater than 10 times 1990 levels (Marchal 2008; Carpentier et al. 2009). Yet, the species still has no assigned quota in this region, with quantitative monitoring of exploitation rates only commencing in 2007 (ICES 2012).

Paper II focuses on the northern subpopulation, one that displays strong phenotypic differences and little mixing with either the 'southern zone subpopulation' (in the Bay of Biscay) (Mahé et al. 2014) and the 'mixing zone subpopulation' (in the Celtic Sea and the Western English Channel) (Benzinou et al. 2013). Despite, indications of a recent, warming-induced, northwards range expansion by this northern subpopulation (Beare et al. 2005; Poulard and Blanchard 2005; Mahé et al. 2014), the role of sea surface temperature and other environmental factors thought to influence habitat choice in mullet (e.g. salinity, bathymetry, sediment type) (ICES 2017a) requires clarification using data spanning the full geographic range of the subpopulation, over several years. Understanding how these extrinsic processes shape the migration and distribution patterns of this subpopulation is the primary objective of **Paper II**. To do this, we united multiple fishery and survey datasets with differing spatial and temporal extents within a series of hierarchical Bayesian models, again fitted using the SPDE approach (Rue et al. 2009; Lindgren et al. 2011; Krainski et al. 2016). We found that mullet occurrence was positively correlated with water temperature and salinity, and that mullet distribution was widespread and rather uniform in some years and small and patchy in others. Despite marked inter-annual variability in distributional range, we observed relatively consistent patterns in seasonal migration in this subpopulation, with mullet occupying waters in the north-east of the North Sea in winter, moving south during spring/summer and entering the Eastern English Channel in autumn.

Our analysis is timely, as the regular fluctuations in abundance experienced by this northern subpopulation have increased in magnitude over the past five years, concurrent with the loss of the largest, oldest spawners (ICES 2015, 2017a). Moreover, a recent assessment of length-based indicators provided strong evidence of 'growth overfishing' (ICES 2017a). Taken together, these results point to a stock that is exploited beyond sustainable limits, with further declines in biomass likely given recent poor recruitment (ICES 2017a). There is currently no total allowable catch (TAC) specified for this subpopulation, and the implementation of more restrictive management actions is currently being debated. We believe that the new insights gained here into the environmental sensitivity and space use of the species near its northern range limit could contribute to making wiser, spatially-informed management decisions in this regard.

1.4 Connectivity among populations and stocks

Of equal, if not even greater importance for managing migratory species distributed across wide geographic domains are reliable data on how populations or stocks of conspecifics are connected (Cowen et al. 2007; Fogarty and Botsford 2007). Understanding the ecological

and evolutionary processes that give rise to contemporary patterns of connectivity, and defining the scales of this connectivity itself (e.g. across space, time and through ontogeny) provides a basis for delineating management boundaries that better reflect the scales at which populations (or stocks) actually function (Leis et al. 2011; Moore et al. 2018).

Recent advances in applied-tag technology (e.g. acoustic, archival and satellite tags), in genetic techniques (e.g. next-generation sequencing, detection of Single Nucleotide Polymorphisms – SNPs) and in linkages between ocean models and species' biological characteristics are allowing researchers to define these scales with increasing confidence (Treml et al. 2012; Grewe et al. 2015; Bárðarson et al. 2017; Halfyard et al. 2017; Scutt Phillips et al. 2018). However, questions on how life history stages are linked, both geographically and ecologically, remain open for many exploited fish populations (Cowen et al. 2007). Juveniles and adults of the same species often prefer different habitats, vary in their environmental tolerances and have distinct diets, and as such, these groups can find themselves biologically and spatially isolated throughout much of their lives (e.g. Tsukamoto et al. 2002). Even within juvenile cohorts, striking variation is sometimes seen in individual size, physiological and behavioural traits (Fiksen et al. 2007), past experience (Shima and Swearer 2010, 2016) and personality (Cote et al. 2010). These individual-level (intrinsic) differences might, in conjunction with local environmental (extrinsic) pressures, manifest in marked phenotypic diversity among groups of similarly aged juveniles (Freshwater et al. 2019), in turn influencing migratory capacity/tendency (Nanninga and Berumen 2014), survival to adulthood (Shima and Swearer 2010; Jørgensen et al. 2014) and the composition and spatial arrangement of nursery 'source' populations across an ocean scape.

In studies of 'source-sink' dynamics, quantifying the scales at which such spatially-structured populations might differ, both in their expression of intrinsically-driven traits, and in their exposure to extrinsic factors, can also reveal the scales at which they connect. In a fishery-management context, two often interlinked applications of such information are to estimate mixing rates among putative 'source' populations in order to assess their relative contributions to adult 'sink' populations.

Fish otoliths (ear stones) contain arguably the richest repositories of data for this purpose. These structures, composed mainly of $CaCO_3$ and located within the inner ear of all teleost fishes, play a vital role in the fish's sensory functioning, balance and hearing, and comprise lifetime, individual-level data on phenotypic traits that can vary strongly within and among populations or stocks (Macdonald and Crook 2010; Huey et al. 2014; Libungan et al. 2015). The discovery that permanent growth increments are deposited daily onto the otolith makes them the gold standard of accurate age recorders (Campana and Neilsen 1985). Yet, the sensitivity of both otolith morphology and otolith chemical constituents to intrinsic processes (e.g. physiology, metabolism, growth, age, genetics) and/or extrinsic (e.g. environmental) factors, also highlights otoliths' unique potential as 'natural tags' in population connectivity studies, used either alone (e.g. Burke et al. 2008; Neubauer et al. 2010; Libungan et al. 2015; Wright et al. 2018), or in combination with other complimentary approaches (e.g. Ashford et al. 2012; Bárðarson et al. 2017; Taillebois et al. 2017).

1.4.1 Harnessing otoliths' true potential

To optimise otoliths' value for these types of population-delineation applications, we need to acknowledge that the external environment can place strict limits on intrinsic processes (Pörtner and Peck 2010; Holt and Jørgensen 2014), and to quantify how these factors jointly influence the expression of traits that we measure in these structures. Moreover, innovations in statistical approaches that use the chemical traits locked within otoliths as population markers may allow us to honour their full potential for such applications. Traditional modelling approaches, while evolving (see Mercier et al. 2011; Jones et al. 2017; Niklitschek and Darnaude 2016), often fail to consider the mechanisms driving inter-individual variability in chemical traits, and how these manifest at the site-, population- or stock-level. Moreover, they rarely assess data- and model-related uncertainties explicitly. In the context of understanding connections among 'source' populations and their links with mixed 'sink' populations targeted by fisheries, these deficiencies make formal tests of hypotheses on the significance of source location and quality (see Beck et al. 2001) difficult, and might easily lead to sub-optimal management outcomes, especially when sampling is sparse, or sample sizes low.

1.4.2 Papers III and IV

Papers III and **IV** centre on such topics. Again, we use the ISS herring stock for illustration, one that still supports a viable commercial fishery for Iceland (Jakobsson and Stefánsson 1999; ICES 2018) despite undergoing a decade-long decline as a result of serial poor recruitment, severe disease outbreaks (Óskarsson et al. 2018a) and two mass mortality events during the 2012/2013 winter (ICES 2017b; Óskarsson et al. 2018b). Data on the spatiotemporal structure of nursery populations within this stock are limited, and the origins of individuals within the fished adult populations remain largely unknown.

Data for both papers derive from otoliths of juvenile herring captured on their nursery grounds around the Icelandic coast over three autumns (i.e. 2013, 2014, 2015) (Figure 1.4).

*Figure 1.4. A) Chasing juvenile ISS herring aboard w/w Dröfn RE-35. Ísafjarðardjúpi, November 2014. (Photo: Jed Macdonald). B) A selection of age 1 and age 2 ISS herring fresh from the trawl. C) Polished sagittal otoliths from age 2 ISS herring (viewed under reflected light) awaiting the MicroMill (see **Papers III** and **IV** for analytical details).*

We measured the concentrations of a suite of elemental (i.e. Li, Mg, Ca, Mn, Zn, Sr, Ba) and stable isotopic (i.e. $\delta^{13}C$, $\delta^{18}O$) traits (hereafter 'markers') in these otoliths, combining laser-

and solution-based mass spectrometry techniques to analyse otolith material accreted during nursery residence, representing the last weeks of each juvenile's life prior to capture.

In **Paper III**, we present results from a field-based test of intrinsic influences on otolith chemical markers. We take advantage of a sampling scheme in which two age classes were captured simultaneously in the same trawl haul, at a subset of nursery sites, and develop a series of Bayesian mixed effects models to disentangle ontogenetic influences (i.e. age- and growth-related factors) and environmental effects (i.e. ambient salinity and temperature) in shaping otolith chemical expression. We detected strong age-related, site-specific declines in several elemental markers, high individual-level variability within sites, within age classes for all markers, and evidence of temperature and salinity effects on otolith $\delta^{13}C$ and $\delta^{18}O$ at the population-level. We harnessed this information to predict marker concentrations at all nursery sites, both sampled and unsampled, generating maps that accurately reproduced the observed heterogeneity in otolith chemistry across the juveniles' full geographic range. The models developed here were relatively simple, yet provided direct inference on both the scale of individual-, site-, age class- and population-level variation in otolith chemistry through time, and the synergies between marker expression and intrinsic and extrinsic factors. Whilst tuned to ISS herring, we note that spatially-explicit predictions from these types of models could provide valuable initial estimates of population connectivity for other widely-distributed species, particularly when sampling coverage is patchy.

We expand on these ideas in **Paper IV**, in which we tackle some open questions relating to the connections among, and fidelity to nursery areas, and the contribution these make to fished adult populations. Using an extended version of the dataset analysed in **Paper III**, and informed by its findings, we fitted a series of Bayesian multivariate and finite mixture models to address four key aims: 1) to define the scales of spatial and temporal variability in otolith chemical traits in nursery-resident juveniles across their full distributional range; 2) to test the long-held theory that juveniles are retained within specific nurseries following settlement, prior to joining the adult component of the stock at age 3; and 3) to quantify the relative contribution of nursery populations to a sample of age 3 adults caught in the winter fishery operating off the west coast of Iceland in November 2015. Additionally, we explored if/how geographic distance from the wintering grounds, and/or nursery 'quality' (*sensu* the 'nursery-role hypothesis' – Beck et al. 2001) mediate nursery contributions (aim 4).

As part of this work, we used simulations to develop some new rules of thumb for assessing the magnitude of multivariate group differences in a Bayesian setting. We leant on these to classify nursery populations into better-delineated 'source' populations that respect the scale of spatial, temporal, individual- and population-level variation we observe in the data. We found that population-level differences in otolith chemical markers generally increased with both the geographic distance among nursery sites and the temporal distance between sampling periods, manifesting in patterns of coast-wide marker heterogeneity that shifted through time (aim 1). Output from the finite mixture models supported the hypothesis that juvenile herring exhibit strong year-to-year fidelity to nursery sites (aim 2), and demonstrated the collective importance of multiple sources for a fished adult 'sink' population (aim 3). Finally, we found no evidence of a connection between source contribution and distance from the wintering grounds, and no support for the 'nursery-role hypothesis' in this system (aim 4). The results pertaining to aims 2, 3 and 4 must be considered in light of the potential for unsampled, or poorly-characterised source populations to have contributed to the 'mixed samples' of age 2 and 3 herring, an uncertainty

that our finite mixture models cannot account for. Infinite mixture modelling approaches deal with this issue explicitly (Neubauer et al. 2013; Loff and Neubauer 2018; Reis-Santos et al. 2018), and I am exploring these in ongoing work. Notwithstanding these caveats, the Bayesian framework we present for ISS herring offers a quantitative basis for assessing the scale of connections among putative sources, elucidating nursery-residence patterns, and clarifying the role of nurseries as contributors to harvested populations more generally.

1.5 Fishing- and climate-related distribution shifts

The direct impact of fishing on commercially harvested species, including herring, can be immense (Jennings and Kaiser 1998; Corten 2002; Worm et al. 2009; Dickey-Collas et al. 2010). Though we found no clear evidence for a fishing effect in driving winter distribution patterns in the ISS stock (see **Paper I**), it is increasingly recognised that intense exploitation of targeted fish populations may reduce their resilience to environmental change (Planque et al. 2010), and that fishing and climate can interact to influence long-term distribution patterns (Engelhard et al. 2011) and spatial population structure (Ciannelli et al. 2013).

In saying this, changes in climate alone may sometimes be pervasive in rerouting migratory paths and reshaping marine fish distributions (Perry et al. 2005; Astthorsson et al. 2012; Petitgas et al. 2013; Champion et al. 2018), although often, other interactive and/or unmeasured factors are likely at play (Thorson et al. 2017). We saw some sensitivity to environmental factors, particularly temperature and salinity, or the proxies they reflect, in the movements of the northern subpopulation of mullet throughout the North Sea and Eastern English Channel (see **Paper II**), and in the wintering patterns of ISS herring (see **Paper I)**. Similar sensitivities have been noted for other herring stocks during winter (e.g. Corten 1999), and at different times of the year. For example, in a series of papers focused on North Sea herring, Maravelias and colleagues demonstrated strong effects of temperature, salinity, stratification, zooplankton biomass and bottom topography on pre-spawning summer distribution (e.g. Maravelias and Haralabous 1995; Maravelias and Reid 1997; Maravelias et al. 2000a, b). The direction and magnitude of these effects differed substantially from the results presented in **Paper I**, a finding that was anticipated given that the ISS stock is located near the northerly range edge for the species, and is therefore exposed to vastly different environmental conditions to those encountered in the North Sea. Moreover, these North Sea papers and similar studies in Nordic seas (e.g. Misund et al. 1998; Jakobsson and Østvedt 1999; Kvamme et al. 2003; Nøttestad et al. 2007; Broms et al. 2012) have focused largely on herring distributions during spring and summer, periods of high feeding activity in which adult herring can be tightly associated with prey resources either directly (e.g. Holst et al. 1997; Maravelias and Reid 1997; Olsen et al. 2007) or indirectly through hydrographic proxies.

These examples go to illustrate how environmental and biotic factors can interact in complex ways to shape feeding, pre-spawning and overwintering distributions in herring. Moreover, recent experimental evidence for decreased survivorship and growth in larval herring under elevated temperature conditions (Sswat et al. 2018), and historic observations of recruitment suppression in Icelandic herring stocks during the unfavourably cold ‘ice years’ of the late

1960s (Jakobsson and Stefánsson 1998, 1999), highlight the need for further work on the potential consequences of future environmental change on herring population dynamics more broadly. Whilst a simplification of the processes at play, an empirical means to reconstruct lifetime environmental histories for individual fish would, either alone, or in conjunction with process-based or simulation modelling, provide a valuable baseline from which to predict how future ocean warming might drive range contraction or expansion, and for herring and other species of strong commercial interest, to plan how management strategies should best be adapted.

1.5.1 Paper V

In **Paper V**, I present a detailed tutorial on the empirical aspect of this equation. Specifically, I measure stable oxygen isotope ($\delta^{18}O$) profiles in otoliths using secondary ion mass spectrometry (SIMS) to define a thermal niche for five adult (i.e. age 6) ISS herring captured off the east coast of Iceland in 2014. I then apply this data to make predictions on how ISS herring distributions might shift under projected changes in ocean temperature across the region (see Darnaude and Hunter 2018 for details on the processes driving $\delta^{18}O$ incorporation into otoliths, and a recent application). Briefly, through a series of equations that relate $\delta^{18}O$ concentrations in the otolith to ambient $\delta^{18}O$, salinity and temperature, I estimated the life-long temperature histories of each of the five herring and defined an optimal thermal niche for these individuals. In making some rather large assumptions around adherence to this niche throughout life (see **Paper V** for details), I then predicted how a 1°C increase in water temperature throughout a region off the northeast coast forecast to undergo warming of up to 2°C by 2046–2065 (IPCC 2013) might affect the distributional range of adult ISS herring populations. The results suggest that future warming may create opportunities for poleward expansion in the adult component of the stock, all else being equal. I stress the preliminary nature of these results. The tutorial was designed to illustrate the type of information we can glean from otoliths and how it can be used in a forecasting context to predict likely distribution shifts in a rapidly warming ocean (IPCC 2013; Resplandy et al. 2018). I am exploring these approaches further in ongoing work, some of which I detail in the next section.

1.6 Conclusions and further work

By drawing together empirical data from a diverse array of sources and developing new models to suit, the papers presented in this thesis collectively add to a growing body of knowledge on the underlying drivers of movement, migration and connectivity in animals on the move. A unifying theme 'connecting' the analyses revolves around defining the scales at which individuals and populations of commercially-harvested marine fishes connect across an ocean scape, and understanding how these connections are moulded by intrinsic and extrinsic processes. I took a multi-pronged approach to exploring these ideas, using stocks of two species with vastly different life history strategies for illustration. In **Papers I** and **II**, we developed a series space-time regression models for adult ISS herring and the northern subpopulation of striped red mullet to investigate the interplay between sociality, stock demographics, the environment and fishing in shaping occurrence patterns through time. In **Paper III**, we isolated ontogenetic influences on the expression of chemical markers

stored in juvenile herring otoliths, detecting high individual-level variability in marker expression, and capturing this information to predict the scales of marker heterogeneity among spatially- and temporally-separated juvenile populations. We built on these findings in **Paper IV**, in which we established some quantitative rules for assessing multivariate differences in measured traits, and presented a novel Bayesian modelling approach for classifying 'source' population structure. Our rules permitted formal tests of hypotheses on nursery site fidelity and nursery contribution to fished adult populations, offering important insights into the structure and connectedness of ISS herring populations. We hope these findings will help protect key nursery populations and guide spatial management decisions for herring fisheries in Icelandic waters. Finally, in the tutorial presented in **Paper V**, I show how otoliths can be used to estimate the temperature histories of individual fish, to define thermal niches, and to forecast possible range shifts under future warming scenarios.

Yet, there are still many questions left answered. For example, we know that dispersal of eggs, larvae and young juveniles is a key process governing successful recruitment in many marine fishes. For ISS herring, information on larval transport between spawning grounds and nursery fjords remains scarce – a situation that hampers the forecasts of recruitment strength needed to ensure the sustainable management of the fishery. Expanding on the approach used in **Paper V**, one piece of 'work in progress' involves integrating otolith $\delta^{18}O$ and elemental measurements encompassing the full life history histories of juvenile herring within individual-based simulation models. Such a coupling would allow us to estimate herring dispersal trajectories from spawning grounds, test hypotheses on the existence of shared migratory histories, and shed new light on the spatiotemporal connections between spawning and nursery grounds.

It is now widely accepted that individuals within a species can vary strongly in traits associated with personality, behaviour, physiology and past experience (Dall et al. 2004; Fiksen et al. 2007; Cote et al. 2010; Shima and Swearer 2010; Leitão et al. 2018). Indeed, the existence of marked individual-level variability in the expression of such traits in group-living conspecifics of the same age (see **Paper III**) might have important ecological and evolutionary consequences for the structure and function of the populations they reside in, and the movement decisions they make at critical life stages (Kawecki and Ebert 2004; Berdahl et al. 2018; Freshwater et al. 2019). Momentum is growing in this research arena, and our understanding of how individuals' decisions scale to the collective is rapidly improving (Berdahl et al. 2018; Westley et al. 2018; MacCall et al. 2019; **Paper I**). With regard to commercially-targeted fishes, by combining expertise from multiple disciplines, seeking novel empirical data sources and taking advantage of continued advancements in modelling approaches (e.g. see MacCall et al. 2019), we place ourselves in an ideal position to probe deeper into the complex processes that underpin movements, migrations and connections among populations – a noble quest that will help ensure fisheries remain sustainable into the future.

1.7 References

Alerstam, T., Hedenström, A. and Åkesson, S. 2003. Long-distance migration: evolution and determinants. Oikos 103: 247–260.

Andersson, M.Å., Ek, F. and Olsson, R. 2015. Using visual lateralization to model learning and memory in zebrafish larvae. Sci. Rep. 5: 8667.

Ashford, J., Dinniman, M., Brooks, C., Andrews, A.H., Hofmann, E., Cailliet, G., Jones, C., Ramanna, N. and Gillanders, B. 2012. Does large-scale ocean circulation structure life history connectivity in Antarctic toothfish (*Dissostichus mawsoni*)? Can. J. Fish. Aquat. Sci. 69: 1903–1919.

Astthorsson, O.S., Valdimarsson, H., Guðmundsdottir, A. and Óskarsson, G. 2012. Climate-related variations in the occurrence and distribution of mackerel (*Scomber scombrus*) in Icelandic waters. ICES J. Mar. Sci. 69: 1289–1297.

Atlas, W.I., Housty, W.G., Béliveau, A., DeRoy, B., Callegari, G., Reid, M. and Moore, J.W. 2017. Ancient fish weir technology for modern stewardship: lessons from community-based salmon monitoring. Ecosyst. Health and Sustainability 3: 1341284.

Bainbridge, V. and Forsyth, D.C.T. 1972. An ecological survey of a Scottish herring fishery. Part V: The plankton of the northwestern North Sea in relation to the physical environment and the distribution of the herring. Bull. Mar. Ecol. 8:21–52.

Bainbridge, V., Forsyth, D. and Canning, D. 1978. The plankton in the northwestern North Sea, 1948 to 1974. Rapp. P.-v. Réun. Cons. Int. Explor. Mer 172: 397–404.

Banks, J.W. 1969. A review of the literature on the upstream migration of adult salmonids. J Fish. Biol. 1: 85–136.

Bárðarson, H., McAdam, B.J., Thorsteinsson, V., Hjorleifsson, E. and Marteinsdottir, G. 2017. Otolith shape differences between ecotypes of Icelandic cod (*Gadus morhua*) with known migratory behaviour inferred from data storage tags. Can. J. Fish. Aquat. Sci. 74: 2122–2130.

Barrett, J., Beukens, R., Simpson, I., Ashmore, P., Poaps, S. and Huntley, J. 2000. What was the Viking Age and when did it happen? A view from Orkney. Nor. Archaeol. Rev. 33: 1–0. doi:10.1080/00293650050202600.

Bartolino, V., Margonski, P., Lindegren, M., Linderholm, H.W., Cardinale, M., Rayner, D., Wennhage, H. and Casini, M. 2014. Forecasting fish stock dynamics under climate change: Baltic herring (*Clupea harengus*) as a case study. Fish. Oceanogr. 23: 258–269.

Beare, D., Burns, F., Jones, E., Peach, K., and Reid, D. 2005. Red mullet migration into the northern North Sea during late winter. J. Sea Res. 53: 205–212.

Beck, M.W., Heck, K.L., Able, K.W., Childers, D.L., Eggleston, D.B., Gillanders, B.M., Halpern, B., Hays, C.G., Hoshino, K., Minello, T.J., Orth, R.J., Sheridan, P.F. and Weinstein, M.P. 2001. The identification, conservation, and management of estuarine and marine nurseries for fish and invertebrates. BioScience 51: 633–641.

Benzinou, A., Carbini, S., Nasreddine, K., Elleboode, R. and Mahé, K. 2013. Discriminating stocks of striped red mullet (*Mullus surmuletus*) in the Northwest European seas using three automatic shape classification methods. Fish. Res. 143: 153–160.

Berdahl, A., Torney, C.J., Ioannou, C.C., Faria, J.J. and Couzin, I.D. 2013. Emergent sensing of complex environments by mobile animal groups. Science 339: 574–576.

Berdahl, A., Westley, P.A.H., Levin, S.A, Couzin, I.D. and Quinn, T.P. 2016. A collective navigation hypothesis for homeward migration in anadromous salmonids. Fish Fish. 17: 525–542.

Berdahl, A.M., Kao, A.B., Flack, A., Westley, P.A.H., Codling, E.A., Couzin, I.D., Dell, A.I. and Biro, D. 2018. Collective animal navigation and migratory culture: from theoretical models to empirical evidence. Philos. T. Roy. Soc. B 373: 20170009.

Biro, D., Sasaki, T. and Portugal, S. 2016. Bringing a time–depth perspective to collective animal behaviour. Trends Ecol. Evol. 31: 550–562.

Blaxter, H.S. 1985. The herring: a successful species? Can. J. Fish. Aquat. Sci. 42: 21–30.

Brännäs, E. 2014. Time-place learning and leader-follower relationships in Arctic charr *Salvelinus alpinus*. J. Fish Biol. 84: 133–144.

Broms, C., Melle, W. and Horne, J.K. 2012. Navigation mechanisms of herring during feeding migration: the role of ecological gradients on an oceanic scale. Mar. Biol. Res. 8: 37–41.

Brower, L.P. and Malcolm, S.B. 1991. Animal migrations: endangered phenomena. Am. Zool. 31: 265–276.

Brown, C. 2001. Familiarity with the test environment improves escape responses in the crimson spotted rainbowfish, *Melanotaenia duboulayi*. Anim. Cogn. 4: 109–113.

Brown, C. 2015. Fish intelligence, sentience and ethics. Anim. Cogn. 18: 1–17.

Burke, N. Brophy, D. and King, P.A. 2008. Shape analysis of otolith annuli in Atlantic herring (*Clupea harengus*); a new method for tracking fish populations. Fish. Res. 91: 133–143.

Campana, S. and Neilsen, J. 1985. Microstructure of fish otoliths. Can. J. Fish. Aquat. Sci. 42: 1014–1032.

Carpentier, A., Martin, C.S. and Vaz, S., 2009. Channel Habitat Atlas for marine Resource Management (CHARM phase II), INTERREG 3a Programme. Ifremer, Boulogne-sur-mer, France.

Champion, C., Hobday, A.J., Tracey, S.R. and Pecl, G.T. 2018. Rapid shifts in distribution and high-latitude persistence of oceanographic habitat revealed using citizen science data from a climate change hotspot. Global Change Biol. 24: 5440–5453.

Chidester, F. 1924. A critical examination of the evidence for physical and chemical influences on fish migration. J. Exp. Biol. 2: 79–118.

Ciannelli, L., Bartolino, V. and Chan, K. 2012. Non-additive and non-stationary properties in the spatial distribution of a large marine fish population. P. Roy. Soc. B-Biol. Sci. 279: 3635-3642.

Ciannelli, L., Fisher, J.A.D., Skern-Mauritzen, M., Hunsicker, M.E., Hidalgo, M., Frank, K.T. and Bailey, K.M. 2013. Theory, consequences and evidence of eroding population spatial structure in harvested marine fishes: a review. Mar. Ecol. Prog. Ser. 480: 227–243.

Conradt, L. and Roper, T.J. 2005. Consensus decision making in animals. Trends Ecol. Evol. 20: 449–456.

Corten, A. 1993. Learning processes in herring migrations. ICES CM 1993/H:18, Copenhagen, Denmark.

Corten, A. 2000. A possible adaptation of herring feeding migrations to a change in timing of the *Calanus finmarchicus* season in the eastern North Sea. ICES J. Mar. Sci. 57: 1261–1270.

Corten, A. 2002. The role of "conservatism" in herring migrations. Rev. Fish Biol. Fisher. 11: 339–361.

Cosandey-Godin, A., Krainski, E.T., Worm, B. and Flemming, J.M. 2015. Applying Bayesian spatiotemporal models to fisheries bycatch in the Canadian Arctic. Can. J. Fish. Aquat. Sci. 72: 186–197.

Cote, J., Clobert, J., Brodin, T., Fogarty, S. and Sih, A. 2010. Personality-dependent dispersal: characterization, ontogeny and consequences for spatially structured populations. Philos. T. Roy. Soc. B 365: 4065–4076.

Couzin, I.D. 2009. Collective cognition in animal groups. Trends Cogn. Sci. 13: 36–43.

Cowen, R.K., Gawarkiewicz, G., Pineda, J., Thorrold, S.R. and Werner, F.E. 2007. Population connectivity in marine systems: an overview. Oceanography 20: 14–21.

Dall, S.R.X., Houston, A.I. and McNamara, J.M. 2004. The behavioural ecology of personality: consistent individual differences from an adaptive perspective. Ecol. Lett. 7: 734–739.

Darnaude, A.M. and Hunter, E. 2018. Validation of otolith $\delta^{18}O$ values as effective natural tags for shelf-scale geolocation of migrating fish. Mar. Ecol. Prog. Ser. 598: 167–185.

Dawbin W.H. 1966. The seasonal migratory cycle of humpback whales. *In* Whales, dolphins and porpoises. *Edited by* K.S. Norris. University of California Press, Berkeley, California, USA. pp. 145–170.

Dawkins, M. 2001. Who needs consciousness? Anim. Welfare 1: 19–29.

Desbrosses, P. 1933. Contribution a la connaissance de la biologie du rouget-barbet en Atlantique nord (I). Revue des Travaux de l'Office des Pêches Maritimes VI: 249–270.

Desbrosses, P. 1935. Contribution a la connaissance de la biologie du rouget-barbet en Atlantique nord (II). *Mullus barbatus* (Rond) *surmuletus*. Mode septentrional Fage. Revue des Travaux de l'Office des Pêches Maritimes 8: 351–376.

Dickey-Collas, M., Nash, R.D.M., Brunel, T., van Damme, C.J.G., Marshall, C.T., Payne, M.R., Corten, A., Geffen, A.J., Peck, M.A., Hatfield, E.M.C., Hintzen, N.T., Enberg, K., Kell, L.T. and Simmonds, E.J. 2010. Lessons learned from stock collapse and recovery of North Sea herring: a review. ICES J. Mar. Sci. 67: 1875–1886.

Dingle, H. and Drake, V.A. 2007. What is migration? BioScience 57: 113–121.

Dragesund, O., Johannessen, A. and Ulltang, Ø. 1997. Variation in migration and abundance of Norwegian spring spawning herring (*Clupea harengus* L.). Sarsia 82: 97–105.

Dybas, C.L. 2014. Migrations without borders: going, going... gone? BioScience 64: 1067–1072.

Elderd, B.D. and Miller, T.E.X. 2016. Quantifying demographic uncertainty: Bayesian methods for integral projection models. Ecol. Monogr. 86: 125–144.

Engelhard, G.H., Pinnegar, J.K., Kell, L.T. and Rijnsdorp, A.D. 2011. Nine decades of North Sea sole and plaice distribution. ICES J. Mar. Sci. 68: 1090–1104.

Fage, L. 1909. Etude de la variation chez le Rouget (*Mullus barbatus* L., *M. surmuletus* L). Arch. Zool. Expér. Génér. 5: 1–55.

Fernö, A., Pitcher, T., Melle, W., Nottestad, L., Mackinson, S., Hollingworth, C. and Misund, O. 1998. The challenge of the herring in the Norwegian Sea: making optimal collective spatial decisions. Sarsia 83: 149–167.

Fiksen, Ø., Jørgensen, C., Kristiansen, T., Vikebø, F. and Huse, G. 2007. Linking behavioural ecology and oceanography: larval behaviour determines growth, mortality and dispersal. Mar. Ecol. Prog. Ser. 347: 195–205.

Fisher, J. and Frank, K. 2004. Abundance-distribution relationships and conservation of exploited marine fishes. Mar. Ecol. Prog. Ser. 279: 201–213.

Flack, A., Fiedler, W., Blas, J., Pokrovsky, I., Kaatz, M., Mitropolsky, M., Aghababyan, K., Fakriadis, I., Makrigianni, E., Jerzak, L., Azafzaf, H., Feltrup-Azafzaf, C., Rotics, S., Mokotjomela, T.M., Nathan, R. and Wikelski, M. 2016. Costs of migratory decisions: a comparison across eight white stork populations. Sci. Adv. 2: 1–8.

Fogarty, M.J. and Botsford, L.W. 2007. Population connectivity and spatial management of marine fisheries. Oceanography 20: 112–123.
Freshwater, C., Trudel, M., Beacham, T.D., Gauthier, S., Johnson, S.C., Neville, C.-E. and Juanes, F. 2019. Individual variation, population-specific behaviours, and stochastic processes shape marine migration phenologies. J. Anim. Ecol. 88: 67–78.
Fridriksson, Á. and Aasen, O. 1950. The Norwegian - Icelandic herring tagging experiments, Report No. 1. Fisk Skr HavUnders 9: 1–43.
Geffen, A. 2009. Advances in herring biology: from simple to complex, coping with plasticity and adaptability. ICES J. Mar. Sci. 66: 1688–1695.
Gelfand, A.E., Silander Jr, J.A., Wu, S., Latimer, A., Lewis, P.O., Rebelo, A.G. and Holder, M. 2006. Explaining species distribution patterns through hierarchical modeling. Bayesian Anal. 1: 41–92.
Gelman, A. and Hill, J. 2007. Data analysis using regression and multilevel/hierarchical models. Cambridge University Press, New York, USA.
Glover, R. S. 1955. Science and the herring fishery. Advancement of Science 11:426-436.
Grabowski, T.B., Boswell, K.M., McAdam, B.J., Wells, R.J.D. and Marteinsdóttir, G. 2012. Characterization of Atlantic cod spawning habitat and behavior in Icelandic coastal waters. PLoS One 7(12): e51321.
Grewe, P.M., Feutry, P., Hill, P.L., Gunasekera, R.M., Schaefer, K.M., Itano, D.G., Fuller, D.W., Foster, S.D. and Davies, C.R. 2015. Evidence of discrete yellowfin tuna (*Thunnus albacares*) populations demands rethink of management for this globally important resource. Sci. Rep. 5: 16916.
Halfyard, E.A., Webber, D., Del Papa, J., Leadley, T., Kessel, S.T., Colborne, S.F. and Fisk, A.T. 2017. Evaluation of an acoustic telemetry transmitter designed to identify predation events. Methods Ecol. Evol. 8: 1063–1071.
Harris, G., Thirgood, S., Hopcraft, J.G.C., Cromsigt, J.P.G.M., and Berger, J. 2009. Global decline in aggregated migrations of large terrestrial mammals. Endanger. Species Res. 7: 55–76.
Hasler, A.D. and Scholz, A.T. 1983. Olfactory imprinting and homing in salmon. Springer-Verlag, Berlin, Germany.
Heessen, H.J.L. 1996. Time-series data for a selection of forty fish species caught during the International Bottom Trawl Survey. ICES J. Mar. Sci. 53: 1079–1084.
Held, L., Schrödle, B. and Rue, H. 2010. Posterior and cross-validatory predictive checks: a comparison of MCMC and INLA. *In* Statistical Modelling and Regression Structures. *Edited by* T. Kneib and G. Tutz. Springer Verlag, Berlin, Germany. pp. 91–110.
Helfman, G.S. and Schultz, E.T. 1984. Social transmission of behavioural traditions in a coral reef fish. Anim. Behav. 32: 379–384.
Höglund, H. 1955. Swedish herring tagging experiments, 1949–1953. – Rapports et procès-verbaux des réunions/Conseil permanent international pour l'exploration de la mer 40: 19–29.
Holst, J.C., Salvanes, AG.V. and Johansen, T. 1997. Feeding, *Ichthyophonus* sp. infection, distribution and growth history of Norwegian spring-spawning herring in summer. J. Fish Biol. 50: 652–664.
Holt, R.E. and Jørgensen, C. 2014. Climate warming causes life-history evolution in a model for Atlantic cod (*Gadus morhua*). Conserv. Physiol. 2: cou050.
Hotta, T., Takeyama, T., Heg, D., Awata, S., Jordan, L.A. and Kohda, M. 2015. The use of multiple sources of social information in contest behavior: testing the social cognitive abilities of a cichlid fish. Front. Ecol. Evol. 3: 85.

Huey, J.A., Crook, D.A., Macdonald, J.I., Schmidt, D.J., Marshall, J.C., Balcombe, S.R., Woods, R.J. and Hughes, J.M. 2014. Is variable connectivity among populations of a continental gobiid fish driven by local adaptation or passive dispersal? Freshwater Biol. 59: 1672–1686.

Huse, G. 2016. A spatial approach to understanding herring population dynamics. Can. J. Fish. Aquat. Sci. 73: 177–188.

Huse, G., Fernö, A. and Holst, J. 2010. Establishment of new wintering areas in herring co-occurs with peaks in the 'first time/repeat spawner' ratio. Mar. Ecol. Prog. Ser. 409: 189–198.

Huse, G., Railsback, S. and Fernö, A. 2002. Modelling changes in migration pattern of herring: collective behaviour and numerical domination. J. Fish Biol. 60: 571–582.

Huse, I. and Ona, E. 1996. Tilt angle distribution and swimming speed of overwintering Norwegian spring spawning herring. ICES J. Mar. Sci. 53: 863–873.

Hutchinson, G.E. 1957. Concluding remarks. Cold Spring Harbor Symposium on Quantitative Biology 22: 415–427.

ICES. 2012. Report of the Working Group on Assessment of New MoU Species (WGNEW). 5 - 9 March 2012, ICES CM 2012/ACOM:20, Copenhagen, Denmark.

ICES. 2015. Report of the Benchmark Workshop on North Sea Stocks (WKNSEA). 2 - 4 February 2015, ICES CM 2015/ACOM:32, Copenhagen, Denmark.

ICES. 2017a. Report of the Working Group on Assessment of Demersal Stocks in the North Sea and Skagerrak. 26 April - 5 May 2017, ICES CM 2017/ACOM:21, Copenhagen, Denmark.

ICES. 2017b. Report of the North-Western Working Group (NWWG). 27 April - 4 May 2017, ICES CM 2017/ACOM:08, Copenhagen, Denmark.

ICES. 2018. Report of the North-Western Working Group (NWWG). 26 April - 3 May 2018, ICES CM 2018/ACOM:09, Copenhagen, Denmark.

IPCC. 2013. Climate Change 2013: The Physical Science Basis. Contribution of Working Group I to the Fifth Assessment Report of the Intergovernmental Panel on Climate Change. *Edited by* T.F. Stocker, D. Qin, G.-K. Plattner, M. Tignor, S.K. Allen, J. Boschung, A. Nauels, Y. Xia, V. Bex and P.M. Midgley. Cambridge University Press, Cambridge, United Kingdom and New York, New York, USA.

Iles, T.D. and Sinclair, M. 1982. Atlantic herring: stock discreteness and abundance. Science 215: 627–633.

Jakobsson, J. 1969. Síld og sjávarhiti. *In* Hafásinn. *Edited by* M.Á. Einarsson. Reykjavík, Iceland. pp. 497–511.

Jakobsson, J. and Østvedt, O.J. 1999. A review of joint investigations on the distribution of herring in the Norwegian and Iceland Seas 1950-1970. Rit Fiskideildar 16: 209–238.

Jakobsson, J. and Stefánsson, G. 1998. Rational harvesting of the cod–capelin–shrimp complex in the Icelandic marine ecosystem. Fish. Res. 37: 7–21.

Jakobsson, J. and Stefánsson, G. 1999. Management of summer-spawning herring off Iceland. ICES J. Mar. Sci. 56: 827–833.

Jansen, T., Post, S., Kristiansen, T., Óskarsson, G.J., Boje, J., MacKenzie, B.R., Broberg, M. and Siegstad, H. 2016. Ocean warming expands habitat of a rich natural resource and benefits a national economy. Ecol. Appl. 26: 2021–2032.

Jennings, S. and Kaiser, M.J. 1998. The effects of fishing on marine ecosystems. Adv. Mar. Biol. 213: 127–142.

Jones, C.M., Palmer, M. and Schaffler, J.J. 2017. Beyond Zar: The use and abuse of classification statistics for otolith chemistry. J. Fish Biol. 90: 492–504.

Jonsson, B. and Jonsson, N. 2011. Ecology of Atlantic Salmon and Brown Trout: Habitat as a Template for Life Histories. Springer, Dordrecht, Netherlands.
Jørgensen, C., Opdal, A. and Fiksen, Ø. 2014. Can behavioural ecology unite hypotheses for fish recruitment? ICES J. Mar. Sci. 71: 909–917.
Kao, A.B., Miller, N., Torney, C., Hartnett, A. and Couzin, I.D. 2014. Collective learning and optimal consensus decisions in social animal groups. PLoS Comput. Biol. 10: e1003762.
Kawecki, T.J. and Ebert, D. 2004. Conceptual issues in local adaptation. Ecol. Lett. 7: 1225–1241.
Krainski, E.T. Lindgren, F. Simpson, D. and Rue, H. 2016. The R-INLA tutorial on SPDE models. Norwegian Univ. of Science and Technology, Trondheim, Norway.
Kvamme, C., Nøttestad, L., Fernö, A, Misund, O., Dommasnes, A, Axelsen, B., Dalpadado, P. and Melle, W. 2003. Migration patterns in Norwegian spring-spawning herring: why young fish swim away from the wintering area in late summer. Mar. Ecol. Prog. Ser. 247: 197–210.
Langård, L., Fatnes, O., Johannessen, A., Skaret, G., Axelsen, B., Nøttestad, L., Slotte, A., Jensen, K. and Fernö, A. 2014. State-dependent spatial and intra-school dynamics in pre-spawning herring *Clupea harengus* in a semi-enclosed ecosystem. Mar. Ecol. Prog. Ser. 501: 251–263.
Leis, J.M., Van Herwerden, L. and Patterson, H.M. 2011. Estimating connectivity in marine fish populations: what works best ? Oceanogr. Mar. Biol. 49: 193–234.
Leitão, A.V., Hall, M.L., Venables, B. and Mulder, R.A. 2019. Ecology and breeding biology of a tropical bird, the Lovely Fairy-Wren (*Malurus amabilis*). Emu 119: 1–13.
Levin, S. 1992. The problem of pattern and scale in ecology. Ecology 73: 1943–1967.
Levins, R. 1966. The strategy of model building in population biology. Am. Sci. 54: 421–431.
Libungan, L.A. 2015. Identification of herring populations. PhD dissertation, Faculty of Life and Environmental Sciences, University of Iceland.
Libungan, L.A, Óskarsson, G.J, Slotte, A., Jacobsen, J.A. and Pálsson, S. 2015. Otolith shape: a population marker for Atlantic herring *Clupea harengus*. J. Fish Biol. 86: 1377–1395.
Libungan, L.A. and Pálsson, S. 2015. ShapeR: An R package to study otolith shape variation among fish populations. PloS One 10: e0121102.
Lindegren, M., Östman, Ö. and Gárdmark, A. 2011. Interacting trophic forcing and the population dynamics of herring. Ecology 92: 1407–1413.
Lindgren, F. and Rue, H. 2013. Bayesian spatial modelling with R-INLA. J. Stat. Softw. 63: 1–25.
Lindgren, F., Rue, H. and Lindström, J. 2011. An explicit link between Gaussian fields and Gaussian Markov random fields: the stochastic partial differential equation approach. J. R. Stat. Soc. B 73: 423–498.
Loff, J.F. and Neubauer, P. 2018. unmixR: analysis of population structure in R using finite and infinite Bayesian mixture models. R package version 0.4.1. (available from https://github.com/zeloff/unmixR)
Lohmann, K.J., Putman, N.F. and Lohmann, C.M.F. 2008. Geomagnetic imprinting: a unifying hypothesis of long-distance natal homing in salmon and sea turtles. P. Natl. Acad. Sci. U.S.A 105: 19096–19101.
Loots, C., Vaz, S., Planque, B. and Koubbi, P. 2010. What controls the spatial distribution of the North Sea plaice spawning population? Confronting ecological hypotheses through a model selection framework. ICES J. Mar. Sci. 67: 244–257.

Løvschal, M., Bøcher, P.K., Pilgaard, J., Amoke, I., Odingo, A., Thuo, A. and Svenning, J.-C. 2017. Fencing bodes a rapid collapse of the unique Greater Mara ecosystem. Sci. Rep. 7: 41450.

MacCall, A.D., Francis, T.B., Punt, A.E., Siple, M.C., Armitage, D.R., Cleary, J.S., Dressel, S.C., Jones, R.R., Kitka, H., Lee, L.C., Levin, P.S., McIsaac, J., Okamoto, D.K., Poe, M., Reifenstuhl, S., Schmidt, J.O., Shelton, A.O., Silver, J.J., Thornton, T.F., Voss, R. and Woodruff, J.A. 2019. A heuristic model of socially learned migration behaviour exhibits distinctive spatial and reproductive dynamics. ICES J Mar. Sci. 76: 598–608.

Macdonald, J.I. and Crook, D.A. 2010. Variability in Sr:Ca and Ba:Ca ratios in water and fish otoliths across an estuarine salinity gradient. Mar. Ecol. Prog. Ser. 413: 147–161.

Mahé, K., Coppin, F., Vaz, S. and Carpentier, A. 2013. Striped red mullet (*Mullus surmuletus*, Linnaeus, 1758) in the eastern English Channel and southern North Sea: growth and reproductive biology. J. Appl. Ichthyol. 29: 1067–1072.

Mahé, K., Villanueva, M.C., Vaz, S., Coppin, F., Koubbi, P. and Carpentier, A. 2014. Morphological variability of the shape of striped red mullet *Mullus surmuletus* in relation to stock discrimination between the Bay of Biscay and the eastern English Channel. J. Fish Biol. 84: 1063–1073.

Maravelias, C.D. and Haralabous, J. 1995. Spatial distribution of herring in the Orkney/Shetland area (northern North Sea): a geostatistical analysis. Neth. J. Sea Res. 34: 319–329.

Maravelias, C.D. and Reid, D.G. 1995. Relationship between herring (*Clupea harengus*, L.) distribution and sea surface salinity and temperature in the northern North Sea. Sci. Mar. 59: 427–438.

Maravelias, C.D. and Reid, D.G. 1997. Identifying the effects of oceanographic features and zooplankton on prespawning herring abundance using generalized additive models. Mar. Ecol. Prog. Ser. 147: 1–9.

Maravelias, C.D., Reid, D.G. and Swartzman, G. 2000a. Seabed substrate, water depth and zooplankton as determinants of the prespawning spatial aggregation of North Atlantic herring. Mar. Ecol. Prog. Ser. 195: 249–259.

Maravelias, C.D., Reid, D.G. and Swartzman, G. 2000b. Modelling spatio-temporal effects of environment on Atlantic herring, *Clupea harengus*. Environ. Biol. Fish. 58: 157–172.

Marchal, P. 2008. A comparative analysis of métiers and catch profiles for some French demersal and pelagic fleets. ICES J. Mar. Sci. 65: 674–686.

McQuinn, I. 1997. Metapopulations and the Atlantic herring. Rev. Fish Biol. Fisher. 7: 297–329.

Mercier, L., Darnaude, A.M., Bruguier, O., Vasconcelos, R.P., Cabral, H.N., Costa, M.J., Lara, M., Jones, D.L. and Mouillot, D. 2011. Selecting statistical models and variable combinations for optimal classification using otolith microchemistry. Ecol. Appl. 21: 1352–1364.

Misund, O., Vilhjálmsson, H., Jákupsstovu, S., Rottingen, I., Belikov, S., Asthorsson, O., Blindheim, J., Jónsson, J., Krysov, A., Malmberg, S. and Sveinbjornsson, S. 1998. Distribution, migration and abundance of Norwegian spring spawning herring in relation to the temperature and zooplankton biomass in the Norwegian Sea as recorded by coordinated surveys in spring and summer 1996. Sarsia 83: 117–127.

Moore, B.R., Bell, J., Evans, K., Hampton, J., Grewe, P., Marie, A.D., Minte-Vera, C., Nicol, S., Scutt Phillips, J., Pilling, G.M., Tremblay-Boyer, L., Williams, A.J. and Smith, N. 2018. Current knowledge, key uncertainties and future research directions

for defining the stock structure of skipjack, yellowfin, bigeye and South Pacific albacore tunas in the Pacific Ocean. Final Report for SAN 6004150 (CI-3). The Pacific Community, Nouméa, New Caledonia.
Nanninga, G.B. and Berumen, M.L. 2014. The role of individual variation in marine larval dispersal. Front. Mar. Sci. 1: 7.
N'Da, K. and Déniel, C. 1993. Sexual cycle and seasonal changes in the ovary of the red mullet, *Mullus surmuletus*, from the southern coast of Brittany. J. Fish Biol. 43: 229–244.
Neubauer, P., Shima, J.S. and Swearer, S.E. 2010. Scale-dependent variability in *Forsterygion lapillum* hatchling otolith chemistry: implications and solutions for studies of population connectivity. Mar. Ecol. Prog. Ser. 415: 263–274.
Neubauer, P., Shima, J.S. and Swearer, S.E. 2013. Inferring dispersal and migrations from incomplete geochemical baselines: analysis of population structure using Bayesian infinite mixture models. Methods Ecol. Evol. 4: 836–845.
Niklitschek, E.J. and Darnaude, A.M. 2016. Performance of maximum likelihood mixture models to estimate nursery habitat contributions to fish stocks: a case study on sea bream *Sparus aurata*. PeerJ 4: e2415.
Nøttestad, L., Aksland, M., Beltestad, A., Ferno, A., Johannessen, A. and Misund, O. 1996. Schooling dynamics of Norwegian spring spawning herring (*Clupea harengus* L.) in a coastal spawning area. Sarsia 80: 277–284.
Nøttestad, L., Giske, J., Holst, J.C. and Huse, G. 1999. A length-based hypothesis for feeding migrations in pelagic fish. Can. J. Fish. Aquat. Sci. 56: 26–34.
Nøttestad, L., Misund, O.A., Melle, W., Hoddevik Ulvestad, B.K. and Orvik, K.A. 2007. Herring at the Arctic front: influence of temperature and prey on their spatio-temporal distribution and migration. Mar. Ecol. 28: 123–133.
Olsen, E.M., Melle, W., Kaartvedt, S., Holst, J.C. and Mork, K.A. 2007. Spatially structured interactions between a migratory pelagic predator, the Norwegian spring-spawning herring *Clupea harengus* L., and its zooplankton prey. J. Fish Biol. 70: 799–815.
Ono, K., Shelton, A.O., Ward, E.J., Thorson, J.T., Feist, B.E. and Hilborn, R. 2016. Space-time investigation of the effects of fishing on fish populations. Ecol. Appl. 26: 392–406.
Óskarsson, G.J, Guðmundsdóttir, A. and Sigurðsson, Þ. 2009. Variation in spatial distribution and migration of Icelandic summer-spawning herring. ICES J. Mar. Sci. 66: 1762–1767.
Óskarsson, G.J., Ólafsdóttir, S.R., Sigurðsson, Þ. and Valdimarsson, H. 2018a. Observation and quantification of two incidents of mass fish kill of Icelandic summer spawning herring (*Clupea harengus*) in the winter 2012/2013. Fish. Oceanogr. 27: 302–311.
Óskarsson, G.J., Pálsson, J. and Guðmundsdóttir, A. 2018b. An ichthyophoniasis epizootic in Atlantic herring in marine waters around Iceland. Can. J. Fish. Aquat. Sci. 75: 1106–1116.
Pampoulie, C., Slotte, A, Óskarsson, G.J, Helyar, S.J, Jónsson, Á., Ólafsdóttir, G., Skírnisdóttir, S., Libungan, L.A, Jacobsen, J.A, Joensen, H., Nielsen, H.H., Sigurðsson, S.K. and Daníelsdóttir, A.K. 2015. Stock structure of Atlantic herring *Clupea harengus* in the Norwegian Sea and adjacent waters. Mar. Ecol. Prog. Ser. 522: 219–230.
Perry, A., Low, P., Ellis, J. and Reynolds, J. 2005. Climate change and distribution shifts in marine fishes. Science 308: 1912–1915.
Petitgas, P., Reid, D., Planque, B., Nogueira, E., O'Hea, B. and Cotano, U. 2006. The entrainment hypothesis: an explanation for the persistence and innovation in spawning

migrations and life cycle spatial patterns. ICES Document CM 2006/B:07, Copenhagen, Denmark.
Petitgas, P., Rijnsdorp, A.D., Dickey-Collas, M., Engelhard, G.H., Peck, M.A., Pinnegar, J.K., Drinkwater, K., Huret, M. and Nash, R.D.M. 2013. Impacts of climate change on the complex life cycles of fish. Fish. Oceanogr. 22: 121–139.
Planque, B., Bellier, E. and Loots, C. 2011. Uncertainties in projecting spatial distributions of marine populations. ICES J. Mar. Sci. 68: 1045–1050.
Pörtner, H. and Peck, M. 2010. Climate change effects on fishes and fisheries: towards a cause-and-effect understanding. J. Fish Biol. 77: 1745–1779.
Putman, N.F., Lohmann, K.J., Putman, E.M., Quinn, T.P., Klimley, A.P. and Noakes, D.L.G. 2013. Evidence for geomagnetic imprinting as a homing mechanism in Pacific salmon. Curr. Biol. 23: 312–316.
Reebs, S. 2000. Can a minority of informed leaders determine the foraging movements of a fish shoal? Animal Behav. 59: 403–409.
Reis-Santos, P., Tanner, S.E., Aboim, M.A., Vasconcelos, R.P., Laroche, J., Charrier, G., Pérez, M., Presa, P., Gillanders, B.M. and Cabral, H.N. 2018. Reconciling differences in natural tags to infer demographic and genetic connectivity in marine fish populations. Sci. Rep. 8: 10343.
Reñones, O., Massutí, E. and Morales-Nin, B. 1995. Life history of the red mullet *Mullus surmuletus* from the bottom-trawl fishery off the Island of Majorca (north-west Mediterranean). Mar. Biol. 123: 411–419.
Resplandy, L., Keeling, R.F., Eddebbar, Y., Brooks, M.K., Wang, R., Bopp, L., Long, M.C., Dunne, J.P., Koeve, W. and Oschlies, A. 2018. Quantification of ocean heat uptake from changes in atmospheric O_2 and CO_2 composition. Nature 563: 105–108.
Rue, H. and Held, L. 2005. Gaussian Markov Random Fields: Theory and Applications. Monographs on Statistics and Applied Probability 104. Chapman & Hall/CRC, Boca Raton, FL, USA.
Righton, D. and Walker, A.M. 2013. Anguillids: conserving a global fishery. J. Fish Biol. 83: 754–765.
Rizzo, L.Y. and Schulte, D. 2009. A review of humpback whales' migration patterns worldwide and their consequences to gene flow. J. Mar. Biol. Assoc. U.K. 89: 995–1002.
Rose, J.D., Arlinghaus, R., Cooke, S.J., Diggles, B.K., Sawynok, W., Stevens, E.D. and Wynne, C.D.L. 2014. Can fish really feel pain? Fish Fish. 15: 97–133.
Royle, J.A., Kéry, M., Gautier, R. and Schmid, H. 2007. Hierarchical spatial models of abundance and occurrence from imperfect survey data. Ecol. Monogr. 77: 465–481.
Rue, H. and Martino, S. 2007. Approximate Bayesian inference for hierarchical Gaussian Markov random field models. J. Stat. Plan. Infer. 137: 3177–3192.
Rue, H., Martino, S. and Chopin, N. 2009. Approximate Bayesian inference for latent Gaussian models by using integrated nested Laplace approximations. J. R. Stat. Soc. B 71: 319–392.
Sanderson, F.J., Donald, P.F., Pain, D.J., Burfield, I.J. and van Bommel, F.P.J. 2006. Long-term population declines in Afro-Palearctic migrant birds. Biol. Conserv. 131: 93–105.
Schmidt, J. 1907. Marking experiments on plaice and cod in Icelandic waters. Meddr Komm. Hav. Ser. Fisk. 2: No. 6.
Scutt Phillips, J., Sen Gupta, A., Senina, I., van Sebille, E., Lange, M., Lehodey, P., Hampton, J. and Nicol, S. 2018. An individual-based model of skipjack tuna (*Katsuwonus pelamis*) movement in the tropical Pacific ocean. Prog. Oceanogr. 164: 63–74.

Shima, J.S. and Swearer, S.E. 2010. The legacy of dispersal: larval experience shapes persistence later in the life of a reef fish. J. Anim. Ecol. 79: 1308–1314.
Shima, J.S. and Swearer, S.E. 2016. Evidence and population consequences of shared larval dispersal histories in a marine fish. Ecology 97: 25–31.
Sigurðsson, B. Sigurðsson, B., Jóhannesson, G., Gíslason, H., Ragnarsson, H., Jakobsson, J., Þór, J.Þ. and Lúðvíksson, S.J. 2007. Silfur hafsins, gull Íslands. Síldarsaga íslendinga, III Bindi. Nesútgáfan, Reykjavík, Iceland.
Silveira, M.M., Oliveira, J.J. and Luchiari, A.C. 2015. Dusky damselfish *Stegastes fuscus* relational learning: evidences from associative and spatial tasks. J. Fish Biol. 86: 1109–1120.
Smith, C.L. and Steel, B.S. 1997. Values in the valuing of salmon. *In* Pacific Salmon & their Ecosystems. *Edited by* D.J. Stouder, P.A. Bisson and R.J. Naiman. Springer, Boston, MA, USA.
Soberón, J. 2007. Grinnellian and Eltonian niches and geographic distributions of species. Ecol. Lett. 10: 1115–1123.
Spencer, P.D. 2008. Density-independent and density-dependent factors affecting temporal changes in spatial distributions of eastern Bering Sea flatfish. Fish. Oceanogr. 17: 396–410.
Sswat, M., Stiasny, M.H., Jutfelt, F., Riebesell, U. and Clemmesen, C. 2018. Growth performance and survival of larval Atlantic herring, under the combined effects of elevated temperatures and CO_2. PLoS One 13(1): e0191947.
Sumpter, D.J.T., Krause, J., James, R., Couzin, I.D. and Ward, A.J.W. 2008. Consensus decision making by fish. Curr. Biol. 18: 1773–1777.
Sumpter, D.J.T. and Pratt, S.C. 2009. Quorum responses and consensus decision making. Philos. T. Roy. Soc. B 364: 743–53.
Surowiecki, J. 2004. The wisdom of crowds. Anchor, USA.
Swain, D.P. 1999. Changes in the distribution of Atlantic cod (*Gadus morhua*) in the southern Gulf of St Lawrence - effects of environmental change or change in environmental preferences? Fish. Oceanogr. 8: 1–17.
Taillebois, L., Barton, D.P., Crook, D.A., Saunders, T., Taylor, J., Hearnden, M., Saunders, R.J., Newman, S.J., Travers, M.J., Welch, D.J., Greig, A., Dudgeon, C., Maher, S. and Ovenden, J.R. 2017. Strong population structure deduced from genetics, otolith chemistry and parasite abundances explains vulnerability to localized fishery collapse in a large Sciaenid fish, *Protonibea diacanthus*. Evol. Appl. 10: 978–993.
Talbot, L.M. and Talbot, M.H. 1963. The wildebeest in Western Masailand, East Africa. Wildl. Monogr. 12: 3–88.
Treml, E.A., Roberts, J.J., Chao, Y., Halpin, P.N., Possingham, H.P. and Riginos, C. 2012. Reproductive output and duration of the pelagic larval stage determine seascape-wide connectivity of marine populations. Integr. Comp. Biol. 52: 525–537.
Trenkel, V.M., Huse, G., MacKenzie, B.R., Alvarez, P., Arrizabalaga, H., Castonguay, M., Goñi, N., Grégoire, F., Hátún, H., Jansen, T., Jacobsen, J.A., Lehodey, P., Lutcavage, M., Mariani, P., Melvin, G.D., Neilson, J.D., Nøttestad, L., Óskarsson, G.J., Payne, M.R., Richardson, D.E., Senina, I. and Speirs, D.C. 2014. Comparative ecology of widely distributed pelagic fish species in the North Atlantic: implications for modelling climate and fisheries impacts. Prog. Oceanogr. 129: 219–243.
Tsukamoto, K., Aoyama, J. and Miller, M.J. 2002. Migration, speciation, and the evolution of diadromy in anguillid eels. Can. J. fish. Aquat. Sci. 59: 1989–1998.

Walton, A.G. and Moller, P. 2010. Maze learning and recall in a weakly electric fish, *Mormyrus rume proboscirostris boulenger* (Mormyridae, Teleostei). Ethology 116: 904–919.

Ward, A.J.W., Herbert-Read, J.E., Sumpter, D.J.T. and Krause, J. 2011. Fast and accurate decisions through collective vigilance in fish shoals. P. Natl. Acad. Sci. U.S.A 108: 2312–2315.

Ward, A.J.W., Sumpter, D.J.T., Couzin, I.D., Hart, P.J.B. and Krause, J. 2008. Quorum decision-making facilitates information transfer in fish shoals. P. Natl. Acad. Sci. U.S.A 105: 6948–6953.

Ward, E.J., Jannot, J.E., Lee, Y., Ono, K., Shelton, A.O. and Thorson, J.T. 2015. Using spatiotemporal species distribution models to identify temporally evolving hotspots of species co-occurrence. Ecol. Appl. 25: 2198–2209.

Westley, P.A.H., Berdahl, A.M., Torney, C.J. and Biro, D. 2018. Collective movement in ecology: from emerging technologies to conservation and management. Philos. T. Roy. Soc. B 373: 1746.

Wilcove, D.S. and Wikelski, M. 2008. Going, going, gone: is animal migration disappearing? PLoS Biol. 6: 1361–1364.

Worm, B., Hilborn, R., Baum, J.K., Branch, T.A., Collie, J.S., Costello, C., Fogarty, M.J., Fulton, E.A., Hutchings, J.A., Jennings, S., Jensen, O.P., Lotze, H.K., Mace, P.M., McClanahan, T.R., Minto, C., Palumbi, S.R., Parma, A.M., Ricard, D., Rosenberg, A.A., Watson, R. and Zeller, D. 2009. Rebuilding global fisheries. Science 325: 578–585.

Wright, P.J., Régnier, T., Gibb, F.M., Augley, J. and Devalla, S. 2018. Assessing the role of ontogenetic movement in maintaining population structure in fish using otolith microchemistry. Ecol. Evol. 8: 7907–792.

Paper I

Can collective memories shape fish distributions? A test, linking space-time occurrence models and population demographics

Jed I. Macdonald, Kai Logemann, Elias T. Krainski, Þorsteinn Sigurðsson, Colin M. Beale, Geir Huse, Solfrid S. Hjøllo, Guðrún Marteinsdóttir

(Published in *Ecography* 41: 938–957, 2018)

Author contributions – Conceived and designed the experiments: JIM, ÞS, GM; analysed the data: JIM; contributed code: KL, SSH, ETK, CMB; wrote the manuscript: JIM; reviewed and edited the manuscript: JIM, KL, ETK, ÞS, CMB, GH, SSH, GM.

ECOGRAPHY

Research

Can collective memories shape fish distributions? A test, linking space-time occurrence models and population demographics

Jed I. Macdonald, Kai Logemann, Elias T. Krainski, Þorsteinn Sigurðsson, Colin M. Beale, Geir Huse, Solfrid S. Hjøllo and Guðrún Marteinsdóttir

J. I. Macdonald (http://orcid.org/0000-0002-5769-2912) (jedimacdonald@gmail.com), K. Logemann and G. Marteinsdóttir, Faculty of Life and Environmental Sciences, Univ. of Iceland, Askja, Reykjavík, Iceland. JIM also at: School of BioSciences, The Univ. of Melbourne, Parkville, VIC, Australia. KL also at: Inst. of Coastal Research, Helmholtz Zentrum Geesthacht, Geesthacht, Germany. – E. T. Krainski, Dept of Mathematical Sciences, The Norwegian Univ. for Science and Technology, Trondheim, Norway, and Depto de Estatística, Univ. Federal do Paraná, Curitiba, Brazil. – Þ. Sigurðsson and JIM, Marine Research Inst., Reykjavík, Iceland. – C. M. Beale, Univ. of York, Dept of Biology, Heslington, York, UK. – G. Huse and S. S. Hjøllo, Inst. of Marine Research and Hjort Centre for Marine Ecosystem Dynamics, Nordnes, Bergen, Norway.

Ecography
41: 938–957, 2018
doi: 10.1111/ecog.03098

Subject Editor: Lise Comte
Editor-in-Chief: Miguel Araújo
Accepted 28 June 2017

Social learning can be fundamental to cohesive group living, and schooling fishes have proven ideal test subjects for recent work in this field. For many species, both demographic factors, and inter- (and intra-) generational information exchange are considered vital ingredients in how movement decisions are reached. Yet key information is often missing on the spatial outcomes of such decisions, and questions concerning how migratory traditions are influenced by collective memory, density-dependent and density-independent processes remain open. To explore these issues, we focused on Atlantic herring *Clupea harengus*, a long-lived, dense-schooling species of high commercial importance, noted for its unpredictable shifts in winter distribution, and developed a series of Bayesian space-time occurrence models to investigate wintering dynamics over 23 yr, using point-referenced fishery and survey records from Icelandic waters. We included covariates reflecting local-scale environmental factors, temporally-lagged prey biomass and recent fishing activity, and through an index capturing distributional persistence over time, derived two proxies for spatial memory of past wintering sites. The previous winter's occurrence pattern was a strong predictor of the present pattern, its influence increasing with adult population size. Although the mechanistic underpinnings of this result remain uncertain, we suggest that a 'wisdom of the crowd' dynamic may be at play, by which navigational accuracy towards traditional wintering sites improves in larger and/or denser, better synchronized schools. Wintering herring also preferred warmer, fresher, moderately stratified waters of lower velocity, close to hotspots of summer zooplankton biomass, our results indicative of heightened environmental sensitivity in younger cohorts. Incorporating spatiotemporal correlation structure and time-varying regression coefficients improved model performance, and validation tests on independent observations one-year ahead illustrate the potential of uniting demographic information and non-stationary models to quantify both the strength of collective memory in animal groups and its relevance for the spatial management of populations.

NORDIC SOCIETY OIKOS

www.ecography.org

Introduction

Although notions of the 'animal mind' remain equivocal (Dawkins 2001) there is now widespread acceptance that sociality, learning and memory can play important roles in determining migration patterns and space use in group-living animals (Kao et al. 2014, Merkle et al. 2014). In animal groups, decisions about when to migrate, where to feed, or how best to escape from predators are often made collectively, as a result of some consensus being reached among individuals' preferences (Conradt and Roper 2005). Such preferences are thought to arise through relatively simple interactions among close neighbours, with individuals trading-off aspects of their own experience and behavioural state with those of others (Berdahl et al. 2013).

Fishes have proved useful models on which to explore these ideas (Brown 2015 and references therein), and much empirical and theoretical research effort has been devoted to understanding the seemingly complex individual behaviours required to maintain school cohesion and coordinate large-scale migration (Parrish et al. 2002, Berdahl et al. 2016). Within fish schools, neighbouring individuals are usually not closely related, and hence self-interest may shape the nature of group-level movement decisions in which the majority opinion is often adopted (Couzin et al. 2011). In now rather famous experiments on groups of three-spined sticklebacks *Gasterosteus aculeatus*, Sumpter et al. (2008) showed that collective movement decisions can follow non-linear quorum rules, in which the probability of an individual fish choosing a certain route increases abruptly beyond a threshold number of neighbours that have recently chosen that same route. Through simulations, and in later experimental work (Ward et al. 2011), these authors also demonstrated that quorum responses increase decision accuracy, and that larger fish shoals, in general, make better, faster decisions; sensu 'the wisdom of crowds' (Surowiecki 2004). These patterns appear to emerge across a wide range of taxa and ecological functions (Sumpter and Pratt 2009, but see Kao and Couzin 2014), and for fish, can manifest in improved navigation and capacity to sense dynamic environmental gradients, among other benefits (Berdahl et al. 2013, 2016).

Quorum responses may also be initiated, and consensus achieved, through leadership by a minority of more 'experienced' individuals, or those with strongly held preferences (Reebs 2000, Huse et al. 2002). Often, only a knowledgeable few are needed to produce highly accurate movement decisions (Reebs 2000); however, a complete absence of such leaders may result in poor navigational accuracy or lack of directionality (Helfman and Schultz 1984). These observations, in conjunction with growing recognition of the cognitive abilities of group-living fishes (Hotta et al. 2015), give credence to theories purporting the existence of spatial learning and tradition formation in some species (see Brown 2015 for a review), in which information on previously-used migration routes is thought to be passed down from older, experienced fish to younger, naïve ones, communicated within cohorts and remembered (Corten 1993). Further support for such ideas derives from evidence for time-place learning in fishes (Brännäs 2014), and experimental demonstrations of highly accurate short- and long-term memory (Brown 2001, Hotta et al. 2015).

These phenomena may be particularly relevant for long-lived, schooling species like Atlantic herring *Clupea harengus* (hereafter 'herring') (Wynne-Edwards 1962). Herring are widely distributed across the North Atlantic Ocean and support several important commercial fisheries. The species is characterized by complex population dynamics (Iles and Sinclair 1982, Huse 2016) perhaps best described by a metapopulation model (McQuinn 1997), with individuals within local populations forming densely-packed, mixed-age schools for much of the year and undertaking large-scale migrations between spawning, feeding and overwintering areas for which strong fidelity is exhibited in most, but not all years (Fernö et al. 1998, Langård et al. 2014). Several hypotheses have been advanced to explain this fluctuating 'conservatism' in migratory strategies (Jakobsson 1969, Corten 2002), with a particular focus in recent times on the striking shifts in winter distribution observed occasionally (Óskarsson et al. 2009, Huse et al. 2010). Current thinking favours aspects of McQuinn's 'adopted migrant hypothesis' (McQuinn 1997) akin to Petitgas et al.'s 'entrainment hypothesis' (Petitgas et al. 2006). When tuned to wintering herring, these hypotheses contend that naïve, first-time winterers (i.e. age 3) learn about traditional wintering areas by schooling with older, experienced winterers (i.e. age 4 and older, hereafter age 4+), typically returning to these same areas subsequently (Höglund 1955). However, when the learning process is disrupted during a stock collapse, when age classes are segregated, or when strong recruitment leads to numerical domination by naïve fish, dramatic shifts in winter distribution may occur, suggesting a break in tradition when teachers are few (Corten 1999, 2002, Huse et al. 2002, 2010). Understanding why and when distribution shifts might occur is clearly interesting for ecologists, fishers and fisheries managers alike. However, spatially-resolved information on the outcomes of such shifts (i.e. resultant spatial distribution patterns) is currently lacking – a situation that hinders development of spatial management strategies that maximize economic and conservation benefits. Specifically, two longstanding questions remain: 1) can we predict where herring decide to spend the winter, and 2) does tradition and/or spatial memory drive these decisions, or are other factors at play?

We attempt to answer these questions here. First, we derive a spatial similarity index (SSI) to quantify the persistence or transience in spatial distribution between one year t, and the previous year $t - 1$, and demonstrate its utility in describing the recent wintering patterns of Icelandic summer spawning (ISS) herring. In our example, the SSI operates at the scale of the entire wintering population, and we consider it a proxy for the level of geographic attachment to, or spatial memory for, areas occupied previously. Next, using the variables created through the SSI (and others), we develop a series of space-time regression models for wintering ISS herring spanning a 23-yr time series of fishery and acoustic survey data.

We are particularly interested in the role of spatial memory in shaping distribution patterns, and present a Bayesian mixed-modelling framework based on stochastic partial differential equations (SPDE) (Lindgren et al. 2011) to disentangle its influence from factors representing the dynamic and static environment, prey availability during the pre-wintering feeding period, the magnitude of recent fishing effort and density-dependence.

Our specific hypotheses are as follows. 1) We predict that spatial memory for previous wintering areas would be a key driver of occurrence patterns in the present winter, and that its relative influence across the time series may have a demographic basis. That is, spatial memory would be strongest in years where more experienced individuals are present in the wintering population, or when overall adult population size is large. 2) As our study region is near a range edge for herring, we also expect that environmental gradients (e.g. temperature, salinity) would be influential. 3) Moreover, when population size is small, or naïve fish outnumber experienced adults, we hypothesize that environmental and/or other density-independent processes (e.g. prey availability, fishing pressure) may become unmasked, contributing more to shaping occurrence patterns. In addressing these hypotheses, we explore evidence for temporal non-stationarity in model parameters, and test if these dynamics can be harnessed to accurately predict winter occurrence patterns, both within the time series, and to held-out observations one-year ahead.

Material and methods

Fishery and acoustic survey data

We use two point-referenced datasets comprising $T = 23$ yr of fishery and acoustic survey records for our analysis. Logbook data from the autumn/winter purse seine fishery for ISS herring were collated over the period 1991–1992 to 2013–2014. The fishery is highly selective for adult herring (i.e. age 3+), with effort centred on the wintering grounds between October and January each year. We refer to this period as a fishing 'year'. At the outset of each fishing year, extensive searches for wintering schools are made by the fishing fleet of ~ 15 vessels, covering the full (known) distribution of the stock (see Supplementary material Appendix 1 for a discussion of sampling coverage). Our logbook dataset provides information on each fishing event, defined here as an individual purse seine net shot, including the date, location, and biomass of herring captured c (tonnes) per shot. Due to the dependence of c on factors such as fisher behaviour and vessel capabilities (Thorlindsson 1988), we simplified the biomass information to occurrence/non-occurrence records, and retained only confirmed occurrences (i.e. where $c > 0$ tonnes). Although several instances of zero catch were observed, we excluded these records as $c = 0$ is often a function of gear failure, and not the absence of herring per-se (authors' unpubl.).

We augmented the logbook data with fishery-independent acoustic survey records from annual cruises conducted by the Marine Research Inst. (MRI), Reykjavík, between 1991–1992 and 2013–2014. Surveys were targeted towards wintering herring and ran between October and January each year, spanning the full wintering phase and matching the timing of fishing activities. Survey tracks were not consistent across years; however, spatial coverage was typically broad (see Supplementary material Appendix 1 for details). Herring biomass estimates s (tonnes), as calculated from echosounder backscatter strength measurements, were aggregated at 2 km resolution, forming a single survey event, referenced by date and location.

Data on age-class structure per fishing/survey event were unavailable. Hence, our models focused on the entire adult component of the stock (i.e. age 3+) which form mixed-age schools on the wintering grounds. This also meant that we could not determine which age classes contributed to s, estimates of which were likely influenced by a substantial, and unknown proportion of juveniles (i.e. age 0 to 2) in some regions. For this reason, we extracted only zero biomass records from the survey data (i.e. $s = 0$) and consider these true absences. Detection for both fishery and survey datasets is essentially perfect, notwithstanding potential recording errors (Supplementary material Appendix 1). Our dataset, comprising n = 48 724 occurrence/absence records, is visualized in Fig. 1. Wintering patterns showed marked stability spatially across several consecutive years throughout the 23-yr time series, interspersed by occasional, dramatic distributional shifts (Fig. 1a–c). Occurrence records were characterized by strong spatial structuring within years (explored through correlograms), and dense clustering east, west and south of Iceland (Fig. 1d).

Capturing shifting distributions: a spatial similarity index (SSI)

To more formally quantify the spatial and temporal patterns of wintering we constructed the SSI, a metric that unlike those designed for standardized survey data (Woillez et al. 2007) is most useful when fishing/survey locations are inconsistent in space and time, and/or when abundance data are not available (or uncertain), as was the case here. Calculation is based around two georeferenced variables that map 1) the area of occurrence, denoted distrib_t, and 2) the density of occurrences, denoted counts_t, in a given year t, with comparisons made with maps of these variables generated for the previous year (i.e. distrib_{t-1}, counts_{t-1}). We refer readers to Fig. 2a–e and Supplementary material Appendix 2.1, 2.2 for calculation details, and Appendix 2.3 for R code).

Modelling winter occurrence patterns

Covariates for estimation and prediction

We took a hypothesis-driven approach to the inclusion of covariates that capture the strength of spatial memory for previous wintering areas (i.e. spatially-explicit representations of the SSI), features of the dynamic and static environment, the magnitude of recent fishing activity and prey availability during the previous summer (see Table 1 for

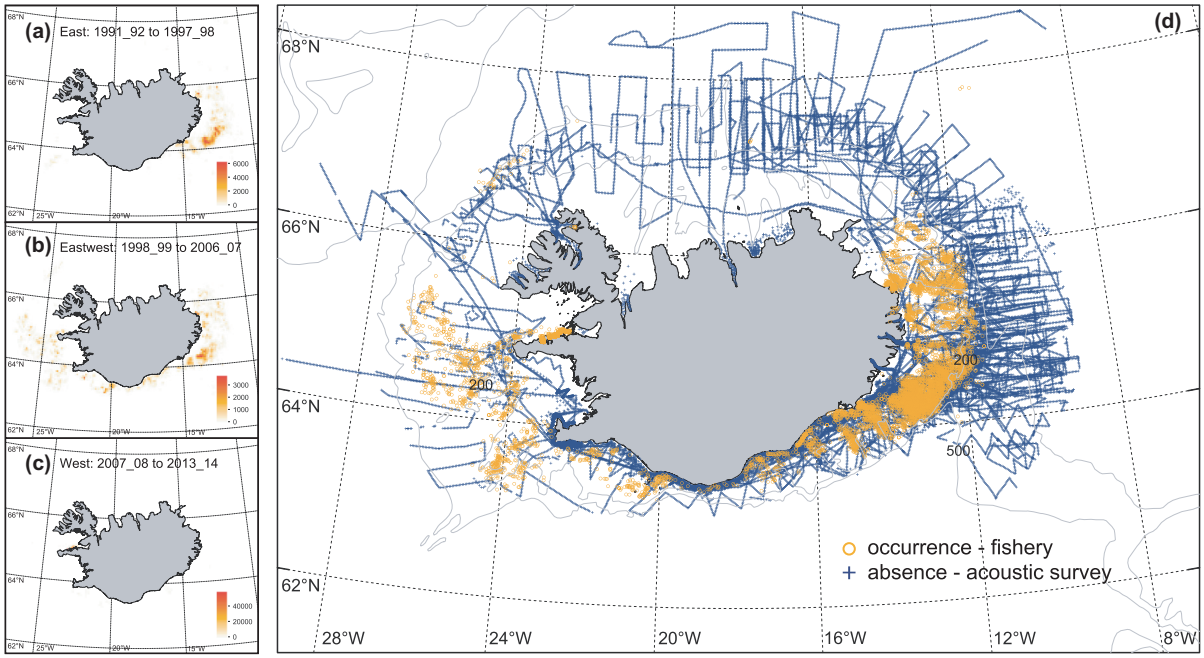

Figure 1. Winter distribution of ISS herring during the period 1991–1992 to 2013–2014. Panels (a–c) illustrate the spatial shifts in landings by the autumn/winter purse seine fishery through time. We identified three major wintering phases over the 23 yr of our time series, and aggregated the landings data (in tonnes per 0.1° longitude × 0.05° latitude grid cell) within each phase: (a) 'East' – 1991_92 to 1997_98; (b) 'Eastwest' – 1998_99 to 2006_07; and (c) 'West' – 2007_08 to 2013_14 (Óskarsson et al. 2009). Note the differences in color bar scales. (d) Twenty-three years of fishery occurrence and survey absence records. Grey lines denote 200 m and 500 m isobaths.

details, and Supplementary material Appendix 3 for derivation). Covariates were either constructed, computed from the CODE ocean model (Logemann et al. 2013) or extracted from other databases (GEBCO, <www.gebco.net>) at varying spatial and temporal scales (Table 1). Given the importance of scale in drawing conclusions about ecological systems (Levin 1992), we balanced ecological knowledge with model resolution in an attempt to select scales for each covariate that best match the processes acting on individual herring schools at the time of capture or survey (Mackinson et al. 1999, see also Table 1 and Supplementary material Appendix 3). Rasters of each covariate were created at the desired scales (see Supplementary material Appendix 3, Fig. A1–A5 for examples), and data for each occurrence or absence record extracted for use in model fitting. To facilitate interpretation of regression coefficients, all continuous inputs were centred and scaled to have mean = 0, SD = 0.5 prior to analysis, with binary inputs centred to have mean = 0 (Gelman 2008). To avoid issues related to collinearity (Dormann et al. 2013), we visualized covariate associations through scatterplots and calculated pairwise correlation coefficients (Pearson's r). If $|r| > 0.7$, we prioritized ecological reasoning in deciding which covariate to retain. Only bottom_depth and dist_to_shore were highly collinear ($r = -0.78$). As bathymetric features may act directly to structure herring school distribution (Maravelias et al. 2000a), we chose to remove dist_to_shore from all further analyses. Prior to model fitting, all covariates were screened graphically for potentially influential values, and data tabulated to test for any separation issues (Zorn 2005). The distributions of fish_magnitude and counts$_{t-1}$ were characterized by many zeros and some high values. Each of these values was checked and found to be measured accurately, and as no clear outliers were detected, all records were retained for modelling.

Model specification

As residual correlation patterns were of direct interest, we considered models that incorporate these patterns explicitly. Let $c_{e,i,t}$ be the total catch (tonnes), and $s_{e,i,t}$ the estimated biomass (tonnes) of an individual fishing/survey event respectively, e, at location i, in year t. We define a new variable, $y_{e,i,t}$ representing observed herring occurrence for each event, location and year (Eq. 1).

$$y_{e,i,t} = \begin{cases} 1, & \text{if } c_{e,i,t} > 0 \\ 0, & \text{if } s_{e,i,t} = 0 \end{cases} \quad (1)$$

As detection probability equals one, $y_{e,i,t}$ also represents the true occurrence state for each observation. Our interest was in estimating the probability of herring occurrenceψ, for event e, at location i, in year t, so we treated each event as an independent trial and modelled $\psi_{e,i,t}$ with a binomial generalized linear mixed model (GLMM) and logit link (Eq. 2, 3).

$$y_{e,i,t} \sim \text{Bernoulli}(\psi_{e,i,t}) \text{ for } e = 1, \ldots, n_i;\ i = 1, \ldots, n_t;\ t = 2, \ldots, T \quad (2)$$

$$\text{logit}(\psi_{e,i,t}) = \alpha + \text{spatial memory} + \text{dynamic environment} + \text{static environment} + \text{predators} + \text{prey} + \beta_{12}\text{year}_t + \omega_{i,t} \quad (3)$$

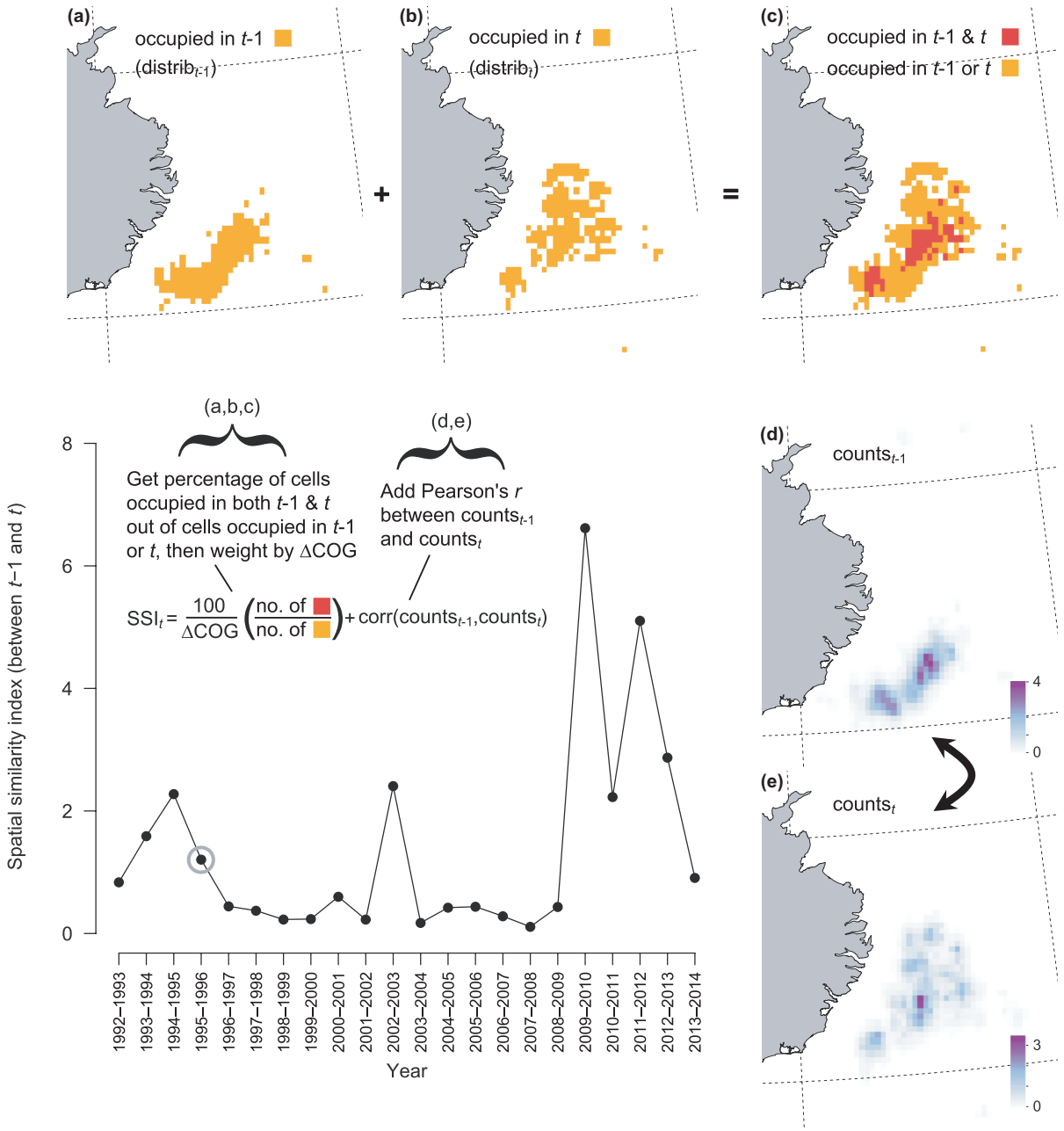

Figure 2. Calculation of the spatial similarity index (SSI). We defined an area of interest inclusive of all occurrence records in our dataset, divided this into 0.1° longitude × 0.05° latitude grid cells, and, for each year $t = 1, 2, \ldots, T$, coded each cell as 1 if herring were captured within it during year t, or 0 if they were not. This resulted in a distrib$_t$ layer for each year. For each $t = 2, 3, \ldots, T$, we then calculated the percentage of cells occupied in both $t-1$ and t, out of the number of cells occupied in $t-1$ or t (a–c). Next, we weighted this value by the change (km) in the center of gravity (ΔCOG) of the stock between $t-1$ and t. Using the counts$_t$ layers that were constructed based on Eq. A1 (see Supplementary material Appendix 2 for details), we then calculated Pearson's r between counts$_{t-1}$ and counts$_t$ and added this value (d, e). Data are presented for 1994–1995 ($t-1$) and 1995–1996 (t), with the SSI value for 1995–1996 circled.

$$\text{spatial memory} = \beta_1 \text{distrib}_{i,t-1} + \beta_2 \text{counts}_{i,t-1}; \quad \text{dynamic environment} = \beta_3 \text{SST}_{e,i,t} + \beta_4 \text{SSS}_{e,i,t} + \beta_5 \text{PEA}_{e,i,t} + \beta_6 \text{change}_{e,i,t} + \beta_7 \text{current\_vel}_{e,i,t}; \quad \text{static environment} = \beta_8 \text{bottom\_depth}_i + \beta_9 \text{slope}_i \quad \text{predators} = \beta_{10} \text{fish\_magnitude}_{e,i,t}; \quad \text{prey} = \beta_{11} \text{CF\_Aug}_{i,t}.$$

Equation 3 represents the full stationary model, where all regression coefficients are static in space and time, α is the intercept and the β's quantify the linear effects of covariates reflecting spatial memory, the dynamic and static environment, predators and prey on ψ (Table 1). For models with no spatiotemporal random field (i.e. 'no-space' and 'time-indep'

Table 1. Covariates considered in space-time regression models for wintering ISS herring (see Supplementary material Appendix 3 for details on their calculation, hypotheses behind their selection, the spatial and temporal scales considered, and examples of raster layers for each covariate used for spatial predictions). F and P represent the range of values used in model fitting and spatial prediction, respectively. Scales for estimation vary by covariate; however, spatial predictions are made to a common 0.1° longitude × 0.05° latitude (i.e. ~5 × 5 km) grid at an annual time-step. ↑, ↓ denote hypothesized directions of the occurrence–covariate relationships, and ↓↑ indicates that the direction of the occurrence–covariate relationship is uncertain. References relate either to the data source, the expected relationship with ψ, or papers contributing to the selection of this covariate for modelling (see Supplementary material Appendix 3 for the full reference list, <www.ecography.org/appendix/ecog-03098>).

Covariate	Abbreviation	Description	Units and derivation	Range (min, max)	Spatial scales for fitting	Temporal scales for fitting	Expected relationship with ψ	Source	References
Spatial memory									
Occurrence in previous year	$distrib_{t-1}$	Using the $distrib_t$ layers created for the spatial similarity index (SSI), we selected the layer for $t-1$ to capture the occurrence pattern one-year earlier.	1 = occurrence in same cell in $t-1$ 0 = absence in same cell in $t-1$	F (0, 1) P (0, 1)	0.1° longitude × 0.05° latitude (i.e. ~5 × 5 km)	Annual	↑, with stronger ↑ influence in years when more 'experienced' individuals are present and/or stock size is large.	Fishery logbooks	Jakobsson 1969, Corten 1993, 2000, 2002, McQuinn 1997, Fernö et al. 1998, Huse et al. 2002, 2010
Density of occurrences in previous year	$counts_{t-1}$	Similar to $distrib_{t-1}$, we used the $counts_t$ layers (created during SSI derivation) and selected the layer for $t-1$ to capture the density of occurrences one-year earlier.	% (see Supplementary material Appendix 2 Eq. A1 for derivation)	F (0, 43.67) P (0, 45.19)	0.1° × 0.05°	Annual	As above	As above	As above
Dynamic environment									Logemann et al. 2013 (for all dynamic variables)
Sea surface temperature	SST	Temperature at 1.25 m depth.	°C	F (–1.76, 9.68) P (–1.36, 9.38)	1 × 1 4 × 4 8 × 8 km	Day of record, mean of 7 d previous	↑, but influence of SST and all other covariates may change with stock demographics.	CODE	Blaxter 1985, Maravelias 1997, Misund et al. 1997, 1998, Maravelias et al. 2000a, Toresen and Østvedt 2000, Corten 2001, Nøttestad et al. 2007, Bartolino et al. 2014
Sea surface salinity	SSS	Salinity at 1.25 m depth.	practical salinity unit (psu)	F (31.51, 35.38) P (33.00, 35.24)	1 × 1 4 × 4 8 × 8 km	Day of record, mean of 7 d previous	↓	CODE	Blaxter 1985, Maravelias and Reid 1995, 1997, Lindegren et al. 2011
Potential energy anomaly	PEA	Energy needed to instantaneously homogenize the water column with a given density stratification. Calculated here as a function of temperature and salinity.	kg m^{-1} s^{-2} $\frac{1}{H}\int_{-h}^{\eta}(\bar{\rho}-\rho)gz\,dz$	F (0, 55.19) P (0, 54.99)	1 × 1 4 × 4 8 × 8 km	Day of record, mean of 7 d previous	↓↑	CODE	Simpson 1981, Huse and Korneliussen 2000, Maravelias and Reid 1997, Maravelias et al. 2000b, Planque et al. 2006, de Boer et al. 2008, Burchard and Hofmeister 2008, Huret et al. 2013

(Continued)

Table 1. (Continued)

Covariate	Abbreviation	Description	Units and derivation	Range (min, max)	Spatial scales for fitting	Temporal scales for fitting	Expected relationship with ψ	Source	References
Difference between SST and bottom temperature	change	SST – temperature at 1.25 m above the sea floor.	°C	F (–8.16, 5.05) P (–4.77, 4.16)	1 × 1 4 × 4 8 × 8 km	Day of record, mean of 7 d previous	↓	CODE	Maravelias and Reid 1997, Maravelias et al. 2000b
Current velocity	current_vel	Mean of the absolute values of the U and V flow vectors at 1.25 m depth.	m s^{-1}	F (0, 0.64) P (3.25e-04, 2.20)	1 × 1 4 × 4 8 × 8 km	Day of record, mean of 7 d previous	↓	CODE	Corten and van de Kamp 1992, Corten 1999a, b
Static environment									
Water depth	bottom_depth	Depth of the water column.	m	F (–2290, –11) P (–2560, 0)	30 arcsec	–	↓↑	GEBCO <www.gebco.net>	Maravelias et al. 2000a, Nøttestad et al. 2007, echosounder data (this study)
Bottom slope	slope	Slope of the sea floor.	°	F (0, 25.37) P (1.44e-02, 0.12)	30 arcsec	–	↓	GEBCO	Maravelias et al. 2000a, echosounder data (this study)
Distance to shore	dist_to_shore	Distance from each occurrence/absence record to the nearest landmass.	km	F (0.01, 334.31) P (0, 344.71)	Exact	–	↓↑	Fishery log-books, 'geo' R package	R package 'geo', MRI, Reykjavík, Iceland <https://r-forge.r-project.org/R/?group_id=945>
Predators									
Fishing magnitude	fish_magnitude	Product of no. of successful fishing events and total landings in tonnes in the week preceding each occurrence/absence record.	tonnes	F (0, 6.15e05) P (0, 7.06e06)	0.1° × 0.05°	Weekly	↓	Fishery logbooks	Olsen 1971, Vabø et al. 2002, Ona et al. 2007, Doksæter et al. 2009, Lindegren et al. 2011
Prey									
Zooplankton biomass	CF_Aug	Biomass estimates for adult *Calanus finmarchicus* (i.e. C4, C5, C6 stages) averaged for the August preceding wintering each year.	μg C m^{-2}	F (0, 1.32e07) P (0, 9.62e06)	20 × 20 km	Annual, but simulation covers 1995–2007 only	↑	Hjøllo et al. 2012. IBM for *C. finmarchicus*	Bainbridge and Forsyth 1972, Holst et al. 1997, Maravelias and Reid 1997, Corten 1999b, Maravelias et al. 2000b, Gislason and Astthorsson 2002, Prokopchuk and Sentyabov 2006, Nøttestad et al. 2007, Hjøllo et al. 2012, Utne et al. 2012

forms of $\omega_{i,t}$ – see Spatiotemporal random effects for details) we included a fixed factor for year. This categorical term captures the overall temporal pattern, common to all locations, and allows for year-to-year fluctuation in occurrence probabilities without assuming a predictable trend among time points.

To explore potential non-linearity in covariate effects, we fitted models that 1) assume linear trends for all covariates, 2) include quadratic terms for all environmental covariates, and 3) treat each environmental covariate as a smooth term, represented by a penalized regression spline with two knots (Crainiceanu et al. 2005, see Supplementary material Appendix 4 for R code). These specifications form a gradient of increasing flexibility in occurrence-covariate relationships, whilst maintaining ecologically realistic functional forms. To control against overfitting, yet maximize biological inference on our hypotheses, we offset this flexibility by specifying additive terms only, and not considering first- or higher-order interactions in our models.

Spatiotemporal random effects

In Eq. 3, $\omega_{i,t}$ is the spatiotemporal random effect, which accounts for residual spatial (and temporal) patterns not explained by the covariates. This term is spatially explicit and estimated for each location i. Three forms of $\omega_{i,t}$ were tested: 1) where $\omega_{i,t} = 0$ (i.e. the 'no-space' case); 2) where $\omega_{i,t}$ is a temporally independent realization of the spatial field for each year (i.e. the 'time-indep' case); and 3) where $\omega_{i,t}$ follows a 1st order autoregressive (ar1) process allowing correlation between years (i.e. the 'time-corr' case) (Eq. 4),

$$\omega_{i,t} = a\omega_{i,t-1} + \xi_{i,t} \; \xi_{i,t} \overset{iid}{\sim} \mathrm{N}(0, \Sigma) \text{ for } t = 2, \ldots, T \tag{4}$$

where the a coefficient denotes the temporal dependence in $\omega_{i,t}$, with $|a| < 1$. When $a = 0$, $\xi_{i,t}$ is the sole representation of the spatial field for year t (i.e. the 'time-indep' case – see Ono et al. (2016) for a similar approach). If $a \neq 0$, the spatiotemporal field in t depends on the intensity and pattern of the field in $t - 1$ (i.e. the 'time-corr' case – see Ward et al. (2015) for an example). In this latter instance, the realization of the spatial process for $t = 1$, $\omega_{i,1}$, is derived from the stationary distribution $\mathrm{N}(0, \Sigma/(1 - a^2))$ (see Cameletti et al. 2013 for details).

In both time_indep and time_corr cases, $\xi_{i,t}$ is a zero mean Gaussian random field assumed to be independent in time and defined by a Matérn covariance function (Eq. 5).

$$\mathrm{Cov}\left[\xi_{i,t}, \xi_{i',t'}\right] = \begin{cases} 0, & \text{if } t \neq t' \\ \Sigma_{i,i'}, & \text{if } t = t' \end{cases} \tag{5}$$

where $i \neq i'$ and,

$$\Sigma_{i,i'} = \frac{\sigma_\omega^2}{\Gamma(\nu) 2^{\nu-1}} \left(\kappa \| i - i' \|\right)^{\nu} K_\nu \left(\kappa \| i - i' \|\right) \tag{6}$$

This is a representation of a Gaussian Markov random field (GMRF). In Eq. 6, $\Sigma_{i,i'}$ is the covariance between locations i and i'. Γ is the gamma function and ν is a smoothing parameter equal to $\alpha_w - d/2$, where α_w governs the smoothness of the random field, and d is the number of dimensions in the model. We set $\alpha_w = 2$ and $d = 2$, hence $\nu = 1$. κ is a scaling parameter associated with the practical range $\rho = \frac{\sqrt{8}}{\kappa}$, which represents the distance at which spatial correlation reduces to ~ 0.13, and K_ν is the modified Bessel function of the second order. With these parameter values set, the marginal variance of the GMRF, σ_ω^2 is given by:

$$\sigma_\omega^2 = \frac{1}{4\pi\kappa^2 \tau^2} \tag{7}$$

where τ in Eq. 7 is the local variance parameter.

General approach

First, we considered a suite of stationary models that assume that the response of the herring population to each covariate is static across the time series (Eq. 3). We began with full models including all covariates, specified as linear, quadratic or spline terms, a fixed year effect and all forms of the spatiotemporal random component $\omega_{i,t}$ (i.e. models s1–s15, Table 2). This approach allowed us to evaluate different random-effect structures, whilst gaining an initial picture of the nature and magnitude of covariate effects (Zuur et al. 2009). After accounting for the overall spatial and temporal trends, the $\mathrm{distrib}_{t-1}$ covariate was found to be strongly influential, exhibiting positive associations with ψ in all cases (Fig. 3, Supplementary material Appendix 7, Table A1). As abrupt shifts in herring winter distribution occurred periodically, interrupting phases of spatial continuity (Fig. 1, 2), we considered that the relative importance of $\mathrm{distrib}_{t-1}$ may also vary in time and be a key indicator of the degree of temporal correlation in winter occurrence patterns. We explored this possibility by fitting a series of partly non-stationary models (i.e. models part_ns1–part_ns9, Table 2), allowing regression coefficients for $\mathrm{distrib}_{t-1}$ to be represented by a time-ordered vector with elements that vary by year according to 1st order random walk (rw1) dynamics. The rw1 models were defined by a Gaussian distribution $\mathrm{N}(0, prec\mathbf{R})$, where $prec$ is the precision parameter assigned a Gamma(1, 5e-05) prior, and $\mathbf{R}$ is a fixed structure matrix (see Supplementary material Appendix 5 for details on alternative model and prior specifications considered). Finally, we fitted a series of fully non-stationary models in which coefficients for all fixed effects could vary annually with the same rw1 specification (i.e. models full_ns1–full_ns9, Table 2). These non-stationary models enabled us to explore associations between covariate influence and changes in population demographics in the ISS herring stock over time, whilst naturally handling temporal dependence among adjacent years (see Supplementary material Appendix 4 for R code).

Model fitting details

Models were fitted in R-INLA (Rue et al. 2009) using the SPDE approach (Lindgren et al. 2011). We grouped models by stationarity level for ease of explanation, and summarize

Table 2. Structure and performance of candidate space-time occurrence models for wintering ISS herring. Each model contains all covariates (full), and results are shown for fitting using simplified Laplace approximation (see Supplementary material Appendix 7 Table A2 for results based on a Gaussian approximation strategy). s1–s15, stationary models; part_ns1-part_ns9, partly non-stationary models; full_ns1-full_ns9, fully non-stationary models. Covariate form refers to models that include linear terms only (linear), and quadratic terms (quadratic) or penalized regression spline terms for environmental covariates (spline). Space/time structure describes the form of the spatiotemporal random effect $\omega_{i,t}$, and if a fixed factor for year (year$_t$) was included; no-space/no-time, no spatially or temporally structured effects; time_indep, independent realization of the spatial random field at each *t*; time_corr, temporal correlation (ar1) is considered in the realization of the spatial random field at each *t*. The best-performing model within each stationarity class is shown in bold.

Model	Covariate form	Structure	DIC	Mean log score	Brier score	AUC
Stationary						
s1	linear	full (no-space/no-time)	49104.2	0.504	0.157	0.934
s2	linear	full + year$_t$	48353.6	0.496	0.154	0.974
s3	linear	full + time_indep $\omega_{i,t}$	41872.1	0.429	0.123	0.993
s4	linear	full + year$_t$ + time_indep $\omega_{i,t}$	41811.9	0.429	0.122	0.993
s5	linear	full + time_corr $\omega_{i,t}$	41877.0	0.429	0.123	0.992
s6	quadratic	full (no-space/no-time)	48917.2	0.502	0.156	0.943
s7	quadratic	full + year$_t$	48059.1	0.493	0.152	0.981
s8	quadratic	full + time_indep $\omega_{i,t}$	41732.1	0.428	0.122	0.994
s9	**quadratic**	**full + year$_t$ + time_indep $\omega_{i,t}$**	**41629.0**	**0.427**	**0.122**	**0.995**
s10	quadratic	full + time_corr $\omega_{i,t}$	41733.0	0.428	0.122	0.993
s11	spline	full (no-space/no-time)	49232.2	0.505	0.158	0.917
s12	spline	full + year$_t$	48365.1	0.496	0.154	0.973
s13	spline	full + time_indep $\omega_{i,t}$	41907.0	0.430	0.123	0.993
s14	spline	full + year$_t$ + time_indep $\omega_{i,t}$	41833.3	0.429	0.123	0.993
s15	spline	full + time_corr $\omega_{i,t}$	41908.3	0.430	0.123	0.992
Partly non-stationary						
part_ns1	linear	full (no-space/no-time)	48953.2	0.502	0.157	0.952
part_ns2	linear	full + time_indep $\omega_{i,t}$	41733.4	0.428	0.122	0.993
part_ns3	linear	full + time_corr $\omega_{i,t}$	41742.0	0.428	0.122	0.992
part_ns4	quadratic	full (no-space/no-time)	48725.5	0.500	0.155	0.960
part_ns5	**quadratic**	**full + time_indep $\omega_{i,t}$**	**41621.5**	**0.427**	**0.122**	**0.994**
part_ns6	quadratic	full + time_corr $\omega_{i,t}$	41625.5	0.427	0.122	0.994
part_ns7	spline	full (no-space/no-time)	49080.7	0.504	0.157	0.943
part_ns8	spline	full + time_indep $\omega_{i,t}$	41780.0	0.428	0.122	0.993
part_ns9	spline	full + time_corr $\omega_{i,t}$	41785.5	0.428	0.122	0.992
Fully non-stationary						
full_ns1	linear	full (no-space/no-time)	47330.3	0.486	0.148	0.989
full_ns2	linear	full + time_indep $\omega_{i,t}$	41334.7	0.424	0.120	0.996
full_ns3	linear	full + time_corr $\omega_{i,t}$	41342.3	0.424	0.120	0.995
full_ns4	quadratic	full (no-space/no-time)	46756.0	0.480	0.146	0.995
full_ns5	**quadratic**	**full + time_indep $\omega_{i,t}$**	**41047.1**	**0.421**	**0.119**	**0.997**
full_ns6	quadratic	full + time_corr $\omega_{i,t}$	41055.3	0.421	0.119	0.997
full_ns7	spline	full (no-space/no-time)	46972.0	0.482	0.147	0.993
full_ns8	spline	full + time_indep $\omega_{i,t}$	41219.1	0.422	0.119	0.996
full_ns9	spline	full + time_corr $\omega_{i,t}$	41226.4	0.423	0.119	0.996

key details in Table 2 and Supplementary material Appendix 7, Table A2. Prior to fitting, we created a triangulated mesh upon which to build the GMRFs, covering a spatial domain that encompassed all of our observations (see Krainski et al. 2016 for details, and Supplementary material Appendix 4 for R code). We initially used a Gaussian approximation strategy to enable fast model comparison. We then refitted all models using simplified Laplace approximation – providing a compromise between correcting the Gaussian approximation for errors in location and/or skewness (Rue et al. 2009) whilst retaining good computational properties. Vague normal priors were assigned to all fixed effects N(0, 1000), and the intercept N(0, ∞). To assess sensitivity to prior choice, we refitted all stationary 'no-space' models using weakly informative Cauchy priors with mean = 0 and scale = 2.5 for the fixed effects, and 10 for the intercept using the 'bayesglm' function in the 'arm' package in R (Gelman et al. 2008). Both prior specifications produced stable, highly congruent posterior estimates, so we proceeded using normal priors only. Priors for the SPDE model hyper-parameters (a, κ, τ), the latter two defining ρ and σ^2_ω, are provided in Supplementary material Appendix 5.

Assessing fit and predictive performance

We calculated the deviance information criterion (DIC) (Spiegelhalter et al. 2002) and a series of metrics based on the conditional predictive ordinate (CPO) (Pettit 1990) to check model fit and assess predictive performance. For each model, we used the CPO$_{e,i,t}$ given by $\pi(y_{e,i,t}|y_{-(e,i,t)})$, which represents the cross-validated (cv) 'leave-one-out' predictive density at

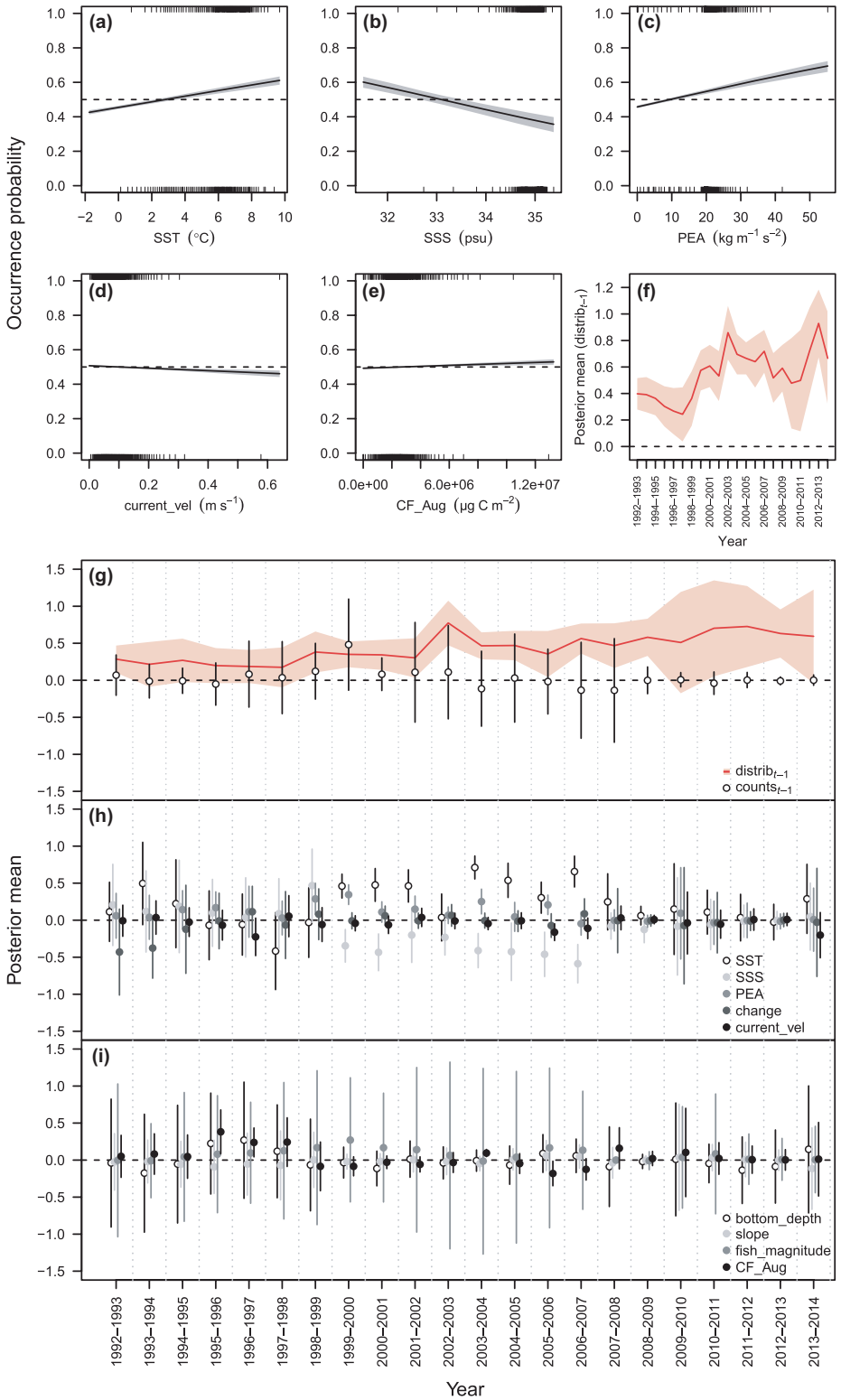

Figure 3. (a–e) Marginal effect plots for influential covariates in the part_ns5 model (see Table 1 for covariate codes), and (f) time series of posterior mean estimates (red line) and 95% credible intervals (CIs) (red-shaded region) for the distrib$_{t-1}$ covariate. In (a–e), black lines are median estimates of 1000 draws from the posterior distribution for a sequence of 100 values across the full range of each covariate, and grey-shaded regions are 95% CIs. Tick marks denote the percentile distribution of raw data for each covariate for occurrence records (top of plots) and absence records (bottom of plots). Plots (a–c) represent quadratic effects, and (d, e) the linear effect of the covariate. (g–i) Time series of posterior mean estimates for the linear term (circles) and 95% CIs (vertical lines) for all covariates from the full_ns5 model. Symbols are offset slightly, and results for the distrib$_{t-1}$ covariate plotted as a red line (posterior mean) and red-shaded region (95% CIs) in panel (g).

observation $y_{e,i,t}$ with the $y_{e,i,t}$th observation removed, to derive the mean logarithmic (log) score (Gneiting and Raftery 2007), a measure of predictive quality, and the cv Brier score (i.e. mean prediction error), a measure of model goodness-of-fit reflecting both discriminatory ability and calibration that evaluates the degree of correspondence between fitted probabilities and observed binary outcomes (Schmid and Griffith 2005, Roos and Held 2011). Lower values on both scores reflect a better model, with Brier scores interpreted in relation to reference values that are a function of sampling prevalence (see Held et al. 2012 for an example). As an additional calibration check for out-of-sample predictions, we examined histograms of probability integral transform (PIT) values for departures from uniformity (Dawid 1984, Gneiting et al. 2007, Held et al. 2010). Despite its known deficiencies (Lobo et al. 2008), given perfect detection in our data, the similarity in both geographic and environmental space in model fitting and prediction domains, and the explicit consideration of spatiotemporal error structure in our modelling approach, we also calculated the AUC for each model.

Covariate importance and model selection

After comparing full models using the aforementioned criteria and determining an optimal structure for $\omega_{i,t}$, we used the best-performing full stationary model (including the fixed year effect and $\omega_{i,t}$) to estimate covariate importance and find an appropriate fixed-effect structure. We first examined parameter estimates and 95% credible intervals (CIs) for each covariate. Next, we dropped one covariate at a time from the full model (i.e. single-term deletion) and compared the DIC, mean log score and Brier score of the reduced models with the full model, and a baseline model comprising only an intercept, year_t and the optimal structure for $\omega_{i,t}$ (see Illian et al. 2013 for a similar approach).

Correlation among covariates and demographic parameters

To examine associations between covariate importance and population demographics, we calculated Pearson's *r* coefficients between time series of posterior means for the linear term for influential covariates (i.e. those with 95% CIs not overlapping 0 in at least one year) in the best non-stationary models, and nine demographic parameters for the ISS stock derived from annual stock assessments coordinated by The International Council for the Exploration of the Sea (ICES). Calculations were made on the first 18, 19, 20, 21, and 22 yr of data. Demographic parameters considered include three ratios of the numbers (millions) of naïve, first-time winterers to older, experienced individuals (i.e. age3:age4to7, age3:age8to13, age3:age4+), spawning stock biomass (SSB – '000 tonnes), spawning stock numbers (SSN – millions), numbers (millions) of young experienced individuals (n age4to7), old experienced individuals (n age8to13), and all experienced individuals (n age4+), and mean age (years) of the spawning stock (mean age).

Spatial prediction and validation

An area of interest for spatial prediction was defined within the extent of the fishery and survey data, covering the entire distributional range of ISS herring. The area, spanning 62.475 to 67.975°N and 9.008 to 28.008°W, was divided into 0.1° longitude × 0.05° latitude (~5 × 5 km) grid cells, matching the resolution of several covariates used in model building and providing a scale useful for fishery management (Supplementary material Appendix 3, 6). Our interest was in predicting herring occurrence probability on an annual time-step. Hence, maps were created for each covariate based on mean grid cell values calculated across each year. The range of covariate values in the prediction space was monitored, and closely matched the values used for model fitting (Table 1).

The different classes of models we built have different utility regarding prediction. The stationary models are very general, making them well suited for predictions to randomly selected data within the time series or for long-term forecasts. By contrast, the fully non-stationary models, with their annually-varying coefficients, are less flexible, but useful in mapping occurrence probabilities for specific years within the time series. The task of short-term forecasting (e.g. to $t+1$) befits the partly non-stationary models, which occupy a middle ground in terms of generality. For these reasons, we used the best performing fully non-stationary model to generate annual prediction maps within the time series. Predictions were made for the last 22 years (i.e. 1992–1993 to 2013–2014), but we present results for four years (i.e. 1994–1995, 2001–2002, 2007–2008, 2013–2014) representative of the different wintering phases. Implementation is straightforward in R-INLA (see Supplementary material Appendix 4 for R code). For predictions to t + 1 we used the best partly non-stationary specification. We ran validation tests on held-out observations by building models for the first 18, 19, 20 and 21 yr of data, and testing how well the predicted probabilities of occurrence match the observations in the 19th, 20th, 21st, and 22nd years, respectively. For this, we needed to estimate the distrib_{t-1} regression coefficient for $t + 1$. We reasoned that if strong correlations exist between the distrib_{t-1} regression coefficients and one or more demographic parameters, and we can estimate these demographic parameter(s) for $t + 1$, then prediction of the distrib_{t-1} regression coefficient in $t + 1$ may be possible. We summarize the main findings in the Results section, but provide full annotated R code (Supplementary material Appendix 4) and explanatory notes in Supplementary material Appendix 6. All analyses were run in R ver. 3.2.2 (R Development Core Team), and datasets and code are available from the Dryad Digital Repository.

Data deposition

Data available from the Dryad Digital Repository: <http://dx.doi.org/10.5061/dryad.9v46k> (Macdonald et al. 2017).

Results

Spatial similarity across years

The SSI accurately reproduced the temporal dynamics of wintering patterns across our time series. The spatial persistence

of the distribution during the 'East' phase (Fig. 1a) was reflected in relatively high SSI values, with the northward shift witnessed between 1994–1995 and 1997–1998 forcing a gradual reduction in the index (Fig. 2). SSI values were lower over the following decade. This is a result of a patchier distribution during these years (Fig. 1b), although year-to-year consistency was sometimes observed (e.g. between 2001–2002 and 2002–2003). From 2007–2008 until 2012–2013, the majority of the adult population wintered inshore, in fjords on Iceland's west coast (Fig. 1c). Strong fidelity to these fjords was observed during this period, resulting in high SSI values. The SSI dropped in 2013–2014, as younger cohorts established a new wintering area off the southeast coast (Óskarsson and Reynisson 2014).

Model performance

Our models generally fitted the data well and showed low mean prediction error, with cross-validated Brier scores falling below the prevalence-based reference value of 0.138 for all models incorporating spatiotemporal random structure (Table 2). Discriminatory ability was high, with AUC values > 0.9 in all cases, and Gaussian and simplified Laplace approximation strategies were in full agreement regarding the best-performing models (Table 2, Supplementary material Appendix 7 Table A2). The inclusion of spatial and temporal structure was beneficial, and results from the stationary models suggest that independent realizations of the spatial random field (i.e. time-indep $\omega_{i,t}$) and a fixed year effect (i.e. year$_t$) more appropriately describe the data than a smooth year-to-year transition in either of these processes (i.e. time-corr $\omega_{i,t}$) (Table 2). Allowing fixed effect parameters to vary in time through the non-stationary models improved goodness-of-fit and predictive capacity over the stationary cases, and there was stronger support for models allowing some non-linearity in occurrence–covariate relationships (i.e. quadratic terms for environmental covariates) (Table 2).

Covariate importance and model selection

The addition of covariates improved model performance. Although posterior 95% CIs overlapped 0 in some cases (Supplementary material Appendix 7 Table A1), backwards selection on the best stationary model (s9) indicated that most covariates added some information and none detrimentally affected predictive capacity (Supplementary material Appendix 7 Table A3). Hence, all covariates were retained, and full models used for further inference.

Nature of occurrence–covariate relationships

Positive associations were found between distrib$_{t-1}$ and ψ in all models – this pattern persisting when spatially and temporally structured terms were included (Fig. 3, Supplementary material Appendix 7 Table A1). This result supports the existence of a strong connection with previously-used wintering sites in most years. The best partly non-stationary model (part_ns5) outperformed s9 (Table 2), suggesting that the predictive ability of the distrib$_{t-1}$ covariate may vary in time. Posterior mean estimates for distrib$_{t-1}$ in the part_ns5 model were always positive however, and 95% CIs never overlapped 0 (Fig. 3f). This model also assumes that the response of the wintering population to all other covariates is static in time. We visualized the nature of these associations by plotting the marginal effect for covariates with posterior 95% CIs that did not overlap 0 (Fig. 3a–e, see Supplementary material Appendix 7 Fig. A7 for plots of all other covariates).

Several local-scale environmental variables were found to be important. Occurrence probability increased in warmer, fresher and moderately stratified waters (Fig. 3a–c), in lower velocity zones (Fig. 3d), and in areas near high zooplankton (i.e. adult *C. finmarchicus*) biomass in the August preceding wintering (Fig. 3e). Notably, dependence on the density of occurrence records from the previous year, as captured by counts$_{t-1}$, was low. Similarly, the vertical temperature gradient, bathymetric features, and the magnitude of recent fishing activity all had little impact (Supplementary material Appendix 7 Fig. A7, Table A1).

These patterns were further investigated in the full_ns5 model – the best model overall – in which all fixed effects could vary by year. Again, distrib$_{t-1}$ was influential; however, the increased number of random effects in the full_ns5 model acted to dampen its effect (Fig. 3g–i). The importance of SST, SSS and PEA shifted in time, with these covariates' influence increasing during the early to mid-2000s when the wintering population was patchily distributed around Iceland (Fig. 1, 3h). Estimates for fish_magnitude were generally small, with large variance (Fig. 3i). Covariates describing bathymetric features showed no strong trends over time, and CF_Aug exhibited a small positive association with ψ in some years (Fig. 3i).

Correlations among covariates and demographic parameters

The importance of the distrib$_{t-1}$ covariate was found to increase most strongly with adult population size (SSN) in both the part_ns5 and full_ns5 models, with positive associations also observed with n age4to7, n age 4 + and SSB (Table 3). Focussing on the full_ns5 model, a stronger positive effect of SST was detected when the ratio of naïve : older, experienced individuals (age3:age8to13) increased (Table 3). The posterior mean estimates for SSS decreased as SSN and SSB increased, and coefficients for PEA were negatively associated with n age8to13. All other correlations were non-significant.

Spatial prediction within the time series

Spatial predictions of occurrence probabilities derived from the full_ns5 model showed high concordance with the observations (Fig. 4). The model accurately predicted the occurrence patterns in years when the wintering population

Table 3. Mean (1 SD) Pearson's *r* coefficients calculated between time series of demographic parameters (Demo.) for the ISS herring stock and posterior mean estimates for influential covariates (Cov.) in the best non-stationary models. Mean and SD were calculated from correlations made for five time series incorporating the first 18, 19, 20, 21 and 22 yr of data. Demographic parameters are age3:age4to7, age3:age8to13, age3:age4+, three ratios of numbers of naïve, first-time winterers to young experienced, old experienced, and all experienced individuals respectively; SSB, spawning stock biomass; SSN, spawning stock numbers; n age4to7, number of young experienced individuals; n age8to13, number of old experienced individuals; n age4+, number of all experienced individuals; mean age, average age of the spawning stock.

Cov. \ Demo.	age3: age4to7	age3: age8to13	age3: age4+	SSB	SSN	n age4to7	n age8to13	n age4+	mean age
Partly non-stationary model (part_ns5)									
$distrib_{t-1}$	0.101	0.418	0.178	0.471	0.575	0.520	0.044	0.479	–0.328
	(0.047)	(0.128)	(0.066)	(0.061)	(0.125)	(0.107)	(0.021)	(0.089)	(0.126)
Fully non-stationary model (full_ns5)									
$distrib_{t-1}$	0.120	0.106	0.113	0.455	0.489	0.372	0.320	0.446	–0.040
	(0.036)	(0.107)	(0.040)	(0.055)	(0.125)	(0.129)	(0.047)	(0.104)	(0.118)
SST	0.113	0.481	0.213	0.404	0.415	0.404	–0.220	0.324	–0.354
	(0.014)	(0.020)	(0.016)	(0.006)	(0.014)	(0.011)	(0.022)	(0.008)	(0.026)
SSS	–0.118	–0.375	–0.187	–0.454	–0.501	–0.435	0.028	–0.405	0.257
	(0.007)	(0.008)	(0.007)	(0.003)	(0.007)	(0.005)	(0.015)	(0.005)	(0.016)
PEA	–0.008	0.156	0.030	–0.386	–0.362	–0.265	–0.481	–0.362	–0.164
	(0.030)	(0.049)	(0.024)	(0.027)	(0.071)	(0.076)	(0.023)	(0.060)	(0.062)
current_vel	–0.134	–0.009	–0.104	0.056	0.101	0.154	–0.011	0.124	–0.131
	(0.019)	(0.034)	(0.026)	(0.004)	(0.017)	(0.012)	(0.021)	(0.010)	(0.032)
CF_Aug	–0.256	–0.444	–0.324	–0.317	–0.405	–0.294	0.088	–0.256	0.385
	(0.007)	(0.027)	(0.010)	(0.002)	(0.017)	(0.016)	(0.013)	(0.010)	(0.029)

was confined to small regions of the prediction space (e.g. 2007–2008), when it was spread out (e.g. 1994–1995), when it was patchily distributed (e.g. 2001–2002), and during distributional shifts (e.g. 2007–2008, 2013–2014) (Fig. 4a). For the four representative years considered here, model predictions were well calibrated, with small mean squared differences between predicted probabilities and actual observations (Brier score: 1994–1995 = 0.162, 2001–2002 = 0.132, 2007–2008 = 0.152, 2013–2014 = 0.168, all below reference values), and showed near-perfect discrimination between observed occurrences and absences (AUC: 1994–1995 = 0.998, 2001–2002 = 0.994, 2007–2008 = 0.999, 2013–2014 = 0.999).

Data were scarce in some years (e.g. 1994–1995, 2013–2014), with large areas of the prediction space containing few observations. The SPDE approach handles this by evaluating the continuous spatial or spatiotemporal random effects as discretely indexed GMRFs, allowing predictions to be made to unsampled locations whilst robustly estimating the uncertainty of these predictions. The SD of ψ was highest in areas where occurrence and absence records were close in geographic space (Fig. 4b), likely due to difficulties in resolving such a steep gradient of probabilities over such short spatial scales. Variance was low and uniform in unsampled regions.

Inclusion of spatiotemporal random effects (ω) improved model fit and predictive performance (Table 2), indicating that the covariate components were not overfitted, but also that factors important in shaping ψ have been missed, and/or were occurring at scales that our models could not resolve. The patterns in ω (Fig. 4c) reveal the presence of spatial dependence at relatively large scales (i.e. 100's of km), confirmed by the posterior estimates for the practical range ρ (Table 3), and likely reflect rapid changes in school shape, size and structure that our models did not capture (Pitcher et al. 1996, Nøttestad and Axelsen 1999, Makris et al. 2009). The trends observed in the random field SD's are a function of data coverage, with uncertainty increasing with distance from the observations (Fig. 4d).

Predicting occurrence patterns in t + 1

We found strong positive correlations between time series of SSN and posterior mean estimates of the $distrib_{t-1}$ covariate in the partly non-stationary models (i.e. part_ns5 specification) fitted to the first 18, 19, 20 and 21 yr of data (Pearson's r mean = 0.623, SD = 0.127) (Fig. 5). Given this degree of correlation, we then were able to predict the posterior mean estimate for $distrib_{t-1}$ in $t + 1$ from the estimate of SSN in $t + 1$ (obtained from MRI surveys – Óskarsson and Reynisson 2014). This allowed us to validate our models on withheld observations one-year ahead, and assess prediction accuracy for the last four years of the time series (see Supplementary material Appendix 6 for details). Predictive performance was high in three out of the four years (19th year: Brier score = 0.142, AUC = 0.961; 20th year: Brier score = 0.137, AUC = 0.976; 21st year: Brier score = 0.128, AUC = 0.976), but dropped sharply in the last year (22nd year: Brier score = 0.194, AUC = 0.588) concurrent with a reduction in correlation strength between time series of SSN and $distrib_{t-1}$ coefficients (Fig. 5).

Discussion

Our study on ISS herring heeds recent calls for a greater focus on the role of collective learning in shaping animal distributions (Keith and Bull 2017), whilst demonstrating that social cues may not necessarily act alone. Consistent

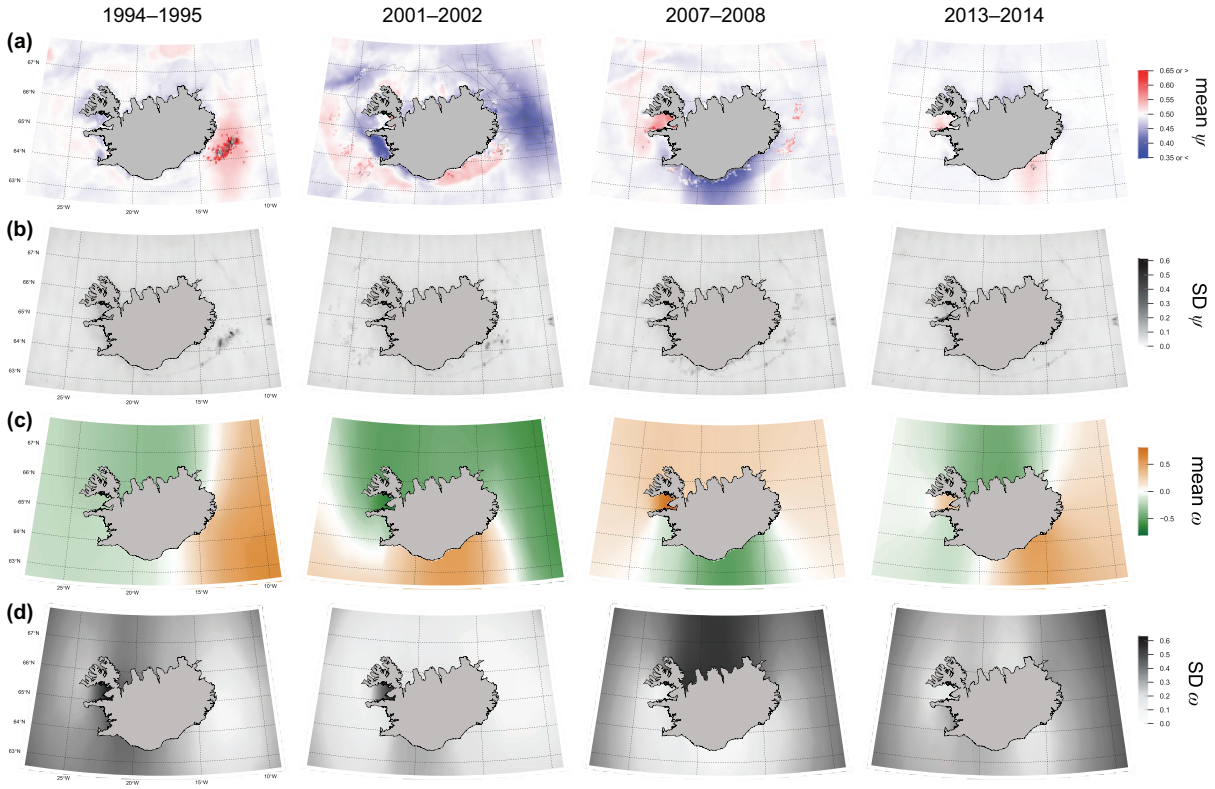

Figure 4. Spatial predictions of occurrence probability for four representative winters of the time series as derived from the full_ns5 model. For each year, (a) is the mean occurrence probability (ψ) and (b) the SD of ψ (expressed as log-odds) for each grid cell. (c) is the mean intensity of the temporally-independent realization of the spatial random field (ω), and (d) is the SD of ω. Observed occurrences (black diamonds) and absences (grey crosses) for each year are overlaid in (a).

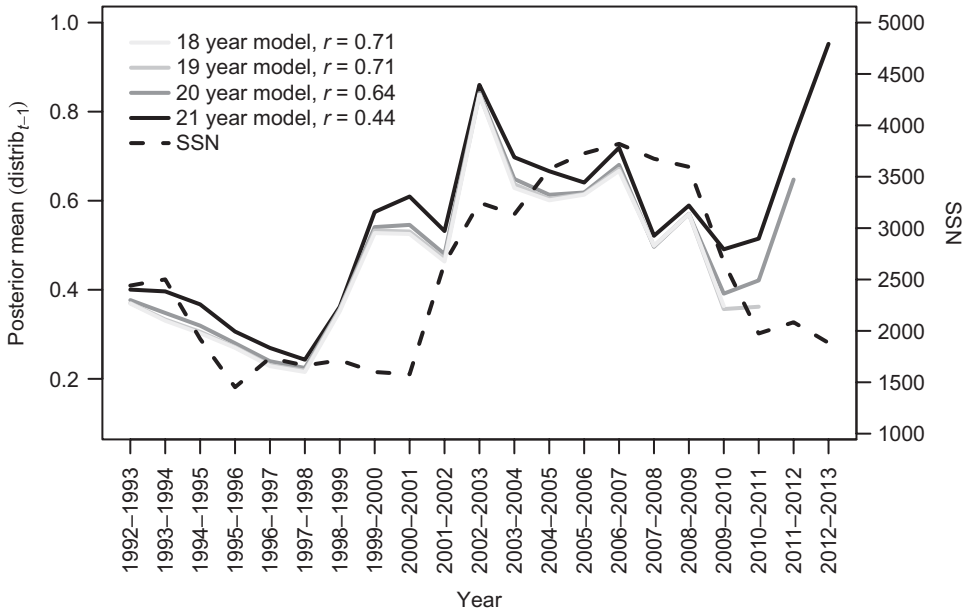

Figure 5. Time series of posterior mean estimates for distrib$_{t-1}$ derived from partly non-stationary models (i.e. part_ns5 specification) fitted to the first 18, 19, 20 and 21 yr of data (solid lines), and estimates of adult population size for the ISS herring stock, represented by spawning stock numbers (SSN – in millions) (dashed line). Pearson's *r* values reflect the degree of correlation between each model time series and SSN in the years included in that model (see Supplementary material Appendix 6 for further details).

with our expectations, we found that the distrib$_{t-1}$ covariate, describing the previous winter's occurrence pattern, imparted strong influence on the present pattern, the magnitude of its effect increasing with adult population size. Moreover, we showed that local-scale environmental and temporally-lagged prey-related factors were sometimes important; our results suggesting a heightened sensitivity of younger age classes to some environmental effects (e.g. SST). Importantly, the accuracy of our predictions to $t + 1$ highlights the potential of combining demographic time series with non-stationary models in exploring evidence for collective memory in fishes and other group-living animals, and in guiding spatial management decisions.

The multiple drivers of spatial distribution

A variety of intrinsic and extrinsic controls, often working synergistically, are known to structure marine fish distributions (Planque et al. 2011). For example, the use of visual stimuli to locate landmarks is well documented (Silveira et al. 2015), whilst geomagnetic and olfactory cues provide important compasses for migrating salmon (Putman et al. 2013). Furthermore, environmental gradients, predators, competitors and prey, population demographics and spatial memory can all be influential (Perry et al. 2005, Rindorf and Lewy 2006, Loots et al. 2010). Many of these factors appear relevant to herring, and work spanning many decades has demonstrated the importance of bottom-up (e.g. climate, local-scale environment, zooplankton biomass), top-down (e.g. predation) and demographic processes in structuring the species' population dynamics (Lindegren et al. 2011, see Huse 2016 for a review). Despite these efforts, the question of what governs where herring spend the winter, a non-feeding period during which schools are heavily targeted by commercial fisheries, has remained largely unresolved. We think that this may be a consequence of three factors. 1) High environmental flexibility in wintering populations (Fig. 3a–d, Supplementary material Appendix 7 Fig. A6) – a trait potentially explaining the marked geographic plasticity in wintering locations observed previously (Óskarsson et al. 2009, Huse et al. 2010). 2) The lack of proximate feeding and spawning cues, or competitive forces acting during the winter months – making underlying mechanisms difficult to pinpoint, and 3) mismatches between the true scale of processes acting on wintering populations and the scales captured by previous studies.

In designing our study, we felt that progress could be made by viewing the realized winter distribution as the result of two behavioural states: (state 1) migrating to, and colonizing wintering areas; and (state 2) living within these areas following colonization; and that herring may be tuned to different stimuli in each. In state 1, decisions must be made on the directionality of migration. Such decisions are thought to have a demographic origin; the probability of following previously-used routes increasing with the proportion of experienced individuals present in the stock, and contingent upon information-sharing opportunities among cohorts during some period preceding wintering. These ideas, supported now by both theory and empirical work (McQuinn 1997, Corten 2002, Huse et al. 2010) have advanced our capacity for predicting when populations are likely to follow suit, returning to traditional grounds, or break tradition and disperse to new areas.

Capturing spatial memory

Through construction of the SSI and in our models, we extend these ideas in a spatially-explicit manner by linking observations from the previous year's distribution to the present year's, and considering demographic parameters as potential mechanisms influencing spatial persistence from year-to-year. In effect, our approach simultaneously tests for geographic attachment to certain wintering areas (sensu Loots et al. 2010) – a well-known herring trait (Höglund 1955), while inclusion of the demographic components allows for an exploration, albeit correlative, of evidence for spatial memory and/or tradition-formation in the species. The strong effect of distrib$_{t-1}$ on ψ in both the stationary (Supplementary material Appendix 7 Table A1) and non-stationary models (Fig. 3f–i), combined with the correlation observed between time series of the distrib$_{t-1}$ coefficients and SSN (Table 3) suggests that although the proportion of naïve: experienced individuals appears fundamental to how decisions on directionality of winter migration are reached (state 1 – Huse et al. (2010)), population size may determine if these decisions are honoured. The mechanisms underpinning these observations remain unclear, but may relate to some form of wisdom through numbers (Surowiecki 2004), or the 'many wrongs principle' (Simons 2004) by which navigational accuracy increases in larger and/or denser schools through pooling many individual directional estimates. Makris et al. (2009) found direct evidence for this in herring. These authors demonstrated that a threshold density of individuals (i.e. 0.2 fish m^{-2}) promoted extremely rapid school-formation and growth at dusk, initiated by joining of small leading groups, and resulting in coordinated spawning migrations towards Georges Bank in the Gulf of Maine. If such processes also operate during the winter migration period, our results suggest that recolonizing previously-used wintering areas is sometimes deemed a good decision by the majority, or at least by some threshold number of influential leaders, and that adherence to these decisions may be stronger when the population is large.

Influence of prey resources and summer feeding distribution

Whilst important, the distrib$_{t-1}$ covariate did not explain all the variation in our observations. We had also speculated that where herring feed during summer might influence winter migration trajectories (Fernö et al. 1998), and used August biomass estimates for the zooplankter *C. finmarchicus* to test

this hypothesis. Wintering areas were often geographically quite close to summer prey patches (Table 3, Fig. 3e) – a situation that could advantage herring approaching wintering grounds, as energy conserved through minimizing dispersal away from profitable feeding areas would be highly valued during the subsequent non-feeding period. Georeferenced data on the summer feeding distribution in addition to empirical measures of *C. finmarchicus* biomass would permit a deeper examination of this idea; first, by providing a validation (in Icelandic waters) of the *C. finmarchicus* IBM used to derive our biomass layers (Hjøllo et al. 2012); and second, by allowing the degree of herring-zooplankton prey overlap to be estimated. Such information would provide useful insights into the importance of pre-wintering actions in general, and where they occur, on subsequent wintering behaviour. We argue that this may be especially relevant to the summer feeding period when several age classes mix (Libungan et al. 2015), offering a perfect arena for decision-making on the nature of the upcoming winter migration.

Wintering and density-dependence

Following settlement in wintering areas (i.e. state 2), herring hardly feed (Slotte 1999), and minimizing metabolic costs is likely prioritized. The absence of competition for food at this time removes a key mechanism thought to promote positive relationships between population abundance and occupied area, now demonstrated for several fish species (Fisher and Frank 2004) and predicted under most models of marine fish spatial dynamics (e.g. the 'basin model' – MacCall (1990)) through 'ideal free distribution' theory (Fretwell and Lucas 1969). Such positive associations are commonly taken as evidence for density-dependent habitat selection (DDHS), although they may also arise via density-independent means (Shepherd and Litvak 2004).

We found no support for any abundance–area association in our data (Supplementary material Appendix 8 Fig. A8), and no evidence for an effect of $counts_{t-1}$, a conservative surrogate for local herring density in $t-1$, on the occurrence pattern in t (Table 3, Fig. 3g, Supplementary material Appendix 7 Fig. A7a). In light of these results, we propose that DDHS is probably not a strong guiding force driving large-scale wintering patterns. Indeed, as the dense schooling behaviour typical of this phase may impart some fitness benefits in terms of predator evasion (Nøttestad and Axelsen 1999), the lack of an abundance–area association, as we found here, might reflect a distribution that is near ideal and free. This idea requires further testing, as density-dependent mechanisms are known to influence feeding and spawning migrations in the species (Ciannelli et al. 2013), and to structure schooling dynamics at micro- (i.e. cm to m) and meso-scales (i.e. 10's of m to 10's of km) (Pitcher et al. 1996, Mackinson et al. 1999).

Environmental effects

Given the nature of our dataset (i.e. 48 724 observations over 23 winters), we suggest that our models provide a broad, yet robust picture of environmental preferences of wintering ISS herring over the time period considered. We found that several local-scale dynamic variables influenced estimates of ψ (Fig. 3, Supplementary material Appendix 7 Tale A1). Whilst we cannot pinpoint the mechanistic basis of these relationships, we contend that this environmental sensitivity can be framed as a balance between maximizing individual fitness and fidelity to traditional wintering sites. Temperature (i.e. SST), the most influential environmental factor in our models, is a pervasive force shaping marine fish distributions (Perry et al. 2005), and although adult herring can tolerate a wide array of temperatures (Nøttestad et al. 2007), studies at the range margins suggest that physiological barriers may exist (e.g. $< \sim 2$°C) which are rarely crossed (Jakobsson 1969, Misund et al. 1997). We observed this here. Wintering ISS herring were never encountered in SST < 1.5°C, and were rarely captured north of 67°N, a region under the influence of cold East Icelandic Current water (Logemann et al. 2013) (Fig. 1, 3a, Supplementary material Appendix 7 Fig. A6a). This is indicative of a lower bound of thermal tolerance below which individual fitness may be compromised. If this is the case, then persistence of SST's far colder than 1.5°C off much of Iceland's north coast during winter, in conjunction with winter SST's in the study region approaching 10°C (Supplementary material Appendix 3 Fig. A2), may neatly explain the monotonic positive trend detected between SST and ψ (Fig. 3a). Even though residence in warmer waters likely involves higher energetic demands, given the species' flexibility in temperature preferences within the ~ 4 to 9°C range as seen here (Fig. 3a, Supplementary material Appendix 7 Fig. A6a), and its capacity to tolerate far higher temperatures elsewhere (Maravelias and Reid 1997) we suggest that our upper temperature bound would not be physiologically constraining.

These findings, in conjunction with pronounced drops in both median SSS and PEA values observed in wintering areas in the latter part of the time series (Supplementary material Appendix 7 Fig. A6b, c), add weight to Huse et al.'s suggestion that winter habitat selection in herring may not be precisely optimized (Huse et al. 2010). However, the consistency in SSS and PEA values seen across several consecutive years; the uniformly low current velocity characteristic of all wintering areas (Supplementary material Appendix 7 Fig. A6d) and the significant relationships detected between ψ and SST, SSS, PEA and current_vel (Fig. 3) indicate a degree of environmental control in wintering site selection, at least in some years (see Supplementary material Appendix 7 for a further discussion).

Temporal non-stationarity

One of the most interesting results of this study came through considering that the response of herring populations to intrinsic and extrinsic factors may alter through time. We found evidence for temporal non-stationarity in some cases (i.e. $distrib_{t-1}$, SST, SSS, PEA) (Fig. 3h); in addition to the $distrib_{t-1}$ – SSN relationship, we showed that the relative

influence of SST increased with the proportion of first-time winterers compared with older, age 8 to 13 individuals in the population (Table 3). This may reflect a heightened sensitivity of younger cohorts to environmental forcing, in combination with an increased tendency to follow traditions as fish get older, as suggested by Corten (2002) (explanation 1). At the population level, such a scenario would manifest in environmental factors, such as temperature, becoming unmasked as strong drivers of wintering area selection when there are fewer older fish to provide guidance.

If we make the assumption that the population truly responds differently to some environmental variables in different years, then our results could also stem from flexibility in population-wide environmental preferences during winter, as suggested by Óskarsson et al. (2009) and Huse et al. (2010) (explanation 2), or from age- or size-related variation in habitat preferences (Bailey et al. 1998, Bartolino et al. 2011) that would act to shape the population's collective reaction dependent on age-class structure (see results for SSS and PEA – Table 3) (explanation 3).

A fourth alternative involves the presence of interactions between density-dependent and environmental factors (explanation 4) (see Ciannelli et al. 2012 for an example). No clear density-dependent environmental responses were observed in our study, a finding in agreement with Maravelias et al. (2000a, b), who reported marked stability in relationships between occurrence, abundance and ambient environmental conditions across a four-year period of population decline in North Sea herring. Our inference is limited to fishery records, but the addition of spatially-consistent survey information would allow a more rigorous exploration of how biomass and environmental factors might interact to influence range size during wintering. Finally, the trends we observed may in part reflect the nature of our datasets (explanation 5). Fishing and survey coverage varied across years; a function of fisher behaviour, catch efficiency, funding and/or time availability and possibly other unknown, annually-varying factors our models did not capture directly (Supplementary material Appendix 1). The year_t term in the stationary models accounts for year-to-year variation in the outcome of such processes, yet with regard to the non-stationary models, tests including or omitting this term, or a temporal component in $\omega_{i,t}$, left parameter estimates essentially unchanged, suggesting that the time-varying patterns we see are not strongly dependent on data availability in a given year, and likely have some other basis.

This list of explanations is not exhaustive; all are plausible, and not necessarily mutually exclusive. However, we propose explanation 1 and/or 3 as most likely on empirical and theoretical grounds (Corten 1993, 2002). Opportunities for fine-tuning the dynamics of connections through time based on ecological or physiological knowledge are emerging through continued advancements in process-based models (Teal et al. 2015), and ongoing work on penalized complexity (PC) priors (Simpson et al. 2015). By combining such approaches, and using outputs from models like those presented here to guide parameterization, we see great potential for identifying the mechanistic fundaments of non-stationarity in ecological time series like ours (see also Supplementary material Appendix 9).

Fishing and predation

The direct impact of fishing on commercially harvested species, including herring, can be immense (Jackson et al. 2001, Dickey-Collas et al. 2010). It is increasingly recognized, however, that intense exploitation can reduce resilience to environmental change, and that fishing and climate can interact to influence long-term distribution patterns (Engelhard et al. 2011) and spatial structure (Ciannelli et al. 2013). In our models, we attempted to capture the impact of recent purse-seine fishing activity whilst considering local-scale environmental variables as additive factors only. This decision reflects an attempt to balance model complexity with meaningful ecological inference (Merow et al. 2014), and although this reduced our power to detect fishing–environment interactions directly, our expectation that increased fish_magnitude would act to reduce ψ at nearby locations in the following week was not met (Supplementary material Appendix 7 Fig. A7e, Table A1). This was surprising, given the known disruptive effects of fishing and vessel activity on the behaviour of pelagic species like herring (Vabø et al. 2002). As herring schools can show incredibly fast predator-evasion responses (Pitcher et al. 1996), we proffer that the weekly window we chose for fish_magnitude was too long, and the 5×5 km grid cell dimensions too large to capture the complexity in fleet dynamics (Branch et al. 2006), or the patchiness and speed of fishing–herring interactions and their cumulative effects over time. Investigating the scale-dependence of harvesting impacts, induced both by fishers and other predators (Similä 1997, Overholtz and Link 2007, Samarra and Foote 2015, Supplementary material Appendix 10) might provide insight into the trade-offs herring and other fishes face in adhering to migratory traditions, whilst avoiding predation in a previously risky arena.

Spatial prediction: implications for fishery management and fisheries

Our space-time models generated predictions that closely matched the observed occurrence patterns of wintering ISS herring. Whilst noting the limitations inherent in fishery and non-standardized survey datasets (Supplementary material Appendix 1, 9), by incorporating time-varying effects, and simultaneously considering spatially- and temporally-structured processes in our analysis, we were able to robustly estimate ψ and its uncertainty across our spatial domain, both within the time series (Fig. 4) and to held-out observations one-year ahead (Supplementary material Appendix 6, 9).

The capacity to predict distribution patterns in $t + 1$ has important implications for the spatial management of herring stocks throughout the North Atlantic, and for other species

exhibiting some homing tendency, for which our models could be easily adapted. In our example, predictive accuracy depended upon the strength of association between SSN and posterior mean estimates for $distrib_{t-1}$, estimated by the part_ns5 model (Table 3, Supplementary material Appendix 6). In three out of four years tested, correlation was strong, models were well calibrated and AUC values exceeded 0.95. Accuracy for the final year – 2013–2014, fell dramatically however, due most likely to two unusual mass-mortality events in a small fjord on Iceland's west coast that forced the 2012–2013 stock assessment estimate of SSN down, despite marked overlap in the area fished in 2011–2012 and 2012–2013 (Fig. 2, 5).

Although preliminary in nature, these results do highlight the potential of temporally non-stationary models in predicting states at one time point based on states at nearby time points. With rapid improvements in uncertainty estimation in stock assessment models for data-poor fish stocks (Kokkalis et al. 2017) coupled with the abundance of information-rich, point-referenced fishery datasets available, the time is ripe for further investigation into the demographic influences on migratory behaviour in other less-studied, commercially-important species. We believe the modelling framework outlined here is a solid starting point for such work.

Conclusions

Despite growing recognition of social learning as a key element in shaping collective movement behaviour, the evolutionary consequences of, and the mechanisms giving rise to, this phenomenon remain unclear for many taxa. Using wintering ISS herring for illustration, we searched for pattern in these behaviours by building space-time models for multi-year, point-referenced fishery and survey datasets and linking model output with time series of demographic parameters. Though we cannot pry too deeply into the 'fish mind', at least at present, our findings lend correlative support to the existence of collective memory in this long-lived, schooling species (Fernö et al 1998, Corten 2002), and suggest that wintering site selection may be tuned to population size and age-class structure, in concert with local-scale environmental factors and temporally-lagged prey distribution. The accuracy of our model predictions implies that considering such processes explicitly in spatiotemporal models could benefit spatial management strategies for fishes and other group-living animals that display a degree of conservatism in migratory behaviour.

Acknowledgements – We are indebted to the skippers and crews of the vessels from which our data came, and in particular, G. Jóhannsson and the crew aboard w/w Dröfn RE-35. Thanks to P. Reynisson for providing access to acoustic survey data and reports, and to H. Rue for hosting JIM at NTNU in Trondheim. We are grateful to D. Ramsey, M. Scroggie and R. Critchlow for suggestions on the statistical approach, I. and K. Macdonald for advice on figure layout and M. Mörsdorf, G. Heard, W. Butler, Z. Cságoly, D. Eme, N. McGinty, and S. Campana for stimulating discussions on ecological theory that shaped the direction of this paper. Comments from the Subject Editor and two reviewers greatly improved a previous version.

Funding – This work was supported by the Nordic Centre for Research on Marine Ecosystems and Resources Under Climate Change (NorMER), through the Norden Top-Level Research Initiative subprogram 'Effect Studies and Adaptation to Climate Change', and research grant 'Rannsóknarsjóðs síldarútvegsins 2013', awarded to JIM and GM from the Icelandic Association of Herring Fisheries. We thank V. Gunnarsson for his efforts in administering this latter fund.

References

Bailey, M. C. et al. 1998. Changes in the spatial distribution of autumn spawning herring (*Clupea harengus* L.) derived from annual acoustic surveys during the period 1984–1996. – ICES J. Mar. Sci. 55: 545–555.

Bartolino, V. et al. 2011. Ontogenetic and sex-specific differences in density-dependent habitat selection of a marine fish population. – Ecology 92: 189–200.

Berdahl, A. et al. 2013. Emergent sensing of complex environments by mobile animal groups. – Science 339: 574–576.

Berdahl, A. et al. 2016. A collective navigation hypothesis for homeward migration in anadromous salmonids. – Fish Fish. 17: 525–542.

Branch, T. A. et al. 2006. Fleet dynamics and fishermen behaviour: lessons for fisheries managers. – Can. J. Fish. Aquat. Sci. 63: 1647–1668.

Brännäs, E. 2014. Time-place learning and leader-follower relationships in Arctic charr *Salvelinus alpinus*. – J. Fish Biol. 84: 133–144.

Brown, C. 2001. Familiarity with the test environment improves escape responses in the crimson spotted rainbowfish, *Melanotaenia duboulayi*. – Anim. Cogn. 4: 109–113.

Brown, C. 2015. Fish intelligence, sentience and ethics. – Anim. Cogn. 18: 1–17.

Cameletti, M. et al. 2013. Spatio-temporal modeling of particulate matter concentration through the SPDE approach. – AStA Adv. Stat. Anal. 97: 109–131.

Ciannelli, L. et al. 2012. Non-additive and non-stationary properties in the spatial distribution of a large marine fish population. – Proc. R. Soc. B 279: 3635–3642.

Ciannelli, L. et al. 2013. Theory, consequences and evidence of eroding population spatial structure in harvested marine fishes: a review. – Mar. Ecol. Prog. Ser. 480: 227–243.

Conradt, L. and Roper, T. J. 2005. Consensus decision making in animals. – Trends Ecol. Evol. 20: 449–456.

Corten, A. 1993. Learning processes in herring migrations. – ICES Document C.M. 1993/H:18 Pelagic Fish Committee, Copenhagen, Denmark.

Corten, A. 1999. A proposed mechanism for the Bohuslan herring periods. – ICES J. Mar. Sci. 56: 207–220.

Corten, A. 2002. The role of "conservatism" in herring migrations. – Rev. Fish Biol. Fish. 11: 339–361.

Couzin, I. D. et al. 2011. Uninformed individuals promote democratic consensus in animal groups. – Science 334: 1578–1580.

Crainiceanu, C. M. et al. 2005. Bayesian analysis for penalized spline regression using WinBUGS. – J. Stat. Softw. 14: 1–24.

Dawid, A. 1984. Statistical theory: the prequential approach (with discussion). – J. R. Stat. Soc. A 147: 278–292.
Dawkins, M. 2001. Who needs conciousness? – Anim. Welfare 10: 19–29.
Dickey-Collas, M. et al. 2010. Lessons learned from stock collapse and recovery of North Sea herring: a review. – ICES J. Mar. Sci. 67: 1875–1886.
Dormann, C. F. et al. 2013. Collinearity: a review of methods to deal with it and a simulation study evaluating their performance. – Ecography 36: 27–46.
Engelhard, G. H. et al. 2011. Nine decades of North Sea sole and plaice distribution. – ICES J. Mar. Sci. 68: 1090–1104.
Fernö, A. T. et al. 1998. The challenge of the herring in the Norwegian sea: making optimal collective spatial decisions. – Sarsia 83: 149–167.
Fisher, J. and Frank, K. 2004. Abundance–distribution relationships and conservation of exploited marine fishes. – Mar. Ecol. Prog. Ser. 279: 201–213.
Fretwell, S. D. and Lucas, H. L. J. 1969. On territorial behaviour and other factors influencing habitat distribution in birds. – Acta Biotheor. 19: 16–36.
Gelman, A. 2008. Scaling regression inputs by dividing by two standard deviations. – Stat. Med. 27: 2865–2873.
Gelman, A. et al. 2008. A weakly informative default prior distribution for logistic and other regression models. – Ann. Appl. Stat. 2: 1360–1383.
Gneiting, T. and Raftery, A. E. 2007. Strictly proper scoring rules, prediction, and estimation. – J. Am. Stat. Assoc. 102: 359–378.
Gneiting, T. et al. 2007. Probabilistic forecasts, calibration and sharpness. – J. R. Stat. Soc. B 69: 243–268.
Held, L. et al. 2010. Posterior and cross-validatory predictive checks: a comparison of MCMC and INLA. – In: Kneib, T. and Tutz, G. (eds), Statistical modelling and regression structures. Springer, pp. 91–110.
Held, U. et al. 2012. Validating and updating a risk model for pneumonia – a case study. – BMC Med. Res. Methodol. 12: 99.
Helfman, G. S. and Schultz, E. T. 1984. Social transmission of behavioural traditions in a coral reef fish. – Anim. Behav. 32: 379–384.
Hjøllo, S. S. et al. 2012. Modelling secondary production in the Norwegian Sea with a fully coupled physical/primary production/individual-based *Calanus finmarchicus* model system. – Mar. Biol. Res. 6: 508–526.
Höglund, H. 1955. Swedish herring tagging experiments, 1949–1953. – Rapports et procès-verbaux des réunions/Conseil permanent international pour l'exploration de la mer 40: 19–29.
Hotta, T. et al. 2015. The use of multiple sources of social information in contest behaviour: testing the social cognitive abilities of a cichlid fish. – Front. Ecol. Evol. 3: 1–9.
Huse, G. 2016. A spatial approach to understanding herring population dynamics. – Can. J. Fish. Aquat. Sci. 73: 177–188.
Huse, G. et al. 2002. Modelling changes in migration pattern of herring: collective behaviour and numerical domination. – J. Fish Biol. 60: 571–582.
Huse, G. et al. 2010. Establishment of new wintering areas in herring co-occurs with peaks in the "first time/repeat spawner" ratio. – Mar. Ecol. Prog. Ser. 409: 189–198.
Iles, T. D. and Sinclair, M. 1982. Atlantic herring: stock discreteness and abundance. – Science 215: 627–633.
Illian, J. B. et al. 2013. Fitting complex ecological point process models with integrated nested Laplace approximation. – Methods Ecol. Evol. 4: 305–315.
Jackson, J. B. C. et al. 2001. Historical overfishing and the recent collapse of coastal ecosystems. – Science 293: 629–638.
Jakobsson, J. 1969. Síld og sjávarhiti. – In: Einarsson, M. Á. (ed.), Hafásinn. Reykjavík, Iceland, pp. 497–511.
Kao, A. B. and Couzin, I. D. 2014. Decision accuracy in complex environments is often maximized by small group sizes. – Proc. R. Soc. B 81: 20133305.
Kao, A. B. et al. 2014. Collective learning and optimal consensus decisions in social animal groups. – PLoS Comput. Biol. 10: e1003762.
Keith, S. A. and Bull, J. W. 2017. Animal culture impacts species' capacity to realise climate-driven range shifts. – Ecography 40: 296–304.
Kokkalis, A. et al. 2017. Estimating uncertainty of data limited stock assessments. – ICES J. Mar. Sci. 74: 69–77.
Krainski, E. T. et al. 2016. The R-INLA tutorial on SPDE models. – Norwegian Univ. of Science and Technology, Trondheim, Norway.
Langård, L. et al. 2014. State-dependent spatial and intra-school dynamics in pre-spawning herring *Clupea harengus* in a semi-enclosed ecosystem. – Mar. Ecol. Prog. Ser. 501: 251–263.
Levin, S. 1992. The problem of pattern and scale in ecology. – Ecology 73: 1943–1967.
Libungan, L. A. et al. 2015. Otolith shape: a population marker for Atlantic herring *Clupea harengus*. – J. Fish Biol. 86: 1377–1395.
Lindegren, M. et al. 2011. Interacting trophic forcing and the population dynamics of herring. – Ecology 92: 1407–1413.
Lindgren, F. et al. 2011. An explicit link between Gaussian fields and Gaussian Markov random fields: the stochastic partial differential equation approach. – J. R. Stat. Soc. B 73: 423–498.
Lobo, J. M. et al. 2008. AUC: a misleading measure of the performance of predictive distribution models. – Global Ecol. Biogeogr. 17: 145–151.
Logemann, K. et al. 2013. The circulation of Icelandic waters – a modelling study. – Ocean Sci. 9: 931–955.
Loots, C. et al. 2010. What controls the spatial distribution of the North Sea plaice spawning population? Confronting ecological hypotheses through a model selection framework. – ICES J. Mar. Sci. 67: 244–257.
MacCall, A. D. 1990. Dynamic geography of marine fish populations. – Univ. of Washington Press.
Macdonald, J. I. et al. 2017. Data from: Can collective memories shape fish distributions? A test, linking space-time occurrence models and population demographics. – Dryad Digital Repository, <http://dx.doi.org/10.5061/dryad.9v46k>.
Mackinson, S. et al. 1999. Cross-scale observations on distribution and behavioural dynamics of ocean feeding Norwegian spring-spawning herring (*Clupea harengus* L.). – ICES J. Mar. Sci. 56: 613–626.
Makris, N. C. et al. 2009. Critical population density triggers rapid formation of vast oceanic fish shoals. – Science 323: 1734–1737.
Maravelias, C. D. and Reid, D. G. 1997. Identifying the effects of oceanographic features and zooplankton on prespawning herring abundance using generalized additive models. – Mar. Ecol. Prog. Ser. 147: 1–9.

Maravelias, C. D. et al. 2000a. Seabed substrate, water depth and zooplankton as determinants of the prespawning spatial aggregation of North Atlantic herring. – Mar. Ecol. Prog. Ser. 195: 249–259.
Maravelias, C. D. et al. 2000b. Modelling spatio-temporal effects of environment on Atlantic herring, *Clupea harengus*. – Environ. Biol. Fish. 58: 157–172.
McQuinn, I. 1997. Metapopulations and the Atlantic herring. – Rev. Fish Biol. Fish. 7: 297–329.
Merkle, J. A. et al. 2014. A memory-based foraging tactic reveals an adaptive mechanism for restricted space use. – Ecol. Lett. 17: 924–931.
Merow, C. et al. 2014. What do we gain from simplicity versus complexity in species distribution models? – Ecography 37: 1267–1281.
Misund, O. et al. 1997. Migration behaviour of Norwegian spring spawning herring when entering the cold front in the Norwegian Sea. – Sarsia 82: 107–112.
Nøttestad, L. and Axelsen, B. E. 1999. Herring schooling manoeuvres in response to killer whale attacks. – Can. J. Fish. Aquat. Sci. 77: 1540–1546.
Nøttestad, L. et al. 2007. Herring at the Arctic front: influence of temperature and prey on their spatio-temporal distribution and migration. – Mar. Ecol. 28: 123–133.
Ono, K. et al. 2016. Space-time investigation of the effects of fishing on fish populations. – Ecol. Appl. 26: 392–406.
Óskarsson, G. J. and Reynisson, P. 2014. Results of acoustic measurements of Icelandic summer-spawning herring in the winter 2013/2014. – Working Document no. 20, ICES North Western Working Group, 24 April–1 May 2014, Copenhagen, Denmark.
Óskarsson, G. J. et al. 2009. Variation in spatial distribution and migration of Icelandic summer-spawning herring. – ICES J. Mar. Sci. 66: 1762–1767.
Overholtz, W. J. and Link, J. S. 2007. Consumption impacts by marine mammals, fish, and seabirds on the Gulf of Maine – Georges Bank Atlantic herring (*Clupea harengus*) complex during the years 1977–2002. – ICES J. Mar. Sci. 64: 83–96.
Parrish, J. K. et al. 2002. Self-organized fish schools: an examination of emergent properties. – Biol. Bull. 202: 296–305.
Perry, A. et al. 2005. Climate change and distribution shifts in marine fishes. – Science 308: 1912–1915.
Petitgas, P. et al. 2006. The entrainment hypothesis: an explanation for the persistence and innovation in spawning migrations and life cycle spatial patterns. – ICES Document C.M. 2006/B:07, Copenhagen, Denmark.
Pettit, L. 1990. The conditional predictive ordinate for the normal distribution. – J. R. Stat. Soc. B 52: 175–184.
Pitcher, T. J. et al. 1996. Adaptive behaviour of herring schools in the Norwegian Sea as revealed by high-resolution sonar. – ICES J. Mar. Sci. 53: 449–452.
Planque, B. et al. 2011. Understanding what controls the spatial distribution of fish populations using a multi-model approach. – Fish. Oceanogr. 20: 1–17.
Putman, N. F. et al. 2013. Evidence for geomagnetic imprinting as a homing mechanism in pacific salmon. – Curr. Biol. 23: 312–316.
Reebs, S. 2000. Can a minority of informed leaders determine the foraging movements of a fish shoal? – Anim. Behav. 59: 403–409.
Rindorf, A. and Lewy, P. 2006. Warm, windy winters drive cod north and homing of spawners keeps them there. – J. Appl. Ecol. 43:445–453.
Roos, M. and Held, L. 2011. Sensitivity analysis in Bayesian generalized linear mixed models for binary data. – Bayesian Anal. 6: 259–278.
Rue, H. et al. 2009. Approximate Bayesian inference for latent Gaussian models by using integrated nested Laplace approximations. – J. R. Stat. Soc. B 71: 319–392.
Samarra, F. I. P. and Foote, A. D. 2015. Seasonal movements of killer whales between Iceland and Scotland. – Aquat. Biol. 24: 75–79.
Schmid, C. H. and J. L. Griffith. 2005. Multivariate classification rules: calibration and discrimination. – In: Armitage, P. and Colton, T. (eds), Encyclopedia of biostatistics, 2nd ed. John Wiley and Sons, pp. 3491–3497.
Shepherd, T. D. and Litvak, M. K. 2004. Density-dependent habitat selection and the ideal free distribution in marine fish spatial dynamics: considerations and cautions. – Fish Fish. 5: 141–152.
Silveira, M. M. et al. 2015. Dusky damselfish *Stegastes fuscus* relational learning: evidences from associative and spatial tasks. – J. Fish Biol. 86: 1109–1120.
Similä, T. 1997. Sonar observations of killer whales (*Orcinus orca*) feeding on herring schools. – Aquat. Mamm. 23: 119–126.
Simons, A. 2004. Many wrongs: the advantage of goup navigation. – Trends Ecol. Evol. 19: 453–455.
Simpson, D. P. et al. 2015. Penalising model component complexity: a principled, practical approach to constructing priors. – arXiv 1403.4630.
Slotte, A. 1999. Differential utilization of energy during wintering and spawning migration in Norwegian spring-spawning herring. – J. Fish. Biol. 54: 338–355.
Spiegelhalter, D. J. et al. 2002. Bayesian measures of model complexity and fit. – J. R. Stat. Soc. B 64: 583–639.
Sumpter, D. J. T. and Pratt, S. C. 2009. Quorum responses and consensus decision making. – Phil. Trans. R. Soc. B 364: 743–753.
Sumpter, D. J. T. et al. 2008. Consensus decision making by fish. – Curr. Biol. 18: 1773–1777.
Surowiecki, J. 2004. The wisdom of crowds. – Random House.
Teal, L. R. et al. 2015. Physiology-based modelling approaches to characterize fish habitat suitability: their usefulness and limitations. – Estuar. Coast. Shelf Sci. doi: 10.1016/j.ecss.2015.11.014
Thorlindsson, T. 1988. The skipper effect in the Icelandic herring fishery. – Hum. Organ. 47: 199–212.
Vabø, R. et al. 2002. The effect of vessel avoidance of wintering Norwegian spring spawning herring. – Fish. Res. 58: 59–77.
Ward, A. J. et al. 2011. Fast and accurate decisions through collective vigilance in fish shoals. – Proc. Natl Acad. Sci. USA 108: 2312–2315.
Ward, E. J. et al. 2015. Using spatiotemporal species distribution models to identify temporally evolving hotspots of species co-occurrence. – Ecol. Appl. 25: 2198–2209.
Woillez, M. et al. 2007. Indices for capturing spatial patterns and their evolution in time, with application to European hake (*Merluccius merluccius*) in the Bay of Biscay. – ICES J. Mar. Sci. 64: 537–550.
Wynne-Edwards, V. C. 1962. Animal dispersion in relation to social behaviour. – Oliver and Boyd.
Zorn, C. 2005. A solution to separation in binary response models. – Polit. Anal. 13: 157–170.
Zuur, A. et al. 2009. Mixed effects models and extensions in ecology with R. – Springer.

Supplementary material (Appendix ECOG-03098 at <www.ecography.org/appendix/ecog-03098>). Appendix 1–10.

Appendix 1. Detection and sampling coverage

Detection

Detection probability for our datasets is essentially = 1, notwithstanding potential recording errors. Occurrence records were included only if $c > 0$ tonnes, and the acoustic output enables accurate identification of herring schools based on area backscatter strength (Jakobsson et al. 1993; Guðmundsdóttir et al. 2007), making false absences highly unlikely. The spatiotemporal distribution of fishing effort in the Icelandic winter purse seine herring fishery is not random however, and has varied markedly over the time series considered here (ICES 2015). Early in the season, fishing locations are often selected based upon knowledge of previous overwintering areas. As the season progresses, information on recent landings, reports from other fishing vessels and input from the MRI acoustic surveys (which typically coincide with the beginning of the fishing season), drive fishing behaviour. Similarly, the location of the acoustic survey tracks is not consistent among years (Guðmundsdóttir et al. 2007; ICES 2015), with the level of survey effort reflecting funding, time availability, weather conditions as well as information exchange between MRI and active fishing vessels (Óskarsson and Pálsson 2015). This situation likely resulted in some level of sampling bias, although given the searching capacity of the purse seine fleet (Guðmundsdóttir and Sigurðsson 2004; Óskarsson et al. 2009), and the wide spatial coverage of the acoustic surveys, we consider this bias to be minimal (see below). Additionally, such bias is generally of lower concern for binomial occurrence models with near perfect detection, as it only acts to reduce precision of the estimation in less-sampled regions, rather than biasing the estimation process itself (Phillips et al. 2009; Guillera-Arroita et al. 2015).

Sampling coverage

It could be argued that the fishery and survey data used here may be biased and may not reflect the true extent of the herring distribution in a given season. We contend that such bias would be minimal for three reasons. First, the fishing fleet for Icelandic herring, which currently consists of 15 large vessels, conducts extensive searches for wintering herring schools each season, covering a substantial portion of the stock's distributional range which is fully captured within the Icelandic exclusive economic zone (EEZ) (Óskarsson et al. 2009; author's personal observation). Second, the annual acoustic surveys, although varying in sampling intensity each year, have covered a large region of the Icelandic EEZ in all years from the mid-1990s onwards. Thirdly, the close working relationship between MRI and the fishing companies results in constant information exchange regarding the distribution of the herring schools during the autumn/winter fishing period. Hence, we contend that although the full extent of the realized distribution may not be captured by the fishery and survey data, it does reflect the major trends in overwintering distribution over the 1991_92 to 2013_14 period. Furthermore, given the near perfect detection in our dataset, there is no need to make assumptions about capturing the full realised niche during the overwintering period. Rather, we use the data we have to build the models.

References

Guðmundsdóttir, A. and Sigurðsson, Þ. 2004. The autumn and winter fishery and distribution of the Icelandic summer-spawning herring during 1978–2003. Report 104, Marine Research Institute, Reykjavík, Iceland.

Guðmundsdóttir, A., Óskarsson, G.J. and Sveinbjörnsson, S. 2007. Estimating year-class strength of Icelandic summer-spawning herring on the basis of two survey methods. ICES J. Mar. Sci. 64: 1182‑1190.

Guillera-Arroita, G., Lahoz-Monfort, J.J., Elith, J., Gordon, A. Kujala, H. Lentini, P.E., McCarthy, M.A., Tingley, R. and Wintle, B.A. 2015. Is my species distribution model fit for purpose? Matching data and models to applications. Global Ecol. Biogeogr. 24: 276–292.

ICES. 2015. Report of the North Western Working Group. 28 April - 5 May 2015. ICES CM 2015/ACOM:07, Copenhagen, Denmark.

Jakobsson, J., Guðmundsdóttir, A. and Stefánsson, G. 1993. Stock-related changes in biological parameters of the Icelandic summer-spawning herring. Fish. Oceanogr. 2: 260–277.

Óskarsson, G.J. and Pálsson. J. 2015. Estimation on number-at-age of the catch of Icelandic summer-spawning herring in 2014/2015 fishing season and the development of *Ichthyophonus hoferi* infection in the stock. Working Document No. 2, ICES North Western Working Group, 28 April - 5 May 2015, Copenhagen, Denmark.

Óskarsson, G.J., Guðmundsdóttir, A. and Sigurðsson, Þ. 2009. Variation in spatial distribution and migration of Icelandic summer-spawning herring. ICES J. Mar. Sci. 66: 1762–1767.

Phillips, S.J., Dudík, M., Elith, J., Graham, C.H., Lehmann, A., Leathwick, J. and Ferrier, S. 2009. Sample selection bias and presence-only distribution models: implications for background and pseudo-absence data. Ecol. Appl. 19: 181–197.

Appendix 2. Details and R code for constructing the 'distrib$_t$' and 'counts$_t$' variables and calculating the spatial similarity index (SSI)

Appendix 2.1. Construction of distrib$_t$ and counts$_t$ layers

To construct the distrib$_t$ layers, we defined an area of interest that encompassed all records in our dataset, then divided this region into 0.1° longitude × 0.05° latitude (i.e. ~ 5 × 5 km) grid cells. Next, for each of the 23 years t = 1, 2, …, T, we summed the number of occurrence records in each cell k, denoted $r_{k,t}$. If $r_{k,t} > 0$, then distrib$_{k,t}$ was coded as 1, otherwise 0. We used these results to produce annual gridded maps of occurrence (distrib$_t$) across our study region (Fig. 2a–c).

Using the same spatial grid, we then computed the counts$_t$ variable which reflects the number of occurrence records (i.e. successful fishing events) in each cell in each year, whilst also accounting for potential joining/splitting interactions among herring schools occupying nearby cells (Mackinson et al. 1999; Nøttestad and Axelsen 1999). For each grid cell k, in year t, counts$_{k,t}$ is the sum of $r_{k,t}$ and the mean number of occurrence records in all 1st order neighbouring cells $n_{k,t,j}$ (j = 1, 2, …, 8), excluding the central cell (eq. 1) (see Appendix 2.3 for R code). To allow for comparisons among years, we converted counts$_{k,t}$ to a percentage of the total number of occurrences recorded across the whole study region in each year, denoted occ_t.

$$\text{counts}_{k,t} = \frac{100}{occ_t}\left(r_{k,t} + \frac{\sum_{j=1}^{8} n_{k,t,j}}{8}\right) \qquad \text{(eq. 1)}$$

Like distrib$_t$, we created annual gridded maps of counts$_t$ for each year of the time series (Fig. 2d, e). The counts$_t$ variable can be considered a proxy for herring abundance that is less prone to error than using landings data directly, as catch rates by vessels using purse seine gears are inherently variable (Hilborn and Ledbetter 1985; Ruttan and Tyedmers 2007; Vázquez-Rowe and Tyedmers 2013).

Appendix 2.2. Calculation of the SSI

For year $t = 2, 3, \ldots, T$, we sum the grid cell values from the gridded occurrence map from the previous year ($distrib_{t-1}$) and those from the current year ($distrib_t$). Where grid cell counts = 2, this cell has been occupied in year t-1 and year t. We then divide this number by the total number of occupied cells in t-1 or t, and convert to a percentage. This last step captures the degree of expansion and contraction in the area occupied from year to year. Next, we calculate the distance change (km) in the centre of gravity (ΔCOG) of the stock between t-1 and t. The COG for fishing year t can be defined as the mean location of the population for that year (Wolliez et al. 2007), and was estimated here by weighting each fishing location by the catch recorded from that location in that year, giving all fishing events equal weight (see eq. 2). For each year t,

$$\mathrm{COG} = \frac{\sum_{i=1}^{M} x_i c_i}{\sum_{i=1}^{M} c_i} \qquad \text{(eq. 2)}$$

where M is the total number of catch locations, x_i is the geographic position (i.e., longitude and latitude) of location i and c_i is the catch (tonnes) at location i. Dividing by ΔCOG down weights the SSI when the distributional centroid has changed dramatically between one year and the next. This calculation generates an 'SSI_overlap' value (see Appendix 2.3). Next, we calculate Pearson's r between the $counts_{t-1}$ and $counts_t$ layers across all grid cells. This captures the change in density of occurrence records from year to year, and generates the 'SSI_pearson' value. Finally, we sum the 'SSI_overlap' and 'SSI_pearson' value to create an 'SSI_estimate' for each year (see Appendix 2.3).

Why use 1st order neighbours?

The decision to use only 1st order neighbouring cells in the calculation for $counts_t$, rather than an autoregressive model, can justified for two reasons. First, this way we have direct control over the distance considered, which can then be tuned to relevant ecological processes. The maximum distance from the outer edge of one of our grid cells to the outer edge of a neighbouring cell is ~ 10 km – a distance representative of the scale at which school joining and splitting behaviour often operates (Mackinson et al. 1999). Second, allowing more flexibility in the numbers of neighbouring cells included in the calculations makes more assumptions outside the spatial range of the occurrence records. In effect, our approach can be viewed as quite conservative, as it only estimates values one-cell removed from where the data actually are. We stress however, that the distance considered in the calculation of $counts_t$ can be easily adjusted if there are reasons to believe that ecological processes are acting at finer or coarser scales.

Excluding catch biomass in the calculation of $counts_t$

Catch biomass (c) for each fishing event can vary based on vessel-, skipper-, gear- and weather-related factors in addition to the actual amount of herring present at a particular location (Branch et al. 2006; Vázquez-Rowe and Tyedmers 2013). Given that we did not explicitly measure the first four of these sources of variability in this study, in addition to the inherent difficulties in accurately capturing these effects in any case (see Squires and Kirkley 1999), we chose to take a conservative approach in computing $counts_t$ – i.e. based on the

number of occurrences per grid cell, per year. We also gave equal weight to occurrence records with $0 < c < 1$ tonne and all $c \geq 1$ tonne, as differences in c may arise through interactions among the aforementioned factors that are unrelated to the point abundance of herring per se. Through this approach we hoped to minimize bias associated with these unquantified sources of variability.

Appendix 2.3. Data and code repository

The folder 'Spatial similarity index.zip' (available from the Dryad Digital Repository: http://dx.doi.org/10.5061/dryad.9v46k) contains R code and data for constructing the $distrib_t$ and countst variables and for calculating the spatial similarity index (SSI), using catch data from the Icelandic winter herring fishery for illustration.

Folder name: 'Spatial similarity index.zip'

Relevant files/subfolders:-

i) 'Create counts(t) rasters.R' (R code to compute and map the $counts_t$ variable).
ii) 'Counts(t) rasters' (folder to store $counts_t$ rasters).
iii) 'Spatial similarity index calculation.R' (R code to compute and map the $distrib_t$ variable and calculate the SSI).
iv) 'SSI_calc_stats.csv' (.csv data file containing 'SSI_overlap 'SSI_pearson' and 'SSI_estimate' values by year, as output from the R script in iii).
v) 'COG_change.csv' (.csv data file containing information on ΔCOG between consecutive years).
vi) 'catch_data.csv' (.csv data file containing georeferenced catch records from the winter herring fishery between 1991_1992 and 2013_14, referenced by day, month and year). Here, 'seine' = the purse-seine shot number, 'sild' = landings per shot (tonnes), and 'pres_abs' denotes if herring were encountered in a given shot (1 = encountered).

References

Branch, T.A., Hilborn, R., Haynie, A.C., Fay, G., Flynn, L. Griffiths, J., Marshall, K.N., Randall, J.K., Scheuerell, J.M., Ward, E.J. and Young, M. 2006. Fleet dynamics and fishermen behavior: lessons for fisheries managers. – Can. J. Fish. Aquat. Sci. 63: 1647–1668.

Hilborn, R. and Ledbetter, M. 1985. Determinants of catching power in the British Columbia salmon purse seine fleet. Can. J. Fish. Aquat. Sci. 42: 51–56.

Mackinson, S., Nøttestad, L., Guénette, S., Pitcher, T., Misund, O.A. and Fernö, A 1999. Cross-scale observations on distribution and behavioural dynamics of ocean feeding Norwegian spring-spawning herring (*Clupea harengus* L.). ICES J. Mar. Sci. 56: 613–626.

Nøttestad, L. and Axelsen, B.E. 1999. Herring schooling manoeuvres in response to killer whale attacks. Can. J. Fish. Aquat. Sci. 77: 1540–1546.

Ruttan, L.M. and Tyedmers, P.H. 2007. Skippers, spotters and seiners : analysis of the "skipper effect" in US menhaden (*Brevoortia* spp.) purse-seine fisheries. Fish. Res.

83: 73–80.
Squires, D. and Kirkley, J. 1999. Skipper skill and panel data in fishing industries. Can. J. Fish. Aquat. Sci. 56: 2011–2018.
Vázquez-Rowe, I. and Tyedmers, P. 2013. Identifying the importance of the “skipper effect” within sources of measured inefficiency in fisheries through data envelopment analysis (DEA). Mar. Policy 38: 387–396.
Woillez, M., Poulard, J.-C., Rivoirard, J., Petitgas, P. and Bez, N. 2007. Indices for capturing spatial patterns and their evolution in time, with application to European hake (*Merluccius merluccius*) in the Bay of Biscay. ICES J. Mar. Sci. 64: 537–550.

Appendix 3. Additional information on covariates for the space-time models

Spatial memory

Our aim was to capture the main features represented in the SSI (Fig. 2, Appendix 2) in covariates that could be used for input into spatially-explicit models to predict seasonally-varying occurrence patterns. We employed the $distrib_t$ and $counts_t$ variables described in the Material and Methods under 'Capturing shifting distributions: a spatial similarity index' for this purpose (see also Appendix 2 for calculation details). By using the layers created for the previous year (i.e. *t*-1), we defined two covariates that represent the occurrence pattern (i.e. $distrib_{t-1}$) and density of occurrence records (i.e. $counts_{t-1}$) one-year earlier (see Fig. A1 for examples of rasters for 2001_02).

These two covariates are able to test the following two hypotheses. 1) Does the occurrence of herring at a particular location in year *t*-1 (represented by the $distrib_{t-1}$ covariate) influence the probability of occurrence in year *t*? 2) Does the relative density of occurrences at a particular location in year *t*-1 (represented by the $counts_{t-1}$ covariate) influence the probability of occurrence in *t*? That is, are herring here in *t* because they were here in numbers in *t*-1 – akin, to a density-dependent effect with one-year lag?

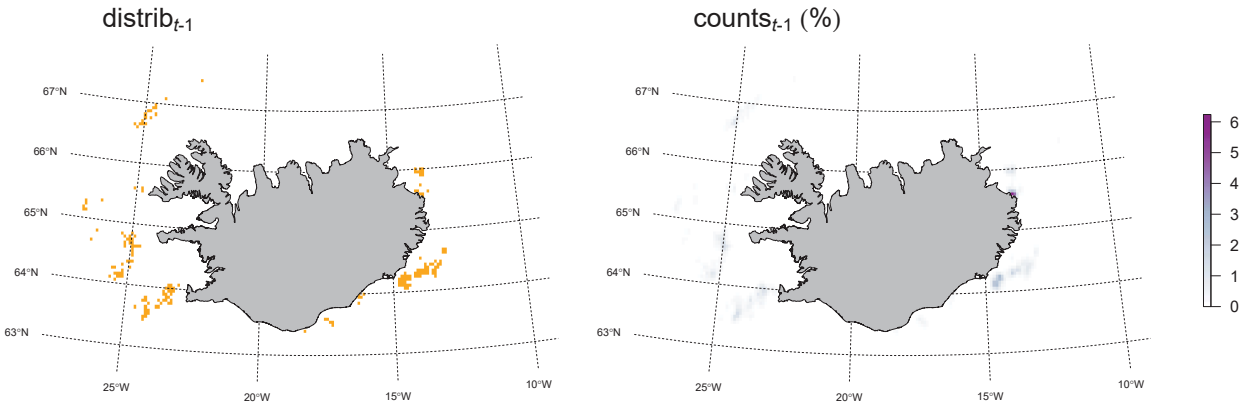

Fig. A1. Rasters of spatial memory covariates for 2001 2002. In $distrib_{t-1}$, orange cells indicate those occupied the previous year (i.e. 2000 2001). See Table 1 in main text for units and derivation for these covariates.

Dynamic environmental variables

As temperature, salinity and flow velocity can impact strongly on herring distribution during several phases of the species' life history (Sinclair and Iles 1985; Maravelias et al. 2000a,b and references therein; Toresen and Østvedt 2000; Lindegren et al. 2011; Bartolino et al. 2014), information on sea surface temperature - SST (°C), sea surface salinity - SSS (psu), and the east-west (U-component) and north-south (V-component) flow vectors (m s^{-1}) were extracted from the CODE model (Logemann et al. 2013) at three spatial scales (i.e. 1 × 1 km, 4 × 4 km and 8 × 8 km buffer distances around each fishing/survey record) and two temporal scales (i.e. day of record, mean of the preceding 7 days) (Fig. A2). From these data,

three new variables were created (at the same scales) to capture mixing processes through the water column that may influence the behaviour of wintering herring: the potential energy anomaly - PEA (kg m^{-1} s^{-2}) a proxy for stratification, and defined as the energy required to vertically mix the water column so that the density is uniform from surface to bottom (Planque et al. 2006; Huret et al. 2013), the temperature gradient between surface and bottom waters - change (°C), and the mean absolute values of the U and V flow vectors in surface waters - current vel (m s^{-1}) (Fig. A2).

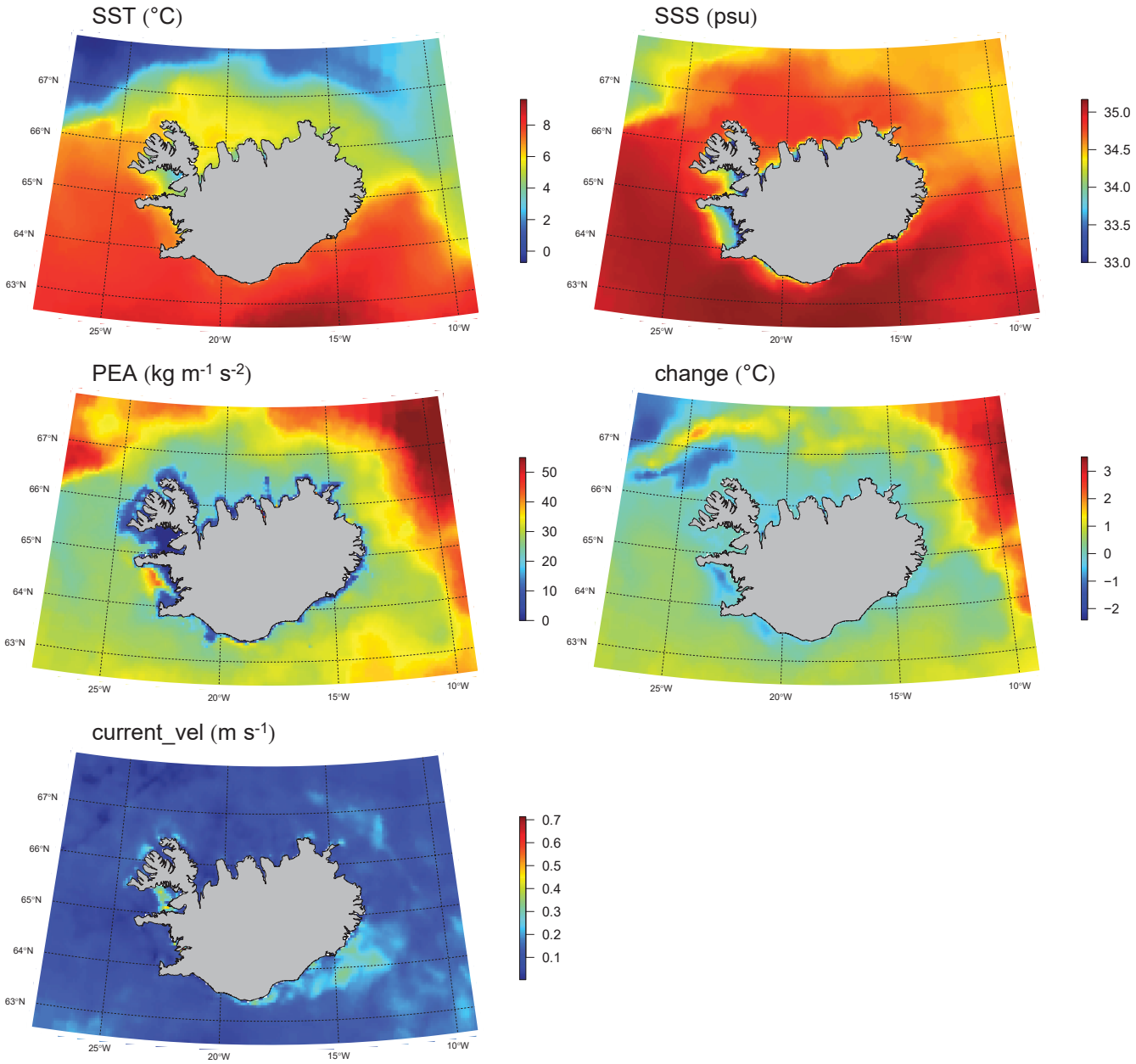

Fig. A2. Rasters of dynamic environmental covariates for 2001_2002. See Table 1 in main text for derivation. For model fitting, these covariates were extracted from the CODE ocean model (Logemann et al. 2013) at 1×1 km resolution on the day of each catch or survey record (see text above). However, rasters presented here are at 0.1° longitude × 0.05° latitude resolution and represent mean grid cell values across the 2001_2002 season. This is the common scale used for spatial prediction for all covariates (see the Material and methods in the main text for further details).

The highest resolution data obtainable from the CODE (i.e. 1 × 1 km grid, day of record) most closely matched both the area sampled by, and the timing of each fishing or survey record, providing the most realistic representation possible of the ambient environment experienced by the school at that time and place. In light of this, in conjunction with the high collinearity found among the spatial and temporal scales considered for each covariate (Pearson's $r > 0.8$ in all cases), we decided to extract data at 1 × 1 km on the day of the record. The CODE model assimilates observational data from CTD (conductivity, temperature, depth) profiles and river discharge data from 46 Icelandic watersheds into its simulation, and excellent concordance was found between modelled and observed temperature, salinity and flow fields across our study region (see Table 1 in Logemann et al. 2013).

Static environmental variables

As both previous work and visual examination of our dataset suggest that herring may favour specific bottom topography during pre-spawning (Maravelias et al. 2000b) and wintering phases (MRI, unpublished data), we extracted information on depth: bottom_depth (m) and slope: slope (degrees) of the sea-floor from the GEBCO website. These data were available at 30 arcsec resolution around each fishing/survey record. As wintering ISS herring have been often been found close to the coast over the past three decades (Óskarsson et al. 2009), we calculated distance to shore: dist_to_shore (km) from each record using the 'gDistance' function in the 'rgeos' package in R (Fig. A3).

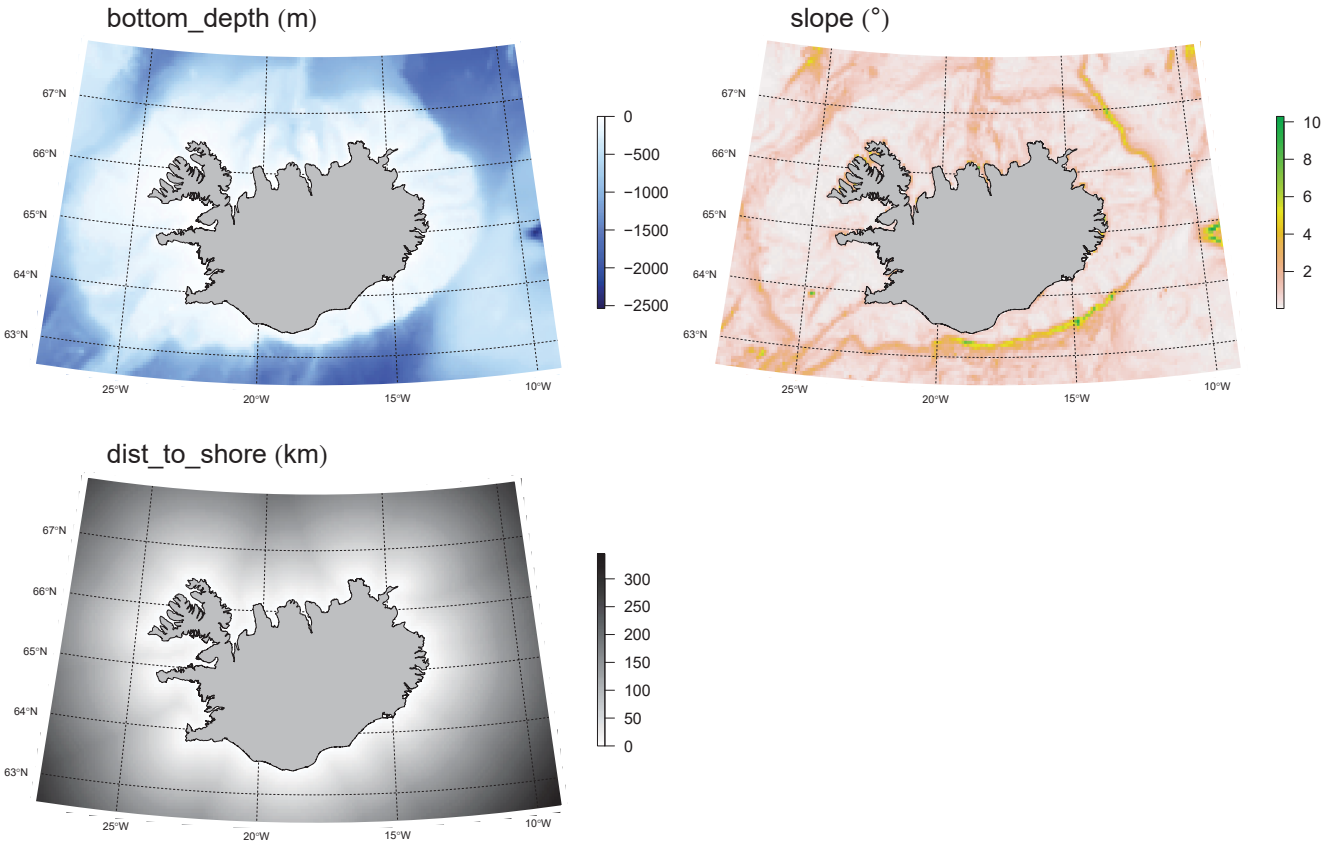

Fig. A3. Rasters of static environmental covariates. See Table 1 for derivation. Rasters are presented at 0.1° longitude × 0.05° latitude resolution.

Zooplankton biomass in August

Although herring hardly feed during the winter (Slotte 1999), adult stages of the zooplankter *Calanus finmarchicus* are a major prey item for herring in the North Atlantic during summer (Holst et al. 1997; Dalpadado et al. 2000; Gíslason and Astthorsson 2002; Prokopchuk and Sentyabov 2006). Hence, we suggest that regions of high summer *C. finmarchicus* biomass is likely be a feeding hotspot for pre-wintering ISS. Further, we propose that selection of wintering areas may be geographically close to where these hotspots are located. To test this, we extracted georeferenced mean August biomass estimates for adult *C. finmarchicus* (i.e. C4, CS, C6 stages), integrated in the upper 400 m of the water column at 20 × 20 km horizontal resolution, from the output of a *C. finmarchicus* IBM – CF_Aug (µg C m^{-2}) (Hjøllo et al. 2012) (Fig. A4). We used this dataset as a proxy for late summer ISS feeding distribution, in lieu of spatially-referenced fishing or survey data that were not available for that time of year during the time series. Temporal coverage of Hjøllo et al.'s simulation spanned 1995 to 2007, and missing values for other years in our dataset were imputed using predictive mean matching in an approximate Bayesian framework in the 'mi' package in R (see below for further details).

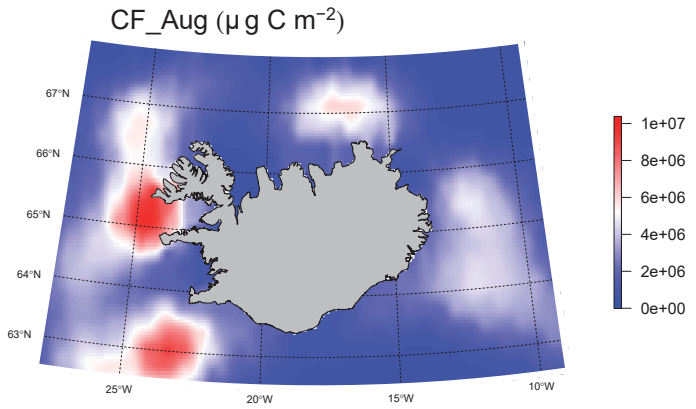

Fig. A4. Raster of mean C. finmarchicus biomass for August 2001. See Table 1 for derivation. Layers were available at 20 × 20 km resolution, and we used this resolution for data extraction and model fitting. Prediction was made to the 0.1° longitude × 0.05° latitude grid presented here, with data resampled using a bilinear interpolation.

Imputation of CF_Aug using the 'mi' package

The 'mi' R package uses a chained equation approach to multiple imputation for datasets with missing values (Su et al. 2011). In our case, we had missing values only for CF_Aug in the years 1992-1994 and 2008-2013. The 'mi' function approximates a Bayesian approach and draws imputed values from the conditional distribution for CF Aug given the observed values of the other covariates. With Student-t priors (mean = 0, df = 1, scale = 2.5) placed on the regression coefficients, we ran four independent chains initialized with different starting values and assessed convergence after 30 (the default), 50 and 80 iterations via $\hat{R}$ statistics. We found acceptable convergence after 80 iterations (CF Aug: mean = 1.01, sd = 1.02) and diagnostic plots (produced by the 'plot' function in 'mi') revealed good congruence between observed and imputed data. Our procedure generated four multiply

imputed datasets (one per chain), and we took the mean imputed values for each across these datasets as our new values for CF Aug.

Fishing magnitude

Given the known disruptive effects of fishing and vessel activity on the behaviour of pelagic schooling species like herring (e.g. Olsen 1971; Fréon et al. 1992; Vabø et al. 2002; Ona et al. 2007; Lindegren et al. 2011) we aggregated data on numbers of successful fishing events (succk) and total landings in tonnes (c_k) in each 0.1° longitude x 0.05° latitude grid cell *k* for each week of winter. We then constructed a measure of local fishing magnitude – fish_magnitude (tonnes) = $succ_k \times c_k$, for each grid cell in each week, month and year across the time series (Fig. A5). Finally, for each fishing/survey event, we calculated a fish_magnitude value in the week prior to that particular observation. Our hypothesis was that a high fishing magnitude would disperse the herring schools in that area, making the probability of capture at that location in the following week less likely.

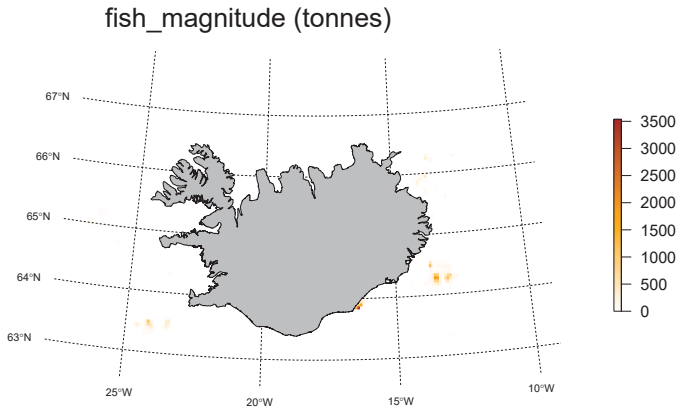

Fig. A5. Raster of mean fishing magnitude for 2001_2002. See Table 1 in main text for derivation. Model fitting was conducted using data extracted at a weekly resolution, but grid cell values (0.1° longitude × 0.05° latitude resolution) were summed across the entire year for spatial predictions.

References (including those cited in Table 1)

Bainbridge, V. and Forsyth, D.C.T. 1972. An ecological survey of a Scottish herring fishery. Part V: The plankton of the northwestern North Sea in relation to the physical environment and the distribution of the herring. Bull. Mar. Ecol. 8: 21–52.

Bartolino, V., Margonski, P., Lindegren, M., Linderholm, H.W., Cardinale, M., Rayner, D., Wennhage, H. and Casini, M. 2014. Forecasting fish stock dynamics under climate change: Baltic herring (*Clupea harengus*) as a case study. Fish. Oceanogr. 23: 258–269.

Blaxter, H. S. 1985. The herring: a successful species? – Can. J. Fish. Aquat. Sci. 42: 21–30.

de Boer, G.J., Pietrzak, J.D. and Winterwerp, J.C. 2008. Using the potential energy anomaly equation to investigate tidal straining and advection of stratification in a region of freshwater influence. Ocean Model. 22: 1–11.

Burchard, H. and Hofmeister, R. 2008. A dynamic equation for the potential energy anomaly for analysing mixing and stratification in estuaries and coastal seas. Estuar. Coast. Shelf Sci. 77: 679–687.

Corten, A. 1993. Learning processes in herring migrations. ICES C.M. 1993/H:18 Pelagic Fish Committee, Copenhagen, Denmark.

Corten, A. 1999a. A proposed mechanism for the Bohuslan herring periods. ICES J. Mar. Sci. 56: 207–220.

Corten, A. 1999b. The reappearance of spawning Atlantic herring (*Clupea harengus*) on Aberdeen Bank (North Sea) in 1983 and its relationship to environmental conditions. Can. J. Fish. Aquat. Sci. 56: 2051–2061.

Corten, A. 2000. A possible adaptation of herring feeding migrations to a change in timing of the *Calanus finmarchicus* season in the eastern North Sea. ICES J. Mar. Sci. 57: 1270.

Corten, A. 2001. Northern distribution of North Sea herring as a response to high water temperatures and/or low food abundance. Fish. Res. 50:189–204.

Corten, A. 2002. The role of "conservatism" in herring migrations. Rev. Fish Biol. Fisher. 11: 339–361.

Corten, A. and van de Kamp, G. 1992. Natural changes in pelagic fish stocks of the North Sea in the 1980s. ICES Mar. Sc. 195: 402–417.

Dalpadado, P., Ellertsen, B., Melle, W. and Dommasnes, A. 2000. Food and feeding conditions of Norwegian spring-spawning herring (*Clupea harengus*) through its feeding migrations. ICES J. Mar. Sci. 57: 843– 857.

Doksæter, L., Rune Godø, O., Olav Handegard, N., Kvadsheim, P.H., Lam, F.-P.A., Donovan, C. and Miller, P.J.O. 2009. Behavioral responses of herring (*Clupea harengus*) to 1-2 and 6-7 kHz sonar signals and killer whale feeding sounds. J. Acoust. Soc. Am. 125: 554–564.

Fernö, A., Pitcher, T., Melle, W., Nottestad, L., Mackinson, S., Hollingworth, C. and Misund, O. 1998. The challenge of the herring in the Norwegian Sea: making optimal collective spatial decisions. Sarsia 83: 149–167.

Fréon, P., Gerlotto, F. and Soria, M. 1992. Changes in school structure according to external stimuli: description and influence on acoustic assessment. Fish. Res. 15: 45–66.

Gíslason, A. and Astthorsson, O. S. 2002. The food of Norwegian spring-spawning herring in the western Norwegian Sea in relation to the annual cycle of zooplankton. Sarsia 87: 236–247.

Hjøllo, S.S., Huse, G., Skogen, M.D. and Melle, W. 2012. Modelling secondary production in the Norwegian Sea with a fully coupled physical/primary production/individual-based *Calanus finmarchicus* model system. Mar. Biol. Res. 6: 508–526.

Holst, J.C., Salvanes, A.G.V. and Johansen, T. 1997. Feeding, *Ichthyophonus* sp. infection, distribution and growth history of Norwegian spring-spawning herring in summer. J. Fish Biol. 50: 652–664.

Huret, M., Sourisseau, M., Petitgas, P., Struski, C., Léger, F. and Lazure, P. 2013. A multi-decadal hindcast of a physical–biogeochemical model and derived oceanographic indices in the Bay of Biscay. J. Mar. Syst. 109-110: S77–S94.

Huse, G., Fernö, A. and Holst, J.C. 2010. Establishment of new wintering areas in herring co-occurs with peaks in the "first time/repeat spawner" ratio. Mar. Ecol. Prog. Ser. 409: 189–198.

Huse, G., Railsback, S. and Fernö, A. 2002. Modelling changes in migration pattern of herring: collective behaviour and numerical domination. J. Fish Biol. 60: 571–582.
Huse, I. and Korneliussen, R. 2000. Diel variation in acoustic density measurements of overwintering herring (*Clupea harengus* L.). ICES J. Mar. Sci. 57: 903–910.
Jakobsson, J. 1969. Síld og sjávarhiti. – *In* Hafásinn. *Edited by* M.Á. Einarsson. Reykjavík, Iceland. pp. 497–511.
Lindegren, M., Östman, Ö. and Gárdmark, A. 2011. Interacting trophic forcing and the population dynamics of herring. Ecology 92: 1407–1413.
Logemann, K., Ólafsson, J., Snorrason, Á., Valdimarsson, H. and Marteinsdóttir, G. 2013. The circulation of Icelandic waters – a modelling study. Ocean Sci. 9: 931–955.
Maravelias, C.D. 1997. Trends in abundance and geographic distribution of North Sea herring in relation to environmental factors. Mar. Ecol. Prog. Ser. 159: 151–164.
Maravelias, C.D. and Reid, D. 1995. Relationship between herring (*Clupea harengus*, L.) distribution and sea surface salinity and temperature in the northern North Sea. Sci. Mar. 59: 427–438.
Maravelias, C.D. and Reid, D. 1997. Identifying the effects of oceanographic features and zooplankton on prespawning herring abundance using generalized additive models. Mar. Ecol. Prog. Ser. 147: 1–9.
Maravelias, C.D., Reid, D.G. and Swartzman, G. 2000a. Modelling spatio-temporal effects of environment on Atlantic herring, *Clupea harengus*. Environ. Biol. Fish. 58: 157–172.
Maravelias, C.D., Reid, D.G. and Swartzman, G. 2000b. Seabed substrate, water depth and zooplankton as determinants of the prespawning spatial aggregation of North Atlantic herring. Mar. Ecol. Prog. Ser. 195: 249–259.
McQuinn, I. 1997. Metapopulations and the Atlantic herring. Rev. Fish Biol. Fisher. 7: 297–329.
Misund, O., Melle, W., and Fernö, A. 1997. Migration behaviour of Norwegian spring spawning herring when entering the cold front in the Norwegian Sea. Sarsia 82: 107–112.
Misund, O., Vilhjálmsson, H., Jákupsstovu, S., Rottingen, I., Belikov, S., Asthorsson, O., Blindheim, J., Jónsson, J., Krysov, A., Malmberg, S. and Sveinbjornsson, S. 1998. Distribution, migration and abundance of Norwegian spring spawning herring in relation to the temperature and zooplankton biomass in the Norwegian Sea as recorded by coordinated surveys in spring and summer 1996. Sarsia 83: 117–127.
Nøttestad, L., Misund, O.A., Melle, W., Hoddevik Ulvestad, B.K. and Orvik, K.A. 2007. Herring at the Arctic front: influence of temperature and prey on their spatio-temporal distribution and migration. Mar. Ecol. 28: 123–133.
Olsen, K. 1971. Influence of vessel noise on the behaviour of herring. *In* Modern fishing gear of the world. *Edited by* H. Kristjonsson. Fishing News Books, London, UK. pp. 291– 293.
Ona, E., Godø, O.R., Handegard, N.O., Hjellvik, V., Patel, R. and Pedersen, G. 2007. Silent research vessels are not quiet. J. Acoust. Soc. Am. 121: EL145.
Óskarsson, G.J., Guðmundsdóttir, A. and Sigurðsson, Þ. 2009. Variation in spatial distribution and migration of Icelandic summer-spawning herring. ICES J. Mar. Sci. 66: 1762–1767.
Planque, B., Lazure, P. and Jegou, A.M. 2006. Typology of hydrological structures

modelled and observed over the Bay of Biscay shelf. Sci. Mar. 70S1: 43–50.
Prokopchuk, I. and Sentyabov, E. 2006. Diets of herring, mackerel, and blue whiting in the Norwegian Sea in relation to *Calanus finmarchicus* distribution and temperature conditions. ICES J. Mar. Sci. 63: 117–127.
Simpson, J. 1981. The shelf-sea fronts: implications of their existence and behaviour. Philos. T. Roy. Soc. A 302: 531–546.
Sinclair, M. and Iles, T. D. 1985. Atlantic herring (*Clupea harengus*) distributions in the gulf of Maine – Scotian shelf area in relation to oceanographic features. Can. J. Fish. Aquat. Sci. 42: 880–887.
Slotte, A. 1999. Differential utilization of energy during wintering and spawning migration in Norwegian spring-spawning herring. J. Fish Biol. 58: 338–355.
Su, Y., Gelman, A., Hill, J. and Yajima, M. 2011. Multiple imputation with diagnostics (mi) in R: opening windows into the black box. J. Stat. Softw. 45: 1–31.
Toresen, R. and Østvedt, J. 2000. Variation in abundance of Norwegian spring-spawning herring (*Clupea harengus*, Clupeidae) throughout the 20th century and the influence of climatic fluctuations. Fish Fish. 1: 231–256.
Utne, K.R., Hjøllo, S.S., Huse, G. and Skogen, M. 2012. Estimating the consumption of *Calanus finmarchicus* by planktivorous fish in the Norwegian Sea using a fully coupled 3D model system. Mar. Biol. Res. 8: 527–547.
Vabø, R., Olsen, K. and Huse, I. 2002. The effect of vessel avoidance of wintering Norwegian spring spawning herring. Fish. Res. 58: 59–77.

Appendix 4. R code and data for space-time occurrence models

The folder 'Space-time models.zip' (available from the Dryad Digital Repository: http://dx.doi.org/10.5061/dryad.9v46k) contains R code and data to run all models described in the paper. Due to confidentially issues, the 'herring_data.csv' dataset is a modified version of that used in the paper, so results of the analyses will differ. However, to encourage further exploration of our specific results, we include the 'quadres2_sLap.Rdata', a list containing model output that allows readers to reproduce the figures and tables presented in the manuscript.

Key components of the R code stored in this folder include:-

1) Preparing the data for modelling using the SPDE approach, allowing for different degrees of linearity and non-stationarity in the covariates and different specifications of the spatiotemporal random effects.
2) Creating a triangulated mesh upon which the GMRFs can be calculated.
3) Fitting the models, assessing model fit and predictive performance.
4) Extracting results from the posterior distribution and plotting summaries.
5) Making spatial predictions to an area of interest within the time series.
6) Assessing predictive performance to years outside the time series.

Folder name: 'Space-time models.zip'

Relevant files/subfolders:-

i) 'Herring models_23yrs.R' (R code and functions for SPDE models).
ii) 'mesh creation.R' (R code for different mesh resolutions).
iii) 'herring_data.csv' (.csv data file containing point- referenced occurrence/absence records and covariates).
iv) bisland.csv' (.csv data file with coordinates of the Icelandic coast).
v) 'Adult-recruit ratios_SSB_numbers.csv' (.csv data file including time series of demographic parameters for Icelandic summer spawning herring – see main text of the paper for parameter codes).
vi) 'space_grid.csv' (.csv data file with coordinates for spatial prediction grid).
vii) 'quadres2_sLap.Rdata' (a four-element list containing model output for plotting Figs. 3-5, A7, reproducing Tables 2, 3, A1-A3, and summarizing key results). This list is accessed directly through the 'Herring models_23yrs.R' R script.
viii) 'Final prediction rasters' (folder containing covariate layers for making spatial predictions for a subset of seasons).

Appendix 5. Prior specification for the space-time models

We assigned vague Gaussian priors for all fixed effects N(0, 1000) and the intercept N(0, ∞) in the *stationary* and *partly non-stationary* models. Although information on the influence of some environmental variables on herring occurrence is available from previous work that could be used to inform prior specification, this information relates to other herring stocks at other times of year. These stocks are exposed to markedly different oceanographic conditions compared with those experienced by the ISS herring during the autumn and winter months.

To this end, we chose to assign vague normal priors to all of our fixed effects, but tested the sensitivity of our results to prior choice by refitting the *stationary* 'no space' models using Cauchy priors with mean 0 and scale = 2.5 for fixed effect covariates and scale = 10 for the intercept in the 'arm' R package (Gelman et al. 2008).

For the *non-stationary* models, the rw1 models specified for the time-varying coefficients were defined by a Gaussian distribution N(0, *prec***R**), where *prec* is the precision parameter assigned a Gamma(1, 5e-05) prior, and **R** is a fixed structure matrix reflecting the model's neighbourhood structure. We also tried various ar1 models for these time-varying terms, using a range of 'Penalized Complexity' priors that control the degree of correlation among seasons (see Simpson et al. 2015 for further details). We found that the rw1 models gave essentially the same results, yet with vast computational benefits, so we used these throughout. The SPDE model is defined by hyperparameters log(τ) and log(κ), (related to the spatial range ρ, and marginal variance σ^2) which were given normal independent priors N(0, 1), and the coefficient 'a' that controls the degree of correlation in the spatial field between seasons, to which we assigned N(0, 0.15).

References

Gelman, A., Jakulin, A., Pittau, M.G. and Yu-Sung, S. 2008. A weakly informative default prior distribution for logistic and other regression models. Ann. Appl. Stat. 2: 1360–1383.

Simpson, D.P., Rue, H., Martins, T.G., Riebler, A. and Sørbye, S.H. 2015. Penalising model component complexity: a principled, practical approach to constructing priors. arXiv 1403.4630 [stat.ME].

Appendix 6. Spatial prediction

Scaling covariates to match prediction grain size

Where the spatial resolution of covariates used in model fitting was smaller (i.e. all dynamic environmental covariates at ~ 1 × 1 km), we aggregated the smaller cells to match the 0.1° longitude × 0.05° resolution of the prediction grid, and used the mean value of the aggregated cells. In the case of the *C. finmarchicus* biomass layers (CF_Aug) (extracted at 20 × 20 km resolution for model fitting), we used bilinear interpolation with the 'resample' function in the 'raster' package in R to create layers with the same extent and resolution as the prediction grid. For the fishing magnitude variable (fish_magnitude), we summed the grid cell values for each week in each fishing year (i.e. October to January inclusive), resulting in one layer reflecting total fishing magnitude for each of year.

Prediction to t+1 (see Appendix 4 for R code for running all analyses)

We used the best *partly non-stationary* model (i.e. part_ns5) specification to fit models to the first 18, 19, 20 and 21 years of data. We wanted to see how well we could predict the observed occurrences and absences in the 19th, 20th, 21st and 22nd years respectively. For this, we need to be able to estimate the $\text{distrib}_{t\text{-}1}$ regression coefficient for t+1. We tested if we could do this by examining relationships between the time series of $\text{distrib}_{t\text{-}1}$ in the fitted models and nine demographic parameters for the ISS herring stock (see *Step 2* below). If a strong correlation existed with one or several demographic factors, we then fitted a GLM to predict the $\text{distrib}_{t\text{-}1}$ coefficient from the demographic factor. Assuming that we have data for (or can estimate) the demographic parameter in t+1, we can then feed this value into the GLM and estimate the $\text{distrib}_{t\text{-}1}$ coefficient in t+1. The steps we used are summarized as follows.

Step 1: Use the more general *partly non-stationary* model. In this model, all covariates are kept stationary in time, except for spatial memory covariate (i.e. $\text{distrib}_{t\text{-}1}$) which is allowed to vary by year according to rw1 dynamics. Note that the $\text{distrib}_{t\text{-}1}$ covariate represents the spatial occurrence pattern in the previous year, t-1.

Step 2: Examine correlations between the 22-year time series of $\text{distrib}_{t\text{-}1}$ coefficients from the above model and time series of the nine demographic parameters for the ISS herring stock described in main text under '*Correlation among covariates and demographic parameters*'. They are as follows:-

i) Number of age3:age4+
ii) Number of age3:age4to7
iii) Number of age3:age8to13
iv) Spawning stock biomass (SSB)
v) Spawning stock numbers (SSN)
vi) Number of experienced individuals (*n* age4+)
vii) Number of young experienced individuals (*n* age4to7)
viii) Number of old experienced individuals (*n* age8to13)
ix) Mean age of the spawning stock (mean age).

Step 3: If a strong correlation with one or more of these parameters is found, run a GLM to model $distrib_{t-1}$ as a function of the demographic parameter.

This analysis revealed a strong positive correlation between SSN on the regression coefficients for $distrib_{t-1}$ across the time series. We then fitted a linear model and found a significant effect of SSN on the $distrib_{t-1}$ regression coefficients. This means that we may be able to predict the $distrib_{t-1}$ coefficient in t+1, given SSN in t+1 is known or can be estimated.

Step 4: Subset full dataset to get first 18, 19, 20 and 21 years of observations and prepare data for model fitting.

Step 5: Fit models to the first 18, 19, 20 and 21 years of the dataset. These models use the same formulation as the best *partly non-stationary* model with linear and quadratic terms for environmental covariates, a rw1 model for $distrib_{t-1}$ and independent realizations of the spatiotemporal random field (ω) each year.

Step 6: For each of the four models in turn, extract the coefficients for the $distrib_{t-1}$ time series.

Step 7: Correlate this time series with the equivalent time series of SSN.

Step 8: If strong correlation with SSN is found, fit a GLM to model the $distrib_{t-1}$ coefficients as function of SSN.

Step 9: Get (or predict) an estimate of SSN for t+1 (i.e. from stock assessment in year t). In our case, we already have the SSN estimates for the 19^{th}, 20^{th}, 21^{st} and 22^{nd} years.

Step 10: Feed this value into the GLM to predict the $distrib_{t-1}$ coefficient in t+1.

Step 11: Calculate a new multiplier for the $distrib_{t-1}$ covariate for the year we want to predict to. For example, for predicting 2010_11, we divide the predicted coefficient from *Step 10* by the estimated coefficient from the fitted 18-year model. This value is the new coefficient we use multiply the $distrib_{t-1}$ covariate values for 2010_11 by in the 'effects' list of the prediction stack.

Step 12: Validate these models on held-out observations in t+1, and assess predictive capacity for the next year (i.e. t+1). Do this by creating a validation stack with covariates referenced for t+1 and refitting the 18, 19, 20 and 21 year models with response = NA, using the spatiotemporal random effect estimated for year t. Examine model calibration and predicted outcomes versus observations (using cross-validated mean Brier scores and AUC).

Step 13: Finally, make spatial predictions across the entire domain for the four t+1 prediction years (i.e. 2010_2011, 2011_2012, 2012_2013, 2013_2014).

Appendix 7. Additional details on wintering area characteristics, modelling output, occurrence-environment relationships and environmental sensitivity in other herring stocks

Environmental characteristics of wintering areas

By charting the hydrographic variability in wintering areas across seasons, we gain some insight into the level of environmental plasticity exhibited by wintering ISS herring. Sea surface temperatures (i.e. SST) in the wintering areas differed somewhat among seasons; however, most estimates were in the range of ~ 4 to 9°C, and rarely below 3°C (Fig. A6a). In 19 out of the 22 seasons, median SST's were higher in wintering areas than in areas where herring were absent. Marked among-year consistency was observed in both sea surface salinity (i.e. SSS) and the degree of stratification (i.e. PEA) during the early to middle part of the time series, yet conditions inshore, inside the fjords occupied during the 'West' phase were substantially more mixed and less saline (Fig. A6b, c). Wintering areas were also typified by relatively small vertical temperature gradients (Fig. A6d), low and uniform current velocities (Fig. A6e), depths ranging from ~500 m off the east coast up to ~ 20 m inshore on the west coast (Fig. A6f), and low bathymetric relief across all seasons (Fig. A6g).

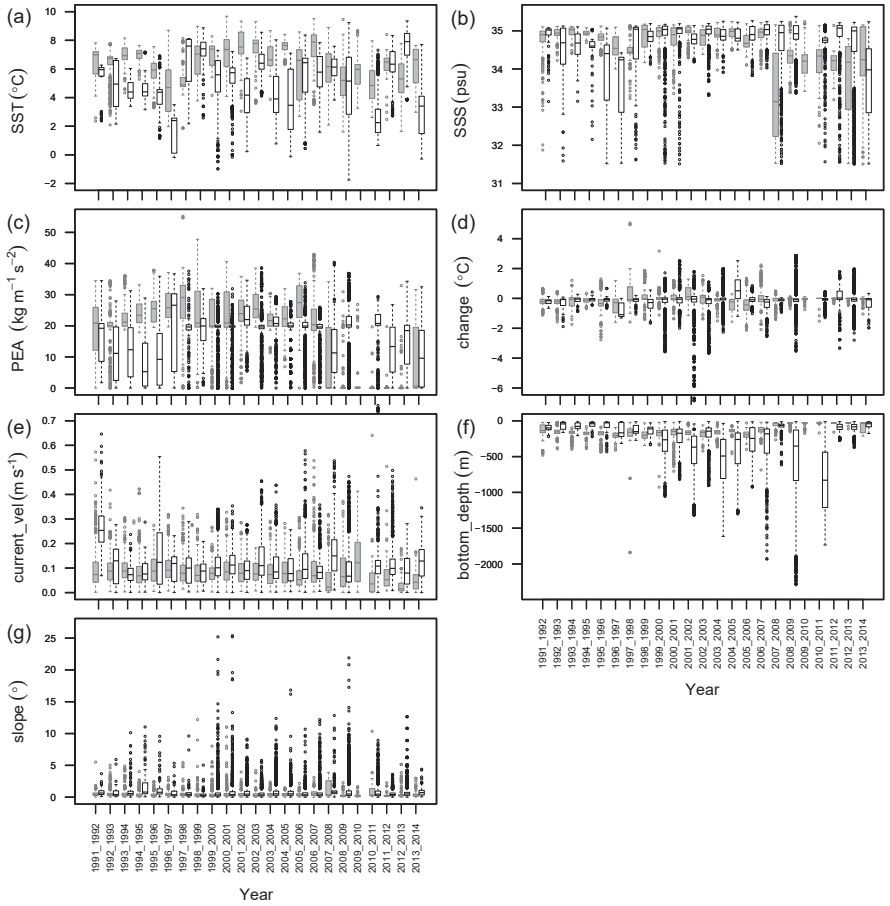

Fig. A6. Seasonal variation in environmental characteristics of wintering areas occupied by ISS herring between 1991_1992 and 2013_2014. Boxplots show the annual distributions of environmental data associated with each occurrence record (grey boxes) and absence record (white boxes) in our dataset.

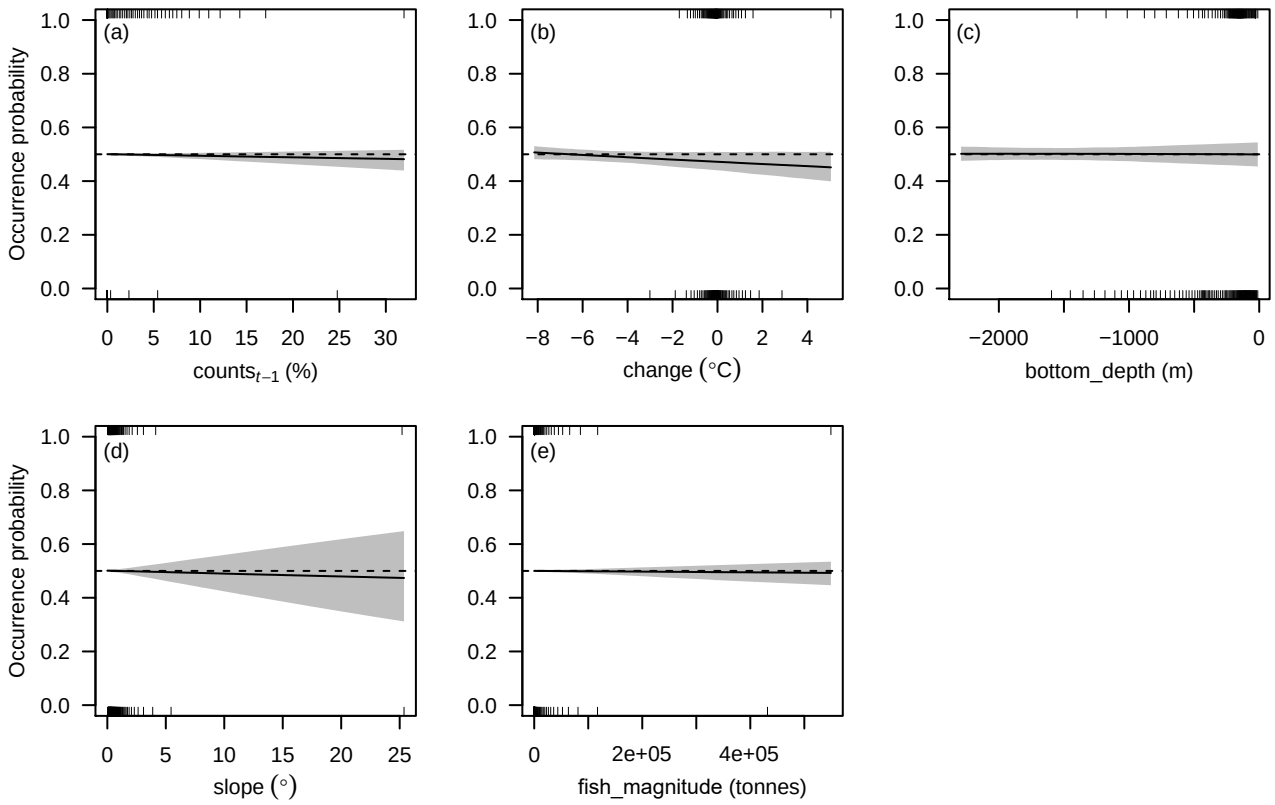

Fig. A7. Marginal effect plots for non-significant covariates in the best partly non-stationary model (part_ns5): (a) density of occurrence records in t-1 (counts$_{t-1}$), (b) vertical temperature gradient (change), (c) bottom depth, (d) bottom slope and (e) fishing intensity in the previous week (see Table 1 for detailed descriptions and derivation). Black lines represent the median estinate of 1000 draws from the posterior distribution for a sequence of 100 values across the full range of each covariate, and grey-shaded regions are 95% CIs. Tick marks denote the percentile distribution of raw data for each covariate for occurrence records (top of plots) and absence records (bottom of plots). Plots (a and e) represent the linear effect and plots (b, c and d) the quadratic effect of the covariate.

Table A1. Posterior mean estimates and 95% credible intervals for fixed effects, the spatial range (ρ) and marginal variance (σ_ω^2) for the best-performing stationary, partly non-stationary and fully non-stationary models. Estimates for random effect covariates with time-varying coefficients in the non-stationary models are presented graphically in Fig. 3. All models were fitted using simplified Laplace approximation.

Parameter	*Stationary model* (s9)			*Partly non-stationary* model (part_ns5)			*Fully non-stationary* model (full_ns5)		
	mean	$Q_{2.5\%}$	$Q_{97.5\%}$	mean	$Q_{2.5\%}$	$Q_{97.5\%}$	mean	$Q_{2.5\%}$	$Q_{97.5\%}$
α	-0.140	-0.206	-0.075	-0.183	-0.204	-0.161	-0.137	-0.170	-0.104
distrib_{t-1}	0.487	0.440	0.534						
counts_{t-1}	0.004	-0.021	0.029	-0.010	-0.041	0.020			
SST	0.247	0.205	0.290	0.170	0.132	0.209			
SST^2	0.146	0.100	0.192	0.090	0.046	0.134			
SSS	-0.168	-0.224	-0.113	-0.109	-0.162	-0.056			
SSS^2	-0.051	-0.070	-0.032	-0.037	-0.056	-0.018			
PEA	0.116	0.087	0.145	0.127	0.098	0.156			
PEA^2	0.083	0.052	0.113	0.076	0.046	0.107			
change	-0.001	-0.026	0.024	-0.005	-0.029	0.020			
change^2	-0.005	-0.014	0.004	-0.005	-0.014	0.003			
current_vel	-0.052	-0.078	-0.026	-0.039	-0.065	-0.014			
current_vel^2	0.017	-0.007	0.041	0.014	-0.010	0.038			
bottom_depth	0.010	-0.044	0.063	-0.003	-0.055	0.049			
bottom_depth^2	0.009	-0.027	0.044	0.000	-0.035	0.034			
slope	-0.009	-0.039	0.020	-0.011	-0.041	0.018			
slope^2	0.000	-0.007	0.006	0.000	-0.006	0.007			
fish_magnitude	-0.003	-0.023	0.018	-0.003	-0.024	0.019			
CF_Aug	0.022	-0.004	0.048	0.036	0.012	0.060			
year_{9394}	-0.147	-0.272	-0.021						
year_{9495}	-0.201	-0.329	-0.074						
year_{9596}	-0.034	-0.164	0.095						
year_{9697}	0.061	-0.075	0.197						
year_{9798}	-0.137	-0.294	0.020						
year_{9899}	-0.055	-0.191	0.081						
year_{9900}	-0.022	-0.102	0.057						
year_{0001}	-0.038	-0.124	0.048						
year_{0102}	-0.068	-0.157	0.020						
year_{0203}	-0.105	-0.186	-0.023						
year_{0304}	-0.016	-0.092	0.060						
year_{0405}	-0.051	-0.139	0.035						
year_{0506}	-0.060	-0.148	0.029						
year_{0607}	-0.050	-0.138	0.037						
year_{0708}	-0.093	-0.202	0.016						
year_{0809}	-0.077	-0.149	-0.004						
year_{0910}	-0.106	-0.427	0.214						
year_{1011}	-0.009	-0.105	0.087						
year_{1112}	-0.093	-0.184	-0.003						
year_{1213}	-0.248	-0.333	-0.162						
year_{1314}	0.003	-0.185	0.189						
ρ	9.945	8.190	11.768	10.395	8.547	12.314	11.247	9.212	13.364
σ_ω^2	0.107	0.081	0.135	0.109	0.081	0.137	0.086	0.063	0.110

Table A2. Structure and performance of candidate space-time occurrence models for wintering Atlantic herring. Each model contains all covariates (full), and results are shown for fitting using Gaussian approximation (see Table 2 in main text for results based on a simplified Laplace approximation strategy). s1-s15, stationary models; part_ns1-part_ns9, partly non-stationary models; full_ns1-full_ns9, fully non-stationary models. Covariate form refers to models that include linear terms only (linear), and quadratic terms (quadratic) or penalized regression spline terms for environmental covariates (spline). Structure details the form of the spatiotemporal random effect $\omega_{i,t}$, and if a fixed factor for year ($year_t$) was included; no-space/no-time, no spatially or temporally structured effects; time_indep, independent realization of the spatial random field at each t; time_corr, temporal correlation (ar1) is considered in the realization of the spatial random field at each t. The best-performing model within each stationarity class is shown in bold.

Model	Covariate form	Structure	DIC	mean log score	Brier score	AUC
Stationary						
s1	linear	full (no-space/no-time)	49104.4	0.504	0.157	0.934
s2	linear	full + $year_t$	48354.0	0.496	0.154	0.974
s3	linear	full + time_indep $\omega_{i,t}$	41877.0	0.429	0.123	0.993
s4	linear	full + $year_t$ + time_indep $\omega_{i,t}$	41816.8	0.429	0.123	0.993
s5	linear	full + time_corr $\omega_{i,t}$	41881.7	0.429	0.123	0.992
s6	quadratic	full (no-space/no-time)	48917.4	0.502	0.156	0.943
s7	quadratic	full + $year_t$	48060.0	0.493	0.152	0.981
s8	quadratic	full + time_indep $\omega_{i,t}$	41737.1	0.428	0.122	0.994
s9	**quadratic**	**full + $year_t$ + time_indep $\omega_{i,t}$**	**41634.0**	**0.427**	**0.122**	**0.995**
s10	quadratic	full + time_corr $\omega_{i,t}$	41738.2	0.428	0.122	0.994
s11	spline	full (no-space/no-time)	49232.4	0.505	0.158	0.917
s12	spline	full + $year_t$	48366.0	0.496	0.154	0.973
s13	spline	full + time_indep $\omega_{i,t}$	41912.0	0.430	0.123	0.993
s14	spline	full + $year_t$ + time_indep $\omega_{i,t}$	41838.2	0.429	0.123	0.993
s15	spline	full + time_corr $\omega_{i,t}$	41913.5	0.430	0.123	0.992
Partly non-stationary						
part_ns1	linear	full (no-space/no-time)	48953.5	0.502	0.157	0.952
part_ns2	linear	full + time_indep $\omega_{i,t}$	41738.2	0.428	0.122	0.993
part_ns3	linear	full + time_corr $\omega_{i,t}$	41746.6	0.428	0.122	0.992
part_ns4	quadratic	full (no-space/no-time)	48726.0	0.500	0.155	0.960
part_ns5	**quadratic**	**full + time_indep $\omega_{i,t}$**	**41626.5**	**0.427**	**0.122**	**0.994**
part_ns6	quadratic	full + time_corr $\omega_{i,t}$	41630.6	0.427	0.122	0.994
part_ns7	spline	full (no-space/no-time)	49081.0	0.504	0.157	0.943
part_ns8	spline	full + time_indep $\omega_{i,t}$	41784.9	0.428	0.122	0.993
part_ns9	spline	full + time_corr $\omega_{i,t}$	41790.5	0.429	0.122	0.992
Fully non-stationary						
full_ns1	linear	full (no-space/no-time)	47333.0	0.486	0.148	0.989
full_ns2	linear	full + time_indep $\omega_{i,t}$	41342.6	0.424	0.120	0.996
full_ns3	linear	full + time_corr $\omega_{i,t}$	41351.8	0.424	0.120	0.995
full_ns4	quadratic	full (no-space/no-time)	46760.2	0.480	0.146	0.995
full_ns5	**quadratic**	**full + time_indep $\omega_{i,t}$**	**41057.3**	**0.421**	**0.119**	**0.997**
full_ns6	quadratic	full + time_corr $\omega_{i,t}$	41065.8	0.421	0.119	0.997
full_ns7	spline	full (no-space/no-time)	46975.4	0.482	0.147	0.993
full_ns8	spline	full + time_indep $\omega_{i,t}$	41228.6	0.423	0.119	0.996
full_ns9	spline	full + time_corr $\omega_{i,t}$	41236.4	0.423	0.120	0.996

Table A3. Results for single-term deletions from the best stationary model (s9). Note that for environmental covariates, this equates to deletion of both linear and quadratic terms.

Model	Covariate form	Structure	DIC	mean log score	mean Brier score
s9	quadratic	full + year$_t$ + time-indep $\omega_{i,t}$	41629.0	0.427	0.122
Deletions from s9					
- distrib$_{t-1}$			42168.6	0.432	0.124
- counts$_{t-1}$			41629.0	0.427	0.122
- SST			41858.6	0.429	0.123
- SSS			41680.3	0.427	0.122
- PEA			41725.6	0.428	0.122
- change		As above	41631.0	0.427	0.122
- current_vel			41653.8	0.427	0.122
- bottom_depth			41629.0	0.427	0.122
- slope			41630.0	0.427	0.122
- fish_magnitude			41630.4	0.427	0.122
- CF_Aug			41637.9	0.427	0.122

Further details on modelled occurrence-environment relationships

Whilst extreme low temperature conditions can impact directly on physiology (see main text for details), and logic dictates that preferences for lower velocity zones may promote energy savings and compensate somewhat for any metabolic costs incurred through residing in warmer waters (see Liao et al. 2003), the search for causality in the relationships we observed between the probability of occurrence, SSS and PEA (see Fig. 3b, c) is more challenging. Given herring's euryhaline nature, and ability to inhabit brackish and fresh waters down to 1 psu in the Baltic Sea (Teacher et al. 2013; Miethe et al. 2014), it is clear that the lowest salinities encountered in Icelandic surface waters (i.e. ~ 31.5 psu) would not impose high physiological demands. Likewise, the highest SSS in the region throughout the study period approached 35.4 psu – a value close to surface measurements made in Ofotfjorden, Norway, during the late 1980s and early 1990s when it harbored the majority of the wintering NSS stock (Dommasnes et al. 1994). As these bounding values are well within the known tolerance range of the species, and that the vertical salinity gradient in the upper water column (between 1 and 100 m) across our dataset never exceeded 2 psu, we argue that wintering ISS herring undertaking diurnal vertical migrations would not have been exposed to strong physiological forcing by salinity, and that any effects we see are likely indirect. With regard to our results for PEA, although it could be argued that selection of less stratified, shallower, fresher waters, as seen during the recent years of our time series (Fig. A6c) could provide energetic benefits to vertically migrating herring (Huse and Ona 1996), we see no direct fitness advantage to wintering fish of inhabiting more stratified waters.

In the absence of any clear mechanistic basis for these findings, we propose two alternatives. First, active avoidance of cold water masses could indirectly influence the population's response to salinity and stratification. The warmer waters encountered at the time and location of the bulk of successful fishing events were also often characterized by higher PEA values (particularly during the 'East' and 'Eastwest' phases), weaker currents and lower SSS (particularly close to the coast during the inshore 'West' phase) compared with conditions associated with survey-derived absence records (Fig. A6). Such hydrographic conditions are common in coastal Icelandic waters (Appendix 3, Fig. A2; authors' unpublished data), and other regions at certain times of year (e.g. North Sea: Maravelias and Reid 1995; Bay of Biscay: Planque et al. 2006; Huret et al. 2013; Lindåspollene, Norway: Langård et al. 2014), and residence in them during winter would shape the response to each of these covariates in the way we observe (see Fig. 3)[1]. Second, preference for moderately-stratified zones, particularly during the early and middle years of the time series (Fig. A6c) could also reflect adaptations for predator-avoidance. During this period, the locations of our occurrence records were typically quite distant from major fronts off the northwest and north coast (i.e. boundaries between strong vertical temperature gradients – see 'change' plot in Appendix 3, Fig. A2; and Pálsson and Thorsteinsson 2003) or strongly-mixed zones offshore (i.e. those associated with lower PEA values) often rich in herring predators like adult cod (Pálsson and Thorsteinsson 2003; Pálsson and Björnsson 2011). Our results may reflect high predator densities in these years, with occupation of more stratified areas affording some release from predation pressure. Although we included recent fishing activity in our analysis as a potential

[1] We note that our PEA estimates may underestimate the true degree of stratification in very shallow zones (i.e. < 15 m deep), due to limits on the minimum vertical bin-depth of the CODE model (= 2.5 m). However, given that only 68 (0.1%) of our records were located in such shallow waters – in all cases near shore in fjords, and that these locations are generally influenced strongly by river run-off and tidal processes which enforce water-column mixing, we contend that slight inaccuracies in our estimates would have negligible effects on model estimation and prediction.

top-down control, spatially-resolved data on the distribution of other non-human predators in the study region during winter are needed to allow a more explicit examination of predator effects and their environmental interactions on herring spatial distribution patterns (see the 'Fishing and predation' in the main text for a further discussion).

Issues of scale

That environmental factors contributed to the wintering patterns we observed (at least in some years) contrasts with recent work on wintering ISS herring (Óskarsson et al. 2009) and NSS herring (Huse et al. 2010). Both studies found no clear evidence for environmental signals as determinants of wintering dynamics. Huse et al. (2010) showed that the six different wintering locations used by the NSS stock over the past 50+ years, were characterized by vastly different environmental conditions. In Iceland, Óskarsson et al. (2009) found no support for a temperature effect on the ISS wintering patterns of the late 1970s up until the mid-2000s, but suggested that temperature may still play a role at finer scales. We agree with this, and posit that the inability to detect a signal in these studies may have arisen from a mismatch between the scale of the temperature data used (i.e. single CTD stations measured annually), and the scale of the process giving rise to the occurrence of herring in that area.

In developing our study, we acknowledged the variable spatial and temporal scales at which stimuli may act (Levin 1992; Witman et al. 2015); shoaling species' responses to them emerging as a result of exposure to, and/or retention of specific cues experienced during early age (e.g. olfactory imprinting), the social transmission of long- standing traditions among generations (e.g. Fernö et al. 2011), or the spontaneous spread of information among individuals, that can manifest in rapid expansion in school size (Makris et al. 2009), and elicit fast, school-wide responses to environmental gradients, prey resources or predation threats (Doksæter et al. 2009; Makris et al. 2009). We deemed it crucial to capture this variability in our models. Therefore, we extracted environmental data from the CODE model (Logemann et al. 2013) at several grain sizes and temporal windows (Table 1, Appendix 3), and, through prioritizing ecological reasoning in the trade-off between data quality and availability, selected scales for the other variables (Table 1, Appendix 3).

Our goal here was to match as closely as possible the scale of processes acting on herring schools in both the pre-wintering period and during residence in the wintering areas (i.e. behavioral states 1 and 2), given the scale of the fishery purse-seine shots that comprise our occurrence data. Although the scales of our covariates likely miss several processes relevant to wintering herring, particularly the complexities of intra-school shoaling dynamics and diurnal vertical migration (Mackinson et al. 1999), the potential impact of larger-scale, non-spatial climatic indices (e.g. North Atlantic Oscillation (NAO) winter index, Atlantic Multidecadal Oscillation (AMO) – see Engelhard et al. 2011) and possibly, interactions between past environmental conditions and spatial persistence in distribution (see Corten 2002; Rindorf and Lewy 2006), we feel that the spatial and temporal resolution we chose provided a plausible linkage between processes and observations. With continuing improvements in the quality of measured and modelled data available for marine systems and the species within them, opportunities are emerging to incorporate more mechanistic information into spatial models (e.g. Teal et al. 2016). Such process-based approaches allow the 'best' scale to emerge naturally from the physiological process of interest, and by their general nature, rooted in data or theory on metabolic rates, hold great promise for predicting

species' distributions when observational data are limited. We anticipate rapid progress in this field in the coming years (see also Appendix 9 'Notes on the modelling approach').

Environmental sensitivity in herring

Sensitivity to environmental forcing has also been seen in other herring stocks during winter (e.g. Corten 1999a), and at different times of the year. For example, in a series of papers focused on North Sea herring, Maravelias and colleagues demonstrated strong effects of temperature gradients, salinity, stratification, zooplankton biomass and bottom topography in shaping pre-spawning summer distribution (e.g. Maravelias and Haralabous 1995; Maravelias and Reid 1997; Maravelias et al. 2000a, b). The direction and magnitude of these effects differed substantially from our study, a finding that was anticipated given that the ISS stock is located near the northerly range-edge for the species, and is therefore exposed to vastly different environmental conditions to those typically encountered in the North Sea. Moreover, these North Sea papers and similar studies in Nordic seas (e.g. Misund et al. 1998, Jakobsson and Østvedt 1999; Kvamme et al. 2003; Nøttestad et al. 2007; Broms et al. 2012) have often focused on distribution patterns during spring and summer, periods of high feeding activity in which adult herring can be tightly linked to prey resources either directly (e.g. Holst et al. 1997; Maravelias and Reid 1997; Olsen et al. 2007) or indirectly through hydrographic proxies. Some examples of the latter include the northwards displacement of the feeding distribution of North Sea herring in the 1980s, posited as a response to intensification of the shelf edge current leading to increased productivity off the Norwegian coast, concurrent with elevated water temperatures causing a range contraction of *C. finmarchicus* to northern waters (Corten and van de Kamp 1992; Corten 2001). And, the reappearance of the Aberdeen Bank spawning population in 1983, suggested as a corollary of increased Atlantic inflow into the North Sea that caused a redistribution of key planktonic prey and their predators (e.g. pre-spawning herring) southwards (Corten 1999b). It has also been suggested that the quality of future spawning habitat (e.g. water depth, seabed roughness – Maravelias et al. 2000b; Langård et al. 2014), and distance to spawning grounds (Jech and Stroman 2012) can affect pre-spawning distribution to some extent. These examples illustrate how environmental and biotic factors can interact in complex ways to shape herring feeding and pre-spawning distributions, yet such processes are largely irrelevant during residence on wintering grounds (i.e. during behavioral state 2 – see main text for definition).

References

Broms, C., Melle, W. and Horne, J.K. 2012. Navigation mechanisms of herring during feeding migration : the role of ecological gradients on an oceanic scale. Mar. Biol. Res. 8: 37–41.

Corten, A. 1999a. A proposed mechanism for the Bohuslan herring periods. ICES J. Mar. Sci. 56: 207–220.

Corten, A. 1999b. The reappearance of spawning Atlantic herring (*Clupea harengus*) on Aberdeen Bank (North Sea) in 1983 and its relationship to environmental conditions. Can. J. Fish. Aquat. Sci. 56: 2051–2061.

Corten, A. 2001. Northern distribution of North Sea herring as a response to high water temperatures and/or low food abundance. Fish. Res. 50: 189–204.

Corten, A. 2002. The role of "conservatism" in herring migrations. Rev. Fish Biol. Fisher. 11: 339–361.

Corten, A. and Van de Kamp, G. 1992. Natural changes in pelagic fish stocks of the North Sea in the 1980s. ICES Mar. Sc. 195: 402–417.

Doksæter, L., Rune Godø, O., Olav Handegard, N., Kvadsheim, P.H., Lam, F.-P.A., Donovan, C. and Miller, P.J.O. 2009. Behavioral responses of herring (*Clupea harengus*) to 1-2 and 6-7 kHz sonar signals and killer whale feeding sounds. J. Acoust. Soc. Am. 125: 554–564.

Dommasnes, A., Rey, F. and Rottingen, I. 1994. Reduced oxygen concentrations in herring wintering areas. ICES J. Mar. Sci. 51: 63–69.

Engelhard, G.H., Pinnegar, J.K., Kell, L.T. and Rijnsdorp, A.D. 2011. Nine decades of North Sea sole and plaice distribution. ICES J. Mar. Sci. 68: 1090–1104.

Holst, J.C., Salvanes, A.G.V. and Johansen, T. 1997. Feeding, *Ichthyophonus* sp. infection, distribution and growth history of Norwegian spring-spawning herring in summer. J. Fish Biol. 50: 652–664.

Huret, M., Sourisseau, M., Petitgas, P., Struski, C., Léger, F. and Lazure, P. 2013. A multi-decadal hindcast of a physical–biogeochemical model and derived oceanographic indices in the Bay of Biscay. J. Mar. Syst. 109-110: S77– S94.

Huse, I. and Ona, E. 1996. Tilt angle distribution and swimming speed of overwintering Norwegian spring spawning herring. ICES J. Mar. Sci. 53: 863–873.

Huse, G., Fernö, A. and Holst, J.C. 2010. Establishment of new wintering areas in herring co-occurs with peaks in the "first time/repeat spawner" ratio. Mar. Ecol. Prog. Ser. 409: 189–198.

Jakobsson, J. and Østvedt, O. J. 1999. A review of joint investigations on the distribution of herring in the Norwegian and Iceland Seas 1950-1970. Rit Fiskideildar 16: 209–238.

Jech, J. M. and Stroman, F. 2012. Aggregative patterns of pre-spawning Atlantic herring on Georges Bank from 1999-2010. Aquat. Living Resour. 25: 1–14.

Kvamme, C., Nøttestad, L., Fernö, A, Misund, O., Dommasnes, A, Axelsen, B., Dalpadado, P. and Melle, W. 2003. Migration patterns in Norwegian spring-spawning herring: why young fish swim away from the wintering area in late summer. Mar. Ecol. Prog. Ser. 247: 197–210.

Langård, L., Slotte, A., Skaret, G. and Johannessen, A. 2014. Thermal stratification influences maturation and timing of spawning in a local *Clupea harengus* population. J. Fish Biol. 84: 1202–1209.

Levin, S. 1992. The problem of pattern and scale in Ecology. Ecology 73: 1943–1967.

Liao, J.C., Beal, D.N., Lauder, G.V. and Triantafyllou, M.S. 2003. Fish exploiting vortices decrease muscle activity. Science 302: 1566–1569.

Logemann, K., Ólafsson, J., Snorrason, Á., Valdimarsson, H. and Marteinsdóttir, G. 2013. The circulation of Icelandic waters – a modelling study. Ocean Sci. 9: 931–955.

Mackinson, S., Nøttestad, L., Guénette, S., Pitcher, T., Misund, O.A. and Fernö, A 1999. Cross-scale observations on distribution and behavioural dynamics of ocean feeding Norwegian spring-spawning herring (*Clupea harengus* L.). ICES J. Mar. Sci. 56: 613–626.

Makris, N.C., Ratilal, P., Jagannathan, S., Gong, Z., Andrews, M., Bertsatos, I., Godo, O.R., Nero, R.W. and Jech, J.M. 2009. Critical population density triggers rapid formation of vast oceanic fish shoals. Science 323: 1734–1737.

Maravelias, C.D. and Haralabous, J. 1995. Spatial distribution of herring in the Orkney/Shetland area (northern North Sea): a geostatistical analysis. Neth. J. Sea. Res. 34: 319–329.

Maravelias, C.D. and Reid, D.G. 1995. Relationship between herring (*Clupea harengus* L.) distribution and sea surface salinity and temperature in the northern North Sea. Sci. Mar. 59: 427–438.

Maravelias, C.D. and Reid, D.G. 1997. Identifying the effects of oceanographic features and zooplankton on prespawning herring abundance using generalized additive models. Mar. Ecol. Prog. Ser. 147: 1–9.

Maravelias, C.D., Reid, D.G. and Swartzman, G. 2000a. Modelling spatio-temporal effects of environment on Atlantic herring, *Clupea harengus*. Environ. Biol. Fish. 58: 157–172.

Maravelias, C.D., Reid, D.G. and Swartzman, G. 2000b. Seabed substrate, water depth and zooplankton as determinants of the prespawning spatial aggregation of North Atlantic herring. Mar. Ecol. Prog. Ser. 195: 249–259.

Miethe, T., Gröhsler, T., Böttcher, U. and van Dorrien, C. 2014. The effects of periodic marine inflow into the Baltic Sea on the migration patterns of Western Baltic spring-spawning herring. ICES J. Mar. Sci. 71: 519–527.

Misund, O., Vilhjálmsson, H., Jákupsstovu, S., Rottingen, I., Belikov, S., Asthorsson, O., Blindheim, J., Jónsson, J., Krysov, A., Malmberg, S. and Sveinbjornsson, S. 1998. Distribution, migration and abundance of Norwegian spring spawning herring in relation to the temperature and zooplankton biomass in the Norwegian Sea as recorded by coordinated surveys in spring and summer 1996. Sarsia 83: 117–127.

Nøttestad, L., Misund, O.A., Melle, W., Hoddevik Ulvestad, B.K. and Orvik, K.A. 2007. Herring at the Arctic front: influence of temperature and prey on their spatio-temporal distribution and migration. Mar. Ecol. 28: 123–133.

Olsen, E.M., Melle, W., Kaartvedt, S., Holst, J.C. and Mork, K.A. 2007. Spatially structured interactions between a migratory pelagic predator, the Norwegian spring-spawning herring *Clupea harengus* L., and its zooplankton prey. – J. Fish Biol. 70: 799–815.

Óskarsson, G.J. and Taggart, C.T. 2009. Spawning time variation in Icelandic summer-spawning herring (*Clupea harengus*). Can. J. Fish. Aquat. Sci. 66: 1666–1681.

Pálsson, Ó.K. and Björnsson, H. 2011. Long-term changes in trophic patterns of Iceland cod and linkages to main prey stock sizes. ICES J. Mar. Sci. 68: 1488–1499.

Pálsson, Ó.K. and Thorsteinsson, V. 2003. Migration patterns, ambient temperature, and growth of Icelandic cod (*Gadus morhua*): evidence from storage tag data. Can. J. Fish. Aquat. Sci. 60: 1409–1423.

Planque, B., Lazure, P. and Jegou, A.M. 2006. Typology of hydrological structures modelled and observed over the Bay of Biscay shelf. Sci. Mar. 70S1: 43–50.

Rindorf, A. and Lewy, P. 2006. Warm, windy winters drive cod north and homing of spawners keeps them there. J. Appl. Ecol. 43: 445–453.

Teacher, A., André, C., Jonsson, P.R. and Merilä, J. 2013. Oceanographic connectivity and environmental correlates of genetic structuring in Atlantic herring in the Baltic Sea. Evol. Appl. 6: 549–567.

Teal, L.R., Marras, S., Peck, M.A. and Domenici, P. 2016. Physiology-based modelling approaches to characterize fish habitat suitability: their usefulness and limitations. Estuar. Coast. Shelf Sci. doi:10.1016/j.ecss.2015.11.014.

Witman, J., Lamb, R. and Byrnes, J. 2015. Towards an integration of scale and complexity in marine ecology. Ecol. Monogr. 85: 475–504.

Appendix 8. Exploring the relationship between adult population size and occupied area

Although the spatial inconsistency of our fishery and survey dataset limits precise quantification of expansion or contraction in Icelandic summer spawning (ISS) herring winter distribution over time, we can consider our occurrence records, and their gridded representations in the spatial similarity index (SSI), as a minimum, yet fairly accurate estimate of the realized winter distribution, reflecting the major spatial trends over the 1991_92 to 2013_14 period (Guðmundsdóttir and Sigurðsson 2004; Óskarsson et al. 2009; and see Appendix 1 for further details). Hence, by summing the number of occupied grid cells within each year $t = 1, 2, \ldots, T$, and plotting these values against fishery-independent estimates of adult population size, represented by spawning stock numbers (SSN), we were able to examine the association between abundance and occupied area for wintering ISS herring. We found no evidence of a positive relationship for our data (Fig. A8).

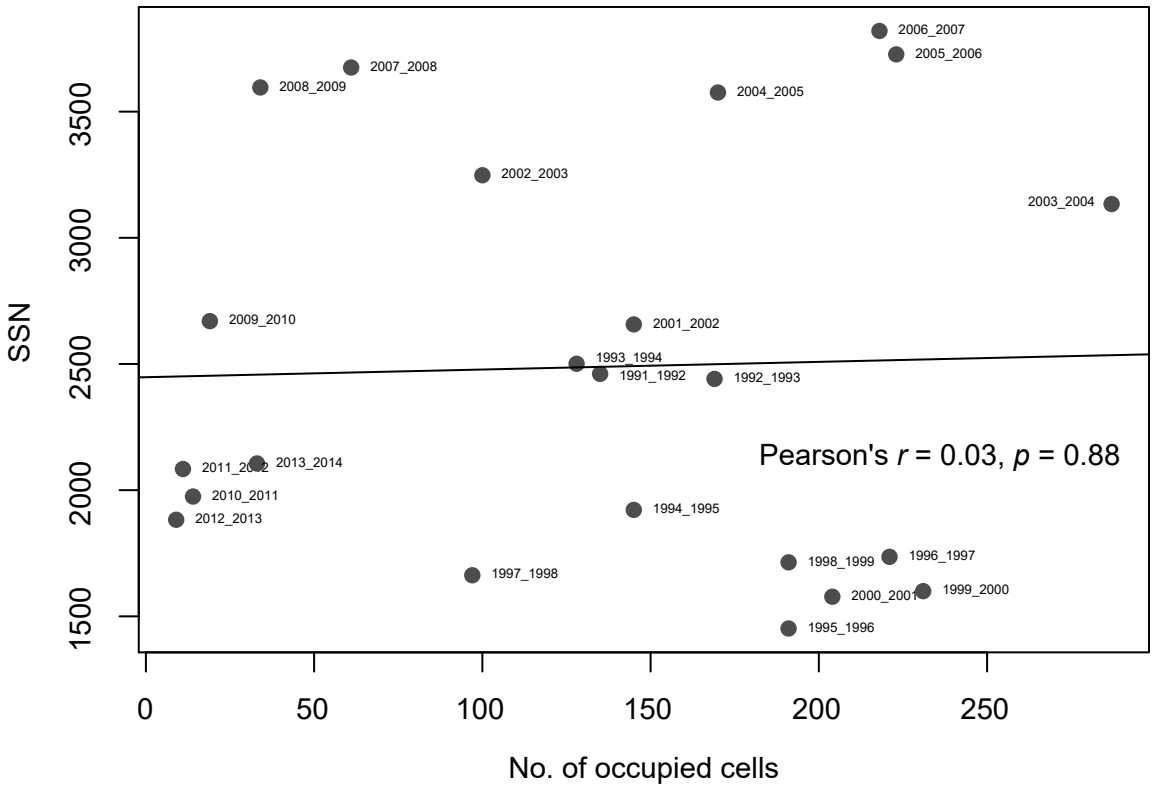

Fig. A8. Plot of adult population size in the ISS herring stock, represented by estimated spawning stock numbers (SSN), against the number of occupied 0.1 longitude × 0.05 latitude grid cells during winter (i.e. October to January) for the 23 years from 1991_92 to 2013_14. Data for the latter are drawn from the distrib$_t$ layers used in the creation of the spatial similarity index (SSI), and are considered as a minimal estimate of occupied area for each year. Estimates for SSN are derived from annual stock assessments for ISS herring conducted by the MRI, Iceland. No evidence of an abundance-occupied area relationship was found for overwintering ISS herring. The black line is the fitted curve from the non-significant linear regression of SSN against the number of occupied cells ($R^2 = 0.001$, $p = 0.885$).

References

Guðmundsdóttir, A. and Sigurðsson, Þ. 2004. The autumn and winter fishery and distribution of the Icelandic summer-spawning herring during 1978–2003. Hafrannsóknastofnunin Fjölrit 104: 1–42.

Óskarsson, G.J., Guðmundsdóttir, A. and Sigurðsson, Þ. 2009. Variation in spatial distribution and migration of Icelandic summer-spawning herring. ICES J. Mar. Sci. 66: 1762–1767.

Appendix 9. Notes on the modelling approach

The mixed effects models we fit in this paper fall broadly within the class of 'empirical' statistical models as defined by Levins (1966). These types of models are in essence correlative, although they may have mechanistic underpinnings related to the fundaments of Grinnellian and Eltonian niches (Hutchinson 1957; Soberón 2007). In lieu of the oft-lacking, detailed physiological knowledge needed for parameterization of an exciting new family of process-based models (e.g. Freitas et al. 2010; Jørgensen et al. 2012; Teal et al. 2012; see Peck et al. 2018 for a review), correlative models, which tend to compromise generality for realism and precision (Levins 1966; Dickey-Collas et al. 2014), remain widely used in ecology to explore the nature of relationships between species' distributions and biotic and abiotic factors, to build hypotheses and to guide management decisions (Guisan and Thuiller 2005; Elith and Leathwick 2009; Robinson et al. 2011).

Increasing recognition of the role of demographic structure, dispersal and density-dependence in shaping fish distribution patterns has motivated recent attempts to incorporate these processes explicitly (Cheung et al. 2009; Loots et al. 2010; Planque et al. 2011; Ciannelli et al. 2012). Moreover, regression models including time-lagged covariates, which provide insights into how the past may impact the present (e.g. Rindorf and Lewy 2006), and those in which covariate coefficients can vary in space and/or time, have proved valuable in understanding the interplay between density-dependent and density-independent controls on observed distributions (Bartolino et al. 2011; Ciannelli et al. 2012). Whilst still not allowing causation to be inferred directly, this class of models implicitly integrate mechanistic processes in their formulation, and hence occupy a space between environmental envelope and process-based models (Beale and Lennon 2012; Peck et al. 2018).

We built our models in line with these ideas. By linking measures of distribution history, output from a spatially-explicit, individual-based model of zooplankton biomass, fine scale environmental fields and estimates of local fishing intensity, we fitted stationary and time-varying coefficient GLMMs for ISS herring occurrence across a 23-year time series. Correlations between the relative influence of these factors across years and time series of demographic parameters were then examined post-hoc, providing a basis for model validation to held-out observations one-year ahead. Our models were fitted in a Bayesian framework in R-INLA, using the SPDE approach to capture spatial and temporal dependence in the data (Rue et al. 2009; Lindgren et al. 2011). The merits of the Bayesian approach for this type of hierarchical model are many (Gelfand et al. 2006; Gelman and Hill 2007; Royle et al. 2007). Without reviewing these exhaustively here (see Elderd and Miller 2016 for a comprehensive appraisal), we highlight the inherent way in which random effects are handled as parameters of interest, resulting in fully specified probability distributions from which information on the intensity and uncertainty of the effects can be drawn; the option to incorporate prior knowledge based on empirical data or theory; and the ability to robustly quantify and propagate uncertainty through all modelling stages. Model fitting using INLA is computationally efficient, and provides accurate approximations of the posterior marginal distributions of model parameters that show high concordance with Markov chain Monte Carlo (MCMC) simulations (Rue and Martino 2007; Rue et al. 2009; Held et al. 2010). Since Lindgren and colleagues proved that a continuously indexed Gaussian field described by a Matérn covariance function can be represented as a discretely indexed GMRF (Rue and Held 2005; Lindgren et al. 2011), rapid development of the SPDE approach within R-INLA has

facilitated fitting of an expanding suite of hierarchical spatial and spatiotemporal models to spatial point patterns (Krainski et al. 2016). This approach has recently proven useful in analyses of georeferenced fisheries datasets, which are often data-rich and where inference at the scale of point locations, rather than grids, is required (e.g. Cosandey-Godin et al. 2015; Ward et al. 2015; Ono et al. 2016).

One of the well-noted criticisms of correlative species distribution models (Elith and Leathwick 2009 for a review of different methods) has been their inability to adequately account for residual autocorrelation in space and/or time. This situation that can violate independence assumptions in regression models, leading to inference errors and/or misrepresentation of covariate importance (Legendre 1993; Dormann 2007; Beale et al. 2010). The SPDE approach considers these correlation structures directly, and allows great flexibility in their specification (e.g. Cosandey-Godin et al. 2015). In our space-time models for example, we specified temporally-independent (time-indep), or temporally-evolving (time-corr) annual realizations of spatially-structured error terms. As wintering herring displayed varying persistence in their spatial distribution from year to year (Fig. 2), our aim was to gain insight into if, and how $\omega_{i,t-1}$ might influence $\omega_{i,t}$. Although model performance did not alter greatly (Table 2), the time-indep structure was preferred for all models. This is most likely due to inclusion of time-lagged covariates (i.e. distrib_{t-1}, counts_{t-1}), the former of which was highly significant in all cases, and captured well the occurrence pattern of the previous year.

We specified covariates as additive effects only in these models, but did allow for varying degrees of non-linearity and temporal non-stationarity in occurrence-covariate relationships. Whilst acknowledging that important interactions among predictors (e.g. environment and fishing intensity – Planque et al. 2010) may have been overlooked, our decision reflects an attempt to balance model complexity with meaningful ecological inference (Merow et al. 2014). Hence, we placed priority on deriving biologically-realistic functional forms that could also vary in time. We found that including quadratic terms for the environmental covariates improved model fit compared with linear specifications alone, or where covariates were represented by penalized regression splines (Table 2), although most relationships approached linearity (Fig. 3). As the wintering stock was often clustered tightly in space, we also did not consider models with spatially-varying coefficients (e.g. Bacheler et al. 2009; Bartolino et al. 2011; Ciannelli et al. 2012). At the spatial scales of our observations, we assumed that any effect of a particular covariate would be imparted roughly equally across the space encompassing all herring schools encountered. This assumption is unlikely to hold if the occupied range expands, for example, during the spring feeding period, or if various ontogenetic stages, inhabiting geographically or environmentally disparate areas, are included in the models (see Bartolino et al. 2011 for an example). In these cases, inclusion of spatially non-stationary terms would likely provide important new insights.

A key limitation of our analysis relates to the lack of age-disaggregated or spatially-standardized catch or survey data available during our temporal window. Because of this, we were forced to consider demographic factors in a non-spatial, correlative context (i.e. estimates across the entire stock for each year), and were unable to incorporate the singular or interactive effects of density-dependence and age-structure directly within the model formulation. Although our results suggest that density-dependence is unlikely to play a major role in governing winter occurrence in herring (see Appendix 8, Fig. A8), and that population size may influence spatial persistence in wintering area use, georeferenced data on age-

structure of each fishing event or survey record would have allowed direct tests of hypotheses around age-related differences in environmental preference, susceptibility to fishing pressure and the tendency to follow traditions and return to previously-used wintering sites. This type of data is available for many other herring stocks, and ongoing work is focused on exploring these ideas.

Our models were specific to wintering ISS herring, limiting their generality. However, the approach used, and the covariates created, are easily adaptable to other herring stocks and species for which questions on the drivers and scales of conservatism or homing remain open. Bolstered by the strong congruence between modelled and observed temperature, salinity and flow fields in Icelandic waters (Logemann et al. 2013), the 23-year dataset we analyzed represents a substantial compilation of georeferenced records on the environmental conditions experienced by wintering ISS herring. The model outputs therefore provide a basis for identifying physiological thresholds that can be used to develop more informative priors and guide variable selection in future regression models (Simpson et al. 2015; Authier et al. 2017), or to aid parameterization of mechanistic models (Teal et al. 2016). We agree with Rochette et al. (2013) who advocate a hierarchical Bayesian framework as an appealing platform upon which to meld different types of data and models together, making it possible to assimilate the processes acting on different life-history phases within the one 'full life cycle' model. Such a model in under development for NSS herring in the Norwegian and Barents Seas (Utne and Huse 2012; Huse 2016) and we see potential for the types of models developed here to contribute to it.

References

Authier, M., Saraux, C. and Péron, C. 2017. Variable selection and accurate predictions in habitat modelling: a shrinkage approach. Ecography 40: 549–560.

Bacheler, N.M., Bailey, K.M., Ciannelli, L., Bartolino, V. and Chan, K.S. 2009. Density-dependent, landscape, and climate effects on spawning distribution of walleye pollock *Theragra chalcogramma*. Mar. Ecol. Prog. Ser. 391: 1–12.

Bartolino, V., Ciannelli, L., Bacheler, N.M. and Chan, K.S. 2011. Ontogenetic and sex-specific differences in density-dependent habitat selection of a marine fish population. Ecology 92: 189–200.

Beale, C.M. and Lennon, J.J. 2012. Incorporating uncertainty in predictive species distribution modelling. Philos. T. Roy. Soc. B 367: 247–258.

Beale, C.M., Lennon, J.J., Yearsley, J.M., Brewer, M.J. and Elston, D.A. 2010. Regression analysis of spatial data. Ecol. Lett. 13: 246–264.

Cheung, W.W.L., Lam, V.W.Y., Sarmiento, J.L., Kearney, K. Watson, R. and Pauly, D. 2009. Projecting global marine biodiversity impacts under climate change scenarios. Fish Fish. 10: 235–251.

Ciannelli, L., Bartolino, V. and Chan, K.-S. 2012. Non-additive and non-stationary properties in the spatial distribution of a large marine fish population. P. Roy. Soc. B 279: 3635–3642.

Cosandey-Godin, A., Krainski, E.T., Worm, B. and Flemming, J.M. 2015. Applying Bayesian spatiotemporal models to fisheries bycatch in the Canadian Arctic. Can. J. Fish. Aquat. Sci. 72: 186–197.

Dickey-Collas, M., Payne, M.R., Trenkel, V.M. and Nash, R.D.M. 2014. Hazard warning: model misuse ahead. ICES J. Mar. Sci. 71: 2300–2306.

Dormann, C. F. 2007. Effects of incorporating spatial autocorrelation into the analysis of species distribution data. Global Ecol. Biogeogr. 16: 129–138.
Elderd, B.D. and Miller, T.E.X. 2016. Quantifying demographic uncertainty: Bayesian methods for integral projection models. Ecol. Monogr. 86: 125–144.
Elith, J. and Leathwick, J. 2009. Species distribution models: ecological explanation and prediction across space and time. Annu. Rev. Ecol. Evol. Syst. 40: 677–697.
Freitas, V., Cardoso, J.F.M.F., Lika, K., Peck, M.A., Campos, J., Kooijman, S.A.L.M. and van der Veer, H.W. 2010. Temperature tolerance and energetics: a dynamic energy budget-based comparison of North Atlantic marine species. Philos. T. Roy. Soc. B 365: 3553– 65.
Gelfand, A.E., Silander Jr, J.A., Wu, S., Latimer, A., Lewis, P.O., Rebelo, A.G. and Holder, M. 2006. Explaining species distribution patterns through hierarchical modeling. Bayesian Anal. 1: 41–92.
Gelman, A. and Hill, J. 2007. Data analysis using regression and multilevel/hierarchical models. Cambridge University Press, New York, USA.
Guisan, A. and Thuiller, W. 2005. Predicting species distribution: offering more than simple habitat models. Ecol. Lett. 8: 993–1009.
Held, L., Schrödle, B. and Rue, H. 2010. Posterior and cross-validatory predictive checks: a comparison of MCMC and INLA. *In* Statistical Modelling and Regression Structures. *Edited by* T. Kneib and G. Tutz. Springer Verlag, Berlin, Germany. pp. 91–110.
Hutchinson, G.E. 1957. Concluding remarks. Cold Spring Harbor Symposium on Quantitative Biology 22: 415–427.
Jørgensen, C., Peck, M.A., Antognarelli, F., Azzurro, E., Burrows, M.T., Cheung, W.W.L., Cucco, A., Holt, R.E., Huebert, K.B., Marras, S., McKenzie, D., Metcalfe, J., Perez-Ruzafa, A., Sinerchia, M., Fleng Steffensen, J., Teal, L.R. and Domenici, P. 2012. Conservation physiology of marine fishes: advancing the predictive capacity of models. Biol. Lett. 8: 900–903.
Krainski, E.T. Lindgren, F. Simpson, D. and Rue, H. 2016. The R-INLA tutorial on SPDE models. Norwegian Univ. of Science and Technology, Trondheim, Norway.
Legendre, P. 1993. Spatial autocorrelation: trouble or new paradigm? Ecology 74: 1659–1673.
Levins, R. 1966. The strategy of model building in population biology. Am. Sci. 54: 421–431.
Lindgren, F., Rue, H. and Lindström, J. 2011. An explicit link between Gaussian fields and Gaussian Markov random fields: the stochastic partial differential equation approach. J. R. Stat. Soc. B 73: 423–498.
Logemann, K., Ólafsson, J., Snorrason, Á., Valdimarsson, H. and Marteinsdóttir, G. 2013. The circulation of Icelandic waters – a modelling study. Ocean Sci. 9: 931–955.
Loots, C., Vaz, S., Planque, B. and Koubbi, P. 2010. What controls the spatial distribution of the North Sea plaice spawning population? Confronting ecological hypotheses through a model selection framework. ICES J. Mar. Sci. 67: 244–257.
Merow, C., Latimer, A.M., Wilson, A.M., Mcmahon, S.M., Rebelo, A.G. and Silander, J.A. 2014. What do we gain from simplicity versus complexity in species distribution models? Ecography 37: 1267–1281.
Ono, K., Shelton, A.O., Ward, E.J., Thorson, J.T., Feist, B.E. and Hilborn, R. 2016. Space-time investigation of the effects of fishing on fish populations. Ecol. Appl. 26: 392–406.

Peck, M.A., Arvanitidis, C., Butenschön, M., Canu, D.M., Chatzinikolaou, E., Cucco, A., Domenici, P., Fernandes, J.A., Gasche, L., Huebert, K.B., Hufnagl, M., Jones, M.C., Kempf, A., Keyl, F., Maar, M., Mahévas, S., Marchal, P., Nicolas, D., Pinnegar, J.K., Rivot, É., Rochette, S., Sell, A.F., Sinerchia, M., Solidoro, C., Somerfield, P.J., Teal, L.R., Travers-Trolet, M. and van de Wolfshaar, K.E. 2018. Projecting changes in the distribution and productivity of living marine resources: a critical review of the suite of modelling approaches used in the large European project VECTORS. Estuar. Coast. Shelf Sci. 201: 40–55.

Planque, B., Fromentin, J.M., Cury, P., Drinkwater, K.F., Jennings, S., Perry, R.I. and Kifani, S. 2010. How does fishing alter marine populations and ecosystems sensitivity to climate? J. Mar. Syst. 79: 403–417.

Planque, B., Bellier, E. and Loots, C. 2011. Uncertainties in projecting spatial distributions of marine populations. ICES J. Mar. Sci. 68: 1045–1050.

Rindorf, A. and Lewy, P. 2006. Warm, windy winters drive cod north and homing of spawners keeps them there. J. Appl. Ecol. 43: 445–453.

Robinson, L.M., Elith, J., Hobday, A.J., Pearson, R.G., Kendall, B.E., Possingham, H.P. and Richardson, A.J. 2011. Pushing the limits in marine species distribution modelling: lessons from the land present challenges and opportunities. Global Ecol. Biogeogr. 20: 789–802.

Rochette, S., Le Pape, O., Vigneau, J., and Rivot, É. 2013. A hierarchical Bayesian model for embedding larval drift and habitat models in integrated life cycles for exploited fish. Ecol. Appl. 23: 1659–1676.

Royle, J., Kéry, M., Gautier, R. and Schmid, H. 2007. Hierarchical spatial models of abundance and occurrence from imperfect survey data. Ecol. Monogr. 77: 465–481.

Rue, H. and Held, L. 2005. Gaussian Markov Random Fields: Theory and Applications. Monographs on Statistics and Applied Probability 104. Chapman & Hall/CRC, Boca Raton, FL, USA.

Rue, H. and Martino, S. 2007. Approximate Bayesian inference for hierarchical Gaussian Markov random fields models. J. Stat. Plan. Inference 137: 3177–3192.

Rue, H., Martino, S., and Chopin, N. 2009. Approximate Bayesian inference for latent Gaussian models by using integrated nested Laplace approximations. J. R. Stat. Soc. B 71: 319–392.

Simpson, D.P., Rue, H., Martins, T.G., Riebler, A. and Sørbye, S.H. 2015. Penalising model component complexity: a principled, practical approach to constructing priors. arXiv 1403.4630 [stat.ME].

Soberón, J. 2007. Grinnellian and Eltonian niches and geographic distributions of species. – Ecol. Lett. 10: 1115–1123.

Teal, L.R., Marras, S., Peck, M.A. and Domenici, P. 2016. Physiology-based modelling approaches to characterize fish habitat suitability: their usefulness and limitations. Estuar. Coast. Shelf Sci. doi:10.1016/j.ecss.2015.11.014.

Teal, L.R., van Hal, R., van Kooten, T., Ruardij, P. and Rijnsdorp, A.D. 2012. Bio-energetics underpins the spatial response of North Sea plaice (*Pleuronectes platessa* L.) and sole (*Solea solea* L.) to climate change. Glob. Change Biol. 18: 3291–3305.

Ward, E.J., Jannot, J.E., Lee, Y., Ono, K., Shelton, A.O. and Thorson, J.T. 2015. Using spatiotemporal species distribution models to identify temporally evolving hotspots of species co-occurrence. Ecol. Appl. 25: 2198–2209.

Appendix 10. Fish and mammal predation on herring

Humans are but one of herring's many predators. Across their distributional range, herring aggregations are targeted by demersal and pelagic fishes, in addition to several species of seals, whales and seabirds (Read and Brownstein 2003; Pitcher et al. 1996; Similä et al. 1996; Nøttestad and Axelsen 1999; Overholtz and Link 2007; Guse et al. 2009; Víkingsson et al. 2014). Herring have developed complex behavioral strategies to combat this; classic examples including diurnal vertical migration (Dommasnes et al. 1994) and extended residence in deep waters, that whilst potentially energetically expensive (Huse and Ona 1996) are suggested as an adaptive response to visual predators like Atlantic cod (*Gadus morhua*) (Langård et al. 2014), surface-feeding fin whales (*Balaenoptera physalus*) (Nøttestad et al. 2002) and killer whales (*Orcinus orca*) (Similä 1997). In-situ observations of killer whale- herring interactions on wintering grounds in Norway have shed further light on the diversity of predator-evasion responses employed by herring schools (Nøttestad 1998; Nøttestad and Axelsen 1999), and the cooperative tactics used by killer whales to overcome such responses (Similä 1997; Domenici et al. 2000).

In Icelandic waters, killer whales specialize on wintering ISS herring, and large numbers of these whales are often present on the wintering grounds between December and March (Samarra and Foote 2015). The ability of killer whales to influence herring schooling behaviour is very real (Nøttestad and Axelsen 1999). However, as herring are typically established on wintering grounds by early October (pre-dating killer whale arrival – Samarra and Foote 2015), and wintering areas are not vacated once colonized (ICES 2014; authors' personal observation), we propose that any displacement by killer whale foraging would occur mainly at localized scales. For these reasons, and due to data scarcity, we did not include killer whale occurrence or density in our analysis. We stress however, that information on arrival times may help expose the evolutionary and contemporary risks herring face in following traditions and returning to the same, predator-rich, wintering grounds.

References

Domenici, P., Batty, R.S., Similä, T. and Ogam, E. 2000. Killer whales (*Orcinus orca*) feeding on schooling herring (*Clupea harengus*) using underwater tail-slaps: kinematic analyses of field observations. J. Exp. Biol. 203: 283–294.

Dommasnes, A., Rey, F. and Rottingen, I. 1994. Reduced oxygen concentrations in herring wintering areas. ICES J. Mar. Sci. 51: 63–69.

Guse, N., Garthe, S. and Schirmeister, B. 2009. Diet of red-throated divers *Gavia stellata* reflects the seasonal availability of Atlantic herring *Clupea harengus* in the southwestern Baltic Sea. J. Sea Res. 62: 268–275.

Huse, I. and Ona, E. 1996. Tilt angle distribution and swimming speed of overwintering Norwegian spring spawning herring. ICES J. Mar. Sci. 53: 863–873.

ICES. 2014. Advice for 2014/2015 Herring in Division Va (Icelandic summer-spawning herring). ICES Advice 2014, Book 2:1–7, Copenhagen, Denmark.

Langård, L., Fatnes, O., Johannessen, A., Skaret, G., Axelsen, B., Nøttestad, L., Slotte, A., Jensen, K. and Fernö, A. 2014. State-dependent spatial and intra-school dynamics in pre-spawning herring *Clupea harengus* in a semi-enclosed ecosystem. Mar. Ecol. Prog. Ser. 501: 251–263.

Nøttestad, L. 1998. Extensive gas bubble release in Norwegian spring-spawning herring (*Clupea harengus*) during predator avoidance. ICES J. Mar. Sci. 55: 1133–1140.
Nøttestad, L. and Axelsen, B. E. 1999. Herring schooling manoeuvres in response to killer whale attacks. Can. J. Fish. Aquat. Sci. 77: 1540–1546.
Nøttestad, L., Fernö, A., Mackinson, S., Pitcher, T.J. and Misund, O.A. 2002. How whales influence herring school dynamics in a cold-front area of the Norwegian Sea. ICES J. Mar. Sci. 59: 393–400.
Overholtz, W.J. and Link, J.S. 2007. Consumption impacts by marine mammals, fish, and seabirds on the Gulf of Maine – Georges Bank Atlantic herring (*Clupea harengus*) complex during the years 1977 - 2002. ICES J. Mar. Sci. 64: 83–96.
Pitcher, T.J., Misund, O.A., Fernö, A., Totland, B. and Melle, V. 1996. Adaptive behaviour of herring schools in the Norwegian Sea as revealed by high-resolution sonar. ICES J. Mar. Sci. 53: 449–452.
Read, A.J. and Brownstein, C.R. 2003. Considering other consumers: fisheries, predators, and Atlantic herring in the Gulf of Maine. Conserv. Ecol. 7: 1–12.
Samarra, F.I.P. and Foote, A.D. 2015. Seasonal movements of killer whales between Iceland and Scotland. Aquat. Biol. 24: 75–79.
Similä, T. 1997. Sonar observations of killer whales (Orcinus orca) feeding on herring schools. Aquat. Mamm. 23.3: 119–126.
Similä, T., Holst, J.C. and Christensen, I. 1996. Occurrence and diet of killer whales in northern Norway: seasonal patterns relative to the distribution and abundance of Norwegian spring-spawning herring. Can. J. Fish. Aquat. Sci. 53: 769–779.
Víkingsson, G.A., Elvarsson, B.Þ., Ólafsdóttir, D., Sigurjónsson, J., Chosson, V., and Galan, A. 2014. Recent changes in the diet composition of common minke whales (*Balaenoptera acutorostrata*) in Icelandic waters. A consequence of climate change? Mar. Biol. Res. 10: 138–152.

Paper II

Combining multiple datasets to unravel the spatiotemporal dynamics of a data-limited fish stock

Cecilia Pinto, Morgane Travers-Trolet, Jed I. Macdonald, Étienne Rivot, Youen Vermard

(Published in *Canadian Journal of Fisheries and Aquatic Sciences* 76: 1338–1349, 2019)

Author contributions – Conceived and designed the experiments: CP, YV, MTT, ER, JIM; analysed the data and contributed code: CP, YV, JIM; wrote the manuscript: CP, JIM, ER; reviewed and edited the manuscript: CP, JIM, ER, MTT, YV.

Combining multiple datasets to unravel the spatiotemporal dynamics of a data-limited fish stock

Cecilia Pinto[1,2], Morgane Travers-Trolet[1], Jed I. Macdonald[3,4], Étienne Rivot[5], Youen Vermard[6]

[1]IFREMER, Département Halieutique de Manche Mer du Nord, 150 Quai Gambetta, BP 699, 62321 Boulogne s/mer, France
[2]Joint Research Centre – Directorate D, Sustainable Resources – Unit D.0, Water and Marine Resources, TP 051, Via Enrico Fermi 2749, 21027 Ispra (VA), Italy
[3]Faculty of Life and Environmental Sciences, University of Iceland, 101 Reykjavík, Iceland
[4]School of BioSciences, The University of Melbourne, Parkville, Victoria 3052, Australia
[5]UMR 985 ESE Ecology and Ecosystem Health, Agrocampus Ouest, INRA, 35042 Rennes, France
[6]IFREMER, Département Ecologie et Modèles pour l'Halieutique, Rue de l'Ile d'Yeu, BP 16 21105, 44311 Nantes cedex 03, France

Abstract

The biological status of many commercially-exploited fishes remains unknown, mostly due to a lack of data necessary for their assessment. Investigating the spatiotemporal dynamics of such species can lead to new insights into population processes, and foster a path towards improved spatial management decisions. Here, we focused on striped red mullet (*Mullus surmuletus*), a widespread, yet data-limited species of high commercial importance. We aimed to quantify range dynamics in this data-poor scenario, and combined fishery-dependent and -independent datasets through a series of Bayesian mixed-effects models designed to capture monthly and seasonal occurrence patterns near the species' northern range limit across 20 years. Combining multiple datasets allowed us to cover the entire distribution of the northern population of *Mullus surmuletus*, exploring dynamics at different spatiotemporal scales, and identifying key environmental drivers (i.e. sea surface temperature, salinity) that shape occurrence patterns. Our results demonstrate that even when process and/or observation uncertainty is high, or when data is sparse, combining multiple datasets within a hierarchical modelling framework can yield accurate and useful spatial predictions.

Introduction

Long-term time series are a valuable resource for testing hypotheses on how temporal variability in recruitment or abundance, or patterns of range expansion or distributional shift may relate to climatic and anthropogenic events (Doney et al. 2012; Hawkins et al. 2013). This is a prerequisite to forecast the response of populations under future scenarios of environmental change and additional anthropogenic stressors, such as fishing pressure (Szuwalski and Punt 2015).

Many fish stocks targeted by fisheries are not subjected to standardized assessment methods (Costello et al. 2012), meaning that both their exploitation level and their resilience to exploitation are uncertain. Non-assessed stocks not only comprise species of low commercial importance; some highly exploited species also fall outside the assessment process. This situation is often due to data scarcity, driven either by a lack of government investment in the fisheries management process, or through the history of the data collection itself (Hilborn and Ovando 2014).

Stock assessment methods for so-called data limited stocks (DLS) have received considerable interest in recent years, with the development of new methods based on life history traits (e.g. body-size frequencies), or trends in abundance and fleets (ICES 2017; Kokkalis et al. 2017). However, data are still missing for many species, and if present, are often only available over short time scales. This can reduce confidence in the evaluation process, with potential consequences for the viability of fish populations and associated fisheries (Costello et al. 2012).

When time series are short or sampling coverage sparse, combining different data sources within a single analysis can help to overcome the limitations of single datasets considered separately. Dependent upon their respective spatiotemporal coverage, amalgamating datasets allows for extending the time series, widening the area covered, and ultimately improving the power of the analysis and our understanding of population dynamics. The development of integrated analysis (as defined in Maunder and Punt (2013)) as a tool to combine data arising from different sampling methods (with their own spatial and temporal heterogeneity) within a single framework, has received attention in the statistical ecology literature (McGeoch and Gaston 2002) and in fisheries sciences (Maunder and Punt 2013 and references therein). Hierarchical modelling approaches explicitly separate out process models from observation models, and therefore offer an efficient framework for this purpose. The process equations allow for modelling multiple dependencies and stochasticity in a hierarchy of scales suitable to depict the spatial and temporal variability present within the data through latent parameters, whilst the set of observation equations define how the data relate to the state variables of the model (Gelfand 2012; Parent and Rivot 2013; Kéry and Royle 2016). This class of models is also particularly well suited to capturing residual correlation patterns through inclusion of spatial (or temporal) correlation structure in the latent variables (Legendre 1993; Elith and Leathwick 2009; Thorson and Minto 2015). Bayesian inference in hierarchical models offers additional technical convenience, and provides outputs in a probabilistic rationale that fully propagates uncertainty (Punt and Hilborn 1997; Harwood and Stokes 2003).

Here, we combine four fishery-dependent and fishery-independent datasets, spanning a 20-year period, within a single hierarchical model to explore monthly and seasonal occurrence

patterns of striped red mullet (*Mullus surmuletus*, Linnaeus, 1758), a demersal Mullid of high commercial importance. We focus on the "northern subpopulation" that resides in the North Sea and eastern English Channel, and shows little mixing with the "southern subpopulation" (Bay of Biscay) (Mahé et al. 2014) and the "mixing zone subpopulation" (Celtic Sea and the Western English Channel) (Benzinou et al. 2013). Despite being commercially targeted across much of its range, information on the sensitivity of this species to changing environmental conditions is scarce. The hypothesized role of dynamic gradients (e.g. sea surface temperature) in shaping the migration and distribution patterns of the northern subpopulation (Beare et al. 2005; Engelhard et al. 2011) requires further enquiry using data covering the full geographic range of the subpopulation, over several years. This northern subpopulation is also characterized by strong oscillations in abundance between consecutive years (Mahé et al. 2005). During the last five years, fluctuations have increased in magnitude, concurrently with the loss of the oldest and most efficient spawners from the population (ICES 2015). These indices suggest an effect of overexploitation (Iglésias et al. 2010) and are an alarm bell for future (and perhaps prolonged) depletion. Implementation of restrictive management options are currently being debated, such as the implementation of quota sharing within the total allowable catch (TAC) for the subpopulation, as already established in a multilateral context for other species in the North Sea (Hannesson 2013).

Indications of a depleted population state, dramatic fluctuations in abundance and high uncertainty regarding the drivers underpinning spatial distribution and migration patterns constitute strong motivations to fill ecological knowledge gaps for this species, and eventually provide more reliable scientific advice for fisheries management. To this end, the objectives of our study are twofold: 1) to clarify the role of environmental factors in shaping occurrence patterns across the full distributional range of the northern subpopulation of striped red mullet; and 2) to gain insight into the mechanisms governing the marked inter-annual variability in abundance and the seasonal migrations that characterize the spatiotemporal dynamics of this subpopulation.

Materials and methods

Presence/absence data

Our data are derived from three scientific bottom-trawl surveys and one set of commercial fishery catch records. The scientific surveys were the winter and summer International Bottom Trawl Survey (IBTS) (ICES 2017) and the Channel Ground Fish Survey (CGFS) (Coppin and Travers-Trolet 1989). The IBTS surveys take place over one month across January and February (winter survey, IBTS-Q1), and one month across August and September (summer survey, IBTS-Q3) and cover the whole of the North Sea. Since 2007, the winter survey has been expanded into the eastern English Channel. The CGFS takes place over one month in October, and has covered the eastern English Channel since 1990. As the North Sea was not systematically sampled twice a year prior to 1995, only survey data from 1995 to 2015 are considered here. The commercial data come from the OBSMER French program (Cornou et al. 2016) which aims to collect data on landings and discards through at-sea observers. Catch data were available throughout the year (for every fishing operation on each sampled trip) from 2003 to 2015.

The four datasets were first reclassified into two new datasets based on their spatial and temporal coverage. Dataset A (n = 8391) comprises observations from IBTS-Q1, IBTS-Q3, CGFS and OBSMER covering the eastern English Channel and the southern North Sea (Figure 1) and spanning the years 1995 to 2015 at a monthly resolution. Dataset B (n = 13853) has the same temporal coverage (1995-2015) but covers a larger spatial area than Dataset A. It includes the whole of the North Sea and comprises fishery-independent records only (i.e. IBTS-Q1, IBTS-Q3 and CGFS), at a seasonal (i.e. winter, summer and autumn) resolution (Figure 1). The number of records available from each data source is presented in Table S1.

For both datasets A and B, georeferenced point records describing the catches of striped red mullet captured at a particular location *s*, and time *t*, were transformed to presence/absence records. This is a critical simplification to limit the effect of heterogeneity in fishing effort and catchability among the various datasets, and allows us to consider that all sampling methods are equivalently informative relative to the presence/absence of the species. To further limit heterogeneity in the catchability and avoid false zeros due to low catchability (Martin et al. 2005) when using OBSMER data, only records from bottom-trawlers using a mesh size between 70-90mm were extracted for the analysis, as larger mesh sizes are typically used by boats targeting other species (e.g. *Pollachius virens*).

Environmental covariates

Presence/absence records were correlated with a set of environmental covariates thought to influence the occurrence of striped red mullet: depth at seabed, sediment type, sea surface temperature (SST) and sea surface salinity (SSS). Depth at seabed (DEP) was extracted from the NORWegian ECOlogical Model system (NORWECOM) database (http://www.imr.no/~morten/wgoofe/). SSS was extracted at a monthly resolution from the NORWECOM website for the time interval from 1990 to 2008, while data for 2009-2015 were obtained directly from the author of the model system. The SST data were obtained from satellite observations at a daily resolution, but for the purposes of this study a monthly mean was computed. SST values from 1990 to 2008 were extracted from the AVHRR Pathfinder Version 5.2 (PFV5.2) dataset, provided by the US National Oceanographic Data Center and GHRSST (http://pathfinder.nodc.noaa.gov) (Casey et al. 2010), whilst data from 2009 to 2015 were extracted from the ODYSSEA processing chain operated within the ESA/MEDSPIRATION project (Gohin et al. 2010). Seabed sediment types (SED) were adapted from Larsonneur et al. (1982) and Schluter and Jerosch (2008), and reclassified into five broad categories: mud, fine sand, coarse sand, gravel and pebbles. To test for collinearity among covariates, we used the 'vif.mer' function (threshold set to 10) on a model object fitted using the 'lme4' package (Bates et al. 2015) in R version 3.3.0 (R Core Team 2016), to calculate variance inflation factors (VIFs) for each predictor (R code available here: https://github.com/aufrank/R-hacks/blob/master/mer-utils.R). No collinearity among covariates was detected, so VIFs are not reported in the Results.

Modelling striped red mullet occurrence

Dataset A and Dataset B were analysed independently but using the same modelling approach. Models were built in a hierarchical Bayesian framework using the SPDE (Stochastic Partial differential Equations) approach in the 'R-INLA' package (Rue et al. 2009; Lindgren et al. 2011; Lindgren and Rue 2015) in R. This approach provides direct

inference on the spatial and temporal dependencies in the data. The process equation models the probability, $p_t(s)$ of striped red mullet presence at time-step *t* (i.e. either month or season) and location *s*, as a random field on the logit scale:-

$$\text{logit}\left(p_t(s)\right) = X_t(s)\beta + \theta_t(s) \qquad \text{(eq. 1)}$$

where $X_t(s)$ represents a vector of covariates (depth at seabed, sediment, SST, SSS) at time-step *t* and at location *s*, β represents a vector of coefficients (fixed effects) to be estimated, and $\theta_t(s)$ is a spatiotemporal random effect to account for variation not explicitly explained by covariates. Random effects are defined by a Gaussian random field that is spatially autoregressive (depending on the distance between locations) and temporally uncorrelated (for details see Cameletti et al. 2013). To avoid computational costs that rapidly arise in continuous space (the so called big-n problem) (Lasinio et al. 2013), the spatial covariation is modelled within a Gaussian Markov random field (GMRF) on a discrete mesh, that defines the area of interest (Krainski et al. 2016) (see Figure S1). This way, the influence of spatial covariance at any point *s* is reduced to a set of neighbours (Cameletti et al. 2013).

Given the latent field of presence probability $p_t(s)$ at any time *t* and location *s*, presence/absence data $y_t(s)$ are modelled as mutually independent and identically distributed Bernoulli variables:-

$$y_t(s) \sim \text{Bernoulli}\left(p_t(s)\right) \qquad \text{(eq. 2)}$$

The full likelihood equation for the model then arises from the product of Bernoulli for all raw data (eq. 2). Because all data sources are considered as presence/absence, the strength of the hierarchical structure is that different data sources are integrated within a single analysis to infer a unique random field model for the probability of presence that captures the spatiotemporal covariations as defined in eq. (1).

Within the SPDE approach, eq. 1 can be rewritten as:-

$$\text{logit}\left(p_t(s)\right) = X_t(s)\beta + \text{A}_t(s)\theta_t \qquad \text{(eq. 3)}$$

where observation matrix $\text{A}_t(s)$ is directly related to the space discretizing mesh (Figure S1) as it extracts the values of the spatiotemporal random field at each location *s* and at each time *t*. The realization of the random field can be represented through its mean density distribution and standard deviation, which in turn can be translated as the level of uncertainty at a certain location depending on the availability of data points (Cameletti et al. 2013). The quantification of such uncertainty, allowed us to account for the heterogeneity across time and space originating from the integration of different datasets.

Several mesh designs were compared visually and the sensitivity of parameter estimation to the different designs assessed (Cosandey-Godin et al. 2015). The best mesh design for each dataset (see Figure S1) includes an outer extension to avoid a 'boundary effect' (Lindgren and Rue 2015) and regularly-shaped triangles, both in the inner and in the outer extension, and at the border between the two extensions (Krainski et al. 2016). Once the best mesh was selected, parameter values defining it were kept constant across models (i.e. at the same spatial resolution).

The simplified Laplace method was used to approximate the posterior marginal distributions (for details see Martins et al. 2013). We built and compared models of increasing complexity, from null models including no covariates to full models including all covariates and random effects. Models were compared through the deviance information criterion (DIC), the log marginal likelihood and by estimating the variance contribution of random effects against that of fixed effects. To evaluate out-of-sample predictive capacity for each fitted model, we derived the conditional predictive ordinate (CPO), defined as the cross-validated (cv) predictive density at observation $y_t(s)$ with that observation removed (Roos and Held 2011). We used the CPO values to compute the cv logarithmic score (CVLS) (Gneiting and Raftery 2007), a measure of predictive quality, and the cv Brier score (i.e. mean prediction error) for each model. This latter score evaluates the correspondence between fitted probabilities and observed binary outcomes (Schmid and Griffith 2005; Roos and Held 2011). Lower values on both scores reflect better predictions, with the Brier score interpreted relative to a reference value equal to sampling prevalence. The probability of presence was predicted across the whole area covered by each dataset, but here we limit our spatial predictions to more reliable areas where the standard deviation of $p_t(s)$ was smaller than a 'cutoff' value, defined here as equal to its mean (Figure S2). Following Ward et al. (2015), we also estimated the predictive accuracy of the best model through the area under the receiver operating characteristic curve (AUC) using the 'ROCR' package (Sing et al. 2005).

Priors

We used the default priors for the fixed effects and hyperparameters as implemented in R-INLA (described in Lindgren and Rue 2015). Hyperparameters currently constitute an active area of research for the R-INLA team (see R-INLA documentation available at http://www.r-inla.org/). The latent field parameters θ_1 and θ_2 were defined by a multivariate normal distribution which is a combination of θ_1 = N(0,10), θ_2 = N(0,10). All fixed parameter priors were defined by a N(0,1000) except the intercept that has a prior distribution N(0,∞).

Results

Model selection

Models with a month within year structure (for dataset A) and season within year (for dataset B) structure for the random effect were always preferred based on DIC. Models including all environmental covariates were selected as the best models on the balance of the DIC, the log marginal likelihood estimates, the reduced variance contribution of the spatial effect and predictive quality (CVLS and Brier score) (Table 1). The spatial correlation range (nominal range) of the best model for dataset A was 2.66 decimal degrees, and 8.51 for dataset B (Table 1). The AUC estimated for the best model for dataset A was 0.61, and 0.69 for dataset B.

Environmental parameters

Though posterior 95% credible intervals overlapped 0 in some cases (Table 2), all covariates appeared to add some information the models and their addition generally improved model fit and predictive capacity (Table 1). SST and SSS were positively correlated with the presence of striped red mullet for dataset A, while for dataset B only SST was significant

(Table 2). Sediment types were not correlated with the presence of striped red mullet at the monthly time scale for dataset A, or at a seasonal scale for dataset B. Finally, depth at seabed alone had little influence on the distribution of striped red mullet in both datasets (Table 2).

Spatial latent field

Posterior estimates of the spatial random effects inform about spatiotemporal variability that was not captured by the covariates in the model. Results are presented from 2009 onwards to allow direct comparison between datasets, as data for all months and seasons are available only from 2009.

For dataset A, posterior estimates of the spatial random effect revealed that the northern subpopulation of striped red mullet changed its distribution month by month, moving into and out of the eastern English Channel (Figure 2). However, due to high variability inherent in commercial sampling and fewer observations per month, as revealed through the patterns in random field standard deviations for dataset A (Figure 4), it is difficult to identify a consistent monthly movement trend. For dataset B, in which sampling was consistent between winter and summer, our models revealed a seasonal distribution shift from the north-east in the winter, to the south in the summer, with higher uncertainty apparent across the region during autumn, as data were available only for the eastern English Channel at that time (Figure 3).

Predicted probability of presence

Our modelling framework also generates predictions of the probability of presence at any point in the region, provided that covariates are available. Figure 5 shows the predicted probability of presence of striped red mullet in the area encompassed by dataset A, but only where predictions were deemed reliable, i.e. where the standard deviation of $p_t(s)$ was lower than 13.23 (see Figure S2). Beyond the inter-annual and seasonal variability in the probability of striped red mullet presence, recurrent patterns can be detected. Results highlight strong seasonal differences, with high predicted probability of presence (>70%) from July to October when the surface waters are warmer and lower probability of presence (<50%) predicted for colder months (late winter) (Figures 5, S3A). We also detected changes across years linked to SST. For example, during the coldest springs of the series (2010 and 2013) (Figure S3B), the probability of presence in the eastern English Channel and the southern North Sea the region was substantially lower than in other years (Figures 5, S3A). Predictions from both datasets also suggest the existence of seasonal movements of striped red mullet across the study area. For example, during the period 2009 to 2015, the northern subpopulation appears to have wintered in two main areas: the English Channel, and the northwest of the North Sea (Figures 5, 6). Monthly predictions from dataset A indicate a distributional shift from the English Channel towards the Strait of Dover in spring, although this pattern varies across years (see Figure 5). Predictions from both datasets then suggest a northward expansion of the distribution into the southern North Sea during late spring and summer, followed by a contraction back towards the Channel in late autumn (Figures 5, 6). We note also that in 2015, the probability of presence remained high in the English Channel throughout the year, a year in which SST showed slightly weaker seasonality compared with previous years (Figure S3).

Discussion

This study provides the first spatially-explicit analysis of how environmental parameters may shape the distribution of striped red mullet near its northern range boundary. We integrated all available georeferenced information on the occurrence of the northern subpopulation within models that directly account for correlation structures in the data, and the sources of uncertainty in data and process. The results provide a substantive contribution to our understanding of the spatiotemporal dynamics of this data-limited stock. Despite marked inter-annual variability in distributional range, we detected clear patterns of seasonal movement; namely, winter residence in the northwest of the North Sea and the English Channel, expansion into the southern North Sea in spring/summer and contraction back into the eastern English Channel in autumn.

Our findings suggest that the occurrence of the northern subpopulation is positively correlated with water salinity and temperature. Results for the latter covariate match suggestions by Beare et al. (2005), who hypothesized that the presence of striped red mullet in northern waters in winter was related to increasing surface water temperatures. Moreover, our predictions show that certain years are characterized by larger occupied areas (e.g. 2011 and 2015) interspersed with years of very low and/or scattered concentrations (e.g. 2013) (see Figures 5, 6). This complements previous descriptions of the strong interannual fluctuations in abundance within this subpopulation (Mahé et al. 2005; Carpentier et al. 2009). Whether range expansion is linked to population size alone in this species (see Fisher and Frank 2004), or synergies between abundance and environmental factors, remains an open question. Striped red mullet has increased in abundance by 30% over the last two decades in the English Channel, concomitant with a shift towards a warmer phase of the Atlantic Multidecadal Oscillation index (Auber et al. 2015), with further increases possible under future warming scenarios (Cheung et al. 2013), all else being equal.

However, higher abundances do not necessarily result in distribution extensions, and further investigation is needed into the strength of the 'abundance–area' relationship for North Sea red striped mullet populations in order to optimize spatial management efforts. That said, presence/absence data are often more easily obtained and more widely available than abundance data, and modelling presence/absence can simplify the integration of data obtained from heterogeneous sources. Indeed, provided that detection probabilities of the survey method(s) are equal to one, or if not, that they can be accounted for, presence/absence models as used in this study allow us to largely ignore variation in catchability among different survey methods and sampling gears.

Although results from both datasets identify a positive effect of SST on the presence of striped red mullet across our study region, some discrepancies in model outputs between the datasets are evident. As an example, estimated $p_t(s)$ during summer in the English Channel is roughly 0.6 higher in dataset A compared with dataset B, although the spatial patterns in $p_t(s)$ are fairly congruent between datasets (Figures 5, 6). One possible explanation for this relates to sampling coverage. Dataset B is derived mainly from IBTS data that are consistently sampled every winter and every summer. Dataset A also contains data from the IBTS surveys, but is complemented by the OBSMER data. Though incorporating true absences, this commercial dataset is potentially biased by variation in nominal and spatial commercial fishing effort that shifts not only between months but also between years (Figure S4, S5). Although we cannot completely rule out seasonally-varying fishing effort as

contributing to our spatial predictions for dataset A, we suggest that any effects are relatively minor given our use of presence/absence data as previously discussed. Building two different models based on the two different datasets allows us to glean the maximum possible information from both, and improve our understanding of the species' dynamics at different spatial and temporal scales. Dataset A provides insight into the spatiotemporal dynamics of the northern population of striped red mullet at a monthly level, while dataset B exposes seasonal dynamics at a larger spatial scale, using spatially-consistent survey information. Importantly, the lower level of sampling heterogeneity in dataset B suggests where, spatially, the predictions from dataset A may be less reliable due to the high uncertainty given by non-consistent sampling.

Integrating data from multiple sampling campaigns increased both the number of observations for our analysis, and our capacity to detect statistical flukes (Maunder and Punt 2013). Moreover, comparing the results from the separate analyses of datasets A and B allowed us to expand our geographical coverage and explore the consistency of inferences across two different spatial scales and at two different temporal resolutions (i.e. monthly for A, and seasonal for B). As noted by Maunder and Punt (2013), when integrating multiple data sources, a trade off must be found that maximizes scientific reward in light of the challenges presented by integrated analysis. Indeed, combining datasets within a single analysis does not necessarily give rise to improved understanding of the target system, as it may lead to conflicts in what the datasets tell us, in addition to increasing statistical complexity and computational costs. Distilling the IBTS-Q1, IBTS-Q3, CGFS and OBSMER datasets into datasets A and B that differed in spatial and temporal resolution, was our trade off.

The major source of uncertainty in our datasets came from the lack of commercial landings information for single months in the years prior to 2003 (the time series is complete for each month only from 2009 onwards). Confidence surrounding model estimates during this time period is therefore relatively low, and further efforts are needed to improve data quality in future analyses. A substantial impediment to progress on this front relates to the difficulties in accessing commercial catch and observer data from countries bordering the North Sea. The advantages of obtaining observer data from foreign fisheries targeting local stocks was demonstrated in US fisheries (French et al. 1982) and stands in stark contrast to the situation in the eastern English Channel and North Sea, where multiple countries similarly share the quota on several harvested stocks. Hannesson et al. (2013) showed that cooperation always brings more advantages than competition when quota is shared among parties. Hence, strong incentive exists to integrate all the available data – both fishery dependent and independent (e.g. national observer programs) – to maximize coverage of spatiotemporal information for commercial stocks.

Species which are commercially exploited, though not formally managed, are particularly vulnerable to overexploitation, as their population dynamics are often not monitored with no limits placed on landings or minimum sizes. Using striped red mullet for illustration, our results have demonstrated some advantages of data integration within models that explicitly account for process and observation uncertainties, providing new insights into the spatiotemporal dynamics of the northern subpopulation within the North Sea and eastern English Channel. It is important to note, however, that such models alone are not the silver bullet for developing successful management directives under data-poor scenarios. Instead, we hope this work inspires future sampling designs, data collection and multilateral data-

sharing programs that in conjunction with appropriate modelling approaches can lead to better adaptive management decisions for data-limited populations more generally (Walters 2007; Maunder and Punt 2013).

Acknowledgements

CP's postdoc was funded by IF and France Filière Peche. We thank Bruno Ernande for the suggestions on the analysis and two anonymous reviewers for their comments which helped to improve the manuscript.

References

Auber, A., Travers-Trolet, M., Villanueva, M.C. and Ernande, B. 2015. Regime shift in an exploited fish community related to natural climate oscillations. PLoS One 10: e0129883.

Bates, D., Mächler, M., Bolker, B.M. and Walker, S.C. 2015. Fitting linear mixed effects models using lme4. J. Stat. Softw. 67: 1–48.

Beare, D., Burns, F., Jones, E., Peach, K., and Reid, D. 2005. Red mullet migration into the northern North Sea during late winter. J. Sea Res. 53: 205–212.

Benzinou, A., Carbini, S., Nasreddine, K., Elleboode, R. and Mahé, K. 2013. Discriminating stocks of striped red mullet (*Mullus surmuletus*) in the Northwest European seas using three automatic shape classification methods. Fish. Res. 143: 153–160.

Cameletti, M., Lindgren, F., Simpson, D. and Rue, H. 2013. Spatio-temporal modeling of particulate matter concentration through the SPDE approach. AStA Adv. Stat. Anal. 97: 109–131.

Carpentier, A., Martin, C.S. and Vaz, S. 2009. Channel Habitat Atlas for Marine Resource Management (CHARM Phase II), INTERREG 3a Programme. IFREMER: Boulognesur-Mer, France.

Casey, K.S., Brandon, T.B., Cornillon, P. and Evans, R. 2010. The Past, Present, and Future of the AVHRR Pathfinder SST Program. *In* Oceanography from Space, revisited. *Edited by* V. Barale, J.F.R Gower and L. Alberotanza. Springer, Dordrecht, Netherlands. pp. 323–341.

Cheung, W.W.L., Watson, R. and Pauly, D. 2013. Signature of ocean warming in global fisheries catch. Nature 497: 365–368.

Coppin, F. and Travers-Trolet, M. 1989. CGFS: Channel Ground Fish Survey. IFREMER, France. Available from http://dx.doi.org/10.18142/11.

Cornou, A.-S., Diméet, J., Goascoz, N., Quinio-Scavinner, M. and Rochet, M.-J. 2016. Captures et rejets des metiers de peche francais Resultats des observations a bord des navires de peche professionnelle en 2015. IFREMER, France.

Cosandey-Godin, A., Krainski, E.T., Worm, B. and Flemming, J.M. 2015. Applying Bayesian spatiotemporal models to fisheries bycatch in the Canadian Arctic. Can. J. Fish. Aquat. Sci. 72: 186–197.

Costello, C., Ovando, D., Hilborn, R., Gaines, S.D., Deschenes, O. and Lester, S.E. 2012. Status and solutions for the world's unassessed fisheries. Science 338: 517–520.

Doney, S.C., Ruckelshaus, M., Emmett Duffy, J., Barry, J.P., Chan, F., English, C.A., Galindo, H.M., Grebmeier, J.M., Hollowed, A.B., Knowlton, N., Polovina, J.,

Rabalais, N.N., Sydeman, W.J. and Talley, L.D. 2012. Climate change impacts on marine ecosystems. Ann. Rev. Mar. Sci. 4: 11–37.
Elith, J. and Leathwick, J.R. 2009. Species distribution models: ecological explanation and prediction across space and time. Annu. Rev. Ecol. Evol. Syst. 40: 677–697.
Engelhard, G.H., Pinnegar, J.K., Kell, L.T. and Rijnsdorp, A.D. 2011. Nine decades of North Sea sole and plaice distribution. ICES J. Mar. Sci. 68: 1090–1104.
Fisher, J. and Frank, K. 2004. Abundance-distribution relationships and conservation of exploited marine fishes. Mar. Ecol. Prog. Ser. 279: 201–213.
French, R., Nelson Jr., R. and Wall, J. 1982. Role of the United States Observer Program in management of foreign fisheries in the Northeast Pacific Ocean and Eastern Bering Sea. North Am. J. Fish. Manag. 2: 122–131.
Gelfand, A.E. 2012. Hierarchical modeling for spatial data problems. Spat. Stat. 1: 30–39.
Gneiting, T. and Raftery, A.E. 2007. Strictly proper scoring rules, prediction, and estimation. J. Am. Stat. Assoc. 102: 359–378.
Gohin, F., Saulquin, B. and Bryere, P. 2010. Atlas de la Température, de la concentration en Chlorophylle et de la Turbidité de surface du plateau continental français et de ses abords de l'Ouest européen. IFREMER, France.
Hannesson, R. 2013. Sharing a migrating fish stock. Mar. Resour. Econ. 28: 1–17.
Harwood, J. and Stokes, K. 2003. Coping with uncertainty in ecological advice: lessons from fisheries. Trends Ecol. Evol. 18: 617–622.
Hawkins, S.J., Firth, L.B., McHugh, M., Poloczanska, E.S., Herbert, R.J.H., Burrows, M.T., Kendall, M.A., Moore, P.J., Thompson, R.C., Jenkins, S.R., Sims, D.W., Genner, M.J. and Mieszkowska, N. 2013. Data rescue and re-use: recycling old information to address new policy concerns. Mar. Policy 42: 91–98.
Hilborn, R. and Ovando, D. 2014. Reflections on the success of traditional fisheries management. ICES J. Mar. Sci. 71: 1040–1046.
ICES. 2015. Report of the Benchmark Workshop on North Sea Stocks (WKNSEA). 2–6 February 2015, Copenhagen, Denmark.
ICES 2017. Report of the ICES Workshop on the Development of Quantitative Assessment Methodologies based on Life-history traits, exploitation characteristics, and other relevant parameters for stocks in categories 3–6 (WKLIFEVI). 3–7 October 2016, Lisbon, Portugal.
Iglésias, S.P., Toulhoat, L. and Sellos, D.Y. 2010. Taxonomic confusion and market mislabelling of threatened skates: important consequences for their conservation status. Aquat. Conserv. Mar. Freshw. Ecosyst. 20: 319–333.
Kéry, M. and Royle, J.A. 2016. What are hierarchical models and how do we analyze them? *In* Applied Hierarchical Modeling in Ecology: Analysis of distribution, abundance, and species richness in R and BUGS – Volume 1 Prelude and Static Models. Academic Press and Elsevier, Amsterdam, The Netherlands. pp. 19–78.
Kokkalis, A., Eikeset, A.M., Thygesen, U.H., Steingrund, P. and Andersen, K.H. 2016. Estimating uncertainty of data limited stock assessments. ICES J. Mar. Sci. 74: 69–77.
Krainski, E.T., Lindgren, F., Simpson, D. and Rue, H. 2016. The R-INLA tutorial: SPDE models. Norwegian University of Science and Technology, Trondheim, Norway.
Larsonneur, C., Bouysse, P. and Auffret, J.P. 1982. The superficial sediments of the English Channel and its western approaches. Sedimentology 29: 851–864.
Lasinio, G.J., Mastrantonio, G. and Pollice, A. 2013. Discussing the "big n problem". Stat. Meth. Appl 22: 97–112.

Legendre, P. 1993. Spatial autocorrelation: trouble or new paradigm? Ecology 74: 1659–1673.

Lindgren, F. and Rue, H. 2015. Bayesian spatial modelling with R-INLA. J. Stat. Softw. 63: 1–26.

Lindgren, F., Rue, H. and Lindström, J. 2011. An explicit link between Gaussian fields and Gaussian Markov random fields: the stochastic partial differential equation approach. J. R. Stat. Soc. B 73: 423–498.

Mahé, K., Destombes, A., Coppin, F., Koubbi, P., Vaz, S., Roy, D.L. and Carpentier, A. 2005. Le rouget barbet de roche *Mullus surmuletus* (L. 1758) en Manche orientale et mer du Nord. IFREMER/Crpmem 39: 1–199.

Mahé, K., Villanueva, M.C., Vaz, S., Coppin, F., Koubbi, P. and Carpentier, A. 2014. Morphological variability of the shape of striped red mullet *Mullus surmuletus* in relation to stock discrimination between the Bay of Biscay and the eastern English Channel. J. Fish Biol. 84: 1063–1073.

Martin, T.G., Wintle, B.A., Rhodes, J.R., Kuhnert, P.M., Field, S.A., Low-Choy, S.J., Tyre, A.J. and Possingham, H.P. 2005. Zero tolerance ecology: improving ecological inference by modelling the source of zero observations. Ecol. Lett. 8: 1235–1246.

Martins, T.G., Simpson, D., Lindgren, F. and Rue, H. 2013. Bayesian computing with INLA: new features. Comput. Stat. Data Anal. 67: 68–83.

Maunder, M.N. and Punt, A.E. 2013. A review of integrated analysis in fisheries stock assessment. Fish. Res. 142: 61–74.

McGeoch, M.A., and Gaston, K.J. 2002. Occupancy frequency distributions: patterns, artefacts and mechanisms. Biol. Rev. 77: 311–331.

Parent, É. and Rivot, É. 2013. Introduction to Hierarchical Bayesian Modeling for Ecological Data. CRC Press and Chapman and Hall, Boca Raton, FL, USA.

Punt, A.E. and Hilborn, R. 1997. Fisheries stock assessment and decision analysis: the Bayesian approach. Rev. Fish Biol. Fish. 7: 35–63.

R Core Team. 2016. R: a language and environment for statistical computing. R Foundation for Statistical Computing. Vienna, Austria.

Roos, M. and Held, L. 2011. Sensitivity analysis in Bayesian generalized linear mixed models for binary data. Bayesian Anal. 6: 259–278.

Rue, H., Martino, S. and Chopin, N. 2009. Approximate Bayesian inference for latent Gaussian models by using integrated nested Laplace approximations. J. R. Stat. Soc. B 71: 319–392.

Schluter, M. and Jerosch, K. 2008. Digital atlas of the North Sea (DANS). Geo-information regarding geology, geochemistry, oceanography and biology. Available from http://www.awi.de/en/research/research_divisions/geosciences/marine_geochemistry/marine_gis/digital_atlas_of_the_north_sea/.

Schmid, C.H. and Griffith, J.L. 2005. Multivariate classification rules: calibration and discrimination. *In* Encyclopedia of Biostatistics, second edition. *Edited by* P. Armitage and T. Colton. John Wiley & Sons, London, UK. pp. 3491–3497.

Sing, T., Sander, O., Beerenwinkel, N. and Lengauer, T. 2005. ROCR: visualizing classifier performance in R. Bioinformatics 21: 3940–3941.

Szuwalski, C.S. and Punt, A.E. 2015. Can an aggregate assessment reflect the dynamics of a spatially structured stock? Snow crab in the eastern Bering Sea as a case study. Fish. Res. 164: 135–142.

Thorson, J.T. and Minto, C. 2015. Mixed effects: a unifying framework for statistical modelling in fisheries biology. ICES J. Mar. Sci. 72: 1245–1256.

Walters, C.J. 2007. Is adaptive management helping to solve fisheries problems? Ambio J. Hum. Environ. 36: 304–307.

Ward, E.J., Jannot, J.E., Lee, Y., Ono, K., Shelton, A.O., Thorson, J.T., Division, C.B., Fisheries, N., Fisheries, N.M., Oceanic, N., Resource, F., Division, M., Fisheries, N., Service, M.F., Oceanic, N., Division, M., Fisheries, N., Marine, N., Service, F., Oceanic, N. and Sciences, F. 2015. Using spatiotemporal species distribution models to identify temporally evolving hotspots of species co-occurrence. Ecol. Appl. 25: 2198–2209.

Tables

Table 1. Models' DIC and log marginal likelihood, estimated spatial autocorrelation range (ρ), variance contribution of the spatial effect to the total variance (σ^2), cross-validated logarithmic score (CVLS) and Brier score. Best models for each dataset are highlighted in grey.

Dataset A	DIC	log marg. likelihood	ρ	σ^2	CVLS	Brier score
SED+DEP+SSS+SST	7529	-4204	2.657	4.604	0.4469	0.0757
SED+DEP+SSS	7556	-4222	2.768	4.856	0.4483	0.1461
SED+DEP	7558	-4219	2.726	4.836	0.4484	0.1461
SED	7557	-4210	2.770	4.880	0.4483	0.1461
SSS+SST	7541	-4221	2.432	5.183	0.4472	0.1458
No covariates	7569	-4237	2.554	5.496	0.4486	0.1462
Dataset B						
SED+DEP+SSS+SST	6881	-3841	8.510	6.555	0.2533	0.0786
SED+DEP+SSS	6894	-3854	8.018	6.659	0.2536	0.0786
SED+DEP	6895	-3848	8.001	6.626	0.2537	0.0786
SED	6900	-3839	7.890	6.483	0.2538	0.0787
SSS+SST	7672	-4257	7.475	6.466	0.2467	0.0589
No covariates	7021	-3907	7.214	6.803	0.2584	0.0807

Table 2. Estimated coefficients for the best models for dataset A and dataset B. Values are posterior means and intervals (CI) are 95% Bayesian credible intervals. Intervals not containing 0 are highlighted in grey.

Covariate	Dataset A	Dataset B
Mud	-4.428 (-30.036, 21.029)	-0.785 (-26.155, 24.435)
Fine sand	-4.537 (-30.148, 20.922)	-0.810 (-26.180, 24.411)
Gravels	-4.091 (-29.706, 21.372)	-0.634 (-26.005, 24.587)
Pebbles	-5.086 (-30.700, 20.377)	-1.749 (-27.120, 23.472)
Coarse sand	-3.863 (-29.475, 21.598)	0.319 (-25.051, 25.540)
SST	0.208 (0.151, 0.266)	0.268 (0.181, 0.356)
SSS	0.652 (0.034, 1.267)	-0.063 (-0.182, 0.056)
DEP	-0.005 (-0.014, 0.003)	0.002 (-0.002, 0.006)

Figures

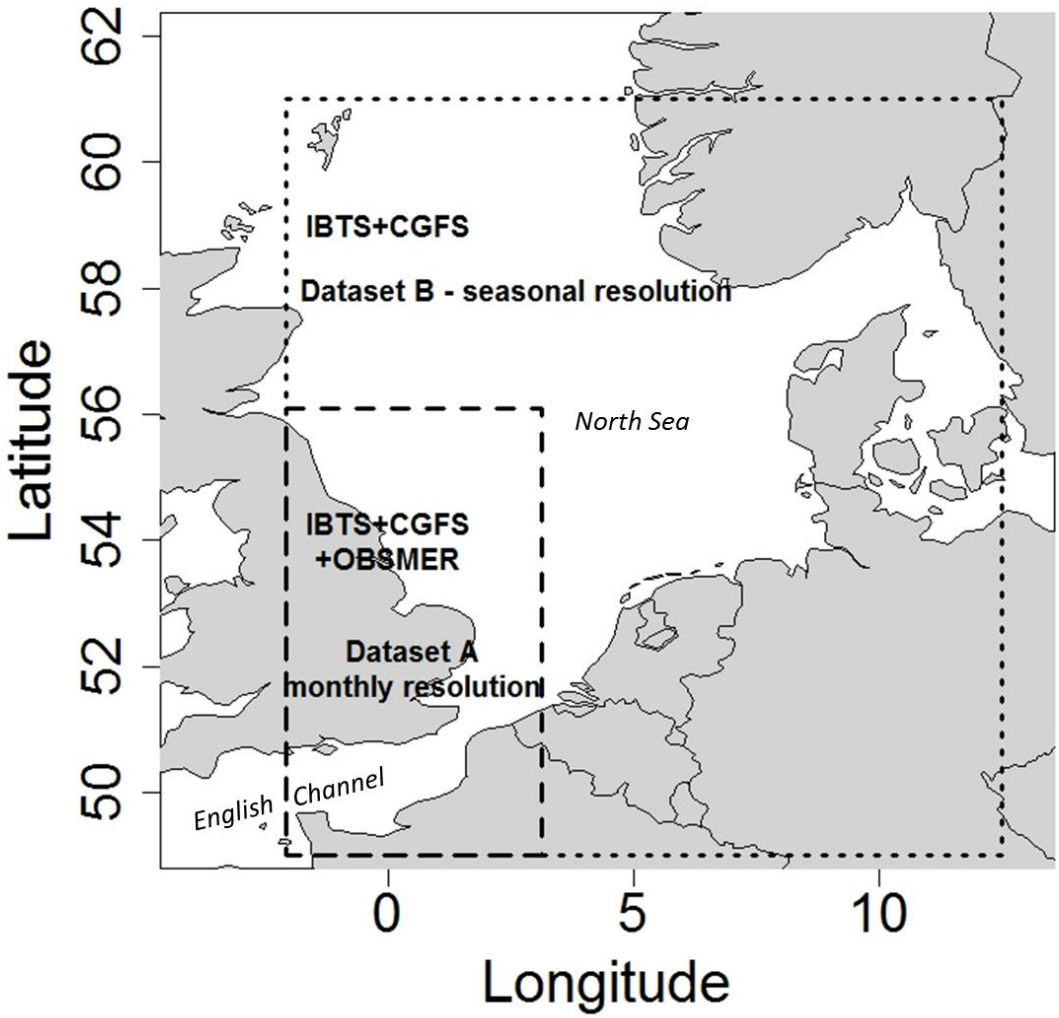

Figure 1. Spatial coverage of the two datasets (A and B) used in the modelling.

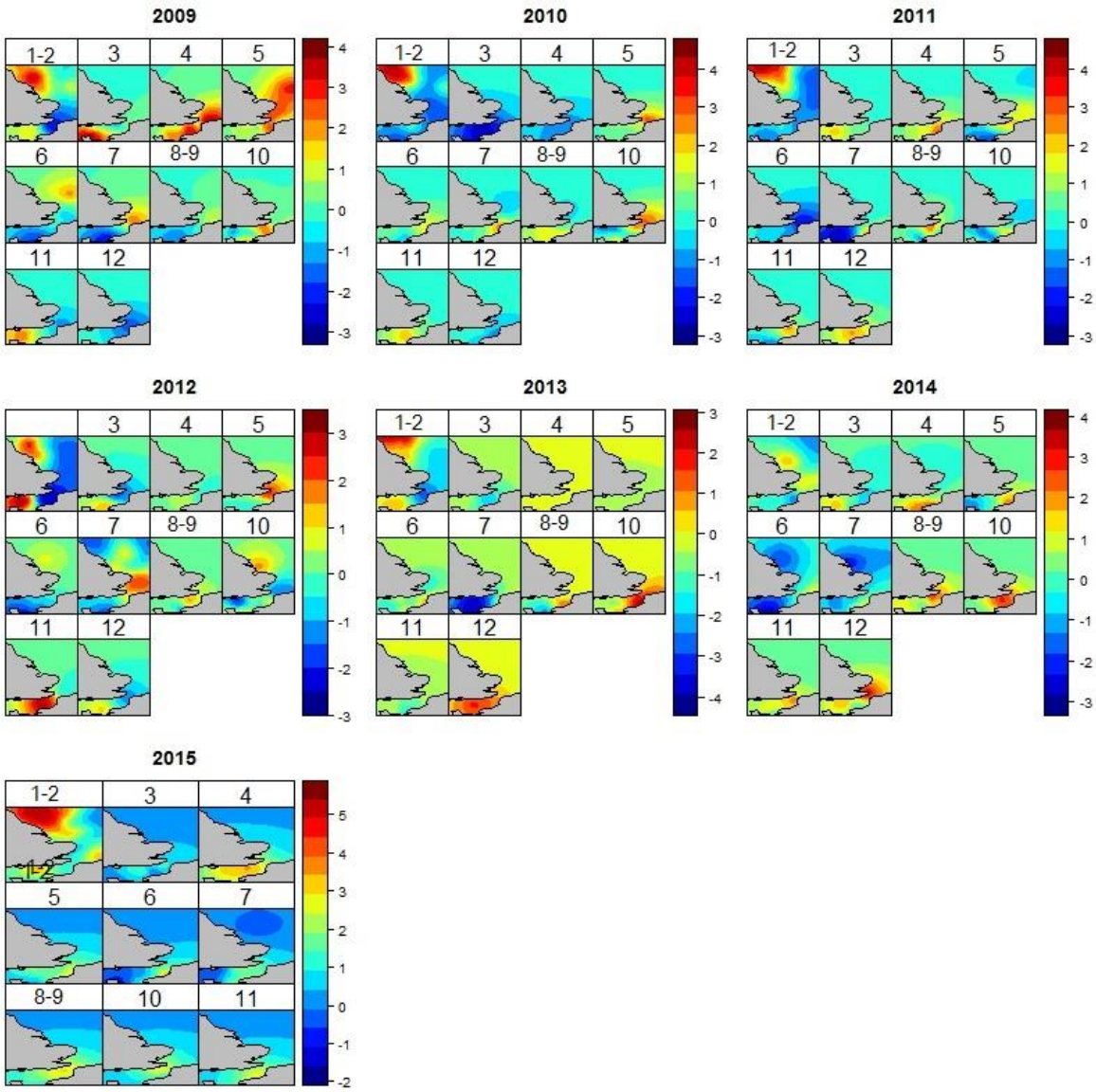

Figure 2. Posterior mean of the spatial random effect for dataset A – positive values indicate a high density of presence data while negative values indicate a high density of absence data. The months of January–February and August–September were grouped together to combine the parts of the IBTS survey that straddled months.

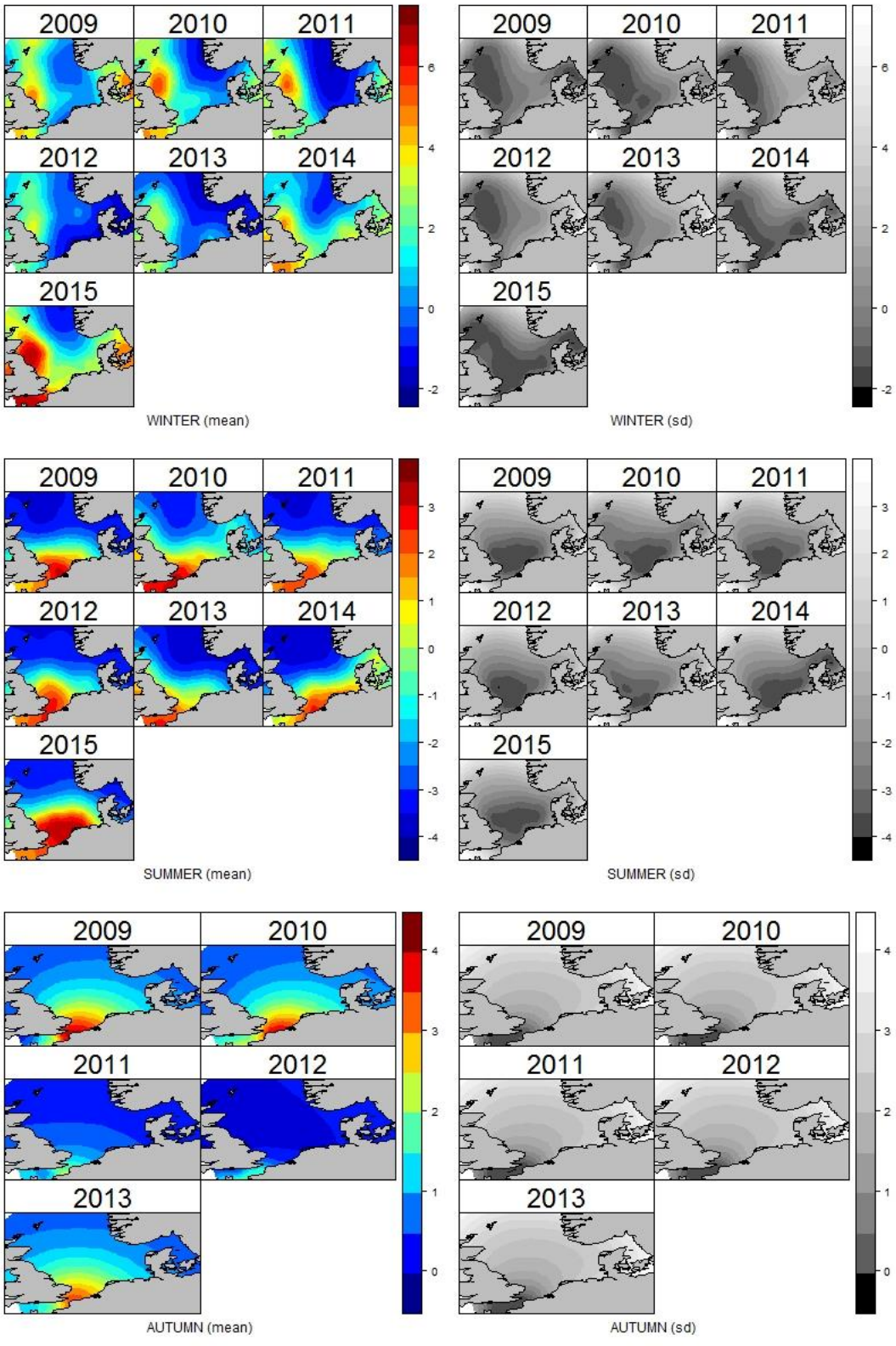

Figure 3. Mean (left-hand side) and standard deviation (right-hand side) of the spatial random effect at a seasonal resolution for dataset B – positive values of the mean indicate a high density of presence data while negative values indicate a high density of absence data. The standard deviation increases with distance from the data points.

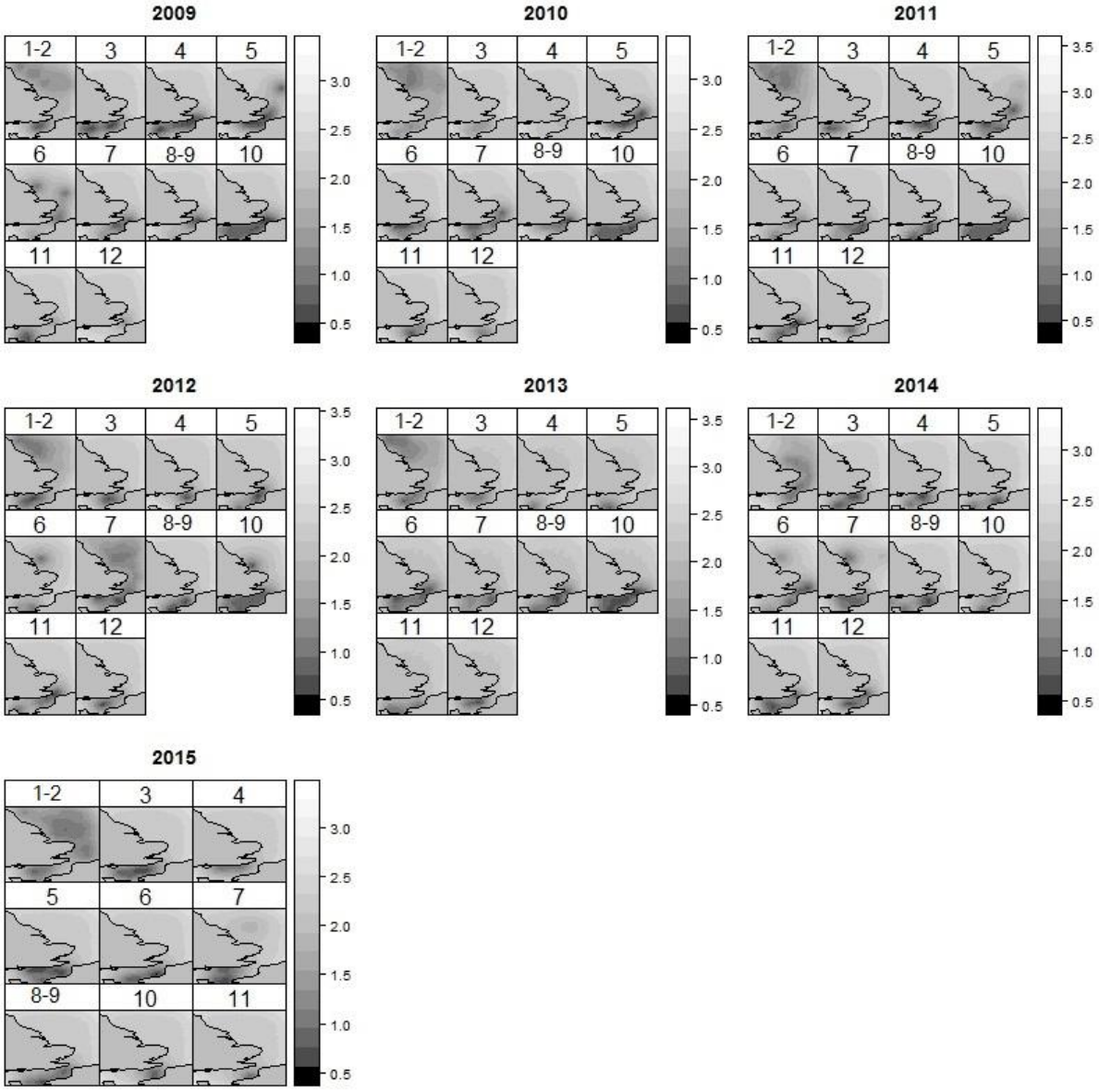

Figure 4. Standard deviation of the spatial random effect for dataset A. The months of January–February and August–September were grouped together to combine the parts of the IBTS survey that straddled months.

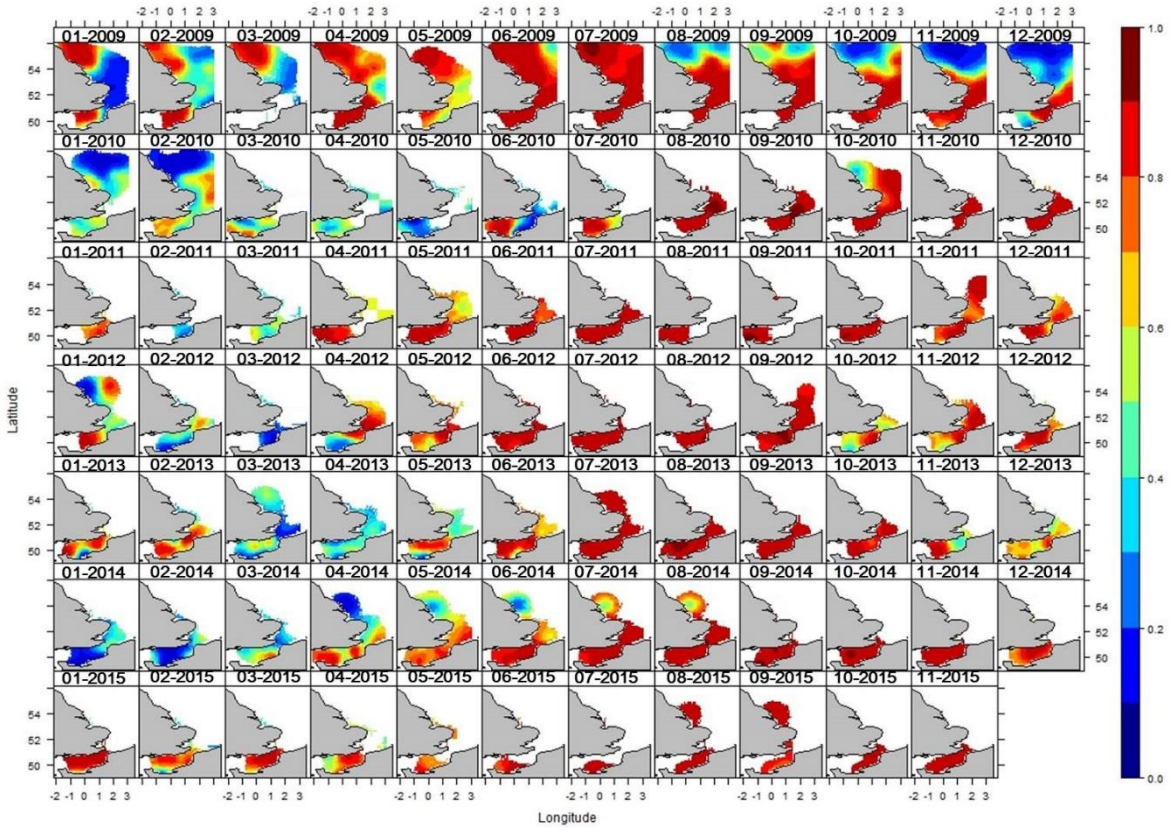

Figure 5. Spatial predictions of the probability of presence of striped red mullet in the eastern English Channel and southern North Sea at a monthly resolution from 2009 (top) to 2015 (bottom), as output from the best model for dataset A. The colour bar scales from blue (low occurrence probability) to red (high occurrence probability). White areas represent grid cells in which the standard deviation was higher than the mean standard deviation (on the logit scale) (see Figure S2).

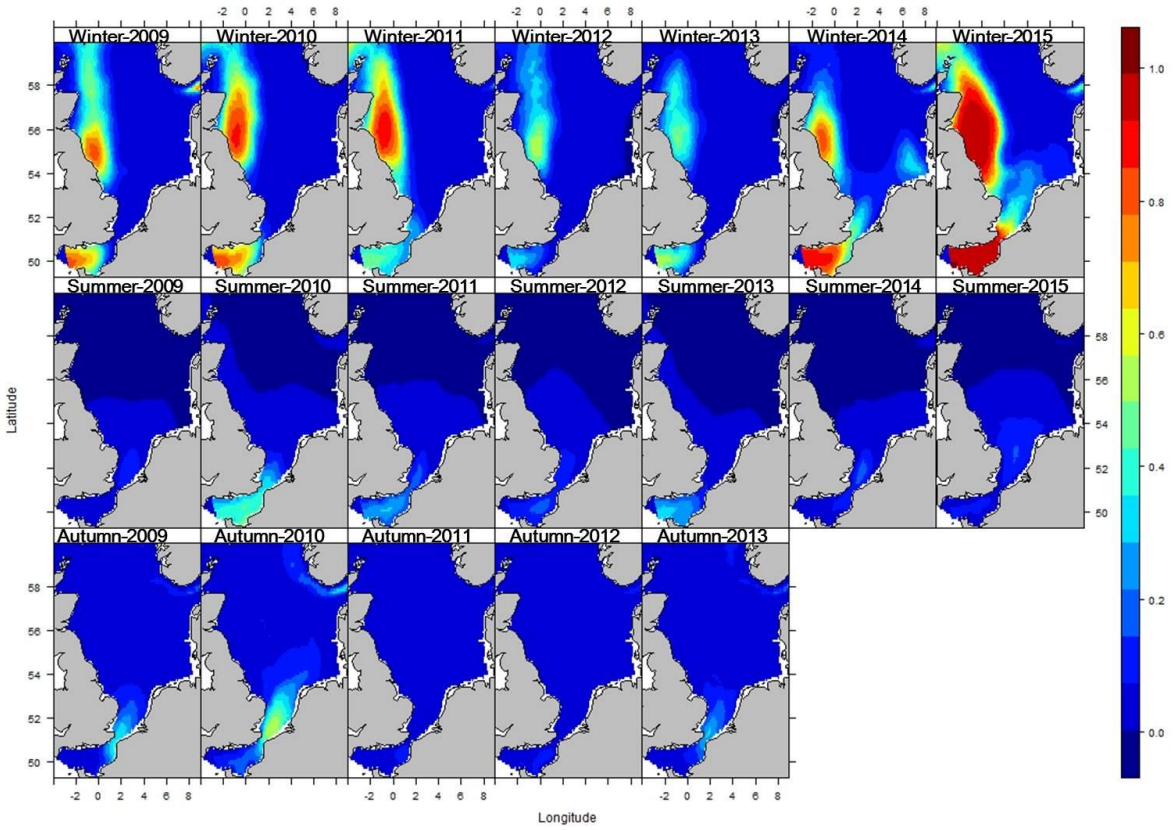

Figure 6. Spatial predictions of the probability of presence of striped red mullet in the eastern English Channel and the North Sea at a seasonal resolution from 2009 (left) to 2015 (right), as output from the best model for dataset B. The colour bar scales from blue (low occurrence probability) to red (high occurrence probability).

Supplementary material

Table S1. Details of the four data sources used in this study, the total number of records (n) available for each, and the number of records where striped red mullet was present.

Data source	Spatial coverage	Temporal coverage	n records	n presences
IBTS-Q1 survey data	North Sea & English Channel included since 2007	January/February (1995-2015)	7496	912
IBTS-Q3 survey data	North Sea & English Channel included since 2007	August/September (1995-2015)	6202	445
CGFS survey data	English Channel	October (1990-2014)	1814	922
OBSMER commercial data	English Channel and Southern North Sea	Monthly (2003-2015)	4331	2041
Dataset A	See Figure 1	1995-2015	8391	3371
Dataset B	See Figure 1	1995-2015	13853	2279

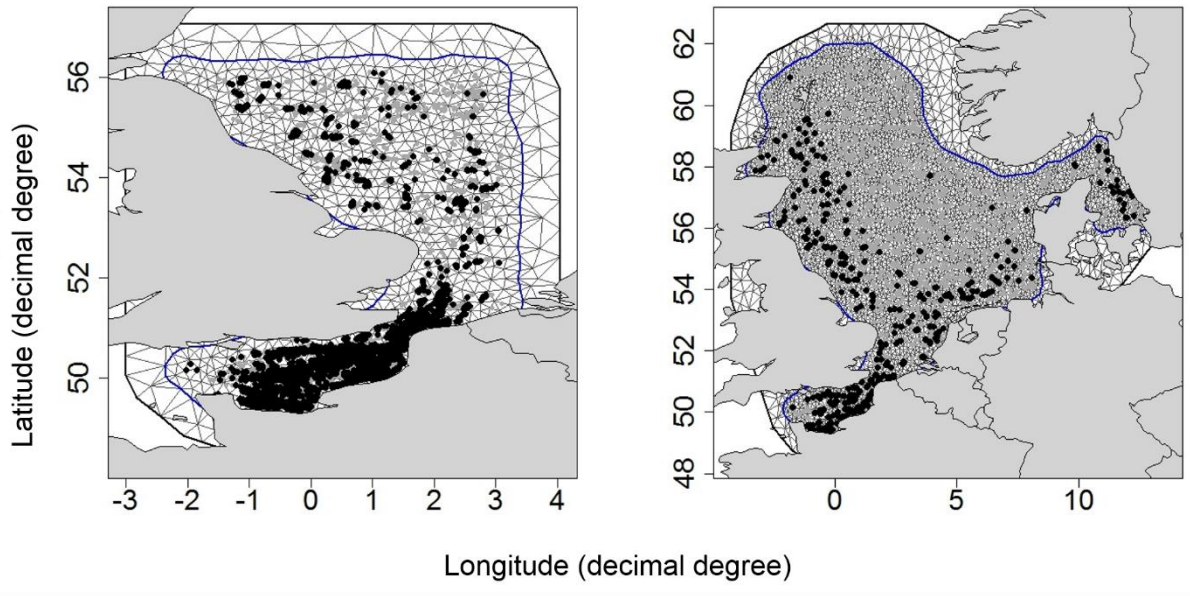

Figure S1. Best meshes built and selected for the SPDE model for dataset A (left) (max edge=0.3,0.8; offset=0.05,0.6) and dataset B (right) (max edge=0.25,0.6; offset=0.05,0.6). The black and grey points represent the distribution of data (presence/absence in our case).

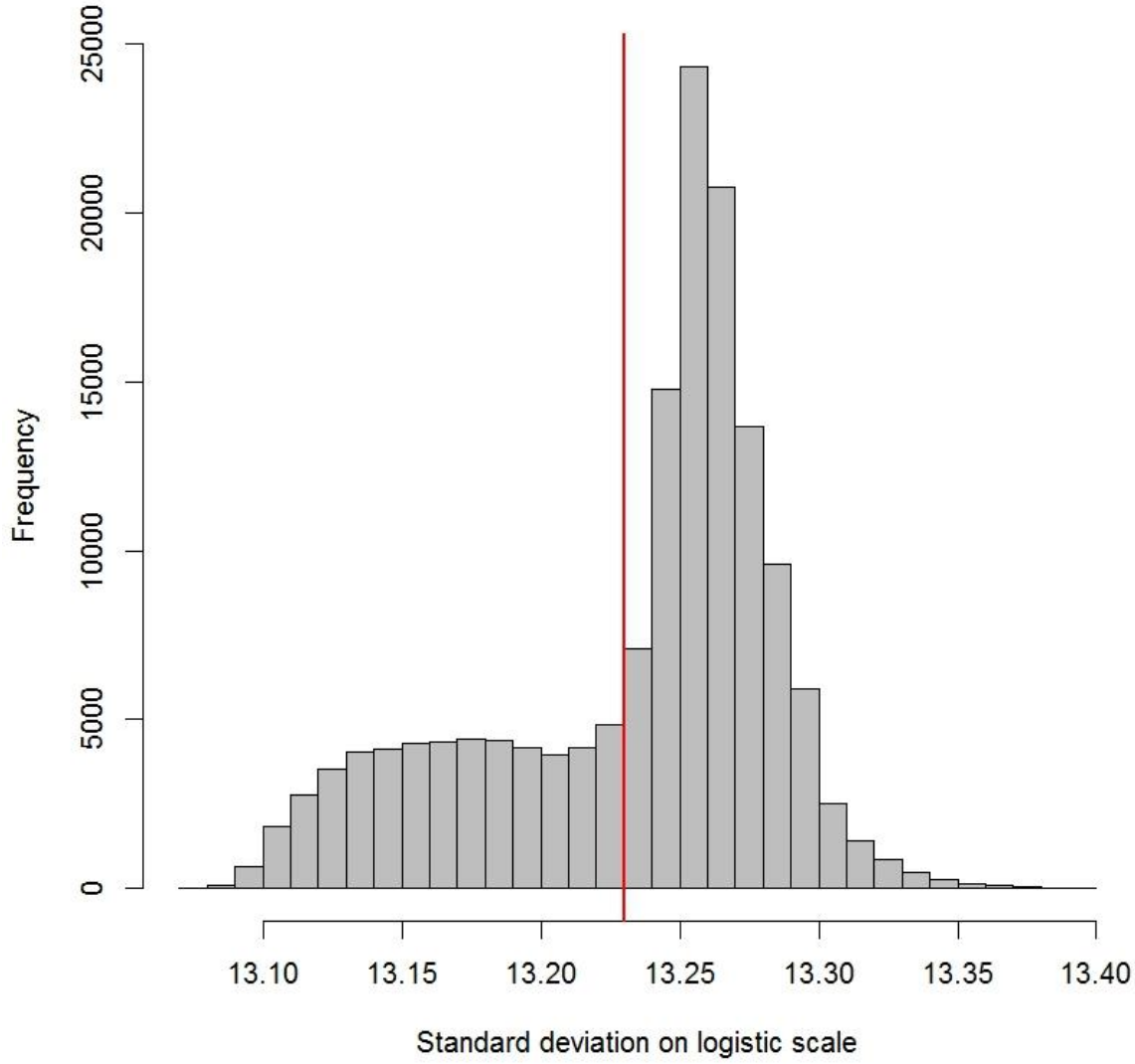

Figure S2. Distribution of the values of the predictions' standard deviation used to define an upper 'cutoff' (red vertical line) corresponding to an uncertainty too high to consider the predictions on the probability of presence of striped red mullet reliable.

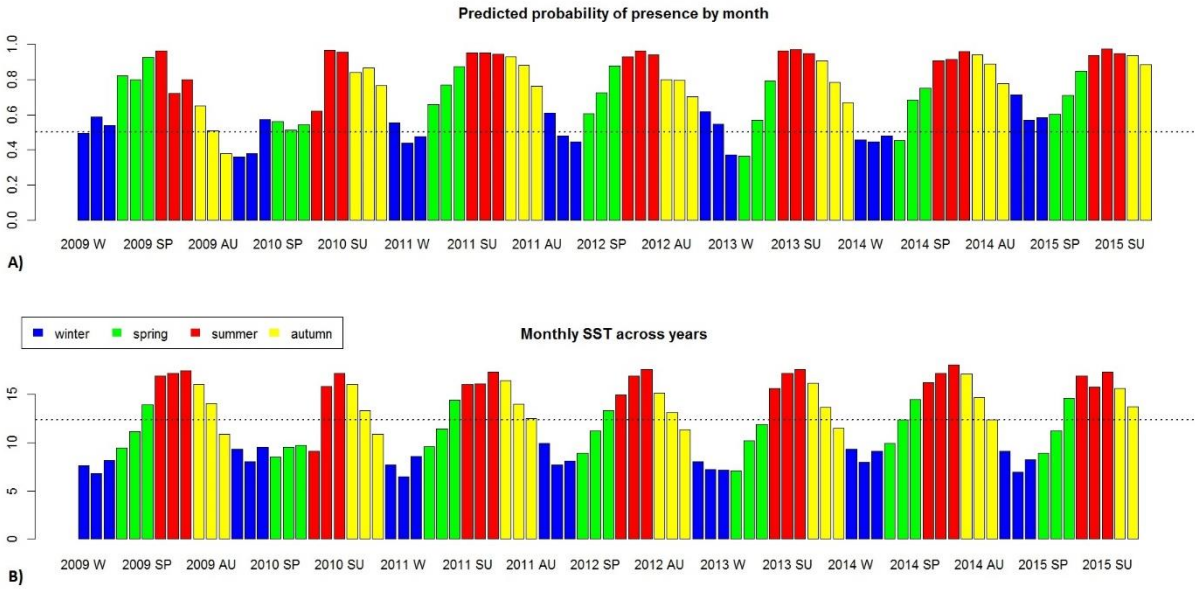

Figure S3. A) Monthly predicted probability of presence obtained from dataset A, from 2009 to 2015. Each colour represents a seasonal quarter and the horizontal dotted line marks the average predicted probability of presence across all years. B) Monthly average SST used to analyse dataset A, from 2009 to 2015. Each colour represents a seasonal quarter and the horizontal dotted line marks the average SST across all years.

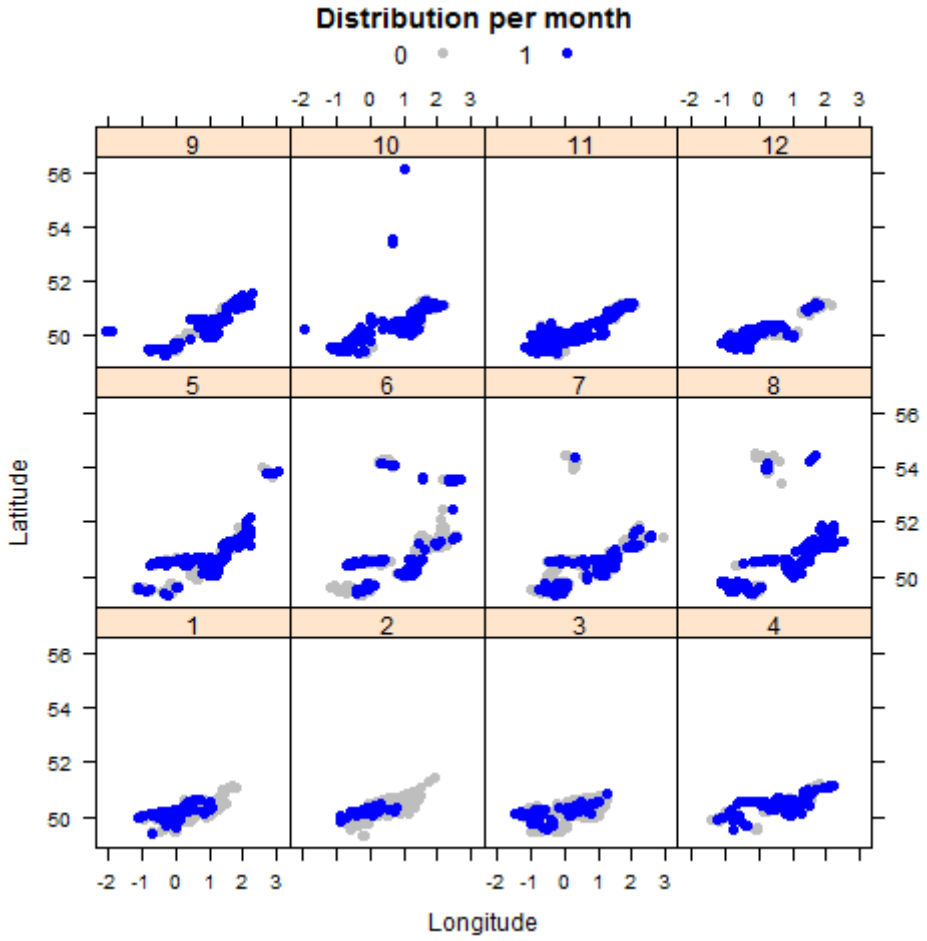

Figure S4. Summary of the monthly catch locations across years available from the OBSMER program, for bottom-trawlers using a mesh size between 70-90mm. Both total records (grey plus blue dots) and records where striped red mullet was present (blue dots) are indicated.

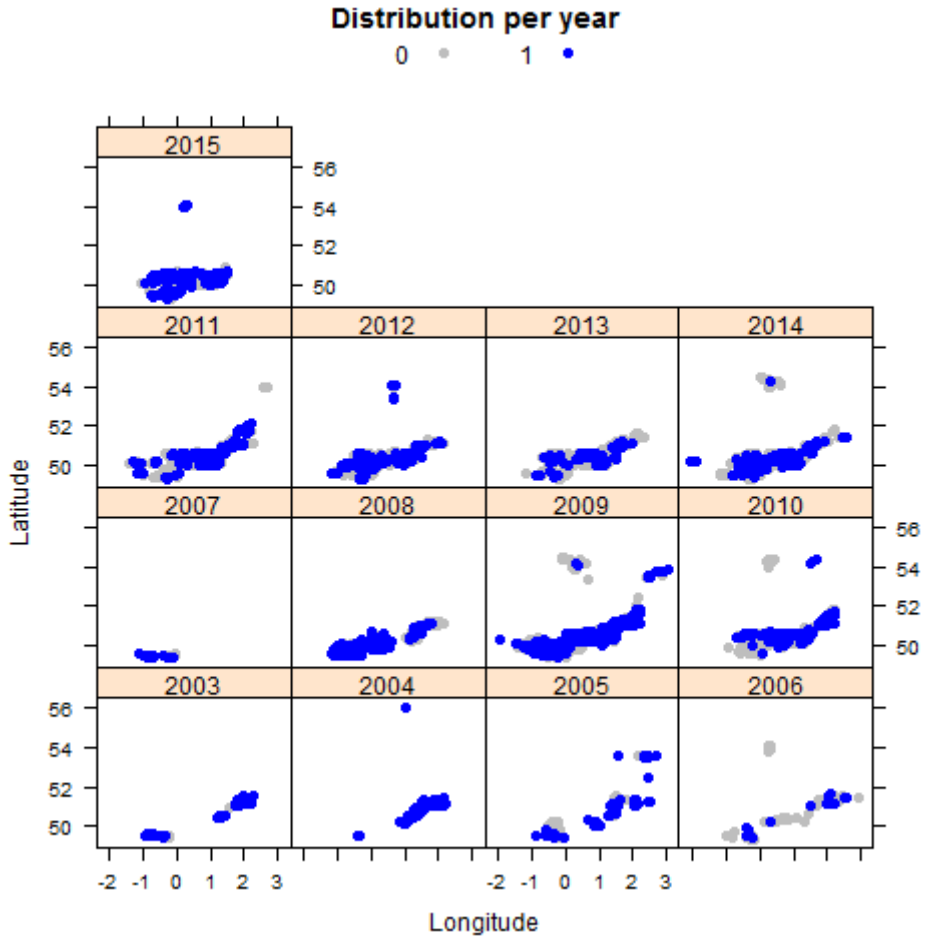

Figure S5. Summary of the yearly catch locations across years available from the OBSMER program, for bottom-trawlers using a mesh size between 70-90mm. Both total records (grey plus blue dots) and records where striped red mullet was present (blue dots) are indicated.

Paper III

Isolating the influence of ontogeny helps predict island-wide variability in chemical traits stored in fish otoliths

Jed I. Macdonald, Russell N. Drysdale, Roman Witt, Zsófia Cságoly, Guðrún Marteinsdóttir

(In review in *Reviews in Fish Biology and Fisheries*)

Author contributions – Conceived and designed the experiments: JIM; extracted and prepared the otoliths: JIM, ZC; analysed the data: JIM, RND, RW; wrote the manuscript: JIM; reviewed and edited the manuscript: JIM, RND, RW, ZC, GM.

Isolating the influence of ontogeny helps predict island-wide variability in chemical traits stored in fish otoliths

Jed I. Macdonald[1,2], Russell N. Drysdale[3], Roman Witt[3], Zsófia Cságoly[1], Guðrún Marteinsdóttir[1]

[1]Faculty of Life and Environmental Sciences, University of Iceland, 101 Reykjavík, Iceland
[2]School of BioSciences, The University of Melbourne, Parkville, Victoria 3052, Australia
[3]School of Geography, The University of Melbourne, Carlton, Victoria 3053, Australia

Abstract

Populations of animals often comprise individuals with strikingly diverse phenotypes. The interplay between individual-level (intrinsic) and environmental (extrinsic) variability can magnify these phenotypic differences, leading to the emergence of strong trait variation among ecologically- or geographically-separated populations. For commercially-exploited marine fishes, defining the scales (in space and time) at which nursery 'source' populations vary in such traits can allow researchers to assess source contribution to harvested adult 'sink' populations, and managers to identify and protect critical nursery habitats. The chemical constituents of fish otoliths (ear stones) have emerged as powerful tools for this purpose, as they provide life-long, bio-environmental markers for individuals and populations. However, substantial uncertainty still surrounds how intrinsic and extrinsic processes shape chemical incorporation into otoliths, limiting our capacity to predict the scales of marker variability when sampling coverage is patchy, or data are few. To tackle these issues, we analysed otolith elemental (Li, Mg, Ca, Mn, Zn, Sr, Ba) and stable isotopic ($\delta^{13}C$, $\delta^{18}O$) concentrations from two age-classes of juvenile Atlantic herring (*Clupea harengus*) captured simultaneously at nursery sites around Iceland, and fitted a series of Bayesian mixed effects models to isolate ontogenetic (i.e. age- and growth-related) influences from environmental influences on otolith chemistry. We tested for ontogenetic effects *within* sites, and detected strong declines in four of six element:Ca ratios with age (Li:Ca, Mg:Ca, Mn:Ca, Sr:Ca), the slopes of these relationships differing *among* sites for Li:Ca and Mg:Ca. Otolith Sr:Ca was consistently lower in larger individuals within an age-class. Our models also revealed high individual-level variability (i.e. within site, within age-class) for all otolith markers, whilst highlighting the importance of temperature and salinity (or the proxies these represent) in explaining population-level trends for $\delta^{13}C$ and $\delta^{18}O$. Age- and year-specific predictions for each otolith marker, at each nursery site, generally accorded well with empirical observations, providing inference on island-wide heterogeneity in otolith chemistry across the juveniles' full distributional range. Such spatially-resolved predictions, generated from mechanistically-focused models as presented here, might hold value for other animals whose source-sink dynamics remain uncertain, or where sampling limitations hamper the effectiveness of spatial management efforts.

Introduction

Animals within a species often display dramatic phenotypic variability. In populations of conspecifics, this can arise via inter-individual differences in traits associated with behaviour and personality (Sih et al. 2004; Fiksen et al. 2007; Cote et al. 2010), which may be adaptive (Dall et al. 2004), or those related to age, physiology, sex and/or past experience (e.g. Shima and Swearer 2010; Leitão et al. 2019), all mediated through intra-individual plasticity in trait expression through ontogeny (Stamps 2016). Dependent upon the species and setting, it is conceivable that the existence of such intrinsic (i.e. individual-level) trait differences *within* populations, in conjunction with local extrinsic (e.g. environmental) forcing, might also give rise to marked divergence in trait expression *among* geographically- and/or ecologically-segregated populations (see Kawecki and Ebert 2004; Freshwater et al. 2019) – differences pronounced enough to shape the spatial structure and connectedness of these populations, as well as the attributes of their members.

Commercially-harvested species can face additional selective pressures (Allendorf et al. 2008), and for those distributed over wide geographic domains, defining the scales at which spatially-separated populations differ in key traits provides a platform upon which to develop spatial management directives that balance sustainable harvest and conservation objectives. Whilst a worthy goal, such information is often lacking, particularly in the context of marine fisheries (Cowen et al. 2007; Moore et al. 2018; but see Williams et al. 2012). This arena is arguably where data needs are most pressing, as climate change redistributes species subject to heavy commercial fishing pressure across new international or jurisdictional borders (e.g. Jansen et al. 2016), leading to mismatches between the scale of management units and population processes (Moore et al. 2018). A means to characterise how individual-level trait variability scales to the population level, with explicit consideration of intrinsic and extrinsic influences on trait expression, would constitute a major step towards resolving these issues. For example, it would enhance researchers' ability to clarify the structure of populations across an ocean scape, and to assess nursery 'source' contributions to harvested adult 'sinks', enabling managers to delineate ecologically-relevant management boundaries and to protect key nurseries with a view to ensuring future fishery sustainability.

Fish otoliths (ear stones) offer one powerful tool for such applications, as they comprise life-long, individual-level data on chemical traits (or markers) that can vary strongly within and among populations (Thorrold et al. 1998; Macdonald and Crook 2010). Although well known for their accurate age- and growth-recording properties, the discovery that concentrations of certain elements and stable isotopes in otoliths are sensitive to environmental gradients (i.e. in salinity, temperature, ambient water chemistry, pH) (Elsdon and Gillanders 2004; Martin and Wuenschel 2006; Mirasole et al. 2017), physiological changes associated with fish age (Chittaro et al. 2006; Grammer et al. 2017) and growth (Sadovy and Severin 1994; Stanley et al. 2015), sex (Sturrock et al. 2015), metabolic activity (Kalish 1991a; Høie et al. 2003), diet (Ranaldi and Gagnon 2008) and genetic variation (Clarke et al. 2011) underscores otoliths' unique potential as bio-environmental recorders for individuals and populations (see Grønkjær 2016; Izzo et al. 2018 for reviews).

Notwithstanding this potential, the environment can place strict limits on intrinsic processes (Pörtner and Peck 2010; Holt and Jørgensen 2014), and decoupling how these factors interact to shape otolith chemical traits remains a key challenge for accurate data interpretation. Evidence for non-environmentally driven elemental enrichment at, or near to, the otolith

core (Brophy et al. 2004) further complicates matters, and individual- (Macdonald and Crook 2010) and species-level (Chang and Geffen 2013) variation in elemental uptake rates makes generalising trends within and among taxa problematic (but see Swearer et al. 2003). Yet there is hope. Recent assays of blood and endolymph chemistry (Sturrock et al. 2014, 2015; Thomas et al. 2017) in conjunction with investigations into elemental binding processes within the otolith (Melancon et al. 2009; Doubleday et al. 2014; Izzo et al. 2016) have shed new light on the bio-environmental regulation of chemical trait variability. Taken together, these studies open a pathway towards deeper process-based insights in this field.

Though complete mechanistic understanding is not a strict requirement for using otoliths as natural tags in fishery management applications, isolating the drivers of otolith chemical variability in wild fish populations may advantage studies of this kind. For example, several commercially-targeted marine species are known to form mixed-age and/or origin schools during critical life phases (e.g. during spawning – Grabowski et al. 2012; or nursery residence – Brophy and Danilowicz 2002), with populations distributed over broad geographic ranges and/or steep environmental gradients. For juveniles of these species, predictions from spatially-explicit models of otolith chemistry that appropriately capture both ontogenetic and environmental influences could provide first-order estimates of trait heterogeneity across a network of nursery sites. Indeed, by encompassing all potential nursery source populations, relevant time-points, age-classes, age-specific growth rates and environmental features, these models would generate reliable baselines for quantifying population mixing rates, particularly when sampling coverage is sparse.

Here, we illustrate the value of such models using data from wild, juvenile Atlantic herring (*Clupea harengus*) (hereafter herring) residing in Icelandic waters (i.e. Icelandic summer spawners – ISS), and take advantage of a sampling scheme in which two age-classes were captured simultaneously from the same nursery sites, in the same trawl tow. Following larval dispersal from spawning grounds, ISS herring settle in nurseries that are distributed widely across the Icelandic coast. Juveniles exhibit strong nursery-site attachment through the first two years of life before leaving to join the adult component of the stock, which is subject to heavy commercial fishing pressure (Jakobsson and Stefánsson 1999; Guðmundsdóttir et al. 2007). This situation provided us an opportunity to isolate ontogenetic influences on otolith chemical traits *within* nursery sites, using the sharp environmental gradients present around Iceland to explore the additional contribution of environmental effects *among* sites. Spatially-explicit inference on how these factors are expressed in otoliths, and at which scales, is particularly pertinent for ISS herring. The population has been declining for the past decade due to a combination of regular *Ichthyophonus hoferi* outbreaks and a series of poor recruitment years (ICES 2017), and a lack of quantitative data on the spatio-temporal structure of nursery populations has hindered efforts to identify and protect key nursery areas.

To this end, we measured the elemental (Li, Mg, Mn, Zn, Sr, Ba) and stable isotopic ($\delta^{13}C$, $\delta^{18}O$) concentrations at the edges of juvenile ISS herring otoliths, and developed a series of Bayesian mixed effects models incorporating both ontogenetic and environmental covariates to address three specific aims (1) to seek evidence for age- and growth-related effects on elemental and stable isotopic markers *within* sites; (2) to explore variation in relationships between these markers and temperature and salinity gradients *among* sites; and (3) to harness this information to map site-level predictions for each marker at an island-wide scale, for the two juvenile age-classes, and across three sampling years. Our modelling approach provides

direct inference on the scale of individual-, site-, cohort- and population-level variation in phenotypic traits, and their synergies with intrinsic and extrinsic factors – data useful both for identifying connections among broadly-distributed animal populations, and for our management of them.

Materials and methods

Fish sampling and rationale

Juvenile age 1 (i.e. ~15-month old) and age 2 (i.e. ~27-month old) herring were captured from 26 inshore nursery sites, concentrated on the Icelandic north coast, over three autumns (i.e. 2013, 2014, 2015) (Table 1, Figure 1). Sampling took place in late October and early November each year during the juvenile herring (acoustic and trawl) and northern shrimp (*Pandalus borealis*) (trawl) surveys that aim to provide recruitment/biomass indices for input into stock assessments. Juvenile herring are a common bycatch item in the shrimp trawls. We used a standard bottom trawl of 1010 meshes, with the cod-end comprising a 37-mm diamond-mesh. Tows were conducted during daylight hours, covering between 0.1 and 1.2 nautical miles, with the vessel travelling at ~2 knots.

At a subset of capture sites (n = 6), age 1 and age 2 herring were collected simultaneously in the same tow, allowing us an opportunity to isolate age- and growth-related effects on otolith chemistry within sites. After settlement in nursery sites, juvenile ISS herring exhibit strong site fidelity over the subsequent two years (Guðmundsdóttir et al. 2007), often forming dense, mixed-age schools that move little (in the horizontal dimension) from late autumn through the winter months. Under these circumstances, and given the location and characteristics of the capture sites, it follows that within each site, the environmental conditions (e.g. salinity, temperature, ambient water chemistry, pH) experienced by both age-classes in the weeks preceding capture would be near identical. Hence, we contend that any variation in chemical markers detected at the otolith edge (representing recently accreted otolith material) would be driven primarily by intrinsic and/or dietary factors. Upon capture, fish were measured for standard length (SL) (±1 mm), and frozen for transport to the laboratory.

Otolith analysis

Extensive details on otolith preparation, the analyses conducted and the instruments used are provided in Appendix S1. Briefly, sagittal otolith pairs were removed, cleaned of adhering tissue, rinsed with ultrapure water (Milli-Q®; www.merckmillipore.com) and stored dry in 0.5-ml polypropylene microtubes. For each fish, we polished one sagitta to near the primordium and used laser ablation-inductively coupled plasma-mass spectrometry (LA-ICP-MS) to measure the concentrations of seven elemental markers (i.e. ^{7}Li, ^{25}Mg, ^{43}Ca, ^{55}Mn, ^{66}Zn, ^{88}Sr, ^{138}Ba) in a ~40-µm wide × 11-µm deep disc of otolith material at the dorsal margin. We estimate that these discs reflected otolith material accreted during the final < 2 weeks of each fish's life (Appendix S1).

We used the second sagitta for analyses of stable carbon and oxygen isotope ratios (i.e. δ^{13}C, δ^{18}O). Whole age 1 otoliths were ground, individually, to a fine powder, of which between 0.05 and 0.1 mg was analysed using isotope ratio mass spectrometry (IRMS). Each powder

sample represented a full lifetime (i.e. ~15-month) record of $\delta^{13}C$ and $\delta^{18}O$ for each age 1 fish. Age 2 otoliths were sub-sampled. We used a high-resolution MicroMill system to plot a 200-µm wide × ~25-µm deep drill path along the otolith edge (see Appendix S1 for details). Again, between 0.05 and 0.1 mg of powder was analysed per sample using IRMS, encompassing otolith material deposited during the last ~2 months of life.

Elemental data are expressed as molar ratios to Ca throughout (e.g. Li:Ca), with stable isotopic measurements reported relative to the Vienna Pee Dee Belemnite (VPDB) reference standard, and expressed in δ-notation (in ‰). Note that second sagittae were not available for age 1 herring captured in 2014. In addition, sample sizes were often lower for stable isotopic compared with elemental measurements due to technical issues with the MS operation and subsequent loss of samples (Table 1). We consider these data as 'missing completely at random' (Rubin 1976).

Statistical analysis

A series of univariate and multivariate linear mixed effects models were developed to investigate how age, growth and environmental covariates might influence the elemental and stable isotopic composition of juvenile herring otoliths. All analyses were run in R 3.4.0 (R Core Team 2017). Datasets and R code are available from the Dryad Digital Repository.

Covariates

We selected covariates that reflect, either directly or indirectly, some key mechanisms thought to underpin chemical uptake into fish otoliths, and tuned them to the ecology of the juvenile herring sampled here. To capture possible ontogenetic effects, we included age in years (Age), and a variable representing individual-level 'anomalies' from the mean standard length calculated within each site and age-class (SL_anom). The former provides a proxy for any physiological, metabolic and/or dietary changes occurring *between* the two juvenile cohorts, while the latter tests if individual variation in somatic growth, or by association, condition or metabolism *within* a cohort can influence chemical incorporation. Inclusion of SL_anom also tests if faster growers (positive anomalies) differ from slower growers (negative anomalies) in chemical uptake, irrespective of Age. Conductivity, temperature and depth (CTD) profiles were collected at 12 out of 26 capture sites, allowing us empirical measurements of water temperature (Temp) and salinity (Sal) at 1-m depth intervals. We used these measurements to calculate mean values for both parameters across the entire water column at the time and location of each tow. Our aim here was to mirror the environmental conditions recently experienced by juvenile herring during their diel vertical migrations (Cardinale et al. 2003), rather than conditions at the exact depth of the tow. For the remaining 14 sites, we used data hindcast from the CODE ocean model (Logemann et al. 2013). Modelled temperature and salinity estimates were extracted at a 1 × 1 km horizontal resolution around each capture site at 2.5-m depth intervals, and mean values calculated through the entire water column for the day of capture. As empirical measurements were recorded on the capture date, we aimed to match this temporal resolution with our modelled estimates. Yet, given the potential for time-lags in elemental incorporation into otoliths (e.g. Macdonald and Crook 2010), we checked how representative the daily estimates were of local environmental variability in the week, and month preceding capture. Correlations (Pearson's *r*) between day and week, week and month, and day and

month were > 0.94 for both modelled environmental parameters, so we elected to use daily estimates for subsequent model fitting (see Table 1).

Data organisation

In order to build, validate and predict from the models, we split our dataset in three: (1) A 'training' set (n = 176), comprising data from the six sites where age 1 and age 2 fish were captured simultaneously was used for model building, within-sample validation and posterior predictive simulation (see below). (2) A 'test' set (n = 190), consisting of data from a further 12 sites in which only one age-class was captured, and site-level environmental variables fell within the range of the training set was used for out-of-sample (oos) validation. (3) An 'extras' set (n = 92), comprising data from the remaining eight sites, in which one age-class was captured, and the environmental variables fell outside the range of the training data (Table 1). We combined the three datasets to make spatial predictions for each otolith chemical marker across all nurseries sampled.

Exploratory data analysis

Prior to model fitting, the distributions of the response variables (i.e. Li.Ca, Mg:Ca, Mn:Ca, Zn:Ca, Sr:Ca, Ba:Ca, $\delta^{13}C$, $\delta^{18}O$) and covariates (Age, SL_anom, Temp, Sal) were visualised and screened for potentially influential values. Three samples with extreme values on Zn:Ca were detected in the training set, identified as measurement errors, and removed from subsequent analysis. All elemental ratios were natural log transformed, which acted to improve normality of residuals and stabilise the error variance in subsequent modelling. $\delta^{13}C$ and $\delta^{18}O$ values were left untransformed. We assessed covariate associations through scatterplots and calculated pairwise correlation coefficients (Pearson's r). As $|r|$ was always < 0.7 (Dormann et al. 2013), all covariates were retained for modelling. To facilitate interpretation of regression coefficients, continuous inputs were centred and scaled to have mean = 0 and SD = 0.5, with the binary input, Age, left unscaled (Gelman 2008).

Modelling approach - univariate models

Univariate models were fitted in both a Bayesian framework using Monte Carlo Markov chain (MCMC) simulations in the 'MCMCglmm' package (Hadfield 2010), and using restricted maximum likelihood (REML) and ML estimation in the 'lme4' package (Bates et al. 2015). Coupling these approaches proved useful for model comparison, checking and validation. The model structure differed for elemental and stable isotopic markers. For each elemental marker, we began with 'full' models containing all covariates coded as linear terms, and first-order interactions that allowed the relationships between SL_anom, Temp and Sal and the marker of interest to vary with Age. Examination of residuals from preliminary linear models revealed moderate within-site correlations for some markers. In light of this, and given (1) that our interest lay in age and growth effects *within* sites, and (2) that our sites are a random sample of all possible nursery sites, we opted to treat 'site' as a random effect. After specifying the full model, we next searched for the optimal random effect structure (Zuur et al. 2009) – six of which were considered (Table 2). These encompass a range of scenarios regarding how intrinsic and extrinsic processes might shape herring otolith chemistry differently at different sites. Once the best random structure was identified, we then found an optimal fixed structure (Zuur et al. 2009) by fitting and comparing sub-

models containing all possible fixed effect combinations, and null (i.e. intercept-only) models where appropriate (see Appendix S2: Table S1). The full model equation for random structure 5, the most complicated structure in Table 2, is:-

$$y_{ij} = (\beta_0 + \text{site}_{0j}) + (\beta_1 + \text{site}_{1j})\text{Age}_{ij} + (\beta_2 + \text{site}_{2j})\text{SL\_anom}_{ij} + \beta_3\text{Temp}_j + \beta_4\text{Sal}_j + (\beta_5 + \text{site}_{5j})\text{Age}_{ij}\,\text{SL\_anom}_{ij} + \beta_6\text{Age}_{ij}\,\text{Temp}_j + \beta_7\text{Age}_{ij}\,\text{Sal}_j + \varepsilon_{ij}$$

$$\begin{pmatrix} \text{site}_{0j} \\ \text{site}_{1j} \\ \text{site}_{2j} \\ \text{site}_{5j} \end{pmatrix} \sim \text{MVN}(0, \Omega_{\text{site}}), \qquad \Omega_{\text{site}} = \begin{pmatrix} \sigma^2_{\text{site}_0} & & & \\ \text{cov}_{\text{site}_0,\text{site}_1} & \sigma^2_{\text{site}_1} & & \\ \text{cov}_{\text{site}_0,\text{site}_2} & \text{cov}_{\text{site}_1,\text{site}_2} & \sigma^2_{\text{site}_2} & \\ \text{cov}_{\text{site}_0,\text{site}_5} & \text{cov}_{\text{site}_1,\text{site}_5} & \text{cov}_{\text{site}_2,\text{site}_5} & \sigma^2_{\text{site}_5} \end{pmatrix}$$

$$\varepsilon_{ij} \sim \text{N}(0, \sigma^2_\varepsilon) \qquad \text{(eq. 1)}$$

Here, y_{ij} represents the (natural log transformed) otolith edge element:Ca concentration measured in µmol/mol (for Li:Ca, Mn:Ca, Zn:Ca, Ba:Ca) or mmol/mol (for Mg:Ca, Sr:Ca) for fish *i* sampled at capture site *j*. β_0 is the overall mean concentration across sites, and site_{0j} is the random site-level deviation from this mean. β_1 to β_7 are regression coefficients for the fixed effects, and site_{1j}, site_{2j} and site_{5j} denote random site-level differences from the mean slopes for Age (β_1), SL_anom (β_2) and their interaction (β_5), respectively. The random site effects are assumed to be multivariate normally distributed with mean 0 and covariance matrix Ω_{site}, which defines the site-level variances (σ^2) for, and covariances (cov) among, the random intercept and slopes (Eq. 1). ε_{ij}, representing individual-level variation, is modelled as normally distributed with mean 0 and variance σ^2_ε.

The 'full' models for otolith $\delta^{13}C$ and $\delta^{18}O$, did not include an Age term. This was necessary, as analyses of these markers differed in temporal resolution (i.e. age 1: whole otolith; age 2: last ~2 months of life pre-capture), precluding direct comparisons between cohorts. Due to sample size constraints, we considered age 2 samples only and modelled each of $\delta^{13}C$ and $\delta^{18}O$ (in ‰) as a function of SL_anom, Temp and Sal, entered as additive, linear terms. Random effect structures 1 and 3 were tested and compared with models without random effects (i.e. structure 6) (see Table 2).

Modelling approach - multivariate models

Next, we fitted a series of multivariate (response variables = six elemental ratios), and bivariate (response variables = $\delta^{13}C$, $\delta^{18}O$) mixed models in the 'MCMCglmm' package, incorporating the same fixed and random effect structures as the univariate models. A key advantage of multi/bivariate models is their ability to quantify the covariances between response variables, both among and within captures sites, while also estimating the (co)variances described in Ω_{site} (eq. 1) (Dingemanse and Dochtermann 2013). A drawback, however, is that these models act to smooth covariate effects across all response variables, reducing precision if different markers are sensitive to different covariates. As covariances between random intercepts and slopes for Age and/or SL_anom were very low for all chemical markers in the univariate models, we chose not to include these in the multi/bivariate cases. We did estimate among-site variances in random intercepts and Age

and/or SL_anom slopes and their interaction (if included) for each marker (i.e. the long diagonal in Ω_{site}), the among-site covariances between all marker pairs (e.g. $cov_{site_0(Li:Ca,\ Mg:Ca)}$ represents the covariance between random intercepts for Li:Ca and Mg:Ca), and the among-individual variances (σ^2_ε) and covariances (e.g. $cov_{\varepsilon(Li:Ca,\ Mg:Ca)}$) captured by the residual terms. All response variables were scaled to have mean = 0, SD = 1 prior to model fitting (Hadfield 2010). Multivariate normality was checked using functions in the 'MVN' package, and we screened for multivariate outliers based on robust Mahalanobis distances (Korkmaz et al. 2015). The assumption of homogeneity of variance-covariance matrices was assessed using Box's M test in the 'biotools' package (da Silva 2017). Again, we used a top-down approach to arrive at optimal random and fixed effect structures for each model.

Bayesian model fitting

We fitted each 'MCMCglmm' model to the data three times, obtaining three independent Markov chains initialised using dispersed values. We ran each chain for 250,000 iterations, discarding the first 50,000 as burn-in, and using the remaining 3 × 200,000 = 600,000 samples for the calculation of posterior summaries. We initially used a thinning interval of 10 to aid efficiency, then refitted the final models using unthinned chains to maximise precision in our estimates (Link and Eaton 2012). Convergence of the chains was assessed via visual inspection of trace plots and by computing Gelman-Rubin diagnostics ($\hat{R}$). Autocorrelation between successive samples was explored using the set of 'autocorr' functions in the 'coda' package (Plummer et al. 2006). Finally, we calculated Monte Carlo standard errors for all estimated parameters using overlapping batch means in the 'mcmcse' package (Flegal et al. 2016). Details of priors, and results from a sensitivity analysis on prior choice for the random effect variance components are presented in Appendix S2 and Figure S1.

Model selection

Model selection was based on several metrics: the deviance information criterion (DIC), the deviance (computed for the Bayesian models), the small-sample corrected Akaike's information criterion (AICc), and the restricted log likelihood (LL) (computed for models fitted with REML). In addition, we calculated oos mean squared prediction error ($MSPE_{oos}$) by comparing Bayesian point predictions from the models to observed values in the test data. From these metrics, we arrived at two final univariate models for each otolith chemistry marker – one that maximised explanatory power (denoted 'explan') and one that maximised oos predictive accuracy (denoted 'oos.pred') – and two final multi/bivariate models selected for these same attributes (Table 3, Appendix S2: Table S1). For each final 'explan' model, we checked model residuals, and, in the univariate cases, calculated the marginal, conditional and semi-partial R^2 (R^2_m, R^2_c, $R^2_{\beta_f}$, respectively) to estimate the variance explained by all fixed effects (R^2_m), fixed and random effects combined (R^2_c), and each fixed effect, *f*, separately ($R^2_{\beta_f}$) (Nakagawa and Schielzeth 2013; Johnson 2014; Jaeger et al. 2017). We also estimated adjusted repeatability (± 95% bootstrapped confidence intervals) for each marker at the site level, using the 'rptR' package (Stoffel et al. 2017). These repeatability estimates adjust for the fixed covariates, with estimates for random slope models based on the mean random effect variance across all values/levels of the covariate.

As fitting in 'lme4' and 'MCMCglmm' yielded the same final models on the balance of the selection criteria examined (Appendix S2: Table S1), we focused on the Bayesian models for further inference, and ran posterior predictive checks as an additional test of within-sample predictive capacity. We generated 200,000 simulated datasets from each final 'explan' model, and gauged how closely these data matched the observed otolith chemistry by plotting the observations for each marker against the simulated means (± 95% prediction intervals) and assessing the correlation (i.e. r_{sim}) between them (Table 3, Appendix S2: Figure S2). This let us judge whether the univariate or the multi/bivariate 'explan' models performed better. The simulations also allowed us to calculate posterior predictive p-values (i.e. ppp-values) – the proportion of simulated means > empirical means – for two test quantities: the observed mean and SD of the marker(s) of interest. Values close to 0 or 1 indicate discrepancies between simulated and observed data distributions. Lastly, to determine the models providing the most accurate oos prediction, we compared the correlation strength between observations and predictions on the test data (i.e. r_{oos}) for each 'oos.pred' model version/otolith marker combination (Table 3).

Spatial predictions

We used the best-performing 'oos.pred' models to predict otolith elemental and stable isotopic chemistry for each capture site, for each of the two age-classes captured, and for each of the three years of sampling[1]. To build the prediction matrix, we first extracted mean daily Temp and Sal values at each capture site from CODE (measured through the full water column) for October 2013, 2014 and 2015, and calculated monthly means for October each year. For the intrinsic covariates, when age 1 and/or age 2 herring were captured from a given site, the mean SL_anom value from the sampled population of each cohort at that site was used. In the event of no fish being captured at a site in a particular year, we followed a series of steps to estimate the SL_anom value (see Appendix S2 for details). We produced annual maps of site-specific predicted values for each age-class, and plotted the observed (± SD) versus predicted (± 70% highest posterior density (HPD) credible intervals) values across all sites and years. Finally, at each capture site, and for each otolith chemistry marker separately, we calculated Pearson's *r* between the mean observed and predicted values, and the MSPE across (1) all years, (2) by age-class, (3) by year, and (4) by age-class within year.

Results

Sampling coverage and environmental data

Our sampling targeted the key nursery areas for juvenile ISS herring in each year of the study (Figure 1). We observed large variation in juvenile size within each age-class (i.e. age 1: 55–118 mm SL, age 2: 97–149 mm SL), and in mean water column temperatures (0.97–8.80°C) and salinities (23.54–35.21‰) at capture sites across the Icelandic coast (Table 1).

[1] Spatial predictions are made for age 1 and age 2 herring for all element:Ca, and for age 2 only for $\delta^{13}C$ and $\delta^{18}O$.

Model adequacy and diagnostics

Fitting the univariate models in both 'MCMCglmm' and 'lme4' resulted in comparable parameter estimates and the selection of the same final explanatory 'explan' models for each otolith marker based on DIC and AICc (Appendix S2: Table S1). This allowed us to couple the functionality of 'lme4' for repeatability and R^2 estimation, with the benefits of posterior predictive checks to assess model adequacy (see below and Table 3). The Markov chains for the estimated parameters were well mixed for all univariate and multi/bivariate MCMCglmm models, displaying low serial dependence. Mean (± SD) lag-one autocorrelation for individual chains was 0.01 (± 0.06), < 0.01 (± 0.02) and 0.03 (± 0.09) for the final uni-, multi- and bivariate models, respectively, and mean $\hat{R}$ (± SD) was 1.01 (± 0.03), 1.00 (± 0.01) and 1.02 (± 0.06), respectively, indicating chain convergence and reliable samples for computing posterior summaries. Monte Carlo standard errors were always < 0.073, 0.177 and 0.100 in the uni-, multi- and bivariate models, respectively.

Models for explanation

The final univariate and multi/bivariate 'explan' models selected for each otolith marker differed in their fixed and random effect structures (see Table 3, Figure 2). In general, however, they showed strong and comparable performance with regard to within-sample predictive capacity as measured through posterior predictive simulation. Correlation (i.e. r_{sim}) between observed values for each marker and predicted mean values from the simulations was ≥ 0.6, with the exception of Zn:Ca (~0.3) and Ba:Ca (~0.4) (see Table 3, Appendix S2: Figure S2), with the spread of ppp-values obtained for the test quantities we considered (i.e. observed mean and SD of each marker) indicating no major discrepancies between observed and simulated distributions (Table 3). For five out of eight markers (Mg:Ca, Zn:Ca, Sr:Ca, Ba:Ca, $\delta^{13}C$) the multi/bivariate 'explan' models displayed slightly higher r_{sim} values compared with the univariate equivalents (Appendix S2: Figure S2). The final univariate models explained between 9 and 64% of the total variance (R^2_c) in the response, and in all cases where random effects were included, they contributed strongly to R^2_c. Adjusted repeatabilities varied widely. For example, after controlling for the fixed Age and SL_anom effects, > ~50% of the total variance in Li:Ca and Mn:Ca was explained by differences among sites, indicating strong within-site correlation in otolith measurements for these markers. By contrast, the low among-site, and high individual-level variability estimated for Zn:Ca (Figure 2) resulted in low repeatability (0.05) for this marker (Table 3).

Our analyses support the assertion that intrinsic processes can shape otolith elemental concentrations. The fixed Age term was retained in all final element:Ca models (Table 2, Figure 2), and contributed most to the population-level outcome for four out of six elements (see $R^2_{\beta_f}$ in Table 3). Models with the best within-sample predictive capacity (i.e. highest r_{sim}; see underlined models in Figure 2) showed consistent negative Age trends for Mg:Ca, Mn:Ca, Sr:Ca, and Ba:Ca at both the population and site levels (Figure 3, left-hand panels). Some site-level variation in the element:Ca–Age relationship was observed for Li:Ca, Mg:Ca, Mn:Ca and Sr:Ca, as confirmed by the magnitude of the random intercept and/or Age slope variances for these elements (Figure 2, 3). Otolith Zn:Ca concentrations did not differ between cohorts.

Our covariate for age-specific fish growth, SL_anom, was also influential for five of six elements, but trends varied across markers (Table 3, Figure 2, 3). Sr:Ca was consistently

lower in larger juveniles within each cohort. For Li:Ca, the interaction between SL_anom and Age at the population level indicates that the positive effect of SL_anom was weaker for age 2 compared with age 1 juveniles (Figure 3, top-right panel). Among-site variability in element:Ca – SL_anom relationships was generally small, as evidenced by the low estimated random SL_anom slope (co)variances for most markers (see Figure 2), and the consistent site-level trends (Figure 3, right hand panels). Ba:Ca was the exception, with site-level relationships for SL_anom varying widely (Figure 3). This result drove the inclusion of the random SL_anom slope term in the final multivariate model for the elemental markers (Table 3, Figure 2). We found no evidence for growth-related effects on otolith $\delta^{13}C$ and $\delta^{18}O$ (Table 3, Figure 2).

Environmental parameters, which here differed only *among* and not *within* capture sites, also explained some of the population-level variance for certain otolith markers (see $R^2_{\beta_f}$ estimates in Table 3). In the univariate models, salinity (Sal) was retained as a main effect for Zn:Ca (positive association), $\delta^{13}C$ and $\delta^{18}O$ (both negative associations), and showed a positive interaction with Age for Mg:Ca and Sr:Ca. Given that the main effects for Age and Sal were negative for Mg:Ca and Sr:Ca, a positive interaction coefficient suggests that the influence of Sal on these two elements is dampened in older (i.e. age 2) versus younger (age 1) individuals. Temperature (Temp) was retained in the univariate model for Sr:Ca and interacted with Age. Similar to the result for Sal, this interaction effect suggests that the weak overall negative association observed between Temp and Sr:Ca was weaker for age 2 than age 1 individuals. Temp was the most important predictor in the uni- and bivariate models for both $\delta^{13}C$ and $\delta^{18}O$, showing relatively strong negative associations with these markers in all four models (Figure 2, bottom four panels). A bivariate, and a univariate model, both including random intercepts, exhibited the best within-sample predictive accuracy for $\delta^{13}C$ and $\delta^{18}O$, respectively (underlined in Figure 2). Among-site variance in intercepts was low for $\delta^{13}C$ and moderate for $\delta^{18}O$.

Models for out-of-sample prediction

The final 'oos.pred' models had the highest oos predictive accuracy (i.e. the lowest $MSPE_{oos}$) of all candidate models considered. We observed substantial variation in $MSPE_{oos}$ across the candidate models (Appendix S2: Table S1), and also between the final 'explan' and 'oos.pred' models selected (Table 3). These two model suites often contained different fixed effect structures (e.g. see Li:Ca in Table 3); however, at least one intrinsic covariate was always included in the final 'oos.pred' models. The univariate models for the elemental markers out-performed the multivariate model in terms of correlation strength between observed and predicted values on the test data (r_{oos}) (Table 3). The bivariate 'oos.pred' model for $\delta^{13}C$ and $\delta^{18}O$ did better than the univariate versions.

Spatial predictions

Predictions from the best performing 'oos.pred' models revealed strong spatial structuring in several otolith markers across the Icelandic coast (Figure 4, Appendix S2: Figure S3). These patterns were generally consistent among the three sampling years within each age-class. Age 1 individuals were predicted to show enriched elemental concentrations relative to age 2 fish for five out of six elemental markers (see maps of Li:Ca, Sr:Ca, Mg:Ca, Mn:Ca, Zn:Ca) (Figure 4, Appendix S2: Figure S3), and displayed more pronounced variation in

elemental concentrations among capture sites; with the spatial scale of this variability differing by element (e.g. coarse north–south gradient in Li:Ca; finer, fjord-scale east–west and north–south gradient in Sr:Ca; homogenous pattern at the island-scale for Mn:Ca). Predictions for $\delta^{13}C$ and $\delta^{18}O$ depended solely on water temperature (Table 3), which increased year-on-year at most sites between 2013 and 2015. This drove the annual decrease in predicted values for these stable isotopic markers for age 2 fish, in addition to the strong north–south gradients observed (Figure 4, Appendix S2: Figure S3).

Overall, our predictions showed good concordance with the observations (Figure 5). Correlation (Pearson's *r*) between observed and predicted values for all captures sites was > 0.6 for Sr:Ca and $\delta^{13}C$, and ≥ 0.4 for Li:Ca and $\delta^{18}O$. Mg:Ca and Ba:Ca were poorly predicted, yet in the case of Mg:Ca, this was a consequence of high within-site variability in this marker observed in 2013. MSPE for 2013 ($MSPE_{2013}$) was an order of magnitude greater than $MSPE_{2014}$ and $MSPE_{2015}$, with *r* increasing from 0.09 to 0.57 for Mg:Ca if data from 2013 were excluded. No further clear trends emerged for individual markers with regard to MSPEs calculated by age-class, year, or by age-class within year (Appendix S2: Table S2).

Discussion

The natural schooling behaviour of juvenile ISS herring on their nursery grounds afforded us a rare, direct test of ontogenetic influences on otolith chemical traits in the field. Through the co-occurrence of two age-classes with shared recent environmental experience, captured in the same trawl tow, we were able to isolate age- and growth-related effects and demonstrate their importance in shaping otolith elemental and stable isotopic concentrations. Our models revealed how inter-individual variability in otolith chemistry scales to the site level, exposing site-level variation in relationships between some elemental concentrations and these intrinsic traits, whilst also highlighting the additional contribution of salinity and temperature variability (and/or the mechanisms these proxies represent) in explaining population-level trends. We made use of this information to predict observations at nursery sites across the Icelandic coast over three years, providing first-order estimates of the scales at which juvenile otolith chemistry might vary in space and time. The accuracy achieved here using relatively simple models parameterised with only four easily-calculated and routinely-measured covariates, suggests that these scales might, in fact, be quite predictable more generally. Given appropriate data, our modelling approach could test this on other species and systems, and serve as a valuable template for resolving management-related questions on source-sink dynamics when field observations are scarce or sampling coverage patchy.

Intrinsic influences on elemental and isotopic ratios

Using fish otoliths for illustration, our results add field-based support for the contention that intrinsic processes related to ontogeny can act, either alone, or in concert with environmental factors, to shape phenotypic trait variability (Walther et al. 2010; Grammer et al. 2017). The Age covariate was retained in the final 'explan' models for all elemental markers, and the SL_anom covariate in five of six (Table 3), with older age 2 juveniles typically displaying lower element:Ca ratios at the otolith edge relative to the younger conspecifics, both at the site- and population-level (Figure 3). Similar age-associated trends in these elements have been documented for other marine fishes (Sadovy and Severin 1994; Chittaro et al. 2006;

Grammer et al. 2017). However, the direction and magnitude of such relationships vary across species and systems (e.g. Walther et al. 2010), making generalisations difficult to draw, and underlying mechanisms difficult to pinpoint. Our ability here to discount environmental influences on otolith chemistry *within* capture sites implies that any clear deviation from a zero Age or SL_anom slope at the site-level must have an intrinsic and/or dietary basis, notwithstanding constraints enforced by sample size and between-cohort variability in otolith growth near the ablation site. Below, we present some ideas to explain our results in the context of recent theoretical and empirical advances.

Our Age covariate was included as a proxy for physiological and/or dietary changes occurring at an ~annual time step. Such changes were outwardly expressed as variation in fish size and growth rates between age-classes (Table 1), but internally, both theory and experiments suggest that these changes might regulate ion availability and transport through most stages of the journey from the surrounding water to blood to endolymph to otolith surface (Kalish 1989, 1991b; Sturrock et al. 2014, 2015; Limburg et al. 2018). How this occurs is complex, and Loewen et al. (2016) recently stressed the need to consider the functional role of each element in terms of life maintenance in teasing apart the stage-specific physiological processes giving rise to otolith concentrations. For example, accumulation of biologically 'essential' elements like Mg, Mn and Zn, that facilitate enzyme functioning (Watanabe et al. 1997; Crichton 2008), may be closely tuned to diet (Zn) (Ranaldi and Gagnon 2008), growth (Mg, Mn) (Martin and Thorrold 2005; Turner and Limburg 2015), and metabolism (Mg) (Limburg et al. 2018). Whereas, 'non-essential' elements like Sr and Ba, which likely substitute directly for calcium in the otolith matrix (Campana 1999; Doubleday et al. 2014), may be more sensitive to ambient Ca concentrations and Ca homeostasis at the water–blood and blood–endolymph boundaries (Payan et al. 2004; Loewen et al. 2016). Yet, other work at the water–blood interface has also illustrated the interplay between ontogeny and blood-bound protein concentrations in regulating ion exchange (Sturrock et al. 2014). In their 12-month mesocosm experiment on European plaice (*Pleuronectes platessa*), Sturrock et al. (2014) showed that plasma protein concentration varied with age, shifting through the year within the same groups of fish. They also reported a positive correlation between plasma protein level and somatic growth rate, and found that one or both of these variables were strong predictors of blood plasma concentrations of Mg, Ca, Mn, Zn, and Sr – elements found to be under limited environmental control in their experiment (Sturrock et al. 2014).

We did not collect blood composition data in our study. However, considering Sturrock et al. (2014)'s findings in conjunction with the evidence for tight links between (1) protein and ion concentrations in the plasma, and endolymph and otolith ion concentrations (Mugiya 1966; Kalish 1991b; Sturrock et al. 2015), and (2) otolith composition and endolymph composition (Kalish 1989; Borelli et al. 2001), it seems clear that physiologically-sensitive constituents of marine teleost blood are capable of mediating both endolymph and otolith chemistry. In light of this, one possible contribution to the negative element:Ca–Age relationships we observed might stem from a reduction in plasma protein concentrations due to slower growth in older versus younger juveniles, as seen in ISS herring (authors' unpublished data) and other herring populations (see Berg et al. 2018). Although this explanation may be particularly pertinent for transition metals like Zn, which associate closely with plasma (Sturrock et al. 2012) and otolith (Izzo et al. 2016) proteins, we contend that it may also apply to Sr. Sr is present in both mineral and protein fractions of the endolymph (Thomas et al. 2017) and otolith (Izzo et al. 2016), suggesting both endogenous

and exogenous regulation. In fully marine fishes, otolith Sr:Ca rarely reflects ambient water concentrations (Brown and Severin 2009), and instead, appears tied to internal factors that shift with age and growth, mediated by environmental variability (Kalish 1989, 1991b; Sturrock et al. 2015; Grammer et al. 2017). However, if we assume a positive link between somatic growth and plasma protein concentration (Sturrock et al. 2014), the consistent site- and population-level decreases in Sr:Ca with Age that we observed appear reasonable.

Reasonable that is, except that larger individuals within each age-class consistently exhibited lower otolith Sr:Ca than their smaller nursery-mates (Figure 3). From first glance, it appears that faster growth in early life may actually depress Sr:Ca uptake, as reported in previous studies (e.g. Sadovy and Severin 1994; Walther et al. 2010). Whilst we cannot rule this out, we offer an alternative. As spawning occurs over a ~30-day period in ISS herring (Óskarsson and Taggert 2009), we presumed that larger fish are faster growers in a pool of similarly-aged juveniles, rather than being older, 'average' growers. Spawning can occur in two or more waves in this stock, however (Óskarsson and Taggert 2009), so larger individuals could actually be older, and to have experienced slower recent growth than their younger, smaller conspecifics – an explanation that aligns more closely with the negative Age effects we detected, and one that could be resolved with more extensive daily increment analyses. Few published data exist on blood composition in herring (but see Ewart and Fletcher 1990 regarding 'antifreeze' proteins), and to our knowledge, none on endolymph composition. Controlled experiments that examine plasma protein levels in relation to growth variability in this species, whilst concurrently monitoring environmental Ca, endolymph and otolith composition would allow these ideas to be explored more rigorously.

But the constituents of ambient water, blood and endolymph are not necessarily the sole determinants of otolith chemical composition. In linking the seasonal fluctuations in otolith Mg:Ca observed for several marine-dependent fishes (including herring) with otolith growth and modelled standard metabolic rates (SMR), Limburg et al. (2018) make the case for a metabolic basis to Mg incorporation into the otolith. Briefly, their hypothesis originates at the blood–endolymph interface, where the authors propose that the activity of ion-transport cells (i.e. ionocytes) in the saccular epithelium correlates positively with the metabolic rate of the fish. This increases during high feeding activity, which in turn provides the energy needed for faster growth, and for the ionocytes to pump large, hydrated Mg^2 ions actively into the endolymph. Once within the saccule, Limburg et al. (2018) then argue the importance of the otolith surface environment for Mg^{2+} inclusion, pointing to the ratio of water soluble to insoluble proteins in the organic matrix as a key determinant – a ratio that can be well predicted by fish size (negative effect) and temperature (positive effect) (Hüssy et al. 2004).

Using Baltic flounder (*Platichthys flesus*) and American shad (*Alosa sapidissima*) for illustration, Limburg et al. (2018) demonstrated significant positive relationships between otolith Mg:Ca concentrations and both daily and annual otolith growth. Moreover, all species examined in their study displayed Mg:Ca enrichment during the early juvenile phase, with concentrations declining towards the otolith margin whilst tracking the seasonality of the species' particular environment (see their Figure 3). These patterns closely match the model of negative allometry in fish metabolism (Goolish 1995; Rosenfeld et al. 2015) that, in general, predicts higher metabolic, otolith and somatic growth rates as juveniles, and a non-linear decline in these parameters with size and/or age. We contend that this model might neatly explain the negative otolith Mg:Ca–Age relationships observed here for juvenile ISS

herring, and for other marine fishes (Macdonald et al. 2013; Grammer et al. 2017). Daily increment widths at the otolith edge, potential proxies for recent somatic growth, decreased with age in our samples (age 1 mean ± SD = 3.83 ± 0.08, n = 10; age 2 mean ± SD = 3.03 ± 0.09, n = 10). The uncoupling of otolith and somatic growth in herring larvae (Moksness 1992) fits within the general view that otolith growth is more closely tied to metabolic rate (see Mosegaard et al. 1988), and under this scenario, Limburg et al.'s proposal of a metabolic control on Mg:Ca incorporation appears to hold for our data. We did not measure individual metabolic rates, but note that metabolism in juvenile fishes can be linked to growth (Rosenfeld et al. 2015), social status (Metcalfe et al. 1995), food intake (Van Leeuwen et al. 2012) and temperature (Bernreuther et al. 2013), some of which may be selected for (Rosenfeld et al. 2015) and all of which may covary. Further integration of experimental results with dynamic energy budget theory (e.g. Fablet et al. 2011) would help disentangle these effects, clarifying the value of otolith Mg as a metabolic recorder, and perhaps shedding new light on the mechanisms underlying the consistent cycling in other elements (e.g. Mn, Sr, Ba) often detected in scans across marine fish otoliths (e.g. Macdonald et al. 2013).

Our results for Mn warrant some further discussion along these lines. We found strong negative relationships between Mn:Ca and Age at all sites, but no evidence for an age-specific growth effect (Figure 3). The maternal basis for Mn enrichment at the otolith core of Atlantic herring has been identified previously (Brophy et al. 2004), and this phenomenon has since been widely observed in marine fishes (e.g. Ruttenberg et al. 2005). However, patterns seen in Mn:Ca across outer growth zones have been less easily explained. In the Baltic Sea, Limburg et al. (2011) linked Mn:Ca in Atlantic cod otoliths to periodic hypoxia, but also reported a decline in concentrations through the first five years of life irrespective of the hypoxia level experienced. Drawing on these results, they proposed a model for Mn:Ca uptake as a function of (1) decreasing somatic growth with age, following an inverse von Bertalanffy growth curve, and (2) ambient Mn^{2+} (see SI Appendix in Limburg et al. 2011). Under non-hypoxic conditions *within* capture sites where ambient Mn^{2+} is equally available to age 1 and age 2 juveniles, this model would then predict a reduction in otolith Mn:Ca with age and/or growth, as we observed at all sites (Figure 3), consistent with other studies (Sturrock et al. 2015; Turner and Limburg 2015). Under non-hypoxic conditions, it therefore appears likely that ontogenetic patterns in otolith Mn may be associated with growth-related changes in physiology, which in our case were strong enough between age-classes (Age plot in Figure 3), but not within age-classes (SL_anom plot in Figure 3) to illicit a response in Mn:Ca levels.

We found less convincing evidence for ontogenetic influences on otolith Zn:Ca, Li:Ca and Ba:Ca at the site level. Assuming that both juvenile cohorts have experienced a common environment in the lead up to capture, these results might indicate either (1) a primarily extrinsic control on these elements, (2) that physiological processes driving the expression of an intrinsic signal are not sufficiently different between cohorts within sites, and/or (3) that inter-individual variation in physiological processes swamps any site- or population-level signals. Whilst we cannot fully disentangle these alternatives, useful insight may be gained from recent investigations into ion-binding affinities within the saccular endolymph, and at the precipitating otolith surface.

Zinc, a transition metal, associates with the 'proteinaceous fraction' of the endolymph and is tightly bound to soluble proteins in the otolith matrix (Izzo et al. 2016; Thomas et al.

2017). Zinc exhibits strong catalytic properties (Crichton 2008), and its presence in otoliths likely reflects its physiological significance as a co-factor, rather than being environmentally driven (Thomas et al. 2017), although sensitivity to diet has also been noted (Ranaldi and Gagnon 2008). Within nursery sites, we would expect that a distinct difference in dietary Zn between cohorts would result in some shift in otolith Zn concentrations (Ranaldi and Gagnon 2008). This was not observed, implying either that both cohorts share a similar diet, a notion supported by findings in other seas (e.g. Last 1989), that diets are variable, but Zn-concentrations within them are similar, or that alternatives (2) and/or (3) (previous paragraph), may be acting. Among-individual repeatability for Zn:Ca was very low, as a result of high variability in Zn:Ca concentrations within sites and cohorts, making option (3) a likely contributor to the (lack of) trends we see.

The alkali metal, Li was found only in the 'mineral fraction' of estuarine black bream (*Acanthopagrus butcheri*) endolymph as free ions (Thomas et al. 2017), and has low affinity for otolith proteins (Izzo et al. 2016). Lithium cations are small and univalent, hence regular substitution for Ca^{2+} in the otolith matrix is unlikely; random trapping providing a more plausible incorporation route. It is conceivable that otolith growth rates could influence ion-trapping opportunities, a scenario which would regulate Li incorporation according to otolith growth, both decreasing with age. We observed this Age trend at four of six capture sites (Figure 3), although the inconsistency in site-level relationships hints that a growth-based mechanism may not be universal. Nevertheless, as the positive impact of somatic (and likely otolith) growth on otolith Li:Ca appears to diminish in older juveniles (Figure 3, top-right panel), and as growth potential can vary markedly at the island-wide scale (see *Site- and individual-level variation*) this could explain our results in the context of growth variability alone. We stress though, that the interaction of Age and SL_anom was retained only at the population-level (i.e. across all capture sites), constraining our ability to disentangle intrinsic from unmeasured extrinsic processes (e.g. ambient water concentrations).

Bivalent barium ions associate mainly with the mineral phase of the otolith (Izzo et al. 2016) and likely follow a similar uptake pathway to Sr^{2+}, i.e. via Ca^{2+} replacement (Campana 1999). However, there is some suggestion of both intrinsic and extrinsic control on Ba incorporation (Walther et al. 2010; Clarke et al. 2011; Thomas et al. 2017). We observed small, consistent decreases in otolith Ba:Ca with Age at all sites, but no clear relationship with fish growth (Figure 3). Our data provide no strong evidence to refute the notion that otolith Ba concentration is under substantial environmental control (i.e. alternative 1 above), or at least control by internal processes (e.g. metabolism) themselves influenced by environmental factors (e.g. temperature). The predictive capacity of our Ba models was poor (Table 3, Figure 5), adding weight to the argument that external factors can largely determine otolith Ba levels in marine fishes (Martin and Wuenschel 2006; Walther and Thorrold 2006).

Still at the growing otolith surface, a strong element:Ca–Age relationship could also reflect differences in the ratios of $CaCO_3$: protein occurring in outer otolith growth bands for age 1 and age 2 juveniles, depending on the binding sites of particular elements (Thorrold and Swearer 2009; Izzo et al. 2016), or simply between-cohort variation in the growth period ablated. However, given that our 40-µm ablation spots sampled, at most, the final two weeks of otolith growth in both age-classes, we consider any impact of the latter to be slight.

Otolith stable carbon and oxygen isotope ratios were explained solely by environmental effects in all models. These findings were initially surprising, given the former's known links

to metabolism, growth and diet (Kalish 1991c; Solomon et al. 2006; Geffen 2012), and the potential for 'vital' effects to impact the relationship between $\delta^{18}O$ and temperature (Darnaude and Hunter 2018). We discuss these points further below.

Environmental influences across sites

The oceanography around Iceland during autumn is characterised by marked north-south temperature variation and steep inshore-offshore salinity gradients that shape conditions on the ISS herring nursery grounds (Figure 1, Valdimarsson et al. 2012; Logemann et al. 2013). Such environmental variability is uncommon across ocean scapes at this small a spatial scale, allowing us to field-test the effects of two parameters known to directly and/or indirectly affect otolith chemical concentrations across the full distributional range of ISS juveniles. In interpreting our results, we note that we were unable to isolate the influence of Temp or Sal from other unquantified extrinsic (e.g. pH, ambient water concentrations) factors here, as our comparisons were made *across* sites. Though any relationships we see must be viewed as correlative only, some interesting trends emerged. Salinity was found to influence Mg:Ca, Zn:Ca, and to a lesser extent, Sr:Ca concentrations in both univariate and multivariate 'explan' models, with a mild negative temperature effect detected in the univariate model for Sr:Ca (Figure 2). Importantly, Mg:Ca and Sr:Ca displayed significant interactions between Age and Sal, and Age and both environmental covariates, respectively, in the univariate models. These patterns point to decreased environmental sensitivity in Mg and Sr markers for older juveniles. This is in line with work by Grammer et al. (2017), who reported both a steeper rate of change in elemental assimilation in younger compared with older reef ocean perch (*Helicolenus percoides*) traversing the same environmental gradients, and interactions between age and environmental features such as upwelling intensity.

The search for an unambiguous record of an individual fish's environmental history inspired initial efforts to understand how the environment might shape chemical uptake into otoliths (e.g. Radtke 1984). The commercial importance of herring positioned them at the forefront of early work in this field. In experiments on larvae and juveniles, Townsend et al. (1989) and Radtke et al. (1990) sought evidence for temperature dependence on otolith Sr:Ca. Both studies demonstrated a negative relationship; however, the results were questioned due to artificially introduced stress effects. In a follow-up study on age 0 juveniles, Townsend et al. (1992) interpreted the decrease in Sr:Ca with temperature (also observed in our study) in terms of physiology. They suggested that at lower temperatures, where metabolism slows, Sr may be transported more readily into the endolymph, increasing opportunities for accretion onto the otolith surface (*sensu* Kalish 1989). More recent work has added support for a degree of internal control, not just on Sr, but on concentrations of several commonly-measured elements (e.g. Mg, Mn, Ba) (Brophy et al. 2004; Clarke et al. 2011; Sturrock et al. 2014, 2015; Izzo et al. 2018; Limburg et al. 2018; this study), mediated by temperature (e.g. growth, metabolism) (Holt and Jørgensen 2014) or salinity (e.g. osmoregulation) (Holliday and Blaxter 1960). Ocean-resident species generally experience less environmental heterogeneity throughout life than their freshwater and estuarine cousins, a situation in which environmental influences on otolith chemistry may be swamped by intrinsic signals (Sturrock et al. 2012; 2014). Indeed, a primarily internal control on uptake of such elements into marine fish otoliths might explain the pronounced species- and system-level variability seen among studies that test for environmental influences alone (Chang and Geffen 2013).

To our knowledge, our study is the first to report $\delta^{13}C$ and $\delta^{18}O$ measurements in herring otoliths. Stable oxygen isotopes in age 2 otoliths appeared insensitive to variation in growth rate. However, a clear negative association was found between $\delta^{18}O$, Temp and Sal across all capture sites. A negative temperature trend is in agreement with previous laboratory- and field-based investigations into temperature dependence in otolith $\delta^{18}O$ (e.g. Kalish 1991a, b; Geffen 2012; Darnaude and Hunter 2018). Moreover, our results mirror those from work on juvenile Atlantic cod (Høie et al. 2003; Stanley et al. 2015) and plaice (Geffen 2012) that reported no effect of somatic growth, and reduced otolith $\delta^{18}O$ at higher temperatures. Interestingly, in contrast to these three studies, otolith $\delta^{13}C$ was not influenced by herring growth variability within or across nursery sites, but like $\delta^{18}O$, did decline strongly with increasing temperature. We suggest that the marked temperature and salinity variation existing across the Icelandic coast might have indirectly shaped site-level differences in individuals' metabolic rates. Previous investigations have predicted otolith $\delta^{13}C$ depletion at higher metabolic rates (Kalish 1991c; Schwarcz et al. 1998), and given that metabolic activity increases with temperature in herring (Bernreuther et al. 2013), our results are perhaps not wholly unexpected (see Radtke 1984). As changes detected in stable isotopic concentrations as a function of otolith growth are nearly certainly of metabolic, rather than kinetic origin (Høie et al. 2003), the absence of a growth-related signal here might reflect similarity in metabolic rates between similar-age juveniles across the size range we captured. Monitoring of individual SMRs would have allowed us to explore this further. But we highlight recent analytical advances in assessing the contribution of dietary $\delta^{13}C$ and $\delta^{15}N$ to otolith values of these isotopes, which hold great promise for generating retrospective estimates of individual metabolism from otoliths alone (Shiao et al. 2018).

We did not collect water chemistry data in our study. Ambient water concentrations are known to be major predictors of otolith elemental, $\delta^{13}C$ and $\delta^{18}O$ concentrations (Bath et al. 2000; Elsdon and Gillanders 2004; Solomon et al. 2006), and we recognise that inclusion of such data would likely have improved the fit and predictive capacity of our models at the population scale. However, our main focus in this paper was to test for ontogenetic effects *within* capture sites, whereby all juveniles present were exposed to identical ambient water concentrations, temperatures, salinities and pH in their recent past. This provided us a quasi-controlled, natural-laboratory setting, allowing us direct inference on intrinsic effects both between and within cohorts.

A second issue relates to our use of modelled environmental data at a subset of inshore capture sites. The hydrographic conditions within fjords receiving high inflows are difficult to quantify accurately, either with empirical snapshots of ambient conditions, or with ocean models. Yet, as such areas are the primary nursery grounds for ISS herring on Iceland's north coast, we sought the most realistic representation possible. Empirical measurements were available through the water column at 12 of 26 capture sites at the time of sampling, and importantly, at five of six sites in the 'training' dataset. For the remaining sites, we extracted data from the CODE model, which assimilates observations from CTD profiles and river discharge data from 46 watersheds into its simulation. Excellent concordance was found between modelled and observed temperature and salinity fields across our study region (see Table 1 in Logemann et al. 2013). However, given the bias of the CTD data towards offshore waters, we acknowledge that some uncertainty surrounds our estimates for the inshore sites within the 'test' and 'extras' datasets. We are confident though, that our covariates reflect the main environmental gradients present across the Icelandic coast at the time of sampling. We believe also that the 'explan' and 'oos.pred' models, fitted using a predominance of

empirical observations, incorporate a reliable description of the ambient conditions experienced by juvenile ISS herring on their nursery grounds.

Site- and individual-level variation

An important result from our study was the degree of among-site variation detected in relationships between some otolith elemental markers and the intrinsic covariates (Figure 2, 3). This is a notable finding, suggesting that the characteristics of particular areas might generate pronounced site-level divergence in phenotypic expression (Freshwater et al. 2019). The nursery fjords in our training dataset differ markedly in topography, and are separated by up to ~400 km of coastline. At this scale, strong potential exists for differences in food availability/quality, predation or density-dependent pressures, and environmental heterogeneity – characteristics capable of impacting individuals' behaviour and emergent phenotypic traits (e.g. growth, metabolic activity) (Fiksen et al. 2007; Holt and Jørgensen 2014) that may themselves covary (e.g. Rosenfeld et al. 2015). If the phenotypes of individuals residing within a site are affected similarly by local characteristics, and these characteristics differ sufficiently between sites, then one would expect phenotypic differences to scale from the individual- to the site-level. We saw some evidence for this through the non-overlapping size distributions of age 1 juveniles captured from different nursery sites (e.g. Table 1: site D7-2014C c/w site D9-2014-6). In light of the potential sensitivity of Li and Mg to development-related factors, we speculate that site-level differences in phenotypic traits, driven at least in part by site-specific conditions, may have contributed to the among-site variability seen in Age slopes.

The phenotypic composition of nursery-resident juveniles might also be influenced by events occurring prior to nursery settlement. The ability and tendency of animals to disperse during early life is increasingly being seen as the product of context (environmental drivers) and condition (an individual's internal state). On an individual, intra-specific level, variation in genotype, physiology, behaviour, history and parental history coupled with environmental heterogeneity might lead to marked inter-individual variation in dispersal trajectories (Fiksen et al. 2007; Cote et al. 2010; Nanninga and Berumen 2014). In turn, dispersal history can have consequences for individual fitness later in life, affecting settlement patterns, and hence the spatial structure of populations (Shima and Swearer 2010). With regard to dense-schooling species like herring, if similarly 'conditioned' individuals, with similar phenotypes share similar dispersal histories, the chances of them colonising the same nursery habitats may increase (Shima and Swearer 2016). We are exploring this idea by linking particle-tracking simulations with otolith $\delta^{18}O$ life-history transects from a subset of our age 2 herring (authors' unpublished data). If this is the case, and assuming a level of intrinsic control on elemental uptake, then phenotypic variability emerging both pre- and post-settlement, may have jointly found expression in the site-level otolith chemical variability we detected.

Of course, any site-level variation we see must originate at the level of the individual. We noticed marked inter-individual variation in otolith chemistry within age-classes, within capture sites for several elements (Table 3, Figure 2, 3); variation that cannot be attributed to environmental heterogeneity. The magnitude of the σ^2_ε terms in Figure 2 provides some clues on the degree of individual variability at the population level. However, the spread of raw data, disaggregated by capture site and age-class (see Figure 3, element:Ca–Age plots), and the adjusted repeatability estimates (i.e. 'Adj. rep') in Table 3, both directly demonstrate

strong inter-individual variation for some markers (i.e. Mg:Ca, Zn:Ca and Ba:Ca) and lower variability in others (i.e. Li:Ca, Mn:Ca, Sr:Ca, $\delta^{18}O$).

Such individual-level variability in trait expression is well known in animals (Dall et al. 2004; Stamps 2016), and is not uncommon in otolith chemistry studies. Indeed, Kalish (1989) first observed individual differences in otolith Sr:Ca in Australian salmon (*Arripis trutta*) kept under identical environmental conditions, and more recently, Macdonald and Crook (2010) and Panfili et al. (2015) have demonstrated clear inconsistencies in otolith Sr:Ca and/or Ba:Ca profiles among juvenile Australian bass (*Macquaria novemaculeata*) and tilapia (*Sarotherodonmelanotheron heudelotii*), respectively, held within the same treatment tanks. We are not currently in a position to pin down the mechanisms governing these patterns. However, evidence for inter-individual behavioural plasticity within species and populations is growing (e.g. Crook et al. 2017; Freshwater et al. 2019). And, as individual behaviour can feedback to affect growth (Fiksen et al. 2007) and physiology, factors than may influence elements like Mg and Zn (Turner and Limburg 2015; Thomas et al. 2017), we suggest that the existence of a variety of behavioural traits within each age-class and capture site played a part in driving the individual variability in otolith chemical traits we observed.

Spatial predictions: application to source-sink dynamics and fishery management

The accuracy achieved in predicting most elemental and both stable isotopic markers at our nursery sites was unexpected (see Figure 4, 5, Appendix S2: Figure S3). We found moderate to good congruence (i.e. r = 0.26 to 0.64) between site-level observations and predictions from the 'oos.pred' models for six out of eight markers, and for seven of eight markers (all except Ba:Ca) when data from 2013 were excluded (Table 3, Figure 5). All final 'oos.pred' models for element:Ca ratios included Age and/or SL_anom in their structure, further highlighting the role of age- and/or growth-associated factors in predicting elemental chemistry on oos test data. Our prediction maps exposed island-wide heterogeneity in each marker, providing us a reliable initial estimate of the scales of otolith chemical variability in space, time and for both juvenile cohorts across their entire distributional range (Figure 4).

To some notable results. We detected fine, fjord-scale variation in otolith Sr:Ca across the north coast (Figure 4). Sr:Ca was the best predicted marker, exhibiting the lowest MSPE overall (Table 3), by year (Figure 5), age-class, and age-class within year (Appendix S2: Table S2). Ambient Sr is known to be rather invariant in marine systems (Sturrock et al. 2012), often reducing its utility as a population discriminator in open-ocean settings. This was found to be the case at sites located further offshore (Figure 4); however, given the inclusion of Age, SL_anom and Sal in the final 'oos.pred' model for Sr:Ca, we were able to resolve a finer-scale spatial pattern inshore, across the north coast fjords. By contrast, Ba:Ca was predicted poorly, both non-spatially to oos data, and at the site-level (Table 3, Figure 4, 5). We believe this result stems from a primary dependence of otolith Ba:Ca on ambient Ba:Ca in marine fishes (Bath et al. 2000; Walther and Thorrold 2006), a variable we did not measure here. Site-level predictions of $\delta^{18}O$ matched the observations well in most instances (Figure 5), exhibiting a stark north-south decline that tracked the temperature gradient around Iceland. Predictions for otolith $\delta^{13}C$ reflected the salinity gradient and agreed well with the observations (r = 0.64, Figure 5), suggesting that salinity may be a good proxy for either metabolically-derived carbon sourced from the diet, or for water-borne dissolved

inorganic carbon (Gillikin et al. 2006), both key contributors to otolith $\delta^{13}C$ values (Solomon et al. 2006). Interestingly, evidence for strong annual variation in otolith chemistry was absent, and, as also inferred from the 'explan' models, older juveniles were generally predicted to exhibit lower, more homogenous elemental chemistry across the study region (Figure 4, 5, Appendix S2: Figure S3).

Our predictions are based on snapshots of the local environmental conditions and the nursery populations, both of which may fluctuate over seasonal and annual time scales. Otolith chemistry can also differ markedly in time at the same location, particularly for elemental markers (Reis-Santos et al. 2012), suggesting that the among-year consistency we predicted likely underestimates the system's true variability. We also note that predictions to sites within the 'test' and 'extras' datasets, where observations were few, or totally absent, would be more sensitive to how our intrinsic covariates were derived (see Appendix S2).

Notwithstanding these limitations, the prediction accuracy we achieved generates confidence in our modelling approach. Using combinations of only four covariates that are routinely collected during sampling programmes, we provide a framework for inferring island-wide variability in otolith chemistry, by age-class and through time. Such inference could confer important benefits for fishery-management applications further afield, particularly in data-limited situations. For example, our models return direct estimates of source-source connectivity across all potential source populations, allowing 'baseline' samples of otolith chemical signatures to be constructed at appropriate scales, even when sampling coverage is incomplete. A reliable baseline, together with methods that affirm the number of sources within it (e.g. Neubauer et al. 2013), adds potency to source-assignment tests for older individuals mixing on fishing grounds. These tests provide fundamental data for management, allowing key sources contributing to a fishery to be identified, and protected. Secondly, accurate predictions could aid future juvenile sampling programmes by reducing time and/or costs associated with targeting populations with chemically-homogenous otoliths (if the research or management goal is population delineation). Third, they could allow temporal stability in otolith chemistry in each site/region to be estimated, and if present, remove the need to resample all sites when establishing a reference atlas of source otolith chemical signatures. And lastly, at the otolith analysis stage, they could help identify subsets of chemical markers that maximise discriminatory ability for the target species, potentially negating redundant, often expensive analyses.

Conclusions

By accessing times series of chemical traits stored in otoliths, this study demonstrates the importance of ontogeny in shaping trait expression, and shows how such information can be harnessed to predict trait heterogeneity at multiple scales. Our analysis focussed on otoliths of ISS herring, a fish stock exploited heavily by commercial fishers and undergoing a decade-long decline as a result of recurring *I. hoferi* infection and persistent poor recruitment. Ongoing pressures from these and other top-down stressors (e.g. the potential for high juvenile bycatch in the northern shrimp fishery) provided the impetus for this work. That said, our modelling approach, which explicitly captures individual- to population-level variation in trait expression through ontogeny could be easily applied to other taxa for which time-stamped, individual-level data are available (e.g. via statoliths in aquatic invertebrates, implantable data loggers in aquatic and terrestrial organisms). In a commercial-harvest

context, a tighter union of experimental work and modelling would help disentangle the intrinsic and extrinsic controls on traits stored in such repositories, thereby building trust in them as guides for the effective spatial management of targeted species. The present work represents a step in this direction.

Acknowledgements

This work was funded by the Icelandic Association of Herring Fisheries under 'Rannsóknarsjóður síldarútvegsins 2013', and by the Norden Top-Level Research Initiative subprogram 'Effect Studies and Adaptation to Climate Change', through the Nordic Centre for Research on Marine Ecosystems and Resources Under Climate Change (NorMER). We thank P. Reynisson, I. Jónsdóttir, G. Óskarsson, M. Danielsen, G. Jóhannsson and the crew aboard w/w Dröfn RE-35 for assistance with sample collection, and A. Greig for technical support during the LA-ICP-MS analyses. Thanks also to D. Eme and J. Morrongiello for lively discussions on the modelling approach, and to J. Morrongiello, D. Crook, G. Huse, G. Óskarsson, I. Jónsdóttir, Þ. Sigurðsson and A. Leitão for reviewing early drafts and providing insightful suggestions that greatly improved the paper.

References

Allendorf, F.W., England, P.R., Luikart, G., Ritchie, P.A. and Ryman, N. 2008. Genetic effects of harvest on wild animal populations. Trends Ecol. Evol. 23: 327–337.

Bates, D., Mächler, M., Bolker, B. M. and Walker, S. C. 2015. Fitting linear mixed-effects models using lme4. J. Stat. Soft. 67: 1–48.

Bath, G.E., Thorrold, S.R., Jones, C.M., Campana, S.E., McLaren, J.W. and Lam, J.W.H. 2000. Strontium and barium uptake in aragonitic otoliths of marine fish. Geochim. Cosmochim. Acta 64: 1705–1714.

Berg, F., Almeland, O.W., Skadal, J., Slotte, A. Andersson, L. and Folkvord, A. 2018. Genetic factors have a major effect on growth, number of vertebrae and otolith shape in Atlantic herring (*Clupea harengus*). PLoS One 13: e0190995.

Bernreuther, M., Herrmann, J.P., Peck, M.A., and Temming, A. 2013. Growth energetics of juvenile herring, *Clupea harengus* L.: food conversion efficiency and temperature dependency of metabolic rate. J. Appl. Ichthyol 29: 331–340.

Borelli, G., Mayer-Gostan, N., De Pontual, H., Boeuf, G. and Payan, P. 2001. Biochemical relationships between endolymph and otolith matrix in the trout (*Oncorhynchus mykiss*) and turbot (*Psetta maxima*). Calcified Tissue Int. 69: 356–364.

Brophy, D. and Danilowicz, B.S. 2002. Tracing populations of Atlantic herring (*Clupea harengus* L.) in the Irish and Celtic Seas using otolith microstructure. ICES J Mar. Sci. 59: 1305–1313.

Brophy, D., Jeffries, T.E. and Danilowicz, B.S. 2004. Elevated manganese concentrations at the cores of clupeid otoliths: possible environmental, physiological, or structural origins. Mar. Biol. 144: 779–786.

Brown, R.J. and Severin, K.P. 2009. Otolith chemistry analyses indicate that water Sr:Ca is the primary factor influencing otolith Sr:Ca for freshwater and diadromous fish but not for marine fish. Can. J. Fish. Aquat. Sci. 66: 1790–1808.

Campana, S. 1999. Chemistry and composition of fish otoliths: pathways, mechanisms and applications. Mar. Ecol. Prog. Ser.188: 263–297.

Cardinale, M., Casini, M., Arrhenius, F. and Håkansson, N. 2003. Diel spatial distribution and feeding activity of herring (*Clupea harengus*) and sprat (*Sprattus sprattus*) in the Baltic Sea. Aquat. Living Resour. 16: 283–292.

Chang, M.Y. and Geffen, A.J. 2013. Taxonomic and geographic influences on fish otolith microchemistry. Fish Fish. 14: 458–492.

Chittaro, P.M., Hogan, J.D., Gagnon, J., Fryer, B.J. and Sale, P.F. 2006. In situ experiment of ontogenetic variability in the otolith chemistry of *Stegastes partitus*. Mar. Biol. 149: 1227–1235.

Clarke, L.M., Thorrold, S.R. and Conover, D.O. 2011. Population differences in otolith chemistry have a genetic basis in *Menidia menidia*. Can. J. Fish. Aquat. Sci. 68: 105–114.

Clausen, L.A.W., Bekkevold, D., Hatfield, E.M.C. and Mosegaard, H. 2007. Application and validation of otolith microstructure as a stock identification method in mixed Atlantic herring (*Clupea harengus*) stocks in the North Sea and western Baltic. ICES J. Mar. Sci. 64: 377–385.

Cote, J., Fogarty, S., Weinersmith, K., Brodin, T. and A. Sih. 2010. Personality traits and dispersal tendency in the invasive mosquitofish (*Gambusia affinis*). P. Roy. Soc. B-Biol. Sci. 277:1571–1579.

Cowen, R.K., Gawarkiewicz, G., Pineda, J., Thorrold, S.R. and Werner, F.E. 2007. Population connectivity in marine systems: an overview. Oceanography 20:14–21.

Crook, D.A., Buckle, D.J., Allsop, Q., Baldwin, W., Saunders, T.M., Kyne, P.M., Woodhead, J.D., Maas, R., Roberts, B. and Douglas, M.M. 2017. Use of otolith chemistry and acoustic telemetry to elucidate migratory contingents in barramundi *Lates calcarifer*. Mar. Freshwater Res. 68: 1554–1566.

da Silva, A. 2017. 'biotools'. Tools for biometry and applied statistics in agricultural Science. R package version 3.1. https://cran.r-project.org/web/packages/biotools/

Dall, S.R.X., Houston, A.I. and McNamara, J.M. 2004. The behavioural ecology of personality: Consistent individual differences from an adaptive perspective. Ecol. Lett. 7: 734–739.

Darnaude, A.M. and Hunter, E. 2018. Validation of otolith $\delta^{18}O$ values as effective natural tags for shelf-scale geolocation of migrating fish. Mar. Ecol. Prog. Ser. 598: 167–185.

Dingemanse, N.J. and Dochtermann, N.A. 2013. Quantifying individual variation in behaviour: mixed-effect modelling approaches. J. Anim. Ecol. 82: 39–54.

Dormann, C.F., Elith, J., Bacher, S., Buchmann, C., Carl, G., Carré, G., García Marquéz, J.R., Gruber, B., Lafourcade, B., Leitão, P.J., Münkemüller, T., McClean, C., Osborne, P.E., Reineking, B., Schröder, B., Skidmore, A.K., Zurell, D. and Lautenbach, S. 2013. Collinearity: a review of methods to deal with it and a simulation study evaluating their performance. Ecography 36:27–46.

Doubleday, Z.A., Harris, H.H., Izzo, C. and Gillanders, B.M. 2014. Strontium randomly substituting for calcium in fish otolith aragonite. Anal. Chem. 86: 865–869.

Elsdon, T.S. and Gillanders, B.M. 2004. Fish otolith chemistry influenced by exposure to multiple environmental variables. J. Exp. Mar. Biol. Ecol. 313: 269–284.

Ewart, K.V. and Fletcher, G.L. 1990. Isolation and characterization of antifreeze proteins from smelt (*Osmerus Mordax*) and Atlantic herring (*Clupea harengus harengus*). Can. J. Zool. 68: 1652–1658.

Fablet, R., Pecquerie, L., de Pontual, H., Høie, H., Millner, R., Mosegaard, H. and Kooijman, S.A.L.M. 2011. Shedding light on fish otolith biomineralization using a bioenergetic approach. PLoS One 6:e27055.

Fiksen, Ø., Jørgensen, C., Kristiansen, T., Vikebø, F. and Huse, G. 2007. Linking

behavioural ecology and oceanography: larval behaviour determines growth, mortality and dispersal. Mar. Ecol. Prog. Ser. 347: 195–205.
Flegal, J.M., Hughes, J. and Vats, D. 2016. mcmcse: Monte Carlo standard errors for MCMC. R package version 1.2-1. https://cran.r-project.org/web/packages/mcmcse/
Freshwater, C., Trudel, M., Beacham, T.D., Gauthier, S., Johnson, S.C., Neville, C.-E. and Juanes, F. 2019. Individual variation, population-specific behaviours, and stochastic processes shape marine migration phenologies. J. Anim. Ecol. 88: 67–78.
Geffen, A.J. 2012. Otolith oxygen and carbon stable isotopes in wild and laboratory-reared plaice (*Pleuronectes platessa*). Environ. Biol. Fish. 95: 419–430.
Gelman, A. 2008. Scaling regression inputs by dividing by two standard deviations. Stat. Med. 27: 2865–2873.
Gillikin, D., Lorrain, A., Bouillon, S., Willenz, P. and Dehairs, F. 2006. $\delta^{13}C$ in *Mytilus edulis* shells: relation to salinity, DIC, phytoplankton and metabolism. Org. Geochem. 37: 1371–1382.
Goolish, E.M. 1995. The metabolic consequences of body size. . Biochem. Mol. Biol. Fishes 4: 335–366.
Grabowski, T.B., Boswell, K.M., McAdam, B. J., Wells, R.J.D. and Marteinsdóttir, G. 2012. Characterization of Atlantic cod spawning habitat and behavior in Icelandic coastal waters. PLoS One 7: e51321.
Grammer, G., Morrongiello, J., Izzo, C., Hawthorne, P., Middleton, J. and Gillanders, B. 2017. Coupling biogeochemical tracers with fish growth reveals physiological and environmental controls on otolith chemistry. Ecol. Monogr. 87: 487–507.
Grønkjær, P. 2016. Otoliths as individual indicators: a reappraisal of the link between fish physiology and otolith characteristics. Mar. Freshwater Res. 67: 881–888.
Guðmundsdóttir, A., Óskarsson, G.J. and Sveinbjörnsson, S. 2007. Estimating year-class strength of Icelandic summer-spawning herring on the basis of two survey methods. ICES J. Mar. Sci. 64: 1182–1190.
Hadfield, J. 2010. MCMC methods for multi-response generalised linear mixed models: the MCMCglmm R package. J. Stat. Softw. 33: 1–22.
Høie, H., Folkvord, A. and Otterlei, E. 2003. Effect of somatic and otolith growth rate on stable isotopic composition of early juvenile cod (*Gadus morhua* L) otoliths. J. Exp. Mar. Biol. Ecol. 289: 41–58.
Holliday, F.G.T. and Blaxter, J.H.S. 1960. The effects of salinity on the developing eggs and larvae of the herring. J. Mar. Biol. Assoc. U.K. 39: 591–603.
Holt, R.E. and Jørgensen, C. 2014. Climate warming causes life-history evolution in a model for Atlantic cod (*Gadus morhua*). Conserv. Physiol. 2:cou050.
Hüssy, K., Mosegaard, H. and Jessen, F. 2004. Effect of age and temperature on amino acid composition and the content of different protein types of juvenile Atlantic cod (*Gadus morhua*) otoliths. Can. J. Fish. Aquat. Sci. 61: 1012–1020.
ICES. 2017. Report of the North-Western Working Group, 27 April - 4 May 2017. ICES CM 2017/ACOM:08, Copenhagen, Denmark.
Izzo, C., Doubleday, Z.A. and Gillanders, B.M. 2016. Where do elements bind within the otoliths of fish? Mar. Freshwater Res. 67: 1072–1076.
Izzo, C., Reis-Santos, P. and Gillanders, B.M. 2018. Otolith chemistry does not just reflect environmental conditions: a meta-analytic evaluation. Fish Fish. 19: 441–454.
Jaeger, B.C., Edwards, L.J., Das, K. and Sen, P.K. 2017. An R^2 statistic for fixed effects in the generalized linear mixed model. J. Appl. Stat. 44: 1086–1105.
Jansen, T., Post, S., Kristiansen, T., Óskarsson, G.J., Boje, J., MacKenzie, B.R., Broberg, M. and Siegstad, H. 2016. Ocean warming expands habitat of a rich natural resource

and benefits a national economy. Ecol. Appl. 26: 2021–2032.
Jakobsson, J. and Stefánsson, G. 1999. Management of summer-spawning herring off Iceland. ICES J. Mar. Sci. 56: 827–833.
Johnson, P.C.D. 2014. Extension of Nakagawa & Schielzeth's R^2_{GLMM} to random slopes models. Methods Ecol. Evol. 5: 944–946.
Kalish, J.M. 1989. Otolith microchemistry: validation of the effects of physiology, age and environment on otolith composition. J. Exp. Mar. Biol. Ecol. 132: 151–178.
Kalish, J.M. 1991a. Oxygen and carbon stable isotopes in the otoliths of wild and laboratory-reared Australian salmon. Mar. Biol. 47: 37–47.
Kalish, J.M. 1991b. Determinants of otolith chemistry: seasonal variation in the composition of blood plasma, endolymph and otoliths of bearded rock cod *Pseudophycis barbatus*. Mar. Ecol. Prog. Ser. 74: 137–159.
Kalish, J.M. 1991c. ^{13}C and ^{18}O isotopic disequilibria in fish otoliths: metabolic and kinetic effects. Mar. Ecol. Prog. Ser. 75: 191–203.
Kawecki, T.J. and Ebert, D. 2004. Conceptual issues in local adaptation. Ecol. Lett. 7: 1225–1241.
Korkmaz, S., Goksuluk, D. and Zararsiz, G. 2015. MVN: An R Package for assessing multivariate normality. The R Journal 6: 151–162.
Last, J.M. 1989. The food of herring, *Clupea harengus*, in the North Sea, 1983–1986. J Fish Biol. 34: 489–501.
Leitão, A.V., Hall, M.L., Venables, B. and Mulder, R.A. 2019. Ecology and breeding biology of a tropical bird, the Lovely Fairy-Wren (*Malurus amabilis*). Emu 119: 1–13.
Limburg, K.E., Olson, C., Walther, Y., Dale, D., Slomp, C.P. and Høie, H. 2011. Tracking Baltic hypoxia and cod migration over millennia with natural tags. Proc. Natl Acad. Sci. USA 108: E177–E182.
Limburg, K.E., Wuenschel, M.J., Hüssy, K. and Heimbrand, Y. 2018. Making the otolith magnesium chemical calendar-clock tick: plausible mechanism and empirical evidence. Rev. Fish. Sci. Aquac. 26: 479–493.
Link, W.A. and Eaton, M.J. 2012. On thinning of chains in MCMC. Methods Ecol. Evol. 3: 112–115.
Loewen, T.N., Carriere, B., Reist, J.D., Halden, N.M. and Anderson, W.G. 2016. Linking physiology and biomineralization processes to ecological inferences on the life history of fishes. Comp. Biochem. Physiol. A Mol. Integr. Physiol. 202: 123–140.
Logemann, K., Ólafsson, J., Snorrason, Á., Valdimarsson, H. and Marteinsdóttir, G. 2013. The circulation of Icelandic waters – a modelling study. Ocean Sci. 9:.931–955.
Macdonald, J.I. and Crook, D.A. 2010. Variability in Sr:Ca and Ba:Ca ratios in water and fish otoliths across an estuarine salinity gradient. Mar. Ecol. Prog. Ser. 413: 147–161.
Macdonald, J.I., Farley, J.H., Clear, N.P., Williams, A.J., Carter, T.I., Davies, C.R. and Nicol, S.J. 2013. Insights into mixing and movement of South Pacific albacore *Thunnus alalunga* derived from trace elements in otoliths. Fish. Res. 148: 56-63.
Martin, G.B. and Thorrold, S.R. 2005. Temperature and salinity effects on magnesium, manganese, and barium incorporation in otoliths of larval and early juvenile spot *Leiostomus xanthurus*. Mar. Ecol. Prog. Ser. 293: 223–232.
Martin, G.B. and Wuenschel, M.J. 2006. Effect of temperature and salinity on otolith element incorporation in juvenile gray snapper *Lutjanus griseus*. Mar. Ecol. Prog. Ser. 324: 229–239.
Melancon, S., Fryer, B.J. and Markham, J.L. 2009. Chemical analysis of endolymph and the growing otolith: Fractionation of metals in freshwater fish species. Environ. Toxicol. Chem. 28: 1279–1287.

Mirasole, A., Gillanders, B.M., Reis-Santos, P., Grassa, F., Capasso, G., Scopelliti, G., Mazzola, A. and Vizzini, S. 2017. The influence of high pCO2 on otolith shape, chemical and carbon isotope composition of six coastal fish species in a Mediterranean shallow CO_2 vent. Mar. Biol. 164:191.

Moksness, E. 1992. Validation of daily increments in the otolith microstructure of Norwegian spring-spawning herring (*Clupea harengus*). ICES J. Mar. Sci. 49: 231–235.

Moore, B.R., Bell, J., Evans, K., Marie, A.D., Nicol, S., Scutt Phillips, J., Smith, N., Tremblay-Boyer, L. and Williams, A.J. 2018. Current knowledge, key uncertainties and future research directions for defining the stock structure of skipjack, yellowfin, bigeye and South Pacific albacore tunas in the Pacific Ocean. Final Report for SAN 6004150 (CI-3). The Pacific Community, Nouméa, New Caledonia.

Mosegaard, H., Svedäng, H. and Taberman, K. 1988. Uncoupling of somatic and otolith growth rates in Arctic char (*Salvelinus alpinus*) as an effect of differences in temperature response. Can. J. Fish. Aquat. Sci. 45: 1514–1524.

Nakagawa, S. and Schielzeth, H. 2013. A general and simple method for obtaining R^2 from generalized linear mixed-effects models. Methods Ecol. Evol. 4: 133–142.

Nanninga, G.B. and Berumen, M.L. 2014. The role of individual variation in marine larval dispersal. Front. Mar. Sci. 1: 7.

Neubauer, P., Shima, J.S. and Swearer, S.E. 2013. Inferring dispersal and migrations from incomplete geochemical baselines: Analysis of population structure using Bayesian infinite mixture models. Methods Ecol. Evol. 4: 836–845.

Óskarsson, G.J. and Taggart, C.T. 2009. Spawning time variation in Icelandic summer-spawning herring (*Clupea harengus*). Can. J. Fish. Aquat. Sci. 66: 1666–1681.

Panfili, J., Darnaude, A.M., Vigliola, L., Jacquart, A., Labonne, M. and Gilles, S. 2015. Experimental evidence of complex relationships between the ambient salinity and the strontium signature of fish otoliths. J. Exp. Mar. Biol. Ecol. 467: 65–70.

Payan, P., De Pontual, H., Edeyer, A., Borelli, G., Boeuf, G. and Mayer-Gostan, N. 2004. Effects of stress on plasma homeostasis, endolymph chemistry, and check formation during otolith growth in rainbow trout (*Oncorhynchus mykiss*). Can. J. Fish. Aquat. Sci. 61: 1247–1255.

Plummer, M., Best, N., Cowles, K. and Vines, K. 2006. CODA: convergence diagnosis and output analysis for MCMC. R News 6: 7–11.

Pörtner, H. and Peck, M. 2010. Climate change effects on fishes and fisheries: towards a cause-and-effect understanding. J. Fish Biol. 77: 1745–1779.

Radtke, R. 1984. Formation and structural composition of larval striped mullet otoliths. Trans. Am. Fish. Soc. 113: 186–191.

Radtke, R.L., Townsend, D.W., Folsom, S.D. and Morrison, M.A. 1990. Strontium:calcium concentration ratios in otoliths of herring larvae as indicators of environmental histories. Environ. Biol. Fish. 27: 51–61.

Ranaldi, M.M. and Gagnon, M.M. 2008. Zinc incorporation in the otoliths of juvenile pink snapper (*Pagrus auratus* Forster): the influence of dietary versus waterborne sources. J. Exp. Mar. Biol. Ecol. 360: 56–62.

Reis-Santos, P., Gillanders, B.M., Tanner, S.E., Vasconcelos, R.P., Elsdon, T.S. and Cabral, H.N. 2012. Temporal variability in estuarine fish otolith elemental fingerprints: implications for connectivity assessments. Estuar. Coast. Shelf Sci. 112: 216–224.

Rosenfeld, J., Van Leeuwen, T., Richards, J. and Allen, D. 2015. Relationship between growth and standard metabolic rate: measurement artefacts and implications for habitat use and life-history adaptation in salmonids. J. Anim. Ecol. 84: 4–20.

Rubin, D. 1976. Inference and missing data. Biometrika 63: 581–592.
Ruttenberg, B.I., Hamilton, S.L., Hickford, M.J.H., Paradis, G.L., Sheehy, M.S., Standish, J.D., Ben-Tzvi, O. and Warner, R.R. 2005. Elevated levels of trace elements in cores of otoliths and their potential for use as natural tags. Mar. Ecol. Prog. Ser. 297: 273–281.
Sadovy, Y. and Severin, K. 1994. Elemental patterns in red hind (*Epinephelus guftatus*) otoliths from Bermuda and Puerto Rico reflect growth rate, not temperature. Can. J. Fish. Aquat. Sci. 51: 133–141.
Schwarcz, H., Gao, Y., Campana, S., Browne, D., Knyf, M. and Brand, U. 1998. Stable carbon isotope variations in otoliths of Atlantic cod (*Gadus morhua*). Can. J. Fish. Aquat. Sci. 55: 1798–1806.
Shiao, J., Shirai, K., Tanaka, K., Takahata, N., Sano, Y., Hsiao, S., Lee, D. and Tseng, Y. 2018. Assimilation of nitrogen and carbon isotopes from fish diets to otoliths as measured by nanoscale secondary ion mass spectrometry. Rapid Commun. Mass Spectrom. 32: 1250–1256.
Shima, J.S. and Swearer, S.E. 2010. The legacy of dispersal: larval experience shapes persistence later in the life of a reef fish. J. Anim. Ecol. 79: 1308–1314.
Shima, J.S. and Swearer, S.E. 2016. Evidence and population consequences of shared larval dispersal histories in a marine fish. Ecology 97: 25–31.
Sih, A., Bell, A. and Johnson, J.C. 2004. Behavioral syndromes: An ecological and evolutionary overview. Trends Ecol. Evol. 19: 372–378.
Solomon, C.T., Weber, P.K., Cech Jr., J.J., Ingram, B.L., Conrad, M.E., Machavaram, M. V., Pogodina, A.R. and Franklin, R.L. 2006. Experimental determination of the sources of otolith carbon and associated isotopic fractionation. Can. J. Fish. Aquat. Sci. 63: 79–89.
Stamps, J.A. 2016. Individual differences in behavioural plasticities. Biol. Rev. 91: 534–567.
Stanley, R., Bradbury, I., DiBacco, C., Snelgrove, P., Thorrold, S. and Killen, S. 2016. Environmentally mediated trends in otolith composition of juvenile Atlantic cod (*Gadus morhua*). ICES J. Mar. Sci. 73: 250–262.
Stoffel, M.A., Nakagawa, S. and Schielzeth, H. 2017. rptR: repeatability estimation and variance decomposition by generalized linear mixed-effects models. Methods Ecol. Evol. 8: 1639–1644.
Sturrock, A.M., Hunter, E., Milton, J.A., Johnson, R.C., Waring, C.P., Trueman, C.N. and EIMF. 2015. Quantifying physiological influences on otolith microchemistry. Methods Ecol. Evol. 6: 806–816.
Sturrock, A., Trueman, C., Darnaude, A. and Hunter, E. 2012. Can otolith elemental chemistry retrospectively track migrations in fully marine fishes? J. Fish Biol. 81: 766–95.
Sturrock, A., Trueman, C., Milton, J., Waring, C., Cooper, M. and Hunter, E. 2014. Physiological influences can outweigh environmental signals in otolith microchemistry research. Mar. Ecol. Prog. Ser. 500: 245–264.
Swearer, S.E., Forrester, G.E., Steele, M.A., Brooks, A.J. and Lea, D.W. 2003. Spatio-temporal and interspecific variation in otolith trace-elemental fingerprints in a temperate estuarine fish assemblage. Estuar. Coast. Shelf Sci. 56: 1111–1123.
Thomas, O., Ganio, K., Roberts, B. and Swearer, S. 2017. Trace element–protein interactions in endolymph from the inner ear of fish: implications for environmental reconstructions using fish otolith chemistry. Metallomics 9: 239–249.
Thorrold, S.R., Jones, C.M., Swart, P.K. and Targett, T.E. 1998. Accurate classification of

juvenile weakfish *Cynoscion regalis* to estuarine nursery areas based on chemical signatures in otoliths. Mar. Ecol. Prog. Ser. 173: 253–265.
Thorrold, S.R. and Swearer, S.E. 2009. Otolith Chemistry. *In* Tropical fish otoliths: information for assessment, management and ecology. *Edited by* B.S. Green, B.D. Mapstone, G. Carlos and G.A. Begg. Springer, Netherlands. pp. 249–295.
Townsend, D., Radtke, R., Corwin, S. and Libby, D.A. 1992. Strontium:calcium ratios in juvenile Atlantic herring *Clupea harengus* L. otoliths as a function of water temperature. J. Exp. Mar. Biol. Ecol. 160: 131–140.
Townsend, D., Radtke, R., Morrison, M. and Folsom, S. 1989. Recruitment implications of larval herring overwintering distributions in the Gulf of Maine, inferred using a new otolith technique. Mar. Ecol. Prog. Ser. 55: 1–13.
Turner, S.M. and Limburg, K.E. 2015. Does daily growth affect the rate of manganese uptake in juvenile river herring otoliths? Trans. Am. Fish. Soc. 144: 873–881.
Valdimarsson, H., Astthorsson, O.S. and Palsson, J. 2012. Hydrographic variability in Icelandic waters during recent decades and related changes in distribution of some fish species. ICES J. Mar. Sci. 69:816–825.
Van Leeuwen, T.E., Rosenfeld, J.S. and Richards, J.G. 2012. Effects of food ration on SMR: Influence of food consumption on individual variation in metabolic rate in juvenile coho salmon (*Onchorhynchus kisutch*). J. Anim. Ecol. 81: 395–402.
Walther, B.D., Kingsford, M.J., Callaghan, M.D.O. and McCulloch, M.T. 2010. Interactive effects of ontogeny, food ration and temperature on elemental incorporation in otoliths of a coral reef fish. Environ. Biol. Fish. 89: 441–451.
Walther, B.D. and Thorrold, S.R. 2006. Water, not food, contributes the majority of strontium and barium deposited in the otoliths of a marine fish. Mar. Ecol. Prog. Ser. 311: 125–130.
Watanabe, T., Kiron, V. and Satoh, S. 1997. Trace minerals in fish nutrition. Aquaculture 151: 185–207.
Williams, A.J., Farley, J.H., Hoyle, S.D., Davies, C.R. and Nicol, S.J. 2012. Spatial and sex-specific variation in growth of albacore tuna (*Thunnus alalunga*) across the South Pacific Ocean. PLoS One 7: 1–10.
Zuur, A.F., Ieno, E.N., Walker, N.J., Saveliev, A.A. and Smith, G.M. 2009. Mixed effects models and extensions in ecology with R. Springer, New York, New York, USA.

Table 1. Sampling details for juvenile ISS herring captured during October/November 2013, 2014 and 2015, and associated environmental variables. Shown are the nurseries, and capture sites within them (Site code), numbers of fish collected (n), mean standard length (SL) and range (in brackets) of the sample, numbers of otoliths analysed for Li, Mg, Ca, Mn, Zn, Sr, Ba using LA-ICP-MS at the otolith edge (El_{edge}), numbers analysed for $\delta^{13}C$ and $\delta^{18}O$ using IRMS on whole age 1 otoliths (C/O_{whole}), and at the edge of age 2 otoliths (C/O_{edge}). Mean empirical ($_{emp}$) or modelled ($_{mod}$) temperature (Temp) and salinity (Sal) through the water column on the day of capture is shown for each site, with the range (in brackets). Sites used in 'training', 'test' and 'extras' datasets for subsequent modelling are highlighted in bold, italics and plain text, respectively.

Year	Nursery	Site code	Age 1				Age 2				Temp (°C)	Sal (‰)
			n	SL (mm)	El_{edge}	C/O_{whole}	*n*	SL (mm)	El_{edge}	C/O_{edge}		
2013	Öxarfjörður	531	4	76 (69-86)	4	2					5.22 (4.76-5.69)	34.15 (33.79-34.51) $_{emp}$
	Ísafjarðardjúp	**529**	9	82.7 (77-92)	9	7	14	131.9 (129-139)	14	7	6.52 (6.40-6.65)	34.81 (34.77-34.85) $_{emp}$
		D5-2013-102					9	136.1 (126-149)	9	7	3.47 (3.36-3.50)	30.05 (27.60-30.63) $_{mod}$
		D5-2013-110					11	132.7 (125-147)	11	3	3.50 (3.46-3.53)	31.25 (30.54-31.96) $_{mod}$
		D5-2013-115					10	137.4 (130-145)	10	7	3.31 (3.31-3.31)	26.62 (26.62-26.62) $_{mod}$
	Eyjafjörður	530	11	95.6 (87-100)	11	6					5.30 (4.38-6.23)	33.95 (33.01-34.88) $_{emp}$
	Breiðafjörður	D1-2014-2					18	107.2 (97-115)	18	16	0.97 (0.96-0.97)	33.16 (33.16-33.17) $_{mod}$
2014	Arnarfjörður	D9-2014-7	14	96.1 (76-118)	14						5.06 (4.52-5.59)	33.09 (31.68-34.50) $_{emp}$
		D7-2014	20	67.3 (61-73)	20						7.05 (3.90-10.20)	33.09 (31.68-34.50) $_{emp}$
		D7-2014B	8	73.3 (59-97)	8		18	131.1 (113-146)	18	5	8.80 (8.40-9.20)	28.52 (28.52-28.52) $_{emp}$
		D7-2014C	16	62.2 (57-71)	16						7.05 (4.20-9.90)	28.98 (28.17-29.80) $_{emp}$
	Ísafjarðardjúp	**D9-2014-6**	9	101.0 (81-116)	9		10	139.2 (131-146)	10	7	6.88 (6.86-6.89)	32.26 (31.22-32.79) $_{emp}$
		D7-2014-92	18	76.1 (63-84)	18						7.10 (7.07-7.17)	27.76 (25.11-28.72) $_{mod}$
	Vestmannaeyjar	*B7-2014-468*					10	117.7 (104-126)	10		7.66 (7.33-7.84)	35.11 (35.05-35.15) $_{mod}$
	Jökuldjúp north	*B7-2014-470*					9	123.8 (109-133)	9	2	7.77 (7.75-7.78)	35.21 (35.20-35.21) $_{mod}$
	Jökuldjúp south	*B7-2014-471*					10	119.9 (114-127)	10	2	7.88 (7.86-7.90)	35.20 (35.20-35.20) $_{mod}$
	Eyjafjörður	*D9-2014-4*	18	97.7 (77-118)	18						6.53 (6.09-6.97)	33.11 (31.26-34.96) $_{emp}$
	Miðfjörður	**D7-2014-154**	21	89.8 (72-100)	21		20	141.4 (133-150)	20	14	8.35 (8.20-8.50)	27.36 (24.28-29.44) $_{emp}$
	Öxarfjörður	**D7-2014-140**	22	86.5 (77-99)	22		16	132.4 (120-145)	16	11	8.60 (8.40-8.80)	33.40 (32.14-33.69) $_{emp}$
	Breiðamerkurdjúp	*B7-2014-466*					20	126.2 (115-137)	20	13	8.16 (7.79-8.35)	35.12 (35.04-35.16) $_{mod}$
	Skagafjörður	*D7-2014-113*					20	135.0 (121-147)	20	4	8.45 (8.10-8.80)	34.00 (32.81-34.23) $_{emp}$
2015	Arnarfjörður	*D4-2015-14*					15	121.9 (104-138)	15	15	7.41 (7.41-7.41)	27.12 (27.12-27.12) $_{mod}$
	Hrútafjörður	**D5-2015-18**	18	75.3 (69-81)	17	12	15	154.1 (140-173)	15	15	6.28 (6.08-6.36)	23.54 (20.98-24.52) $_{mod}$
	Ísafjarðardjúp	D4-2015-60					15	121.0 (114-125)	15	15	6.80 (6.80-6.80)	30.85 (30.85-30.85) $_{mod}$
		D4-2015-50					15	132.1 (120-143)	15	15	6.70 (6.64-6.75)	30.60 (27.06-31.51) $_{mod}$
	Miðfjörður	*D5-2015-19*	19	78.5 (63-93)	19	15					6.73 (6.62-6.79)	29.04 (25.56-31.60) $_{mod}$
Tot.			207		206	42	255		255	158		

Table 2. Random effect structures considered in univariate and multivariate linear mixed effects models of otolith elemental and stable isotopic composition in juvenile ISS herring (using 'lme4' syntax). See eq. 1 for further details on the estimated parameters. Terms presented here relate to the univariate models, with the additional parameters estimated in the multivariate models described in the main text.

Random structure	Description	Estimated parameters
1. 1 | site	Random intercept for capture site.	$\sigma^2_{site_0}$, σ^2_{ε}
2. Age | site	Random intercept and Age slope for capture site. Relationship between the response and fish age can vary by site. Correlation allowed between random intercept and slope for Age.	$\sigma^2_{site_0}$, $\sigma^2_{site_1}$, $cov_{site_0,site_1}$, σ^2_{ε}
3. SL_anom | site	Random intercept and SL_anom slope for capture site. Relationship between the response and fish growth can vary by site. Correlation allowed between random intercept and slope for SL_anom.	$\sigma^2_{site_0}$, $\sigma^2_{site_2}$, $cov_{site_0,site_2}$, σ^2_{ε}
4. Age | site + SL_anom | site	Random intercept, Age and SL_anom slopes for capture site. Relationships between the response and fish age and growth can change by site. Fully correlated random effects specified between the two random slopes for Age and SL_anom and between the random slopes and the random intercept.	$\sigma^2_{site_0}$, $\sigma^2_{site_1}$, $\sigma^2_{site_2}$ $cov_{site_0,site_1}$, $cov_{site_0,site_2}$, $cov_{site_1,site_2}$, σ^2_{ε}
5. Age | site + SL_anom | site + Age × SL_anom | site	Random intercept, Age, SL_anom (and their interaction) slopes for capture site. Relationships between the response and fish age and growth and their interaction allowed to vary by site. Fully correlated random effects specified.	Ω_{site}
6. None	No site-level random effects. Tested in the univariate and bivariate models for $\delta^{13}C$ and $\delta^{18}O$.	σ^2_{ε}

Table 3. Structure and performance of final univariate and multi/bivariate 'explan' and 'oos.pred' models for each elemental and stable isotopic marker (see Appendix S4: Table S1 for all details on all candidate models). Mean estimates of DIC and $MSPE_{oos}$ were computed from three replicate MCMCglmm models. SDs were always < 0.08, so are not presented. AICc values were derived from equivalent models fitted using REML or ML estimation. Marginal, conditional and semi-partial R^2 (R^2_m, R^2_c, $R^2_{\beta_f}$, respectively) are shown. Mean adjusted repeatability (±95 CIs) (Adj. rep) is computed at the site level. r_{sim} is the correlation between observed (training data) and predicted values from each 'explan' model. Posterior predictive p-values (ppp-value) are shown for two test quantities: the observed mean (m) and SD of each marker. r_{oos} is the correlation between observed (test data) and predicted values from each 'oos.pred' model.

Model	Structure		DIC	AICc	$MSPE_{oos}$	R^2_m	R^2_c	$R^2_{\beta_f}$	Adj. rep (95% CI)	r_{sim}	ppp-value (m, SD)	r_{oos}
	Fixed	Random										
Univariate models												
$Li:Ca_{explan}$	A + SL + A×SL	A | site	165.07	194.67	0.60	0.05	0.64	A=0.02, SL=0.03, A×SL=0.01	0.62 (0.30, 0.81)	0.79	0.50, 0.61	
$Li:Ca_{oos.pred}$	A + T + S + A×S	A | site	178.20	210.84	0.47							0.54
$Mg:Ca_{explan}$	A + S + A×S	A | site	143.45	152.77	0.24	0.29	0.39	A=0.21, S=0.12, A×S=0.09	0.14 (0.01, 0.36)	0.63	0.50, 0.59	
$Mg:Ca_{oos.pred}$	A + SL + T	A | site	145.09	161.15	0.22							0.29
$Mn:Ca_{explan}$	A	A | site	271.31	284.85	0.54	0.20	0.59	A=0.20	0.48 (0.12, 0.72)	0.79	0.50, 0.59	
$Mn:Ca_{oos.pred}$	A + T	A | site	271.39	286.78	0.52							0.16
$Zn:Ca_{explan}$	A + S	1 | site	496.47	499.75	1.56	0.05	0.09	A=0.02, S=0.03	0.05 (0, 0.18)	0.28	0.50, 0.56	
$Zn:Ca_{oos.pred}$	A + T	1 | site	496.97	501.00	1.38							0.27
$Sr:Ca_{explan}$	A + SL + T + S + A×T + A×S	1 | site	-187.20	-173.77	0.04	0.29	0.48	A=0.18, SL=0.10 , T=0.05, S=0.05, A×T=0.03, A×S=0.02	0.27 (0, 0.57)	0.64	0.50, 0.63	
$Sr:Ca_{oos.pred}$	A + SL + S + A×SL	1 | site	-179.07	-167.37	0.04							0.50
$Ba:Ca_{explan}$	A + SL	SL | site	200.56	208.34	0.28	0.05	0.18	A=0.05, SL=0.01	0.14 (0, 0.33)	0.44	0.50, 0.60	
$Ba:Ca_{oos.pred}$	SL	SL | site	207.97	216.40	0.27							0.00
$\delta^{13}C_{explan}$	T + S	None	91.54	92.23	1.06	0.32	0.32	T=0.31, S=0.15	-	0.56	0.32, 0.56	
$\delta^{13}C_{oos.pred}$	S	None	111.77	112.20	0.32							0.17
$\delta^{18}O_{explan}$	T + S	1 | site	30.87	39.57	0.39	0.41	0.60	T=0.41, S=0.24	0.324 (0, 0.66)	0.76	0.59, 0.56	
$\delta^{18}O_{oos.pred}$	T	1 | site	30.58	42.40	0.20							0.69
Multi/bivariate models												
$multi_{explan}$	A + SL + S	A | site + SL | site	2494.03		1.13							
										Li:Ca: 0.79	0.51, 0.67	
										Mg:Ca: 0.64	0.33, 0.61	
										Mn:Ca: 0.78	0.41, 0.60	
										Zn:Ca: 0.35	0.34, 0.71	
										Sr:Ca: 0.66	0.43, 0.68	
										Ba:Ca: 0.46	0.32, 0.70	
$multi_{oos.pred}$	A + SL + T	A | site + SL | site	2494.80		1.07							
												Li:Ca: 0.22
												Mg:Ca: 0.28
												Mn:Ca: 0.13
												Zn:Ca: 0.23
												Sr:Ca: 0.13
												Ba:Ca: 0.00
$bivar_{explan}$	T + S	1 | site	266.71		2.10							
										$\delta^{13}C$: 0.57	0.45, 0.61	
										$\delta^{18}O$: 0.75	0.55, 0.55	
$bivar_{oos.pred}$	T	1 | site	268.47		0.80							
												δ^1 C: 0.25
												$\delta^{18}O$: 0.69

Notes: Covariate codes are: A = Age; SL = SL_anom; T = Temp; S = Sal. × denotes interaction terms. See Table 2 for descriptions of random effect structures.

Figures

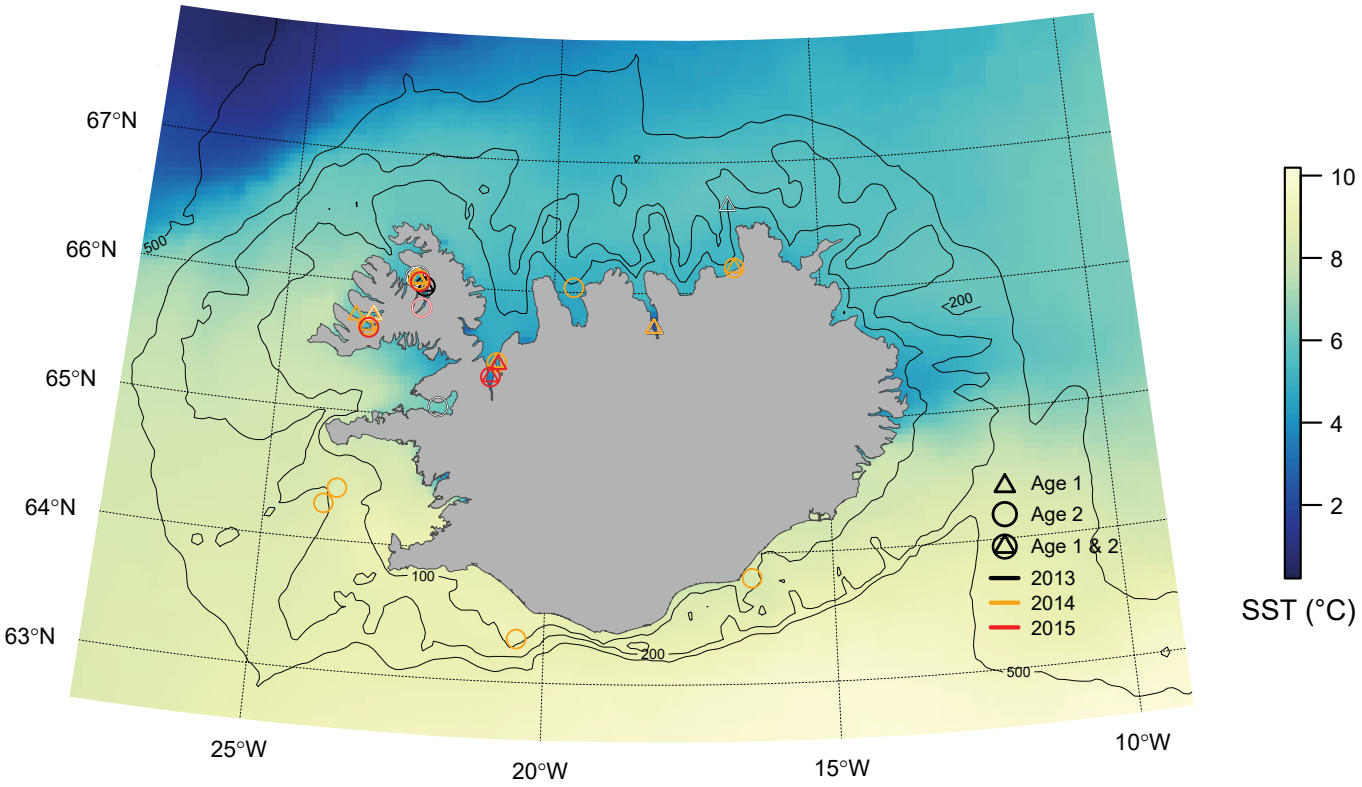

Figure 1. Capture sites for juvenile ISS herring (age 1: triangles; age 2: circles) collected during 2013 (black symbols), 2014 (orange symbols) and 2015 (red symbols). Sites at which age 1 and age 2 herring were captured simultaneously (n = 6) comprise the 'training' data. Sites without an inner white symbol are 'test' sites (n = 12), and those with an inner white symbol are 'extras' sites (n = 8). Sites that overlap exactly in space in different years are offset for clarity. The colour ramp represents modelled mean daily sea surface temperature (SST °C) for October across 2013, 2014 and 2015. Depth contours (in m) (black lines) are overlaid.

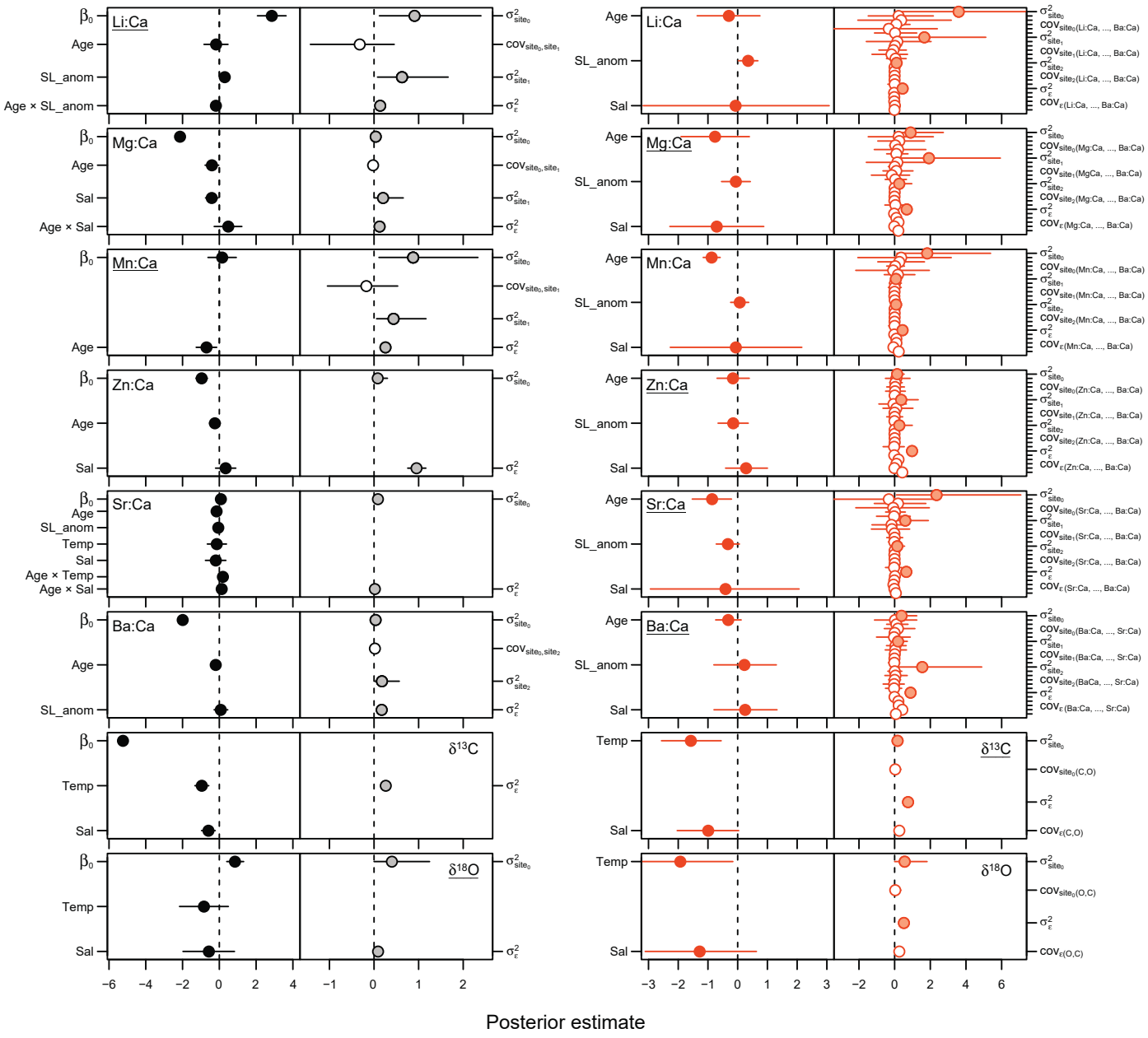

Figure 2. Results from the final univariate (black) and multivariate (red) explanatory 'explan' models for each elemental and stable isotopic marker. Posterior mean estimates (± 95% HPD credible intervals) for fixed (solid symbols) and random effect components (variances – shaded symbols; covariances – open symbols) are presented for each model. See eq. 1, Table 2 and the main text for descriptions of the fixed and random effect parameters estimated. For each marker, underlined models performed better in terms of within-sample predictive capacity (i.e. higher r_{sim}) based on posterior predictive simulations (see Appendix S2: Figure S2).

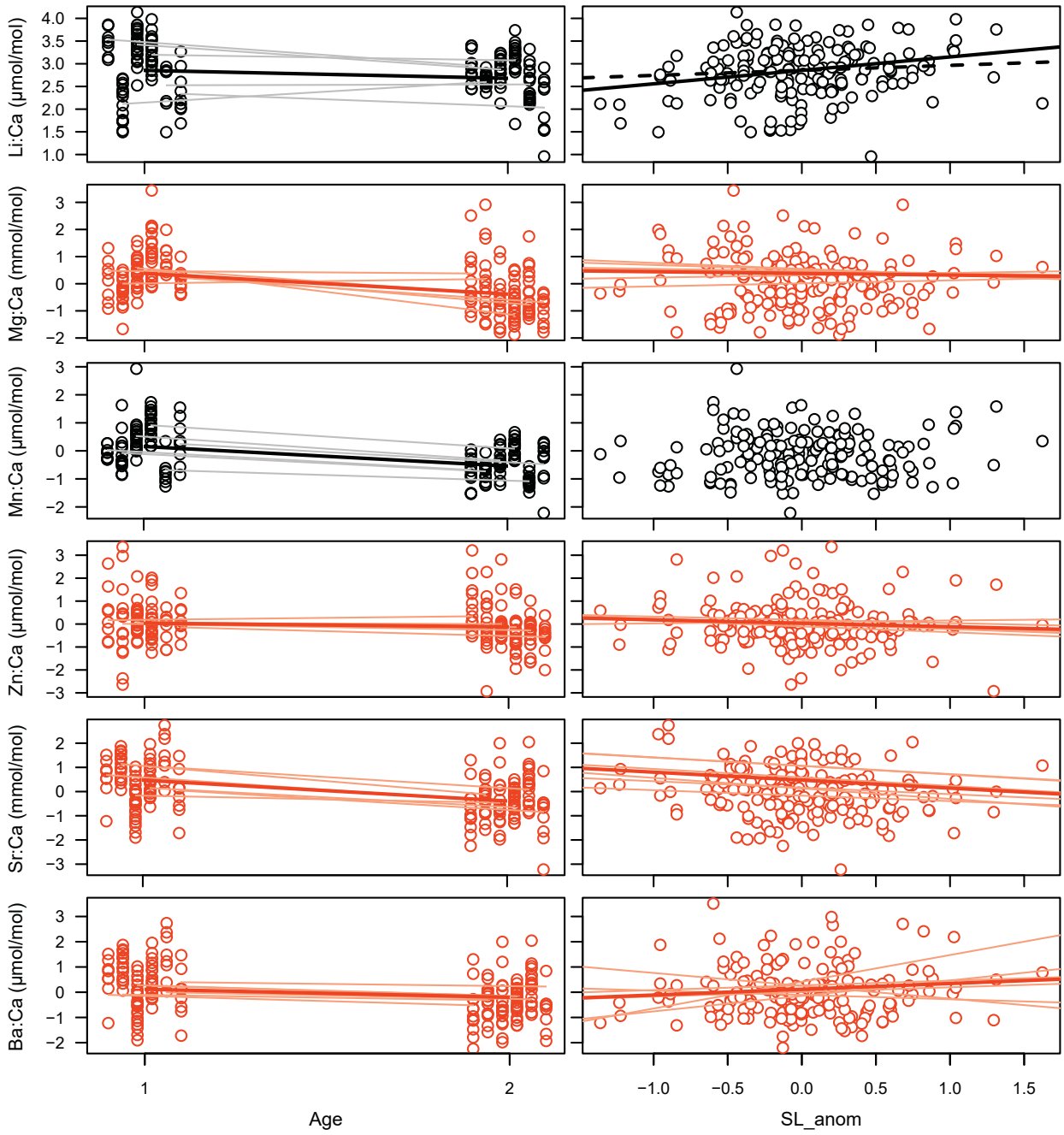

Figure 3. Relationships between each elemental marker and herring age (Age) and growth (SL_anom). Results are derived from the final univariate (black) or multivariate (red) explanatory 'explan' model for each marker (see underlined models in Figure 2). Each open symbol denotes the observation for an individual fish. Grey and pink lines show the site-level relationships estimated from the univariate and multivariate models, respectively, with black and red lines representing the population-level trend across all sites. In the element:Ca–Age plots, observations are disaggregated into vertical columns by capture site (n = 6) to illustrate the degree of individual variation within cohorts and sites. Site codes from left to right are 529, D5-2015-18, D7-2014-140, D7-2014-154, D7-2014B, D9-2014-6 (Table 1). Data are presented on the natural log scale, and have mean = 0 and SD = 1 in the multivariate cases. SL_anom was not included in the final model for Mn:Ca. The data alone are plotted here.

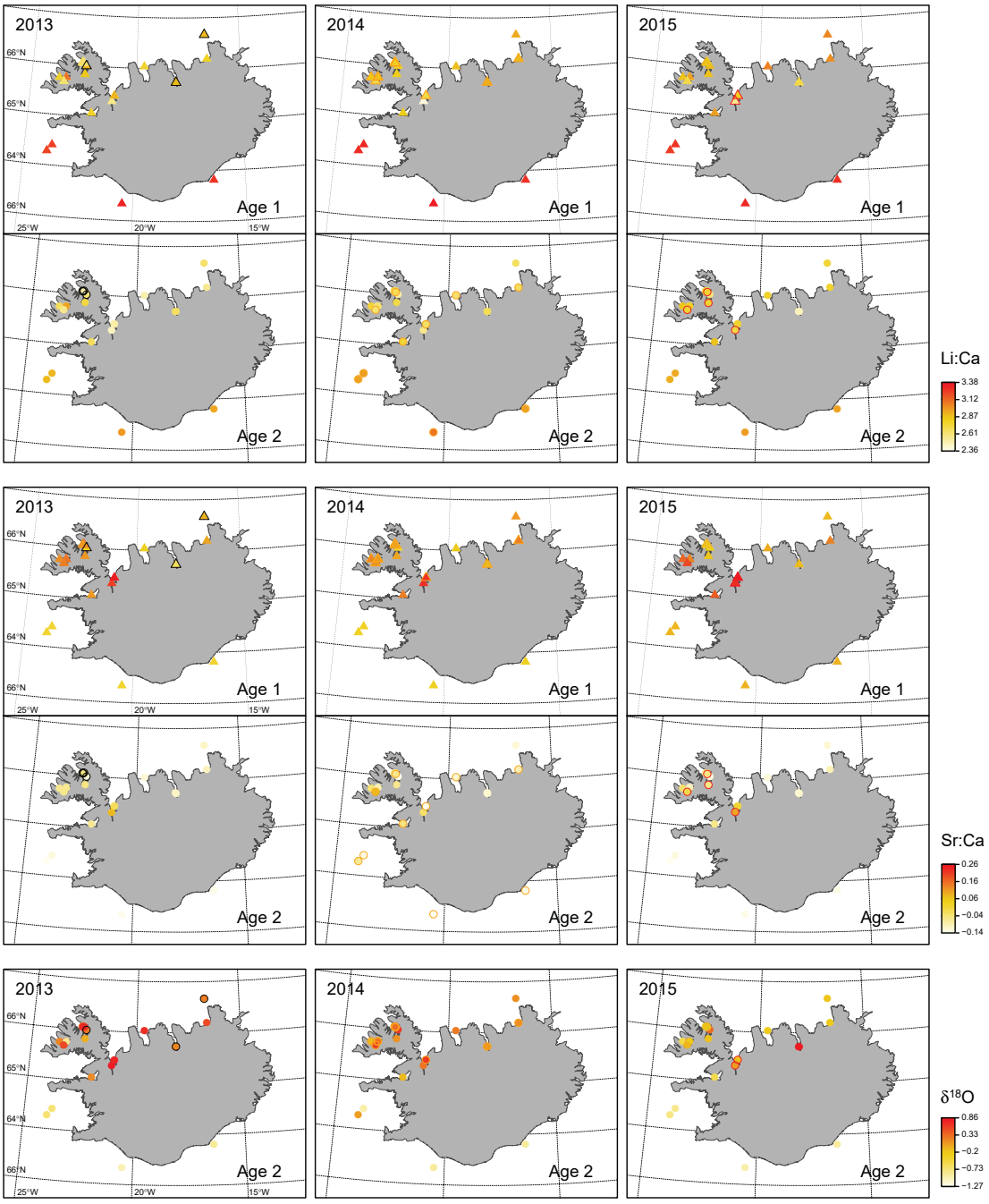

Figure 4. Spatial predictions for otolith Li:Ca, Sr:Ca and $\delta^{18}O$ at all capture sites in each of the three sampling years (2013, 2014, 2015) and for the two age-classes (age 1: triangles, age 2: circles). Results are derived from the final 'oos.pred' models (see Table 3). Colour ramps represent the mean predicted values for each site for the marker of interest. Sites at which fish were captured in a particular year are outlined in black (for 2013), orange (for 2014) and red (for 2015). Predictions for Li:Ca and Sr:Ca are presented on the natural log scale in units of µmol/mol and mmol/mol, respectively, with predictions for $\delta^{18}O$ (in ‰) generated using a bivariate model in which each response variable (i.e. $\delta^{13}C$, $\delta^{18}O$) was scaled to mean = 0 and SD = 1. See Appendix S2: Figure S3 for maps of all other markers.

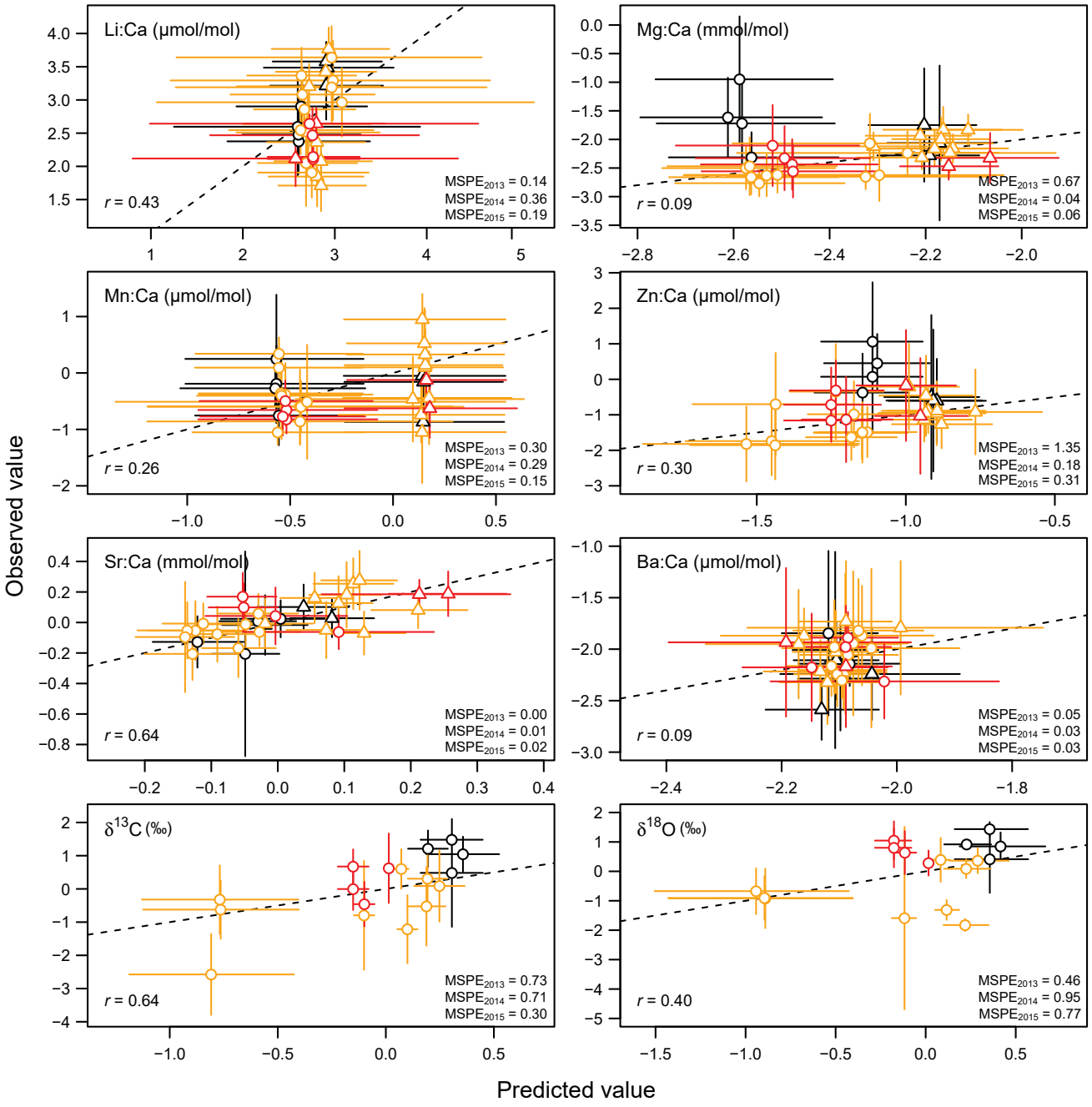

Figure 5. Plots of observed versus predicted values for each otolith marker at all capture sites sampled in 2013 (black), 2014 (orange) and 2015 (red) for age 1 (triangles) and age 2 herring (circles). Symbols are the site-level mean values, vertical lines are ± SD of the observations, and horizontal lines are ± 70% HPD credible intervals on the predictions. In each plot, the correlation (Pearson's r) between site-level mean observed and predicted values is shown, in addition to the MSPE by year. The 1:1 line (dashed black line) is overlaid. See Appendix S2: Table S2 for overall MSPE estimates across years, by age-class, and by age-class within year. Data for each elemental marker are presented on the natural log scale, with $\delta^{13}C$ and $\delta^{18}O$ values scaled to have mean = 0 and SD = 1.

Appendix S1. Details on otolith preparation and analysis

Otolith removal and preparation

Sagittal otolith pairs were removed under a dissecting microscope, cleaned of adhering tissue, rinsed with ultrapure water (Milli-Q®; www.merckmillipore.com) and stored dry in 0.5 ml polypropylene microtubes. One sagitta from each fish was selected for elemental analysis. We mounted these individually, sulcus downwards, on an acid-washed glass slide in thermoplastic glue (Crystalbond™) and polished them to within 10–15 μm of the primordium using a series of wetted lapping films (9, 5, 3 μm). We then reheated the slide and transferred the polished otolith to a master slide, on which otoliths from all capture sites were set in Crystalbond™ and arranged randomly. Master slides were rinsed in ultrapure water and air-dried overnight in a class 100 laminar flow cabinet at room temperature.

Elemental analyses

Laser ablation-inductively coupled plasma-mass spectrometry (LA-ICP-MS) was used to measure elemental concentrations at the otolith edge. Measurements were made using a Varian 810 quadrupole ICP-MS, coupled to a HelEx (Laurin Technic, and The Australian National University) laser ablation system located at The University of Melbourne, Australia. The HelEx system is built around a Compex 110 (Lambda Physik, Gottingen, Germany) excimer laser. Master slides were placed in the sample cell and the primordium of each otolith was located visually with a 400× objective and a video imaging system. The target ablation site on each sample was then digitally plotted using GeoStar v6.14 software (Norris software). We used a depth-profiling approach to ablate a 40-μm spot at the dorsal margin of each otolith, equidistant between the pararostrum and antirostrum. Ablation occurred inside a sealed chamber in an atmosphere of pure He (flow rate: 0.3 L/min) with the vaporised material transported to the ICP-MS in the Ar carrier gas (flow rate: 1.23 L/min) via a signal-smoothing manifold. Prior to data acquisition, a pre-ablation step was implemented in which three laser pulses were fired (at 78 mJ output energy) at the target sites to remove any surface contaminants. Using the same energy settings, the laser was then pulsed at 5 Hz for 40 s per sample. For each otolith sample, the first 3 s of data in the acquisition sequence were excluded, and the next 15 s retained, encompassing a disc of otolith material ~40-μm wide × 11-μm deep. The latter measure was estimated from the drilling rate (i.e., ~0.15 μm per laser pulse) in conjunction with microscopic examination of ablation site geometry post-analysis. Based on measurements of daily growth increment widths taken immediately adjacent to the ablation site on age 1 (n = 10) and age 2 (n = 10) otoliths, we estimate that the ablated discs reflect otolith material deposited during the final < 2 weeks of each fish's life.

Otoliths were analysed for seven elements: ^{7}Li, ^{25}Mg, ^{43}Ca, ^{55}Mn, ^{66}Zn, ^{88}Sr and ^{138}Ba, with ^{43}Ca used as an internal standard. Dwell times were 0.03 s for all elements except Li (0.05 s). Data were processed offline using Iolite version 3.31 (www.iolite-software.com) (Paton et al. 2011). Subtraction of background ion counts from otolith counts was followed by the normalisation of each element to Ca using a glass reference standard (National Institute of Standards and Technology: NIST 612) which was analysed after every 10th otolith sample. Measurement precision (% relative standard deviation [RSD]) was calculated based on 20, 20 s analyses each of NIST 610 and MACS-3 (United States Geological Survey) reference standards run concurrently with the otolith samples. Mean RSDs for the NIST 610/MACS-3, respectively, for normalised data, were Li: 0.60/6.23, Mg: 1.21/6·60, Mn: 0.59/3.95, Zn: 1.10/7.92, Sr: 0.34/6.27, Ba 0.34/3.99. Detection limits (DL) were calculated as the mean + 3

SD of the background samples. Li, Mg, Mn, Sr and Ba were measured well above DL in the otoliths, but Zn was within 5% of DL in 4.6% of cases. Given the relatively low RSD for Zn, and its potential sensitivity to dietary factors (Ranaldi and Gagnon 2008), we elected to include it in our statistical analysis. Elemental data are expressed throughout as molar ratios to Ca (e.g. Li:Ca).

Stable isotopic analysis

We used the second sagitta from each fish for analysis of stable carbon and oxygen isotope ratios (i.e. $\delta^{13}C$, $\delta^{18}O$). Due to their small diameter, whole age 1 otoliths were ground, individually, to a fine powder using a mortar and pestle, and between 0.05 and 0.1 mg of the resulting powder transferred to a 0.5 ml polypropylene microtube. Each powder sample represents a full lifetime (i.e. ~15-month) record of $\delta^{13}C$ and $\delta^{18}O$ for each age 1 individual. Age 2 otoliths were larger, making sub-sampling possible. Age 2 otoliths were polished, mounted, cleaned and dried in an identical manner to those prepared for elemental analyses. We used a high-resolution New Wave Research MicroMill system (New Wave Research Inc., Fremont, California, USA) to plot a 200-µm wide × ~25-µm deep drill path along the otolith edge, beginning at the rostrum, and extending along the ventral margin to the postrostrum. The drill speed was set to 5% and scan speed across the sample was 50 µm/s. Again, between 0.05 and 0.1 mg of powder was collected per individual, encompassing otolith material deposited during the last ~2 months of the fish's life pre-capture (authors' unpublished data). When insufficient material was recovered in the first drill pass, we continued drilling along the otolith's dorsal edge from the pararostrum to the antirostrum.

Otolith powders were analysed using an automated carbonate preparation device (NuCarb) coupled to a Nu Instruments Perspective dual-inlet stable isotope ratio mass spectrometer, located in the School of Geography, The University of Melbourne. Three external standards with known $\delta^{13}C$ and $\delta^{18}O$ values (National Bureau of Standards: NBS19, New1, New12) were run concurrently with the otolith samples. Estimated precision (RSD), based on repeated measurements of NBS19 (n = 5), New1 (n = 18) and New12 (n = 15) across all analysis days was: 3.50, 1.73 and 0.40, respectively for $\delta^{13}C$, and 11.17, 2.43 and 0.53, respectively for $\delta^{18}O$. All stable isotope measurements are reported relative to the Vienna Pee Dee Belemnite (VPDB) reference standard, and expressed in δ-notation (in ‰).

References

Paton, C., Hellstrom, J., Paul, B. and Hergt, J. 2011. Iolite: Freeware for the visualisation and processing of mass spectrometric. J. Anal. At. Spectrom. 26: 2508–2518.

Ranaldi, M.M. and Gagnon, M.M. 2008. Zinc incorporation in the otoliths of juvenile pink snapper (*Pagrus auratus* Forster): The influence of dietary versus waterborne sources. J. Exp. Mar. Biol. Ecol. 360: 56–62.

Appendix S2. Priors, sensitivity analysis and additional modelling results

Priors

In all models, we assigned vague normal priors N(0, 10^4) for the fixed effects and an inverse gamma (IG) prior with shape = scale = 0.001 for the residual variance (σ^2_ε). This latter prior is equivalent to an inverse Wishart (IW) with scale V = 1, and degree of belief parameter nu = 0.002, and is weakly informative when the posterior distribution does not have large support near 0.

We performed an analysis to test the sensitivity of our results to the choice of prior for the random effect variance components (see details on next page). Using the simplest random effect structure (i.e. random intercept for site - structure 1, Table 2 in main text), we tested 5 different prior distributions for the among-site variance ($\sigma^2_{site_0}$) or standard deviation (σ_{site_0}) parameters, refitting the models with each prior, for each elemental and stable isotopic marker separately.

Based on the results of this analysis, we specified IG priors with shape and scale = 0.001 for (co)variance components in the univariate Li:Ca, Mn:Ca and Zn:Ca models, and used 'parameter expanded' (PE) models (Liu et al. 1998, Gelman 2006) for Mg:Ca, Sr:Ca, Ba:Ca, $\delta^{13}C$ and $\delta^{18}O$ and all multi/bivariate models. In random intercept models, for example, the PE settings we used correspond to placing a proper half-Cauchy prior on σ_{site_0}, with location parameter = 0 and scale = $\sqrt{1000}$. These priors are considered weakly informative, performing well near 0, and when the number of capture sites is low (Gelman 2006).

Sensitivity to prior choice for variance components

Motivation and methods

We conducted a sensitivity analysis to explore how the choice of prior for the random effect variance components might influence our results. For each trace-element marker separately (i.e., Li:Ca, Mg:Ca, Mn:Ca, Zn:Ca, Sr:Ca, Ba:Ca), we fitted full univariate models containing all fixed effects specified as linear terms (and some first-order interactions) and the simplest random effect structure (i.e., random intercept for capture site), as in eq. S1.

$$y_{ij} = (\beta_0 + site_{0j}) + \beta_1 Age_{ij} + \beta_2 SL\_anom_{ij} + \beta_3 Temp_j + \beta_4 Sal_j + \beta_5 Age_{ij} SL\_anom_{ij} + \beta_6 Age_{ij} Temp_j + \beta_7 Age_{ij} Sal_j + \varepsilon_{ij}$$

$$site_{0j} \sim N(0, \sigma^2_{site_0})$$

$$\varepsilon_{ij} \sim N(0, \sigma^2_{\varepsilon}) \quad \text{(eq. S1)}$$

This model is a simplification of that specified in Eq. 1 in the main text, where y_{ij} represents the (natural log transformed) otolith edge element:Ca concentration measured in μmol/mol (for Li:Ca, Mn:Ca, Zn:Ca, Ba:Ca) or mmol/mol (for Mg:Ca, Sr:Ca) for fish *i* captured at sampling site *j*. Here, β_0 is the overall mean concentration across sites, $site_{0j}$ is the random site-level deviation from this mean, β_1 to β_7 are regression coefficients for the fixed effects of fish age (Age_{ij}), somatic growth within an age-class (SL_anom_{ij}), ambient temperature ($Temp_j$) and salinity (Sal_j), and some interactions, and ε_{ij} is the observation-level residual. Continuous inputs were centred and scaled to have mean = 0, SD = 0.5 prior to analysis (Gelman 2008), and both $site_{0j}$ and ε_{ij} are assumed to be normally distributed with mean 0 and variance $\sigma^2_{site_0}$ and σ^2_{ε}, respectively.

As the temporal resolution of the otolith material used for $\delta^{13}C$ and $\delta^{18}O$ measurements differed between age 1 and age 2 fish, we dropped Age_{ij} from Eq. S1 and fitted the following model for each (untransformed) stable isotopic marker (eq. S2):-

$$y_{ij} = (\beta_0 + site_{0j}) + \beta_1 SL\_anom_{ij} + \beta_2 Temp_j + \beta_3 Sal_j + \varepsilon_{ij}$$

$$site_{0j} \sim N(0, \sigma^2_{site_0})$$

$$\varepsilon_{ij} \sim N(0, \sigma^2_{\varepsilon}) \quad \text{(eq. S2)}$$

We tested five different prior distributions for the among-site variance ($\sigma^2_{site_0}$) or standard deviation (σ_{site_0}) parameters (see below), refitting the models using each prior specification in turn. In all models, we assigned vague normal priors – $N(0, 10^4)$ for the fixed effects and an inverse gamma (IG) prior with shape = scale = 0.001 for the residual variance (σ^2_{ε}).

The priors considered were as follows:-

Prior set A

- Fixed effects: $N(0, 10^4)$

❖ Variance components:-
- Among-site variance (i.e. 'G' list in MCMCglmm call): IW(V=1, nu=0.002) = IG(0.001, 0.001). Default setting in 'MCMCglmm' package and considered weakly to strongly informative in our examples.
- Residual variance (i.e. 'R' list in MCMCglmm call): IW(V=1, nu=0.002) = IG(0.001, 0.001)

Prior set B

❖ Fixed effects: N(0, 10^4)
❖ Variance components:-
- Among-site variance: IW(V=1, nu=0.02) = IG(0.01, 0.01). An order of magnitude increase in nu results in slightly more mass away from zero than Prior set A.
- Residual variance: IW(V=1, nu=0.002) = IG(0.001, 0.001)

Prior set C

❖ Fixed effects: N(0, 10^4)
❖ Variance components:-
- Among-site variance: IW(V=1, nu=0.2) = IG(0.1, 0.1). Another order of magnitude increase in nu. This prior places more mass away from zero than Prior set B.
- Residual variance: IW(V=1, nu=0.002) = IG(0.001, 0.001)

Prior set D

❖ Fixed effects: N(0, 10^4)
❖ Variance components:-
- Among-site variance: Here we used 'parameter expanded' models (Liu et al. 1998, Gelman 2006) to induce folded non-central *t* priors on the among-site standard deviation parameters (σ_{site_0}). For random-intercept models fitted with the 'MCMCglmm' package, this can be coded by setting the V=1, nu=1, mean (alpha.mu) = 0 and variance (alpha.V) = 10^3, or something large (see Hadfield 2010 for details). These settings correspond to a proper half-Cauchy prior on σ_{site_0}, with location parameter = 0 and scale = $\sqrt{\text{alpha.V}}$, which in our case = $\sqrt{1000}$.
- Residual variance: IW(V=1, nu=0.002) = IG(0.001, 0.001)

Prior set E

❖ Fixed effects: N(0, 10^4)
❖ Variance components:-
- Among-site variance: Improper uniform prior on σ_{site_0} over the interval (0, ∞). Coded as (V=1e-10, nu=-1) in 'MCMCglmm' function call. Non-informative and widely used (e.g. Gelman et al. 2003), although for instances where the number of sites is small (i.e. < 5), the uniform density can inflate the standard deviation estimates.
- Residual variance: IW(V=1, nu=0.002) = IG(0.001, 0.001)

We fitted each model using the 'MCMCglmm' R package (Hadfield 2010), obtaining three independent Markov chains initialized using dispersed values. We ran each chain for 250,000 iterations, discarding the first 50,000 as burn-in, and using the remaining 3 × 200,000 = 600,000 samples for the calculation of posterior summaries. Convergence of the chains was assessed via visual inspection of trace plots and by computing Gelman-Rubin diagnostics ($\hat{R}$)

(Brooks and Gelman 1998). Autocorrelation between successive samples was explored using the set of 'autocorr' functions in the 'coda' package (Plummer et al. 2006).

Results

The Markov chains for the variance components were well mixed across all models, with mean $\hat{R}$(± SD) for the among-site variance parameter ($\sigma^2_{site_0}$) = 1.102 (± 0.088). In general, we observed better mixing properties for parameter expanded models and those using IG(0.001, 0.001) priors. Mean (± SD) lag-one autocorrelation for individual chains was 0.583 (± 0.103), indicating moderate serial dependence, but we chose not to thin chains here in order to maximise precision in our estimates (Link and Eaton 2012). The mean (± SD) effective sample sizes per chain for each prior specification were as follows: 51216 (± 12694) – Prior set A; 45063 (± 6808) – Prior set B; 51568 (± 13202) – Prior set C; 30929 (± 16055) – Prior set D; 47404 (± 13388) – Prior set E. For each otolith chemistry marker, we plotted the posterior densities of $\sigma^2_{site_0}$ derived from models using each of the five priors (Figure S1).

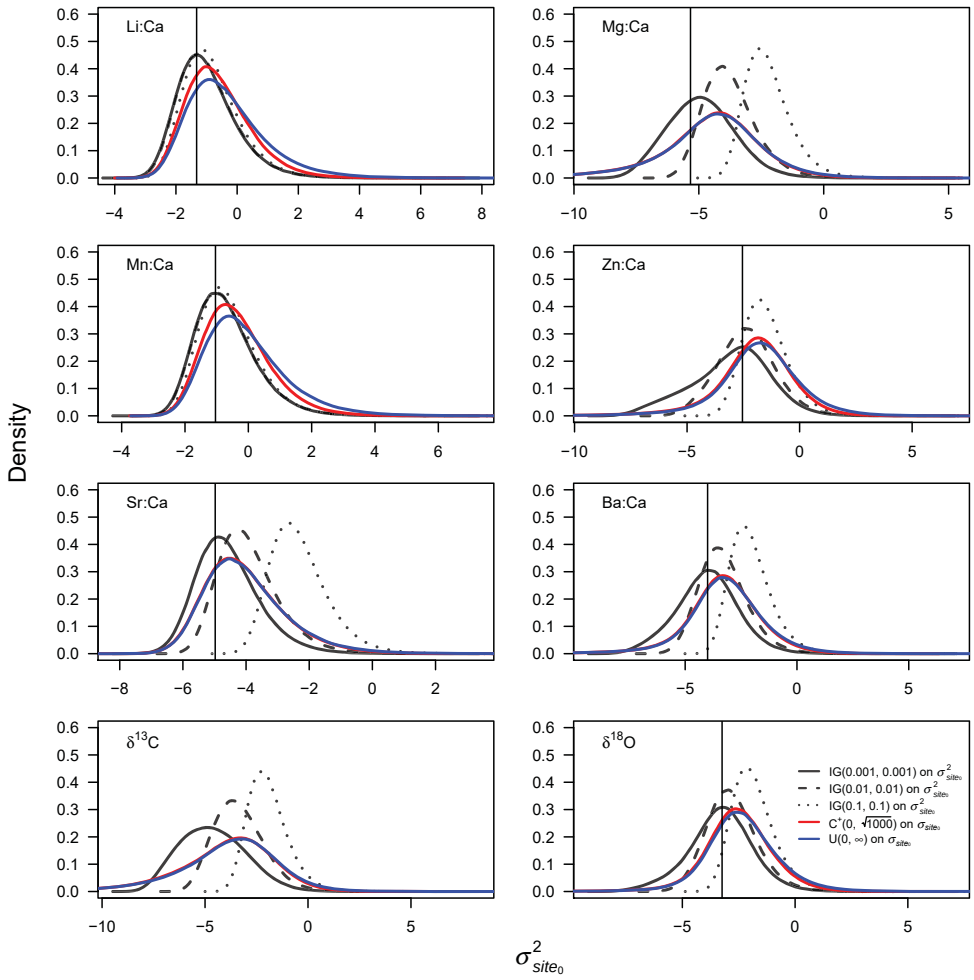

Figure S1. Posterior densities (on natural log scale) for the among-site variance ($\sigma^2_{site_0}$) estimated from MCMCglmm models for each otolith chemistry marker, as specified in eq. S1. Plots show the influence of five different prior distributions placed on $\sigma^2_{site_0}$ or σ_{site_0} (see bottom right panel for colour codes and details). Vertical lines in each plot are (natural log) mean estimates of $\sigma^2_{site_0}$ derived from equivalent models fitted using REML estimation. The REML estimate for $\sigma^2_{site_0}$ in the $\delta^{13}C$ model was ~0, the natural log of which is undefined. Hence, no vertical line in plotted on the bottom left panel.

We then overlaid the mean estimate of the $\sigma^2_{site_0}$ derived from an equivalent model fitted using restricted maximum likelihood (REML) estimation in the 'lme4' package (Bates et al. 2015).

For some otolith markers (i.e. Mg, Sr, Ba, $\delta^{13}C$, $\delta^{18}O$) the among-site variance was small, and in these cases, increasing the degree-of-belief parameter (nu) for the IW prior tended to push the posterior density far beyond the REML estimate. For markers exhibiting σ^2_{site0} estimates well away from zero (i.e. Li, Mn, Zn), the influence of the prior decreased, with REML estimates more closely matching the posterior modes (Figure S1). Parameter expanded models, and those using the flat prior on the site-level standard deviation (σ_{site_0}) resulted in very similar posterior densities for all otolith markers.

Given the tight congruence between REML estimates and the posterior modes from models using an IG(0.001, 0.001) prior on $\sigma^2_{site_0}$ (i.e. Prior set A), the good chain mixing properties observed in these models, and the relatively high effective sample sizes recovered, we decided to use Prior set A in our model selection steps for the Li, Mn and Zn models. As IG priors can be strongly informative when among-site variances approach 0, we elected to use parameter expanded models for Mg, Sr, Ba, $\delta^{13}C$ and $\delta^{18}O$ with proper half-Cauchy priors placed on σ_{site_0} (i.e. Prior set D). These priors are considered weakly informative, and perform well near 0 and when the number of sites is low (Gelman 2006).

References

Brooks, S.P. and Gelman, A. 1998. General methods for monitoring convergence of iterative simulations. J. Comput. Graph. Stat. 7: 434–455.

Gelman, A. 2006. Prior distributions for variance parameters in hierarchical model (Comment on Article by Browne and Draper). Bayesian Anal. 1: 515–534.

Gelman, A. 2008. Scaling regression inputs by dividing by two standard deviations. Stat. Med. 27: 2865–2873.

Hadfield, J. 2010. MCMC methods for multi-response generalised linear mixed models: the MCMCglmm R package. J. Stat. Softw. 33: 1–22.

Link, W.A. and Eaton, M.J. 2012. On thinning of chains in MCMC. Methods Ecol. Evol. 3: 112–115.

Liu, C., Rubin, D. and Wu, Y. 1998. Parameter expansion to accelerate EM, the PX-EM algorithm. Biometrika 85: 755–770.

Plummer, M., Best, N., Cowles, K. and Vines, K. 2006. CODA: convergence diagnosis and output analysis for MCMC. R News 6: 7–11.

*Table S1. Summaries for candidate models describing otolith edge chemistry in juvenile ISS herring. Models were fitted using the best supported random effect structure for each otolith marker (see Table 2 for descriptions). Small sample-size corrected Akaike's information criteria (AICc) and log-likelihood (LL) values were derived from models fitted using restricted maximum likelihood (REML) and ML estimation, and mean (and SD) estimates of the deviance information criterion (DIC), deviance (Dev) and mean squared prediction error on out-of-sample (oos) test data ($MSPE_{oos}$) were computed from three replicate Bayesian models fitted using dispersed starting values in the 'MCMCglmm' package. Bold models were ranked highest in terms of model fit and explanatory power (i.e., 'explan' models in main text), and those underlined were ranked highest regarding oos predictive accuracy (i.e., 'oos.pred' models in main text). All univariate models include an overall intercept, with the intercept suppressed in the multi/bivariate cases to aid interpretation of regression coefficients. × denotes interaction terms; * denotes the additive contribution of two covariates plus their interaction; '1 | site' is a random intercept for capture site; and 'covariate | site' is a random covariate slope and intercept for capture site (see Table 2 for further details). Covariate codes are: A = Age; SL = SL_anom; T = Temp; S = Sal.*

Model	Structure		DIC (SD)	Dev (SD)	AICc	LL	$MSPE_{oos}$ (SD)
	Fixed	Random					
Li:Ca - univariate							
Li_mod.full	A*SL + A*T + A*S	A | site	165.29 (0.01)	150.48 (0.03)	200.68	-87.39	0.582 (0.014)
Li_mod.sub1	A + SL + T + S + A×SL + A×S		165.22 (0.00)	150.47 (0.04)	199.40	-87.89	0.478 (0.000)
Li_mod.sub2	A + SL + T + S + A×SL + A×T		165.23 (0.03)	150.51 (0.03)	199.91	-88.15	0.483 (0.006)
Li_mod.sub3	A + SL + T + S + A×T + A×S		166.18 (0.04)	152.38 (0.03)	201.13	-88.76	0.584 (0.012)
Li_mod.sub4	A + SL + S + A×SL + A×S		165.16 (0.02)	150.43 (0.04)	197.14	-87.90	0.681 (0.003)
Li_mod.sub5	A + SL + T + A×SL + A×T		165.25 (0.02)	150.55 (0.03)	198.41	-88.54	0.531 (0.002)
Li_mod.sub6	A + T + S + A×T + A×S		178.29 (0.02)	165.49 (0.02)	211.99	-95.33	0.587 (0.011)
Li_mod.sub7	A + SL + T + S + A×S		166.09 (0.02)	152.32 (0.03)	199.88	-89.27	0.478 (0.004)
Li_mod.sub8	A + SL + T + S + A×SL		165.11 (0.02)	150.45 (0.05)	197.64	-88.15	0.482 (0.002)
Li_mod.sub9	A + SL + T + S + A×T		166.13 (0.02)	152.40 (0.07)	200.38	-89.52	0.485 (0.004)
Li_mod.sub10	A + SL + S + A×SL		165.07 (0.01)	150.43 (0.04)	195.42	-88.17	0.680 (0.004)
Li_mod.sub11	A + SL + T + A×SL		165.12 (0.03)	150.46 (0.08)	196.17	-88.54	0.529 (0.001)
Li_mod.sub12	A + T + S + A×S		178.20 (0.02)	165.45 (0.01)	210.84	-95.88	0.467 (0.002)
Li_mod.sub13	A + SL + S + A×S		166.04 (0.02)	152.33 (0.05)	197.65	-89.28	0.686 (0.005)
Li_mod.sub14	A + T + S + A×T		178.25 (0.02)	165.54 (0.02)	211.30	-96.11	0.483 (0.004)
Li_mod.sub15	A + SL + T + A×T		166.10 (0.03)	152.37 (0.05)	198.90	-89.91	0.536 (0.001)
Li_mod.sub16	A + SL + T + S		166.02 (0.03)	152.37 (0.04)	198.15	-89.53	0.480 (0.002)
Li_mod.sub17	**A + SL + A×SL**		**165.07 (0.02)**	**150.46 (0.06)**	**194.67**	**-88.90**	**0.596 (0.000)**
Li_mod.sub18	A + S + A×S		178.14 (0.02)	165.42 (0.05)	208.64	-95.89	0.687 (0.003)
Li_mod.sub19	A + T + A×T		178.20 (0.01)	165.52 (0.04)	209.84	-96.49	0.539 (0.001)
Li_mod.sub20	A + T + S		178.07 (0.02)	165.41 (0.03)	209.10	-96.12	0.475 (0.004)
Li_mod.sub21	A + SL + S		165.95 (0.02)	152.32 (0.06)	195.95	-89.54	0.683 (0.004)
Li_mod.sub22	A + SL + T		166.03 (0.01)	152.39 (0.05)	196.69	-89.91	0.532 (0.001)
Li_mod.sub23	A + S		178.03 (0.02)	165.39 (0.01)	206.93	-96.13	0.682 (0.003)
Li_mod.sub24	A + T		178.08 (0.03)	165.44 (0.04)	207.66	-96.50	0.533 (0.001)
Li_mod.sub25	A + SL		165.91 (0.03)	152.31 (0.02)	195.23	-90.28	0.600 (0.001)
Li_mod.sub26	A		177.98 (0.01)	165.41 (0.02)	206.20	-96.85	0.602 (0.001)
Mg:Ca - univariate							
Mg_mod.full	A*SL + A*T + A*S	A | site	145.16 (0.02)	130.48 (0.05)	157.58	-65.83	0.251 (0.003)
Mg_mod.sub1	A + SL + T + S + A×SL + A×S		145.09 (0.02)	130.50 (0.06)	156.64	-66.51	0.233 (0.000)
Mg_mod.sub2	A + SL + T + S + A×SL + A×T		145.07 (0.01)	131.70 (0.02)	156.30	-66.34	0.306 (0.001)
Mg_mod.sub3	A + SL + T + S + A×T + A×S		145.35 (0.01)	130.47 (0.06)	157.52	-66.95	0.248 (0.001)
Mg_mod.sub4	A + SL + S + A×SL + A×S		144.98 (0.03)	130.50 (0.04)	154.67	-66.67	0.239 (0.000)
Mg_mod.sub5	A + SL + T + A×SL + A×T		145.03 (0.05)	130.97 (0.00)	159.24	-68.95	0.254 (0.000)
Mg_mod.sub6	A + T + S + A×T + A×S		143.66 (0.01)	131.67 (0.04)	155.62	-67.14	0.250 (0.003)
Mg_mod.sub7	A + SL + T + S + A×S		145.25 (0.02)	130.47 (0.01)	156.59	-67.63	0.229 (0.000)
Mg_mod.sub8	A + SL + T + S + A×SL		145.01 (0.01)	131.67 (0.03)	158.50	-68.58	0.229 (0.000)
Mg_mod.sub9	A + SL + T + S + A×T		145.24 (0.02)	130.45 (0.04)	156.27	-67.47	0.303 (0.003)
Mg_mod.sub10	A + SL + S + A×SL		144.94 (0.03)	130.45 (0.03)	156.43	-68.67	0.249 (0.000)
Mg_mod.sub11	A + SL + T + A×SL		144.99 (0.01)	130.93 (0.03)	161.22	-71.07	0.226 (0.000)

Mg_mod.sub12	A + T + S + A×S		143.52 (0.02)	131.60 (0.05)	154.72	-67.82	0.231 (0.000)
Mg_mod.sub13	A + SL + S + A×S		145.17 (0.02)	130.95 (0.04)	154.63	-67.77	0.236 (0.000)
Mg_mod.sub14	A + T + S + A×T		143.56 (0.03)	131.64 (0.06)	154.40	-67.66	0.305 (0.000)
Mg_mod.sub15	A + SL + T + A×T		145.19 (0.06)	131.66 (0.03)	159.16	-70.04	0.250 (0.001)
Mg_mod.sub16	A + SL + T + S		145.21 (0.01)	130.52 (0.01)	158.48	-69.70	0.224 (0.001)
Mg_mod.sub17	A + SL + A×SL		145.00 (0.02)	130.87 (0.04)	160.09	-71.61	0.235 (0.000)
Mg_mod.sub18	**A + S + A×S**		**143.45 (0.02)**	**130.93 (0.03)**	**152.77**	**-67.96**	**0.238 (0.000)**
Mg_mod.sub19	A + T + A×T		143.46 (0.02)	130.92 (0.01)	157.29	-70.21	0.252 (0.000)
Mg_mod.sub20	A + T + S		143.50 (0.05)	131.62 (0.03)	156.63	-69.88	0.228 (0.001)
Mg_mod.sub21	A + SL + S		145.11 (0.00)	131.66 (0.01)	156.43	-69.78	0.245 (0.000)
Mg_mod.sub22	A + SL + T		145.09 (0.02)	130.90 (0.01)	161.15	-72.14	0.222 (0.000)
Mg_mod.sub23	A + S		143.39 (0.01)	130.92 (0.05)	154.59	-69.96	0.247 (0.000)
Mg_mod.sub24	A + T		143.42 (0.01)	131.63 (0.03)	159.30	-72.32	0.224 (0.000)
Mg_mod.sub25	A + SL		145.15 (0.02)	132.41 (0.01)	160.00	-72.67	0.231 (0.000)
Mg_mod.sub26	A		143.45 (0.03)	131.72 (0.09)	158.16	-72.83	0.234 (0.000)
Mn:Ca - univariate							
Mn_mod.full	A*SL + A*T + A*S	A | site	275.17 (0.02)	260.56 (0.03)	296.15	-135.12	0.562 (0.005)
Mn_mod.sub1	A + SL + T + S + A×SL + A×S		274.84 (0.04)	260.43 (0.06)	293.88	-135.14	0.558 (0.007)
Mn_mod.sub2	A + SL + T + S + A×SL + A×T		274.88 (0.02)	260.44 (0.04)	294.08	-135.24	0.563 (0.003)
Mn_mod.sub3	A + SL + T + S + A×T + A×S		273.24 (0.03)	259.62 (0.03)	294.03	-135.21	0.560 (0.009)
Mn_mod.sub4	A + SL + S + A×SL + A×S		274.81 (0.06)	260.37 (0.07)	291.63	-135.15	0.566 (0.001)
Mn_mod.sub5	A + SL + T + A×SL + A×T		274.87 (0.02)	260.43 (0.01)	292.40	-135.53	0.521 (0.000)
Mn_mod.sub6	A + T + S + A×T + A×S		272.08 (0.02)	259.45 (0.04)	292.59	-135.63	0.558 (0.012)
Mn_mod.sub7	A + SL + T + S + A×S		272.98 (0.03)	259.50 (0.03)	291.80	-135.23	0.562 (0.003)
Mn_mod.sub8	A + SL + T + S + A×SL		274.47 (0.04)	260.26 (0.03)	291.84	-135.26	0.562 (0.002)
Mn_mod.sub9	A + SL + T + S + A×T		273.01 (0.02)	259.54 (0.01)	291.99	-135.33	0.559 (0.009)
Mn_mod.sub10	A + SL + S + A×SL		274.47 (0.04)	260.24 (0.05)	289.64	-135.28	0.570 (0.001)
Mn_mod.sub11	A + SL + T + A×SL		274.47 (0.02)	260.27 (0.01)	290.18	-135.55	0.521 (0.002)
Mn_mod.sub12	A + T + S + A×S		271.73 (0.03)	259.29 (0.04)	290.39	-135.65	0.546 (0.005)
Mn_mod.sub13	A + SL + S + A×S		272.92 (0.01)	259.53 (0.04)	289.58	-135.25	0.566 (0.001)
Mn_mod.sub14	A + T + S + A×T		271.78 (0.01)	259.32 (0.01)	290.58	-135.75	0.548 (0.004)
Mn_mod.sub15	A + SL + T + A×T		272.99 (0.02)	259.55 (0.05)	290.34	-135.63	0.520 (0.001)
Mn_mod.sub16	A + SL + T + S		272.60 (0.01)	259.33 (0.03)	289.78	-135.35	0.558 (0.005)
Mn_mod.sub17	A + SL + A×SL		274.37 (0.00)	260.19 (0.04)	288.21	-135.67	0.544 (0.001)
Mn_mod.sub18	A + S + A×S		271.73 (0.01)	259.29 (0.02)	288.20	-135.67	0.560 (0.001)
Mn_mod.sub19	A + T + A×T		271.78 (0.03)	259.32 (0.03)	288.95	-136.04	0.515 (0.001)
Mn_mod.sub20	A + T + S		271.42 (0.02)	259.16 (0.04)	288.39	-135.76	0.550 (0.006)
Mn_mod.sub21	A + SL + S		272.59 (0.01)	259.38 (0.06)	287.60	-135.37	0.569 (0.002)
Mn_mod.sub22	A + SL + T		272.60 (0.01)	259.41 (0.01)	288.15	-135.64	0.521 (0.001)
Mn_mod.sub23	A + S		271.36 (0.03)	259.11 (0.04)	286.24	-135.79	0.562 (0.001)
Mn_mod.sub24	A + T		271.39 (0.01)	259.16 (0.00)	286.78	-136.06	0.515 (0.003)
Mn_mod.sub25	A + SL		272.49 (0.03)	259.33 (0.02)	286.20	-135.76	0.546 (0.000)
Mn_mod.sub26	**A**		**271.31 (0.03)**	**259.13 (0.04)**	**284.85**	**-136.18**	**0.538 (0.002)**
Zn:Ca - univariate							
Zn_mod.full	A*SL + A*T + A*S	1 | site	501.51 (0.04)	490.22 (0.10)	506.77	-242.72	1.538 (0.001)
Zn_mod.sub1	A + SL + T + S + A×SL + A×S		499.53 (0.01)	489.29 (0.02)	504.53	-242.72	1.536 (0.001)
Zn_mod.sub2	A + SL + T + S + A×SL + A×T		500.31 (0.03)	490.01 (0.03)	505.37	-243.14	1.523 (0.002)
Zn_mod.sub3	A + SL + T + S + A×T + A×S		501.23 (0.02)	490.96 (0.01)	506.12	-243.52	1.541 (0.003)
Zn_mod.sub4	A + SL + S + A×SL + A×S		498.73 (0.01)	489.46 (0.03)	502.33	-242.73	1.563 (0.002)
Zn_mod.sub5	A + SL + T + A×SL + A×T		500.11 (0.03)	490.30 0.10)	504.45	-243.80	1.386 (0.000)
Zn_mod.sub6	A + T + S + A×T + A×S		500.15 (0.02)	490.88 (0.04)	504.90	-244.02	1.542 (0.003)
Zn_mod.sub7	A + SL + T + S + A×S		499.23 (0.01)	489.97 (0.06)	503.91	-243.52	1.535 (0.005)
Zn_mod.sub8	A + SL + T + S + A×SL		498.52 (0.02)	489.13 (0.05)	503.62	-243.38	1.524 (0.003)
Zn_mod.sub9	A + SL + T + S + A×T		500.01 (0.02)	490.73 (0.03)	504.74	-243.94	1.523 (0.001)
Zn_mod.sub10	A + SL + S + A×SL		497.82 (0.02)	489.36 (0.02)	501.48	-243.41	1.563 (0.001)
Zn_mod.sub11	A + SL + T + A×SL		498.35 (0.01)	489.41 (0.05)	502.69	-244.01	1.375 (0.001)
Zn_mod.sub12	A + T + S + A×S		498.14 (0.00)	489.87 (0.03)	502.71	-244.02	1.537 (0.001)
Zn_mod.sub13	A + SL + S + A×S		498.37 (0.02)	490.10 (0.03)	501.73	-243.53	1.562 (0.002)
Zn_mod.sub14	A + T + S + A×T		498.94 (0.03)	490.66 (0.05)	503.54	-244.44	1.523 (0.003)
Zn_mod.sub15	A + SL + T + A×T		499.82 (0.00)	491.06 (0.05)	503.90	-244.62	1.388 (0.000)

Zn_mod.sub16	A + SL + T + S		498.23 (0.04)	489.89 (0.05)	503.05	-244.19	1.527 (0.001)
Zn_mod.sub17	A + SL + A×SL		498.39 (0.04)	489.77 (0.07)	502.12	-244.81	1.393 (0.000)
Zn_mod.sub18	A + S + A×S		497.33 (0.01)	490.02 (0.03)	500.56	-244.03	1.560 (0.002)
Zn_mod.sub19	A + T + A×T		498.74 (0.01)	490.92 (0.02)	502.71	-245.11	1.386 (0.000)
Zn_mod.sub20	A + T + S		497.11 (0.01)	489.75 (0.03)	501.84	-244.67	1.524 (0.002)
Zn_mod.sub21	A + SL + S		497.50 (0.03)	490.07 (0.01)	500.93	-244.22	1.563 (0.001)
Zn_mod.sub22	A + SL + T		498.05 (0.01)	490.14 (0.01)	502.19	-244.85	1.375 (0.001)
Zn_mod.sub23	SL + T + S		498.95 (0.02)	491.61 (0.02)	503.54	-245.52	1.608 (0.000)
Zn_mod.sub24	**A + S**		**496.47 (0.02)**	**490.00 (0.05)**	**499.75**	**-244.70**	**1.561 (0.001)**
Zn_mod.sub25	A + T		496.97 (0.03)	490.04 (0.03)	501.00	-245.32	1.375 (0.000)
Zn_mod.sub26	A + SL		498.10 (0.01)	490.52 (0.02)	501.62	-245.63	1.394 (0.000)
Zn_mod.sub27	SL + S		498.20 (0.01)	491.81 (0.01)	501.42	-245.54	1.644 (0.001)
Zn_mod.sub28	SL + T		498.83 (0.01)	491.89 (0.03)	502.87	-246.26	1.413 (0.000)
Zn_mod.sub29	T + S		497.91 (0.02)	491.56 (0.06)	502.39	-246.02	1.612 (0.003)
Zn_mod.sub30	A		496.96 (0.02)	490.39 (0.04)	500.47	-246.12	1.394 (0.000)
Zn_mod.sub31	SL		498.84 (0.01)	492.23 (0.01)	502.28	-247.02	1.455 (0.001)
Zn_mod.sub32	T		497.78 (0.01)	491.81 (0.01)	501.74	-246.75	1.413 (0.000)
Zn_mod.sub33	S		497.17 (0.02)	491.75 (0.01)	500.30	-246.03	1.646 (0.000)
Zn_mod.null	-		497.78 (0.03)	492.18 (0.04)	501.18	-247.52	-
Sr:Ca - univariate							
Sr_mod.full	A*SL + A*T + A*S	1 | site	-187.11 (0.02)	-198.93 (0.01)	-173.44	97.39	0.042 (0.000)
Sr_mod.sub1	A + SL + T + S + A×SL + A×S		-176.95 (0.03)	-187.76 0.05	-163.31	91.20	0.040 (0.000)
Sr_mod.sub2	A + SL + T + S + A×SL + A×T		-183.42 0.01	-194.26 0.03	-170.25	94.67	0.040 (0.000)
Sr_mod.sub3	**A + SL + T + S + A×T + A×S**		**-187.20 0.01**	**-198.07 0.03**	**-173.77**	**96.43**	**0.043 (0.000)**
Sr_mod.sub4	A + SL + S + A×SL + A×S		-177.02 0.02	-187.77 0.07	-165.17	91.02	0.039 (0.000)
Sr_mod.sub5	A + SL + T + A×SL + A×T		-183.44 0.01	-194.25 0.03	-170.05	93.45	0.047 (0.000)
Sr_mod.sub6	A + T + S + A×T + A×S		-181.76 0.02	-191.58 0.01	-168.71	92.79	0.043 (0.000)
Sr_mod.sub7	A + SL + T + S + A×S		-177.08 0.02	-186.91 0.05	-163.66	90.26	0.041 (0.000)
Sr_mod.sub8	A + SL + T + S + A×SL		-179.00 0.02	-188.88 0.03	-165.53	91.20	0.040 (0.000)
Sr_mod.sub9	A + SL + T + S + A×T		-183.58 0.04	-193.43 0.03	-170.61	93.74	0.041 (0.000)
Sr_mod.sub10	A + SL + S + A×SL		-179.07 0.03	-188.81 0.05	-167.37	91.02	0.039 (0.000)
Sr_mod.sub11	A + SL + T + A×SL		-179.00 0.01	-188.81 0.05	-165.34	90.00	0.046 (0.000)
Sr_mod.sub12	A + T + S + A×S		-171.86 0.03	-180.72 0.04	-158.82	86.75	0.041 (0.000)
Sr_mod.sub13	A + SL + S + A×S		-177.17 0.02	-186.91 0.04	-165.49	90.08	0.040 (0.000)
Sr_mod.sub14	A + T + S + A×T		-178.38 0.01	-187.23 0.03	-165.77	90.22	0.041 (0.000)
Sr_mod.sub15	A + SL + T + A×T		-183.61 0.01	-193.41 0.05	-170.39	92.53	0.048 (0.000)
Sr_mod.sub16	A + SL + T + S		-179.13 0.00	-188.01 0.04	-165.85	90.26	0.041 (0.000)
Sr_mod.sub17	A + SL + A×SL		-179.07 0.02	-188.77 0.03	-166.88	89.69	0.044 (0.000)
Sr_mod.sub18	A + S + A×S		-171.95 0.01	-180.71 0.02	-160.61	86.55	0.040 (0.000)
Sr_mod.sub19	A + T + A×T		-178.40 0.05	-187.21 0.02	-165.53	89.01	0.048 (0.000)
Sr_mod.sub20	A + T + S		-173.89 0.00	-181.79 0.04	-160.99	86.74	0.041 (0.000)
Sr_mod.sub21	A + SL + S		-179.20 0.04	-187.97 0.04	-167.65	90.08	0.040 (0.000)
Sr_mod.sub22	A + SL + T		-179.12 0.02	-187.96 0.03	-165.64	89.07	0.046 (0.000)
Sr_mod.sub23	SL + T + S		-136.97 0.02	-144.81 0.02	-126.66	69.58	0.043 (0.000)
Sr_mod.sub24	A + S		-174.02 0.01	-181.75 0.04	-162.75	86.55	0.040 (0.000)
Sr_mod.sub25	A + T		-173.92 0.02	-181.74 0.01	-160.75	85.55	0.046 (0.000)
Sr_mod.sub26	A + SL		-179.18 0.01	-187.91 0.02	-167.17	88.76	0.045 (0.000)
Sr_mod.sub27	SL + S		-137.10 0.02	-144.73 0.05	-128.50	69.43	0.045 (0.000)
Sr_mod.sub28	SL + T		-137.04 0.01	-144.77 0.01	-126.41	68.38	0.057 (0.000)
Sr_mod.sub29	T + S		-132.93 0.02	-139.79 0.03	-122.91	66.63	0.043 (0.000)
Sr_mod.sub30	A		-173.98 0.03	-181.71 0.03	-162.28	85.26	0.045 (0.000)
Sr_mod.sub31	SL		-137.05 0.02	-144.69 0.01	-127.81	68.02	0.053 (0.000)
Sr_mod.sub32	T		-132.99 0.01	-139.74 0.02	-122.64	65.44	0.057 (0.000)
Sr_mod.sub33	S		-133.06 0.01	-139.72 0.02	-124.72	66.48	0.045 (0.000)
Sr_mod.null	-		-133.02 0.00	-139.63 0.03	-124.04	65.09	-
Ba:Ca - univariate							
Ba_mod.full	A*SL + A*T + A*S	SL | site	205.68 (0.03)	189.89 (0.03)	216.85	-95.47	0.278 (0.000)
Ba_mod.sub1	A + SL + T + S + A×SL + A×S		204.17 (0.03)	189.37 (0.05)	215.27	-95.83	0.273 (0.000)
Ba_mod.sub2	A + SL + T + S + A×SL + A×T		203.59 (0.03)	188.84 (0.05)	214.58	-95.49	0.280 (0.000)
Ba_mod.sub3	A + SL + T + S + A×T + A×S		204.25 (0.02)	189.50 (0.04)	215.09	-95.74	0.277 (0.000)

Ba_mod.sub4	A + SL + S + A×SL + A×S		203.86 (0.01)	189.52 (0.01)	213.46	-96.06	0.276 (0.000)
Ba_mod.sub5	A + SL + T + A×SL + A×T		203.13 (0.04)	188.76 (0.02)	212.69	-95.68	0.288 (0.000)
Ba_mod.sub6	A + SL + T + S + A×S		202.77 (0.01)	188.97 (0.06)	213.53	-96.10	0.273 (0.000)
Ba_mod.sub7	A + SL + T + S + A×SL		202.89 (0.01)	189.03 (0.03)	214.02	-96.34	0.280 (0.000)
Ba_mod.sub8	A + SL + T + S + A×T		202.15 (0.03)	188.41 (0.03)	212.85	-95.76	0.280 (0.001)
Ba_mod.sub9	A + SL + S + A×SL		202.63 (0.03)	189.24 (0.01)	212.14	-96.53	0.283 (0.000)
Ba_mod.sub10	A + SL + T + A×SL		202.52 (0.04)	189.07 (0.05)	212.26	-96.59	0.285 (0.000)
Ba_mod.sub11	A + SL + S + A×S		202.44 (0.05)	189.12 (0.07)	211.72	-96.32	0.275 (0.000)
Ba_mod.sub12	A + SL + T + A×T		201.75 (0.04)	188.40 (0.06)	210.92	-95.92	0.287 (0.000)
Ba_mod.sub13	A + SL + T + S		201.48 (0.02)	188.68 (0.08)	212.30	-96.61	0.279 (0.000)
Ba_mod.sub14	A + SL + A×SL		201.95 (0.01)	189.12 (0.01)	210.07	-96.60	0.284 (0.000)
Ba_mod.sub15	SL + T + S		208.72 (0.00)	196.92 (0.04)	220.17	-101.65	0.281 (0.000)
Ba_mod.sub16	A + SL + S		201.20 (0.03)	188.81 (0.03)	210.43	-96.78	0.283 (0.000)
Ba_mod.sub17	A + SL + T		201.11 (0.01)	188.68 (0.02)	210.50	-96.82	0.285 (0.000)
Ba_mod.sub18	SL + S		208.51 (0.02)	197.08 (0.01)	218.37	-101.85	0.274 (0.000)
Ba_mod.sub19	SL + T		208.35 (0.01)	196.86 (0.07)	218.55	-101.94	0.272 (0.000)
Ba_mod.sub20	**A + SL**		**200.56 (0.03)**	**188.75 (0.04)**	**208.34**	**-96.84**	**0.284 (0.000)**
Ba_mod.sub21	SL		207.97 (0.04)	197.01 (0.05)	216.40	-101.95	0.271 (0.000)
$\delta^{13}C$ - univariate							
C_mod.full	SL + T + S	None	93.26 (0.00)	88.38 (0.02)	94.29	-41.58	1.066 (0.001)
C_mod.sub1	**T + S**		**91.54 (0.01)**	**87.63 (0.04)**	**92.23**	**-41.75**	**1.063 (0.003)**
C_mod.sub2	SL + S		113.60 (0.00)	109.67 (0.02)	114.28	-52.77	0.323 (0.001)
C_mod.sub3	SL + T		100.94 (0.01)	97.04 (0.01)	101.64	-46.45	0.404 (0.000)
C_mod.sub4	S		111.77 (0.02)	108.82 (0.02)	112.20	-52.88	0.316 (0.000)
C_mod.sub5	T		99.26 (0.01)	96.32 (0.02)	99.69	-46.62	0.396 (0.000)
C_mod.sub6	SL		111.66 (0.02)	108.73 (0.02)	112.09	-52.83	0.328 (0.000)
C_mod.null	-		109.85 (0.00)	107.90 (0.01)	110.09	-52.94	-
$\delta^{18}O$ - univariate							
O_mod.full	SL + T + S	1 | site	32.65 (0.03)	24.92 (0.03)	41.83	-14.09	0.394 (0.003)
O_mod.sub1	**T + S**		**30.87 (0.02)**	**24.14 (0.02)**	**39.57**	**-14.21**	**0.387 (0.003)**
O_mod.sub2	SL + S		32.28 (0.02)	24.57 (0.01)	47.93	-18.39	0.336 (0.003)
O_mod.sub3	SL + T		32.38 (0.00)	24.72 (0.05)	44.50	-16.67	0.200 (0.001)
O_mod.sub4	S		30.55 (0.02)	23.80 (0.01)	45.83	-18.54	0.332 (0.002)
O_mod.sub5	T		30.58 (0.02)	23.91 (0.04)	42.40	-16.82	0.196 (0.001)
O_mod.sub6	SL		32.21 (0.02)	24.60 (0.03)	45.61	-18.43	0.308 (0.000)
O_mod.null	-		30.44 (0.01)	23.83 (0.01)	43.60	-18.58	-
Multi							
multi_mod.full	A*SL + A*T + A*S	A | site + SL | site	2502.92 (0.03)	2397.25 (0.05)	-	-	1.161 (0.007)
multi_mod.sub1	A + SL + T + S + A×SL + A×S		2499.76 (0.09)	2396.20 (0.19)	-	-	1.110 (0.005)
multi_mod.sub2	A + SL + T + S + A×SL + A×T		2500.27 (0.04)	2397.10 (0.02)	-	-	1.148 (0.004)
multi_mod.sub3	A + SL + T + S + A×T + A×S		2502.32 (0.10)	2401.93 (0.12)	-	-	1.164 (0.009)
multi_mod.sub4	A + SL + S + A×SL + A×S		2498.46 (0.08)	2396.38 (0.08)	-	-	1.147 (0.003)
multi_mod.sub5	A + SL + T + A×SL + A×T		2499.67 (0.09)	2397.77 (0.15)	-	-	1.122 (0.002)
multi_mod.sub6	A + SL + T + S + A×S		2499.19 (0.06)	2400.84 (0.06)	-	-	1.113 (0.002)
multi_mod.sub7	A + SL + T + S + A×T		2499.73 (0.09)	2401.72 (0.10)	-	-	1.151 (0.004)
multi_mod.sub8	A + SL + T + S + A×SL		2495.96 (0.06)	2395.16 (0.08)	-	-	1.103 (0.003)
multi_mod.sub9	A + SL + S + A×SL		2494.61 (0.02)	2395.48 (0.13)	-	-	1.133 (0.001)
multi_mod.sub10	A + SL + T + A×SL		2495.39 (0.11)	2395.80 (0.09)	-	-	1.066 (0.001)
multi_mod.sub11	A + SL + S + A×S		2497.71 (0.06)	2401.03 (0.09)	-	-	1.147 (0.001)
multi_mod.sub12	A + SL + T + A×T		2498.85 (0.07)	2402.30 (0.08)	-	-	1.121 (0.002)
multi_mod.sub13	A + SL + T + S		2495.28 (0.02)	2399.75 (0.11)	-	-	1.104 (0.004)
multi_mod.sub14	A + SL + A×SL		2495.00 (0.05)	2396.87 (0.10)	-	-	1.097 (0.001)
multi_mod.sub15	**A + SL + S**		**2494.03 (0.04)**	**2400.09 (0.04)**	**-**	**-**	**1.134 (0.001)**
multi_mod.sub16	A + SL + T		2494.80 (0.06)	2400.45 (0.05)	-	-	1.067 (0.001)
multi_mod.sub17	A + SL		2494.28 (0.06)	2401.47 (0.10)	-	-	1.098 (0.001)
Bivar							
bivar_mod.full	SL + T + S	1 | site	270.44 (0.04)	257.47 (0.03)	-	-	2.111 (0.006)

bivar_mod.sub1	**T + S**	**266.71 (0.04)**	**255.66 (0.08)**	**-**	**-**	**2.103 (0.013)**
bivar_mod.sub2	SL + S	272.46 (0.03)	258.08 (0.06)	-	-	1.112 (0.005)
bivar_mod.sub3	SL + T	272.12 (0.03)	258.47 (0.01)	-	-	0.817 (0.000)
bivar_mod.sub4	S	268.76 (0.08)	256.29 (0.08)	-	-	1.091 (0.003)
bivar_mod.sub5	T	268.47 (0.01)	256.70 (0.05)	-	-	0.797 (0.000)
bivar_mod.sub6	SL	270.91 (0.08)	257.48 (0.02)	-	-	0.999 (0.000)
bivar_mod.null	-	267.59 (0.05)	255.75 (0.08)	-	-	2.111 (0.006)

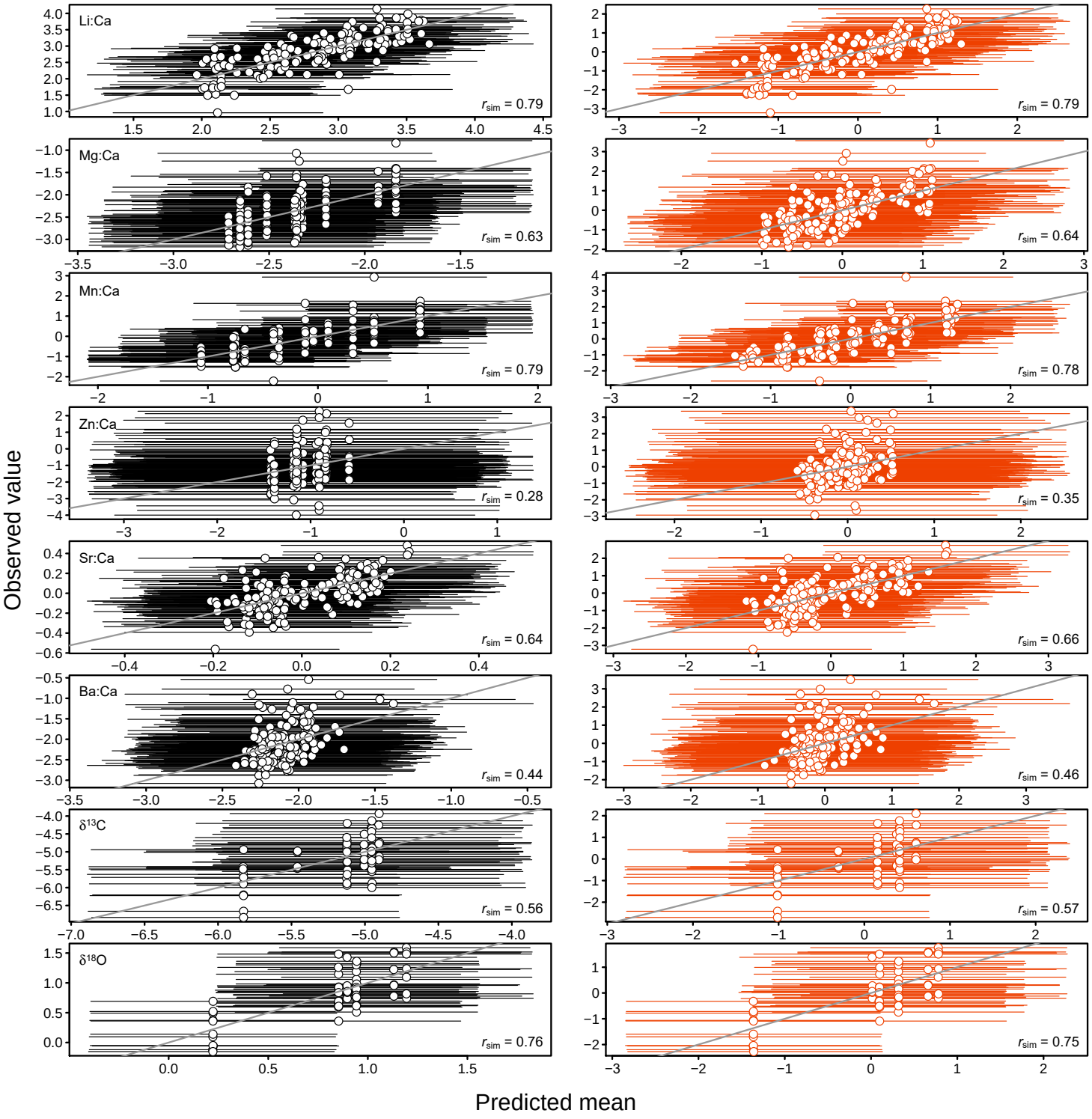

Figure S2. Measurements of elemental and stable isotope markers in the training data plotted against predicted mean values (± 95% prediction intervals – horizontal lines) calculated across 200,000 datasets simulated from the final 'explan' models. Univariate models: black symbols and lines; multi/bivariate models: red symbols and lines models. Correlations (Pearson's r) between observed and predicted values are shown for each plot, and the 1:1 line is shown in grey. Units for Li:Ca, Mn:Ca, Zn:Ca and Ba:Ca are µmol/mol, with Mg:Ca and Sr:Ca measured in mmol/mol, and $\delta^{13}C$ and $\delta^{18}O$ in ‰. Note that all element:Ca ratios are natural log transformed, and all markers used in the multi/bivariate models are scaled to mean = 0, SD = 1.

Calculation of SL_anom values for spatial prediction

At some nursery sites, no age 1 and/or age 2 juveniles were captured in a particular year. We still wanted to make predictions of otolith elemental and stable isotopic markers at these sites for each age-class, so followed a series of steps to estimate the SL_anom covariate value, as follows.

First, we used the median cohort-specific SL_anom value from the nearest capture site (i.e., minimum distance by water) in that year, if this site was located within 10 nautical miles of the site of interest. (2) If no such site existed, we instead used the median cohort-specific SL_anom value from the site of interest in the year in which the fish were collected. (3) If the relevant cohort was never collected from the site of interest across the three sampling years, we used (A) the mean cohort-specific SL_anom value across all sites with data that were located within 10 nautical miles of the site of interest, and across all years; or if no such sites existed, (B) the mean cohort-specific SL_anom value across all sites with data in the year of interest.

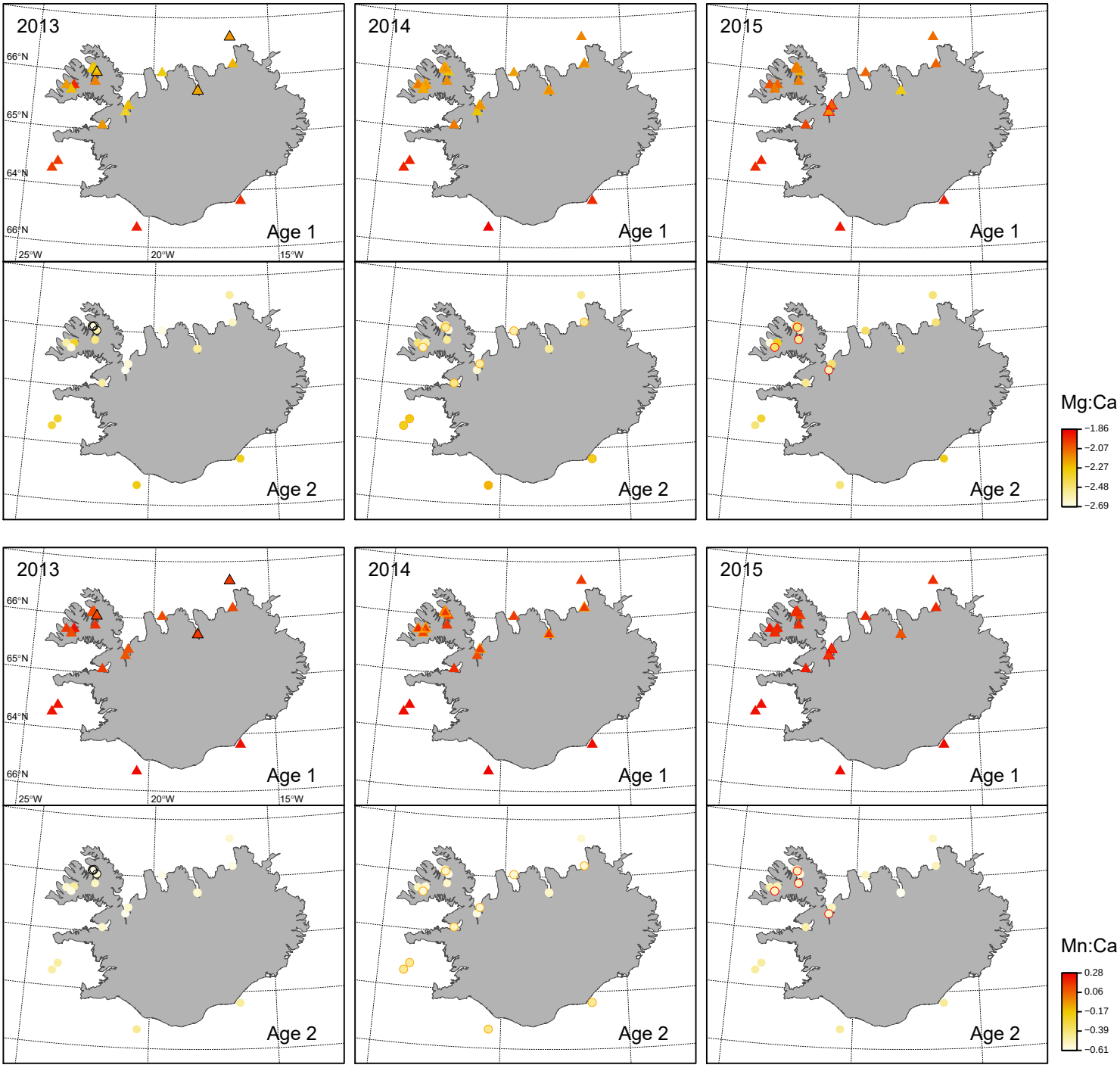

Figure S3. Spatial predictions for otolith Mg:Ca, Mn:Ca, Zn:Ca, Ba:Ca and $\delta^{13}C$ at all capture sites in each of the three sampling years (2013, 2014, 2015) and for the two age-classes (age 1: triangles, age 2: circles). Results are derived from the final 'oos.pred' models (see Table 3). Colour bars represent the mean predicted values for each site for the marker of interest. Sites at which fish were captured in a particular year are outlined in black (for 2013), orange (for 2014) and red (for 2015). Predictions for Mg:Ca (mmol/mol), Mn:Ca, Zn:Ca and Ba:Ca (all µmol/mol) are presented on the natural log scale, with predictions for $\delta^{13}C$ (in ‰) generated using a bivariate model in which each response variable (i.e. $\delta^{13}C$ and $\delta^{18}O$) was scaled to mean = 0 and SD = 1.

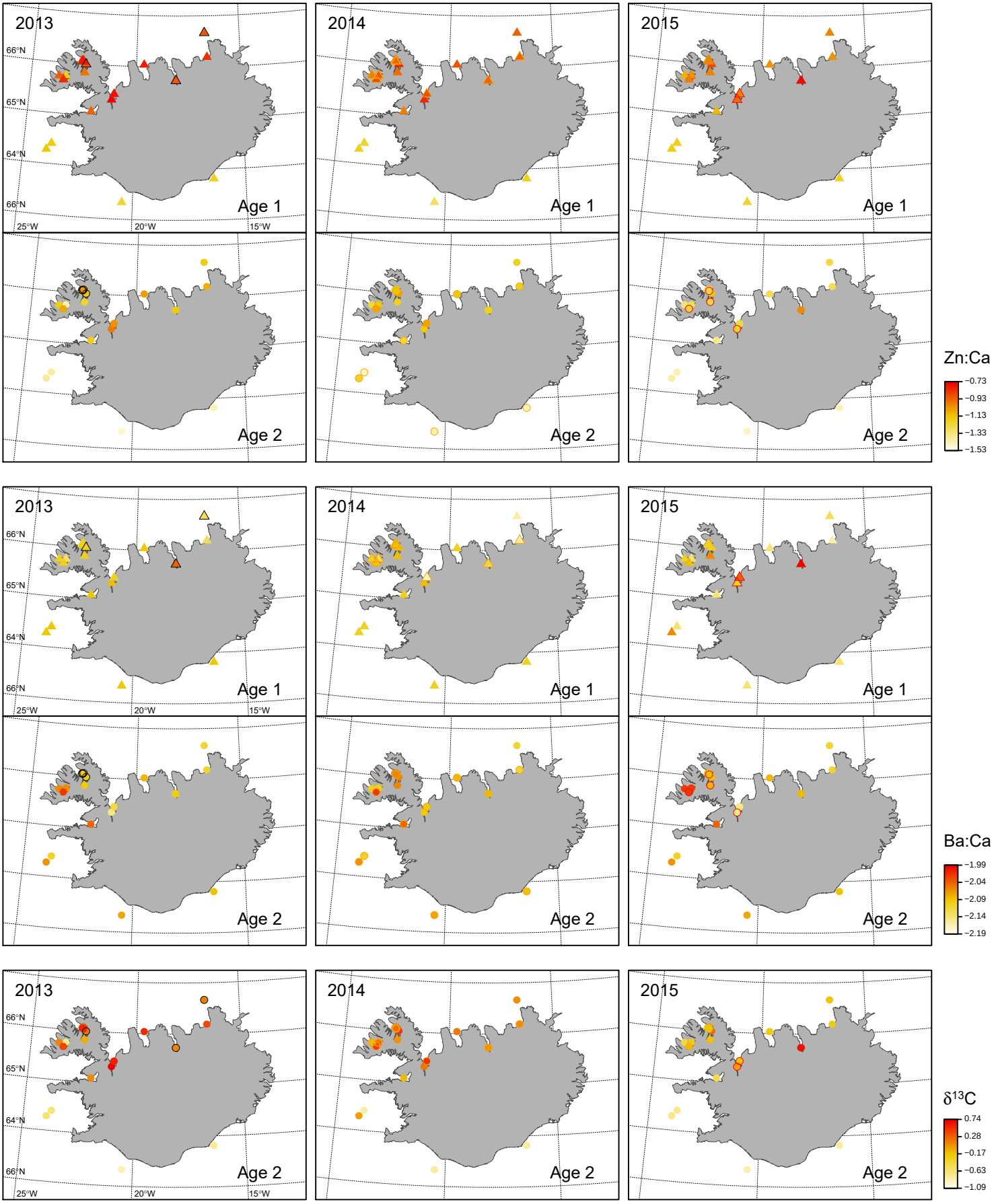

Fig. S3. continued.

Table S2. Mean squared prediction error (MSPE) for spatial predictions of each otolith chemical marker. Estimates are given for all three sampling years (All years) and for each year separately (2013, 2014, 2015). All sites: all capture sites; Age 1: sites where age 1 herring were captured; Age 2: sites where age 2 herring were captured.

Marker	All years			2013			2014			2015		
	All sites	Age 1	Age 2	All sites	Age 1	Age 2	All sites	Age 1	Age 2	All sites	Age 1	Age 2
Li:Ca	0.28	0.38	0.20	0.14	0.29	0.04	0.36	0.47	0.25	0.19	0.12	0.23
Mg:Ca	0.18	0.05	0.28	0.67	0.08	1.12	0.04	0.04	0.04	0.06	0.08	0.05
Mn:Ca	0.26	0.40	0.16	0.30	0.39	0.23	0.29	0.41	0.18	0.15	0.37	0.04
Zn:Ca	0.46	0.15	0.70	1.35	0.12	2.28	0.18	0.12	0.23	0.31	0.34	0.29
Sr:Ca	0.01	0.01	0.01	0.00	0.00	0.01	0.01	0.01	0.01	0.02	0.00	0.02
Ba:Ca	0.04	0.05	0.03	0.05	0.08	0.03	0.03	0.04	0.02	0.03	0.04	0.03
$\delta^{13}C$	0.62	-	0.62	0.73	-	0.73	0.71	-	0.71	0.30	-	0.30
$\delta^{18}O$	0.79	-	0.79	0.46	-	0.46	0.95	-	0.95	0.77	-	0.77

Paper IV

Defining the scales of otolith chemical variability reveals long-term fidelity to nurseries and multiple origins in a fished herring population

Jed I. Macdonald, Ingibjörg G. Jónsdóttir, Russell N. Drysdale, Roman Witt, Þorsteinn Sigurðsson, Páll Reynisson, Guðmundur J. Óskarsson, Zsófia Cságoly, Guðrún Marteinsdóttir

(In review in *Canadian Journal of Fisheries and Aquatic Sciences*)

Author contributions – Conceived and designed the experiments: JIM, ÞS, GM; collected samples: JIM, IGJ, PR, GJÓ; extracted and prepared the otoliths: JIM, ZC; analysed the data: JIM; RND, RW; wrote the manuscript: JIM; reviewed and edited the manuscript: JIM, IGJ, RND, RW, ÞS, PR, GJÓ, GM.

Defining the scales of otolith chemical variability reveals long-term fidelity to nurseries and multiple origins in a fished herring population

Jed I. Macdonald[1,2] , Ingibjörg G. Jónsdóttir[3], Russell N. Drysdale[4], Roman Witt[4], Þorsteinn Sigurðsson[3], Páll Reynisson[3], Guðmundur J. Óskarsson[3], Zsófia Ságoly[1], Guðrún Marteinsdóttir[1]

[1]Faculty of Life and Environmental Sciences, University of Iceland, 101 Reykjavík, Iceland
[2]School of BioSciences, The University of Melbourne, Parkville, Victoria 3052, Australia
[3]Marine and Freshwater Research Institute, 101 Reykjavík, Iceland
[4]School of Geography, The University of Melbourne, Carlton, Victoria 3053, Australia

Abstract

Reliable information on how, and at which scales marine fish populations connect is crucial for the effective management of harvested migratory species. One approach to charting such connections is to quantify the degree to which populations vary in their expression of certain traits, the chemical constituents locked within fish otoliths (ear stones) providing well-known examples. In this study, we develop some new, quantitative rules for assessing the scale of spatial and temporal variation in otolith chemistry within a Bayesian modelling framework. We apply these rules to data on Icelandic summer spawning (ISS) herring *Clupea harengus*, a stock of high commercial importance, to address some long-standing questions on nursery connectivity, nursery fidelity and nursery-specific contributions to the fishery. We show that population-level differences in otolith chemical traits generally scale with both geographic distance among nurseries, and temporal distance between sampling events, manifesting in coast-wide heterogeneity in otolith elemental (i.e. Li:Ca, Mg:Ca, Mn:Ca, Zn:Ca, Sr:Ca, Ba:Ca) and stable isotopic (i.e. $\delta^{13}C$, $\delta^{18}O$) concentrations that vary through time. This information created a data-driven platform for characterising 'source' population structure that explicitly considers individual- to population-level variation in chemical markers through all modelling stages. Such platforms build trust in outputs from mixture models designed to estimate the provenance of fish of uncertain origin; models that here revealed strong attachment to nursery sites as juveniles, and demonstrated the importance of multiple, widely-dispersed nurseries as sources for a portion of the fished adult 'sink' population, irrespective of their presumed quality.

Introduction

From where do fish within fished populations originate? This seemingly simple question remains unresolved for many commercially-targeted marine species, despite the fact that the best fishery-management decisions require reliable answers to it. Knowledge of natal origins, nursery location, arrangement and quality provides a means to identify and protect key juvenile habitats, to track dispersal and recruitment success, and ultimately, to ensure future fishery sustainability (Beck et al. 2001; Botsford et al. 2001; Cowen et al. 2007). Equally important in this context is information on the structure of the nursery-resident populations themselves. For example, quantifying juvenile retention or straying rates and connections among spatially-separated nursery populations can provide valuable inference on if, and how these might act as 'sources' for adult 'sink' populations subject to heavy fishing pressure (Rooker et al. 2008; Garavelli et al. 2018).

Rapid advances in applied-tag technology, in genetic techniques, and in linkages between ocean-circulation models and species' biological characteristics are allowing researchers to define the scales at which populations mix with increasing confidence (Treml et al. 2012; Grewe et al. 2015; Halfyard et al. 2017). Fish otoliths (ear stones) contain a similarly rich store of information for this purpose. Otoliths comprise life-long, individual-level data on chemical and morphological traits whose expression can vary strongly within and among populations (Burke et al. 2008; Macdonald and Crook 2010; Huey et al. 2014; **Paper III**). These aragonitic structures have proved themselves as remarkably effective 'natural tags' in population connectivity studies, used either alone (e.g. Geffen et al. 2011; Neubauer et al. 2010; Wright et al. 2018), or in concert with other complimentary (aforementioned) approaches (e.g. Woods et al. 2010; Ashford et al. 2012; Taillebois et al. 2018). The daily deposition of permanent growth increments onto the otolith surface – increments that incorporate elements and stable isotopes reflecting intrinsic processes (e.g. physiology, metabolism, growth, age) and/or extrinsic (e.g. environmental) factors – highlights otoliths' potential as individual-level, bio-environmental recorders and population markers (see Høie et al. 2003; Grønkjær 2016; Grammer et al. 2017; Izzo et al. 2018; **Paper III**).

Whilst the value of otoliths as population-delineation tools for fishery management is clear (e.g. Burke et al. 2008; Rooker et al. 2008; Libungan et al. 2015), innovations in statistical approaches that use the chemical constituents of these structures as population markers may allow us to honour their full potential for such applications. Current approaches, while evolving (see Mercier et al. 2011; Niklitschek and Darnaude 2016; Jones et al. 2017), often neglect to incorporate new knowledge on the mechanisms driving inter-individual variability in chemical traits, and how this translates to population- or stock-level variability. Moreover, they rarely quantify data-related uncertainties, or those associated with 'source' classification, or source contribution to mixed 'sink' populations. This uncertainty is likely exacerbated when sampling coverage is sparse, or sample sizes low, and if overlooked, may potentially manifest in inaccurate or incomplete characterisation of source populations. Such outcomes can reduce confidence in the results of subsequent source-assignment tests for individuals within fished populations, results upon which management decisions often rest.

Here, we present a Bayesian modelling framework in an attempt to negate many of these issues. We demonstrate our approach using otolith chemistry data from Atlantic herring *Clupea harengus* residing in Icelandic waters, and tackle some open questions pertaining to the connections among, and fidelity to nursery areas, and the contribution these make to fished adult populations. We focus on the Icelandic summer spawning (ISS) herring stock,

one that continues to support an important winter fishery for Iceland (Jakobsson and Stefánsson 1999; ICES 2018) despite undergoing substantial decline in recent years due to a combination of long-lasting and severe *Ichthyophonus hoferi* outbreaks (Óskarsson et al. 2018a), poor recruitment and two mass-mortality events triggered through oxygen depletion in a small fjord in which the majority of the adult biomass overwintered in 2012/2013 (ICES 2017; Óskarsson et al. 2018b).

Following larval dispersal from spawning grounds, ISS herring settle in nurseries (often inshore, within fjords) that are distributed widely across the Icelandic coast (see Figure 1). The current life-history model contends that juveniles exhibit strong fidelity to these nurseries through their first two years of life (Guðmundsdóttir et al. 2007). They then leave at age 3 to join the adult component of the stock, which is targeted with purse-seine and pelagic-trawl gears on the wintering grounds between October and January (ICES 2018). The ecological significance of these nurseries as recruitment sources for the ISS stock remains uncertain. Indeed, although some areas are thought to be consistently important (see Guðmundsdóttir et al. 2007), a paucity of quantitative data on the spatio-temporal structure of the nursery populations has constrained our ability to estimate nursery-specific contributions to the fished wintering populations, and hampered efforts to identify and hence protect key recruitment sources. This is a sub-optimal situation, particularly for a stock already under pressure.

To address these issues, we measured otolith elemental (i.e. Li, Mg, Ca, Mn, Zn, Sr, Ba) and stable isotopic (i.e. $\delta^{13}C$, $\delta^{18}O$) concentrations in three age classes of ISS herring captured over three autumns, and developed a modelling framework based around a series of Bayesian multivariate and finite mixture models with three main objectives. 1) To assess the spatial and temporal variability in otolith chemistry of nursery-resident age 1 and age 2 herring across their full distributional range. Specifically, we conduct a sensitivity analysis on simulated data to derive some new, quantitative rules that allow the scale(s) of variability in elemental and stable isotopic markers to be determined. We then classify juvenile populations from each nursery site into putative 'source' populations based on these rules, in conjunction with the spread of site-level posterior densities derived from the multivariate models. 2) To use the derived source classifications to test the long-standing hypothesis that following settlement, juveniles are retained within the same nursery between the ages of 1 and 2, prior to joining the adult population at age 3. And 3), to estimate the contribution of each source population sampled for age 2 fish in 2014 to a population of age 3 fish captured in the winter fishery in 2015. In relation to this third aim, we ask two questions. First, do geographically 'close' nurseries contribute more to adult populations? And/or, do nurseries with a greater density of juveniles, taken as a proxy for nursery 'quality', contribute more to adult populations (*sensu* the 'nursery-role hypothesis' – Beck et al. 2001)?

By estimating nursery connectivity, nursery fidelity and nursery-specific contributions to the fished ISS herring population, this work provides fundamental data needed to balance conservation, and fishery-management priorities in the region. In addition, we demonstrate a novel and generalisable modelling approach for exploring multivariate group differences in a Bayesian context, one applicable to other species, systems and settings for which continuous multi-response data are available.

Materials and methods

Fish sampling

Juvenile age 1 (i.e. ~15 months old) and age 2 (i.e. ~27 months old) ISS herring were collected from inshore nursery areas across the Icelandic coast, over three consecutive autumns (i.e. 2013, 2014, 2015) (Table 1, Figure 1). Sampling took place in October and November each year during the annual juvenile herring (acoustic and trawl) and northern shrimp *Pandalus borealis* (trawl) surveys that provide recruitment/biomass indices for these species. Juvenile herring are a common bycatch item in the shrimp trawls. We used a standard shrimp bottom trawl of 1010 meshes, with the cod-end comprising a 37-mm diamond-mesh. Tows were conducted during daylight hours, covering between 0.5 and 1.2 nautical miles, with the vessel travelling at ~2 knots. Upon capture, fish were measured for standard length (SL) (± 1 mm), and frozen for transport to the University of Iceland.

In addition, we obtained a sample of age 3 (i.e. ~40 months old) ISS herring (n = 79) from a fishing vessel operating in Kolluáll, west of Iceland, in November 2015 (Figure 1). Fish were frozen immediately upon capture and returned to the University of Iceland for processing. Each fish was measured for SL (± 1 mm) and the sex determined through examination of gonads, if visible, following Bucholtz et al. (2008).

Otolith preparation and analysis

We describe our otolith preparation and analysis steps in brief here, and refer readers to Supplement 1 for further details, including information on instrumentation, standards, analytical precision and detection limit calculations. Sagittal otolith pairs were removed, cleaned of adhering tissue, rinsed thoroughly with Milli-Q – Type 1 Ultrapure water (Merck: www.merckmillipore.com/AU/en) and stored dry in 0.5-ml polypropylene microtubes. We mounted one sagitta from each fish in thermoplastic glue (Crystalbond™) on an acid-washed glass slide, polished it to within 10-15 µm of the primordium in the sagittal plane, and verified the fish's age in years through examination of annual growth increments viewed under reflected light at 20× magnification, and following standard ageing methods (Penttila and Dery 1988). We then used laser ablation-inductively coupled plasma-mass spectrometry (LA-ICP-MS) to measure the concentrations of seven elemental markers (i.e. ^{7}Li, ^{25}Mg, ^{43}Ca, ^{55}Mn, ^{66}Zn, ^{88}Sr, ^{138}Ba) in a ~40-µm wide × 11-µm deep disc of otolith material at the dorsal margin at a position equidistant between the pararostrum and antirostrum. These are termed 'El_{edge}' samples (Table 1). We estimate that these discs reflected otolith material accreted during the final < 2 weeks of each fish's life (see **Paper III**). For age 2 and 3 samples, we used a 40-µm spot size to ablate material accreted 1-year prior to the capture date, again at the midpoint between the pararostrum and antirostrum. These are termed 'El_{mid}' samples (Table 1), and for each individual are representative of a < 2 week period of nursery residence experienced one-year earlier.

The second sagitta from each fish was prepared for analyses of stable carbon and oxygen isotope ratios (i.e. $\delta^{13}C$, $\delta^{18}O$). Individual age 1 otoliths were ground to a fine powder in a mortar and pestle, with between 0.05 and 0.1 mg of the resulting powder analysed using isotope ratio mass spectrometry (IRMS). Each powder sample represented a full lifetime (i.e. ~15-month) record of $\delta^{13}C$ and $\delta^{18}O$ for each age 1 fish, and these are expressed as 'C/O_{whole}' samples throughout (Table 1). Age 2 otoliths were sub-sampled. We used a high-resolution MicroMill system to plot a 200-µm wide × ~25-µm deep drill path along the otolith edge

(see Supplement 1 for details). Again, between 0.05 and 0.1 mg of powder was analysed per sample using IRMS, encompassing otolith material deposited during the last ~2 months of life (Clausen et al. 2007). These are termed 'C/O_{edge}' samples (Table 1). We kept the same drilling parameters for the age 3 otoliths, this time sampling growth increments laid down 1-year prior to capture, i.e. as nursery-resident two year olds. We milled from the rostral end of the otolith along a path parallel to the ventral margin towards the postrostrum, and collected 0.05 and 0.1 mg of powder per sample, reflecting ~2 months of otolith growth deposited within nursery sites the previous year. These samples are termed 'C/O_{mid}' samples.

Elemental data are expressed as molar ratios to Ca throughout (e.g. Li:Ca), with stable isotopic measurements reported relative to the Vienna Pee Dee Belemnite (VPDB) reference standard, and expressed in δ-notation (in ‰). Note that second sagittae were not available for age 1 herring captured in 2014. In addition, sample sizes were often lower for stable isotopic measurements compared with elemental measurements due to technical issues with the MS operation and consequent loss of samples (Table 1). We consider these data as 'missing completely at random' (Rubin 1976).

Statistical analysis

Exploring spatial and temporal variation in otolith chemistry

We developed a series of multivariate linear models to assess variation in juvenile ISS herring otolith chemistry among nursery sites, and among sampling months and years. Models were fitted in a Bayesian framework using Markov Chain Monte Carlo (MCMC) sampling in the 'MCMCglmm' R package (Hadfield 2010). Our models comprised six or eight response variables (i.e. Li.Ca, Mg:Ca, Mn:Ca, Zn:Ca, Sr:Ca, Ba:Ca, $\delta^{13}C$, $\delta^{18}O$), with 'site' or 'year' included as fixed effects. Given recent evidence for strong ontogenetic influence on otolith chemistry in juvenile ISS herring (**Paper III**), we chose to model age-specific spatial variation in otolith chemistry among nursery sites, and built separate models for each year of the study (i.e. 2013, 2014, 2015). This resulted in six final models incorporating all age-class/year combinations. At four nursery sites, we captured juveniles of the same age-class in two or more consecutive years at the same location, so we fitted an additional four models (i.e. one per site) to explore evidence for temporal stability in otolith chemistry at an annual time scale.

In each model, we removed the global intercept to directly obtain site-level and year-level posterior densities for each elemental and stable isotopic marker. We used the model outputs to estimate the scale of spatial and temporal variability in otolith chemical signatures across the full distributional range of the juveniles, creating a framework for characterising 'source' population structure for later assessment of source contribution to a 'mixed' adult population (see 'Mixed stock analyses' below). All analyses were run in R 3.5.1 (R Core Team 2018). Datasets and R code to reproduce these analyses are available from the Dryad Digital Repository.

Exploratory data analysis

Prior to model fitting, the distributions of the response variables were visualised and screened for potentially influential values. Four El_{edge} samples with large values on Li:Ca and/or Mn:Ca and Zn:Ca were detected, identified as measurement errors, and removed from

subsequent analysis. Elemental ratios were natural log transformed, which improved the normality of residuals and stabilised the error variance in subsequent modelling. $\delta^{13}C$ and $\delta^{18}O$ values were left untransformed. All response variables were then scaled to have mean = 0, SD = 1 (Hadfield 2010). Multivariate normality was checked using functions in the 'MVN' package, and we screened for multivariate outliers based on robust Mahalanobis distances (Korkmaz et al. 2015). The assumption of homogeneity of variance-covariance matrices was assessed using Box's M test in the 'biotools' package (da Silva et al. 2017).

Model fitting

We fitted each model to the data three times, obtaining three independent Markov chains initialised using dispersed values. We ran each chain for 250,000 iterations, discarding the first 50,000 as burn-in, and using the remaining 600,000 samples to calculate posterior summaries. Chain convergence was assessed through inspection of trace plots and by computing Gelman-Rubin diagnostics ($\hat{R}$). Autocorrelation between successive samples was explored using the set of 'autocorr' functions in the 'coda' package (Plummer et al. 2006). Finally, we calculated Monte Carlo standard errors for all estimated parameters using overlapping batch means in the 'mcmcse' package (Flegal et al. 2017).

Priors

We assigned vague normal priors N(0, 1000) for the 'site' or 'year' effects and an inverse gamma (IG) prior with shape = scale = 0.001 for the residual variance. This latter prior is equivalent to an inverse Wishart (IW) with scale = 1, and degree-of-belief parameter = 0.002, and is weakly informative when the posterior distribution does not have large support near 0 (see Appendix S2 in **Paper III** for a sensitivity analysis on prior choice).

Model checking

For each model, we examined the spread of residuals and ran posterior predictive checks as a test of within-sample predictive capacity (Gelman et al. 1996). We generated simulated datasets from each model, and gauged how closely these data matched the observed otolith chemistry by calculating posterior predictive p-values (i.e. ppp-values). These values represent the proportion of simulated means that exceed the empirical means for two test quantities: 1) the mean and 2) the SD of the marker(s) of interest. Values close to 0.5 indicate strong concordance between simulated and observed data distributions.

ΔDIC test of multivariate group differences

For each series of among-site and among-year comparisons, we developed an omnibus test of the degree of difference among multivariate group means based on the deviance information criterion (DIC). Put simply, the test involves fitting two Bayesian multivariate models: 1) an intercept-only 'null' model, and 2) an 'effects' model, including a 'site' or 'year' effect, and using the DIC to test if the addition of the 'site' or 'year' term improves model fit compared with the null model.

To gauge the sensitivity of this DIC-based test, we simulated 500 multivariate normal datasets reflecting scenarios typically encountered by otolith chemistry researchers wanting

to assess variation in otolith chemical signatures among 'groups'. To clarify, 'groups' in this context could refer to spatially-distinct sampling sites, or sampling years, among other possibilities. We explored a series of plausible scenarios ranging from 1) no differences, to 2) substantial differences among multivariate group means. We varied the number of groups **n_group** = (2, 3, …, 8); the number of samples within each group **n_sample** = (10, 20, 50); and the number of response variables **rv** = (2, 3, …, 8) in our datasets to encompass the scale of most studies focussed on population delineation using otolith chemistry analyses. Each response variable, representing a simulated elemental or stable isotopic marker, was drawn from a normal distribution with mean μ_{n_group} and common standard deviation $\sigma = 0.5$. Note, we found that varying σ, within- or among-groups had minimal influence on our results.

For each of the simulated datasets, we next ran a one-way MANOVA using the 'lm' function in the 'stats' package, and two Bayesian multivariate models in the 'MCMCglmm' package, using the same priors as stated earlier. To reiterate, the Bayesian models fitted were 1) 'null' models (i.e. no group-level effects), and 2) 'effects' models (i.e. group-level effects included). Our expectation was that if the null hypothesis of no group-level differences is supported by a non-significant MANOVA result (i.e. at $\alpha = 0.05$), the DIC of the 'null' model would be < DIC of the 'effects' model, and vice versa if a significant MANOVA result is returned. If this expectation did not hold, then we trusted that our simulations would expose the consistency of the change in DIC (denoted ΔDIC) between 'null' and 'effects' models. This could be then be related to a range of specified α levels (i.e. 0.001, 0.01, 0.05, 0.1) as returned directly from Pillai's trace statistics in the MANOVA models. Hence, our approach provides some rules of thumb by which the DIC could be used to understand the magnitude of group differences in a Bayesian modelling setting. Full R code for this analysis can be accessed in the Dryad Digital Repository.

Characterising source distributions for use as a baseline

In instances where our ΔDIC test indicated a strong difference among site (or year) means in multivariate space, we developed a *post-hoc* test to determine which sites (or years) differed and on which markers. For each age-class and year separately, we examined the overlap in posterior densities for each marker among all sampled nursery sites. Where 95% highest posterior density credible intervals (hereafter, 95% CIs) overlapped for all markers included in the model, we pooled data from these sites, forming a smaller number of better characterised sources for use as 'baseline' samples in subsequent mixed stock analyses.

Next, we drew samples (n = 100) at random from each source's posterior marginal distributions for each otolith chemical marker, in order to appropriately characterise marker variability within each source. A key advantage of the Bayesian approach for characterising sources in this way is that the models return the full distribution of parameters of interest, allowing us to draw samples of any size from this distribution. This confers at least two benefits: 1) It reduces the influence of sampling bias, as we are not constrained by small samples sizes at certain sites that may be wholly due to patchy or limited sampling coverage rather than the actual density of fish present; and 2) we can assign prior probabilities for source contribution that are consistent with ecological theory, are based on previous data, or are designed to test specific hypotheses concerning source-sink dynamics.

Mixed stock analyses (MSA)

We ran two sets of analyses to assess the relative contribution of the sampled nursery sources (n = *K*) to mixed samples of juveniles or adults of unknown origin. In the first set (i.e. *Nursery retention tests*) we tested the hypothesis that age 2 juveniles have remained within the nursery areas they resided in at age 1. Such tests were possible at five sites in which age 1 herring were captured in one year (i.e. year *t*), and age 2 herring were captured from that same site the following year (i.e. $t + 1$). The five mixed samples of age 2 herring are denoted: $Ísa_m$, $Öxar_m$, $Arna_m$, $ÍsaD4\text{-}50_m$ and $ÍsaD4\text{-}60_m$ (see Table 1 for reference, data highlighted in bold). We treated the El_{mid} data from age 2 fish captured in $t + 1$ as the mixture, with the El_{edge} values from all age 1 fish captured in *t* used as a baseline of possible sources. Assuming all possible sources are adequately characterised, if the capture site is the most likely source, this provides strong evidence of nursery-site fidelity following settlement (at least between age 1 and age 2). This approach enabled us to estimate rates of staying or straying in nursery-resident juveniles.

In the second set of analyses (i.e. *Adult assignment tests*), we treated the El_{mid} and C/O_{mid} data from the fishery-caught age 3 herring as the mixture, denoted $Kolluáll_m$, and estimated the relative contribution of seven putative source populations to this population of first-time wintering adults. The baseline samples in this case comprised the El_{edge} and C/O_{edge} values from age 2 herring captured on the nursery grounds during October/November 2014.

We fitted a series of Bayesian finite mixture models implemented in the 'MixSIAR' R package (Stock and Semmens 2016a; Stock et al. 2018) to estimate source contributions to the mixed samples, and to quantify the uncertainty (i.e. 95% CIs) around these estimates.

Priors for MSA

Priors were needed for the vector of source proportions $\mathbf{p} = (p_{1, \ldots, p_k})$ contributing to a mixed sample. In instances where two putative sources (i.e. $K = 2$) were defined, we specified a uniform prior, U(0, 1), on p_1, making all potential combinations of p_1 and p_2 equally likely *a priori*. When $K > 2$, we used the Dirichlet distribution to place a prior on **p**. The Dirichlet distribution is defined by a vector of concentration parameters $\boldsymbol{\alpha} = (\alpha_1, \ldots, \alpha_k)$, and we set each element of $\boldsymbol{\alpha} = 1$. This prior is considered uninformative on the simplex, giving equal probability to all possible sets of source proportions.

As the variance in each source distribution is directly incorporated through our posterior draws, we decided not to consider process error in our models, and instead, included a 'residual error only' structure for the mixture variance $\boldsymbol{\Sigma}$. Here, $\boldsymbol{\Sigma}$ is given an IW prior, where $\boldsymbol{\Sigma} \sim \text{IW}(\mathbf{I}, J + 1)$, **I** is the identity matrix and *J* is the number of otolith chemical markers included in the model (see Stock and Semmens 2016b; Stock et al. 2018: Supplemental material for details and alternative error structures).

MSA model fitting and checking

The mixture models were implemented using JAGS 4.3.0 (Plummer 2003 – www.sourceforge.net/projects/mcmc-jags) called from R, making use of the 'rjags' (Plummer 2016) and 'R2jags' (Su and Yajima 2015) packages. For each fitted model, we obtained three independent Markov chains of 100,000 iterations each, discarding the first

20,000 as burn-in on each chain. We used a thinning interval of 10, and collated the remaining 3 × 8,000 = 24,000 samples for calculation of posterior summaries. We assessed chain mixing and autocorrelation, and calculated Monte Carlo standard errors for all parameters following the procedures outlined earlier for the 'MCMCglmm' models.

Relationships between source contribution, distance and density of age 2

To test if nursery source contribution scaled with the proximity of source populations to the overwintering grounds, we used Google Earth Pro (www.google.com/earth/versions/#earth-pro) to measure the minimum distance by water (± 0.01 km) from each source location sampled in autumn 2014 to the fishery capture location at Kolluáll (see Figure 1). We then modelled source contribution as a linear function of distance from the overwintering grounds. To test if juvenile densities in the nurseries influenced source contribution, we extracted nursery-specific counts of age 2 herring estimated from acoustic surveys conducted aboard RS Dröfn in November 2014 (see Óskarsson and Reynisson 2015 for datasets used), and used a linear model to explore the relationship between source contribution and the % (by nursery) of the total density of age 2 surveyed.

Results

Sampling and analytical coverage

Our sampling targeted the major nursery grounds for juvenile ISS herring across the three years of the study (Figure 1). The bulk of the juveniles were collected from fjords on the north and west coasts of Iceland, with some age 2 herring also encountered off the south-east and south-west coasts (Figure 1, Table 1). A total of 207 age 1 fish were captured, 206 otoliths of which were analysed for El_{edge} and 42 for C/O_{whole} (Table 1). Some 255 age 2 fish were collected, all otoliths of which were analysed for El_{edge}, with 250 and 158 age 2 otoliths analysed for El_{mid} and C/O_{edge}, respectively. Missing El and C/O analyses were due either to measurement errors or instrumental issues, as described earlier. All 79 age 3 herring captured by the fishery at Kolluáll were analysed for El_{mid} and C/O_{mid}. Substantial length variation was evident within each age-class (i.e. age 1: 55–118 mm SL, age 2: 97–149 mm SL [see Table1], age 3: 170–250 mm SL). Our age 3 sample contained a predominance of males (n = 65), six females and eight fish of indeterminate sex.

Model diagnostics

The individual Markov chains obtained for the estimated parameters displayed low serial dependence at lag one in all fitted models. Values of $\hat{R}$ were always < 1.01, indicating chain convergence to the target distribution and reliable samples for computing posterior summaries. Monte Carlo standard errors were < 0.1 in all cases. Posterior predictive checks revealed no major discrepancies between simulated observed data distributions, with ppp-values for the mean (± 1SE) = 0.53 (± 0.01), and for the SD (± 1SE) = 0.56 (± 0.01) calculated across all MCMCglmm models.

Sensitivity of the ΔDIC test

Our ΔDIC test proved reliable in detecting the magnitude of multivariate group differences for scenarios involving between 2 and 8 multivariate normally distributed response variables (rv's), sampled from between 2 and 8 groups, at sample sizes of 10, 20 and 50 per group (Figures 2, 3). The overall spread of ΔDIC values in the simulations increased with the number of rv's, with the number of groups included in the model, and with the number of observations within each group (Figure 2). We expected *a priori* that if the null hypothesis of no significant group-level differences was true, then the ΔDIC value would be negative. This was true in the vast majority of cases, but not always (e.g. see data above the horizontal zero lines, and right of the vertical dashed p = 0.05 lines in Figure 2). However, the consistency of our results allowed us to develop some guidelines for assessing multivariate differences when fitting Bayesian multivariate linear models. To illustrate, with reference to Figure 3, in a hypothetical study aimed as assessing multivariate differences in otolith chemistry among say four nursery sites, with 20 fish sampled per site, a ΔDIC value > -5 would indicate a significant difference among sites at $\alpha = 0.05$ in 100% of cases. In the same study, a ΔDIC value of > 20 would be needed to ensure (with 100% confidence) a significant site-level difference at $\alpha = 0.001$ (see Figure 3). By contrast, when n = 10 at each of these four sites, any ΔDIC value < -5 would signify a non-significant difference at $\alpha = 0.05$ in 100% of cases.

Spatial (and monthly) variation in age 1 otolith chemistry

Age 1 otolith chemistry varied strongly among nursery sites sampled in 2013 and 2014, but not in 2015, as revealed through ΔDIC values and examination of site-level posterior densities (Figure 4)[1]. Although age 1 herring were captured from just three sites in autumn 2013, we found evidence of variation in otolith chemistry at a coast-wide (i.e. among-fjord) scale across the north coast. Fish from site 531 (Öxarfjörður) were generally lower in most markers compared with individuals from 529 (Ísafjarðardjúp) and 530 (Eyjafjörður). The latter two sites could not be clearly separated, with 95% CIs overlapping for all eight elemental and isotopic markers included in the model (Figure 4, left-hand panels). Among-site variation was driven mainly by Li:Ca, Mn:Ca and $\delta^{13}C$.

Age 1 herring were sampled from nine nursery sites during autumn 2014 (Table 1). Again, we found marked variation in site-level El_{edge} values at a coast-wide scale, with the strongest differences seen in Li:Ca and Mn:Ca (Figure 4, middle panels). In general, El_{edge} values were more similar in juveniles sampled from Arnafjörður and Ísafjarðardjúp than those captured at sites in Miðfjörður, Eyjafjörður and Öxafjörður. We observed some overlap in otolith chemical signatures in geographically-close sites (i.e. within a fjord). For example, age 1 herring from sites D7-C and D7-B (both in Arnafjörður) could not be separated (at the 95% credible level) on all six elemental markers, with a similar pattern evident for sites D7-A and D7-B, and for D9-7 and D7-C (all located in Arnafjörður). However, within-fjord differences were seen in some instances; age 1 El_{edge} values in fish from D7-A and D7-B (both in

[1] In Figures 4 and 5, note that the y-axes for all markers within a year (i.e. within each column) are kept consistent, and although the values on the x-axes may differ, their ranges are consistent. This allows a direct comparison to be made of the shapes of the densities for each nursery site and otolith chemistry marker within a year. The same logic applies for the temporal analyses (see Figure 6).

Arnafjörður) were substantially higher than those from D9-7 (Arnafjörður) (Figure 4), despite being separated by < 14 km by water.

The near-identical location of sites D7-A (Arnafjörður, sampled mid-October 2014) and D9-7 (Arnafjörður, sampled mid-November 2014), and sites D7-92 (Isafjarðardjúp, sampled mid-October 2014) and D9-6 (Isafjarðardjúp, sampled mid-November 2014) gave us an opportunity to investigate this within-fjord variation in further detail. Indeed, we were able to test for monthly variation in El_{edge} values in age 1 herring within these two nurseries. Fish from each pair of sites displayed marked differences in Li:Ca (Figure 4), indicative of temporal shifts in this otolith marker at a monthly scale, though in the case of D7-92 and D9-6, which were separated by ~1.5 km, fine scale spatial differences cannot be ruled out.

Age 1 herring were captured from two sites in 2015. We detected slightly lower El_{edge} Li:Ca and Zn:Ca in Hrútafjörður (site D5-18) compared with the adjacent Miðfjörður site (D5-19), with otoliths from Miðfjörður exhibiting lower Mn:Ca values. These differences were not sufficient to separate the two sites at the 95% credible level (Figure 4, right-hand panels).

Spatial variation in age 2 otolith chemistry

Spatial variability in age 2 otolith chemistry generally increased with geographic distance among nursery sites. Age 2 juveniles were captured from five sites in the autumn 2013 surveys. Fish from D1-2 in Breiðafjörður were lowest in El_{edge} Li:Ca, Mg:Ca, and C/O_{edge} $\delta^{13}C$ and $\delta^{18}O$, and could be delineated from all other sites at the 95% credible level based on one or more of the abovementioned markers (Figure 5, left-hand panels). Sites D5-102, D5-110 and D5-115, all located in close proximity to one another in Ísafjarðardjúp, could not be separated on any of the eight markers considered. Again, we found some evidence of within-fjord variation; herring from site 529 (also in Ísafjarðardjúp) exhibited lower Mg:Ca than those from D5-110. However, fish from both sites differed little on all other markers.

The nine nursery sites sampled for age 2 fish in 2014 covered the full distributional range of ISS herring juveniles. Preliminary analyses revealed that posterior densities from the three capture sites located offshore southwest of Iceland (i.e. Vestmannaeyjar, Jökuldjúp north and south) overlapped strongly on all eight markers, so we pooled these data into a single 'SW' site for further analysis. Each of the resulting seven sites was clearly distinguishable (at the 95% credible level) based on variation in one or more of the measured otolith chemical markers (Figure 5, middle panels). Site-level differences were most pronounced in Li:Ca, Mn:Ca, $\delta^{13}C$ and $\delta^{18}O$.

The four nursery sites from which age 2 juveniles were collected in 2015 overlapped in seven of eight otolith chemical markers analysed at the otolith edge (Figure 5, right-hand panels). Li:Ca exhibited the greatest site-level variability (i.e. D5-18 in Hrútafjörður was higher than D4-50 and D4-60, both in Ísafjarðardjúp, at the 95% credible level). D4-50, D4-60 (both in Ísafjarðardjúp) and D4-14 (Arnafjörður) could not be separated based on all markers at the 95% credible level. Similarly, D5-18 in Hrútafjörður was indistinguishable from D4-14 in Arnafjörður on all markers.

Annual variation in otolith chemistry

We found strong differences among years in most elemental markers at three out of four sites for which multi-year data were available (Figure 6). In Ísafjarðardjúp, age 2 fish captured in 2013 exhibited markedly higher Mg:Ca and Zn:Ca concentrations compared with those sampled in 2014 and 2015. There was also substantial variation in Sr:Ca at this site across the three sampling years, and in $\delta^{13}C$ between 2013 and 2015 (Figure 6, left-hand panels). In Arnafjörður, age 2 fish captured in 2014 and 2015 differed dramatically in Mn:Ca and Zn:Ca, but displayed similar Sr:Ca and Ba:Ca concentrations. $\delta^{13}C$ and $\delta^{18}O$ differed slightly between years, but could not be separated at the 95% credible level (Figure 6, middle-left panels).

Annual variation in El_{edge} was greatest in Miðfjörður (Figure 6, middle-right panels). Li:Ca, Mg:Ca and Mn:Ca were substantially lower (at the 95% credible level) in 2015 compared with 2014. Zn:Ca and Sr:Ca were higher in 2015, but credible intervals for these two markers' distributions overlapped between years. Ba:Ca did not vary through time. A degree of temporal stability was evident in Eyjafjörður, with 95% CIs for all elemental markers in the 2013 samples overlapping those of the 2014 samples (Figure 6, right-hand panels).

Source classifications

The MSAs we wished to conduct necessitated the creation of three 'baseline' datasets comprising otolith chemistry data representative of the putative source populations. For the *Nursery retention tests*, we derived two baseline datasets. The first (i.e. Base1) comprised El_{edge} and C/O_{whole} data for age 1 juveniles captured in 2013. Informed by the spread of the nursery-site level posterior densities (see Figure 4, left-hand panels), we defined two potential sources, classifying site 531 in Öxarfjörður as a north-eastern source, denoted $Öxar_s$, and combining sites 530 (Eyjafjörður) and 529 (Ísafjarðardjúp) into a north/north-western source (i.e. Eyja / $Ísa_s$) (Figure 7a). Our second baseline dataset (i.e. Base2) comprised El_{edge} data from age 1 fish captured in autumn 2014. As D7-92 (Ísafjarðardjúp) and D7-C (Arnafjörður) could not be separated based on all six elemental markers, we chose to exclude these sites. This could be justified as follows. D7-92 exhibited strong overlap with D9-6 in all elements except Li:Ca, so fish from D9-6 would capture the main characteristics of D7-92. Moreover, marker densities for site D7-C closely mirrored those of D7-B and/or D9-7 (Figure 4, middle panels). This left five source populations for Base2: a combination of D7-A and D7-B in Arnafjörður (i.e. $Arna_s$), D9-4 in Eyjafjörður (i.e. $Eyja_s$), D9-6 in Ísafjarðardjúp (i.e. $Ísa_s$), D7-154 in Miðfjörður (i.e. $Mið_s$) and D7-140 in Öxarfjörður (i.e. $Öxar_s$) (Figure 7b).

A third baseline dataset (i.e. Base3) was needed for the *Adult assignment tests*. Base3 comprised El_{edge} and C/O_{edge} data from age 2 fish captured in 2014. Given that each of the seven nursery sites could be clearly delineated based on the posterior densities of the otolith markers (Figure 5, middle panels), we opted to treat each site as a separate source population, and coded these as follows: D7-B in Arnafjörður ($Arna_s$), D9-6 in Ísafjarðardjúp (i.e. $Ísa_s$), D7-154 in Miðfjöður ($Mið_s$), D7-140 in Öxarfjörður ($Öxar_s$), D7-113 in Skagafjörður ($Skag_s$), B7-466 in Breiðamerkurdjúp (i.e. $SthEast_s$) and the SW sites (i.e. $SthWest_s$) (Figure 7c).

Mixed stock analyses

The *Nursery retention tests* were designed to gain inference on rates of nursery-site fidelity in juvenile herring aged between 1 and 2 years old. We estimated nursery contribution to five 'mixed' samples of age 2 fish captured in 2014 and 2015 (see bolded data in Table 1), and in three out of five cases, showed that the major contributor to these mixed populations was the nursery from which they were captured (see '$Ísa_m$' in Figure 7a, '$Arna_m$' and '$Ísa.D450_m$' in Figure 7b). In the remaining two cases, the major contributor was the next most geographically-close nursery (see '$Öxar_m$' in Figure 7a, '$Ísa.D460_m$' in Figure 7b).

The *Adult assignment tests* revealed a relatively even contribution from the seven putative source populations to the mixed population of age 3 herring captured by the fishery in Kolluáll (Figure 7c). Nurseries off the south-east coast ($SthEast_s$), in Miðfjörður ($Mið_s$) and in Arnafjörður ($Arna_s$) were estimated to contribute most, although all sources had a non-zero contribution (Figure 7c). Finally, we found no relationships between source contribution and both the geographic distance of the source from the overwintering location, and the nursery-specific densities of age 2 herring estimated from the acoustic surveys (Supplement 2: Figure S1).

Discussion

In this study we developed some quantitative rules for assessing the scale of spatial and temporal variation in otolith chemistry within a Bayesian modelling framework, and applied them to data spanning the entire geographic range of a commercially-harvested herring stock. Our findings offer several novel insights into the structure and connectedness of juvenile and adult populations of ISS herring. Namely, we show that population-level differences in otolith chemical markers generally scale with both geographic distance among nursery sites, and time between sampling bouts, resulting in patterns of coast-wide heterogeneity in marker expression that vary through time. This information allowed us to define the structure of source populations of ISS herring around Iceland in a statistically robust manner, building confidence in outputs from mixture models designed to estimate source identity for fish of unknown origins. Such models here confirmed a tendency for juvenile herring to exhibit strong year-to-year fidelity to nursery sites, and demonstrated the importance of multiple nurseries as sources for a component of the fished adult population.

Quantifying the scale(s) of otolith chemical variability

For commercially-harvested marine fishes, reliable information on how populations of conspecifics connect across an ocean scape allows management units to be aligned more closely with the true scales of ecological processes. The life-time sensitivity of morphological and chemical traits stored in otoliths to environmental, physiological, metabolic and/or genetic factors (Campana and Casselman 1993; Høie et al. 2003; Cardinale et al. 2004; Grammer et al. 2017; Izzo et al. 2018) underscores the benefits of using these structures to guide spatial management decisions (e.g. Burke et al. 2008; Rooker et al. 2008; Libungan et al. 2015). Yet, to fulfil otoliths' full potential along these lines, appropriate modelling approaches are needed – approaches informed by knowledge on the intrinsic and extrinsic mechanisms governing chemical incorporation into otoliths, while concurrently accounting for data- and model-related uncertainties. Here, we present such a modelling

framework, one that allows the spatial and temporal scale of otolith chemical trait variability to be accurately defined. Focussing on the ISS herring stock, our approach harnesses new information regarding ontogenetic influences on elemental uptake (**Paper III**) and, guided by results from simulation tests, quantifies how individual-level variation in otolith chemical traits translates to variability among spatially- and/or temporally-separated populations.

Our simulations highlight the efficacy of an omnibus test for multivariate group differences based on ΔDIC between 'null' and 'effects' models; the sensitivity of this test allowing quantitative rules of thumb to be developed upon which the scales of multivariate trait variation among putative groups could be estimated with high confidence. Although the scenarios we tested reflected the numbers of groups, response variables, and sample sizes typically encountered in otolith chemistry applications, the derived rules are equally applicable to any situation where trait variation among groups is of interest, and for which individual-level, continuous, multi-response data are available. We focussed on one-way multivariate linear models in these simulations, with 'group' acting as the single fixed effect. This reflected our needs in exploring 'site' or 'year' effects in models fitted to the empirical otolith data. However, the R code we provide could be easily modified to generate similar rules for more complex suites of models, involving multiple fixed and/or random effects.

We adopted these rules in evaluating output from models fitted to El_{edge}, C/O_{edge} and C/O_{whole} data derived from nursery-resident juvenile ISS herring sampled across their full geographic range, over three years. Informed by recent work on this herring stock that found consistent negative effects of fish age on otolith elemental composition, particularly for Li:Ca, Mg:Ca, Mn:Ca and Sr:Ca (**Paper III**), we elected to model each age class separately. This decision enabled us to generate cohort-specific atlases of individual- and population-level trait variability around Iceland that could be compared among months or years at nursery sites for which a particular age class was captured at more than one time point (i.e. to assess the degree of temporal stability in chemical trait expression). Though we accounted for age-related influences on trait expression in our models, the concentrations of several elemental and stable isotopic markers within otoliths are also known to be under strong environmental (e.g. salinity, temperature, water chemistry, pH) control (Elsdon and Gillanders 2004; Martin and Wuenschel 2006; Mirasole et al. 2017), either directly, or indirectly through synergies between environmental and intrinsic processes (see Holt and Jørgensen 2014). Therefore, owing to the island-wide distribution of the nursery sites, many of which are located inshore within fjords fed by rivers that arise in different geological zones, and may vary dramatically in water chemistry (Gíslason et al. 1996; Kristmannsdóttir et al. 2002; Louvat et al. 2008), we still expected to find spatial and temporal heterogeneity in otolith chemistry at the population level. We also expected that island-wide patterns in otolith chemistry would be partly shaped by the steep north-south temperature and inshore-offshore salinity gradients that characterise the local oceanography (Valdimarsson et al. 2012; Logemann et al. 2013), potentially leading to broader-scale differences between inshore and offshore populations.

Indeed, our models exposed marked spatial differences in El_{edge} data among nursery populations (particularly in Li:Ca and Mn:Ca) and less dramatic, but still notable spatial differences in C/O_{edge} and C/O_{whole} for both juvenile cohorts in two out of three years of sampling (Figures 4, 5). Moreover, population-level variability in edge Mg:Ca was greater for age 2 versus age 1 herring, with differences in concentrations of most elemental markers, $\delta^{13}C$ and $\delta^{18}C$ generally increasing with distance between nursery sites across both cohorts. Additionally, we observed strong temporal variation in otolith chemistry at four out of five

sites for which longitudinal sampling of a particular age-class was possible (see Figures 4, 6). Taken together, our results point to a pattern of coast-wide variability in otolith edge chemistry for nursery-resident juvenile herring, one that is temporally dynamic at monthly to annual scales. In the spatial dimension, this scale of marker heterogeneity accords well with predictions from spatially-explicit models of juvenile ISS herring otolith chemistry that included both ontogenetic and environmental covariates (see **Paper III**). Interestingly, the degree of temporal variability we see here far outweighs that predicted from models presented in **Paper III,** which were based on snapshots of local environmental conditions and nursery population composition. Both of these factors can fluctuate over relatively short time scales, and not considering such fluctuations likely led to underestimation of the system's true temporal variability in those models.

As mentioned previously, the mechanisms underpinning the patterns we observed here are likely manyfold, involving interactions between extrinsic and intrinsic processes (see Grammer et al. 2017; Izzo et al. 2018; Reis-Santos et al. 2018a). The relative influences of such processes are challenging to disentangle, even in light of new insights gained into chemical incorporation pathways and ion-binding dynamics within otoliths (Melancon et al. 2009; Sturrock et al. 2014; Thomas et al. 2017). Yet, irrespective of the precise processes at play, if trait differences do exist, and the scale of these differences is measured appropriately while respecting the mechanistic knowledge at hand, we can still glean crucial information on how individual trait variability manifests at the population level, and how source populations are structured – both central foci in this study.

Individual- to population-level variability

The population- (and year-level) variability in otolith chemistry we detected must arise from characteristics of the individuals captured within them. For example, we observed substantial individual-level differences in the expression of otolith chemical markers within populations captured at the same time point, and from the same location (illustrated by the widths of the 95% CIs for site-level posterior densities in Figures 4 and 5). Such individual-level variability in trait expression is widespread in otolith chemistry studies (Kalish 1989; Macdonald and Crook 2010; Panfili et al. 2015), yet is not often acknowledged explicitly; the factors governing it proving difficult to pin down. In our case, this variation cannot be ascribed to environmental heterogeneity, but could be a function of sample size, fish growth variation within sites and cohorts (see Table 1, Stanley et al. 2015; **Paper III**), and/or inter-individual differences in unmeasured intrinsic factors (e.g. physiology, metabolism) thought to influence otolith chemical composition (Høie et al. 2003; Grammer et al. 2017). Moreover, evidence for inter-individual behavioural plasticity within species and populations is growing (e.g. Crook et al. 2017), and as individual behaviour can feedback to affect growth (Fiksen et al. 2007) and physiology, we suggest that behavioural flexibility within each cohort and nursery site might have also contributed to the individual-, and hence population-level variability in otolith chemical traits we found.

Population mixing: insights into juvenile population structure

Results from the multivariate models also contribute to our understanding of connectivity and mixing among ISS nursery populations, the Bayesian approach allowing uncertainties in data and modelling to be fully incorporated in classifying putative source populations for

subsequent MSAs. Our models, in general, uncovered higher among- versus within-population variance in edge chemistry for age 1 and age 2 ISS juveniles sampled across key nursery areas around Iceland. These findings provided us the information needed to confidently define source population structure for each age-class, and to create appropriate baseline samples based on site-level posterior estimates for each otolith chemical marker (see Materials and methods for details). Ecologically-speaking, they also suggest that juvenile movements among distant nurseries are unlikely, and that long-term nursery retention might be the norm.

This idea was investigated further in the finite mixture models. In the *Nursery retention tests*, we tested the hypothesis of limited mixing among geographically-distant juvenile ISS herring populations; specifically, that juveniles are retained within particular nurseries between the ages of 1 and 2. Our results largely support this hypothesis. Three out of five mixed samples of age 2 herring were assigned with highest probability to the nursery site they were captured from, with the remaining two samples assigned to the next closest nursery (Figure 7a,b). Sites deep within Ísafjarðardjúp and Arnafjörður showed the highest retention rates, while > 80% of age 2 herring captured in Öxafjörður in 2014 were assigned to nurseries in either Eyjafjörður or Ísafjarðardjúp. Although the potential for missing sources to contribute in some years is real, given the sparsity of sampling for age 1 fish (e.g. in 2013), our findings strongly infer a high degree of site-attachment in nursery-resident ISS herring as alluded to by Jakobsson and Stefánsson (1999) and Guðmundsdóttir et al. (2007). Our models also highlight the potential for some mixing between geographically-close populations (e.g. within-fjords); however, embarking on large-scale movements between nurseries further afield, while possible (Figure 7a) appears uncommon during the juvenile phase. We speculate that this strategy may have evolved through energetic and mortality costs associated with long-distance, exploratory behaviour outweighing the potential rewards of finding better 'quality' nursery habitats (see Alerstam et al. 2003), although further work is needed to explore this.

Population mixing: insights into source-sink dynamics

The second part of the MSAs was focussed on the *Adult assignment tests*. Our results demonstrated a relatively even contribution of the age 2 source populations to the mixed sample of age 3 fish (Figure 7c), with no source dominating as a supplier of recruits to the fished population at Kolluáll, west of Iceland. The Kolluáll area provided the bulk of the fishery catch during the 2015/2016 winter season (ICES 2016), but harboured only 10% (by numbers) of the age 3 cohort surveyed acoustically, with the remaining 90% located south and east of Iceland (Óskarsson 2016). We recognise that our age 3 samples are representative of only a small fraction of the age 3 population, yet importantly, we estimated that the $SthEast_s$ (i.e. Breiðamerkurdjúp) source contribute most, despite it being the most distant source (i.e. > 500 km by water) from the Kolluáll wintering grounds.

These findings are indicative of substantial mixing of widely-distributed juvenile populations during their first year of adulthood. Whether this occurs first during the summer spawning period when multiple age classes meet on the spawning grounds south of Iceland (Jakobsson and Stefánsson, 1999) (though only ~ 20% of age 3 are estimated as mature – ICES 2018), during the pre- or post-spawning feeding seasons, or on the wintering grounds themselves, is difficult to tease apart based on our data. However, no clear relationship was found between the magnitude of source contribution and the distance of the source to the

wintering grounds (Figure S1a). And, as long-distances themselves (Alerstam et al. 2003), or the ecological costs associated with crossing them, could be expected to act as impediments to the rapid, large-scale, coordinated movements needed for migrants from disparate sources to unite first on these grounds in October/November, we propose that mixing likely occurs prior to overwintering (see also Geffen et al. 2011).

We also failed to detect a relationship between source contribution and nursery-specific densities of age 2 herring surveyed in 2014 (Figure S1b). We considered juvenile density as a proxy for nursery 'quality' that could be used in a test of the 'nursery-role hypothesis' in ISS herring (Beck et al. 2001). In their seminal paper on clarifying the 'nursery-role concept' in the interests of conservation and management of critical juvenile habitats, Beck et al. (2001) laid out their hypothesis along the lines that under certain conditions, some inshore juvenile habitats contribute disproportionally to the production of individuals that recruit to adult populations. Several requirements need to be met for a formal test of this hypothesis, summarised as follows: 1) geographic separation between juvenile and adult habitats; 2) comparisons of nursery quality must be made on a unit-area basis; 3) all potential juvenile habitats must be sampled; 4) nursery habitats are a subset of juvenile habitats; and 5) movement of individuals from juvenile to adult habitats must be estimated.

The life-history transitions between spatially-discrete juvenile and adult habitats in herring make them ideal test subjects (Geffen et al. 2011; Huse 2016), and indeed, at least three out of five of Beck et al.'s requirements were adhered to in our study (i.e. 1, 3 (possibly), 4, 5). Even so, we found no clear evidence in favour of the nursery-role hypothesis based on the data presented here. All sources contributed to the age 3 population captured at Kolluáll, with posterior mean contributions varying at most by 7.6% (Figure 7c). Furthermore, nursery quality appeared to play little role in shaping source contribution, though this may be a function of how 'quality' was defined. We chose to compare nursery quality based on indices of age 2, rather than age 1 abundance derived from acoustic surveys, the latter index currently favoured in forecasting year-class strength at age 3 in assessment models for the stock (see Guðmundsdóttir et al. 2007; ICES 2017, 2018). Our reasoning relates back to the limited sampling coverage of age 1 herring in 2013 (see Table 1) which precluded their use in the *Adult assignment tests*, and to the island-wide sampling of age 2 in 2014 from which we generated a larger, more robust baseline sample. As the age 2 otolith data was used to estimate nursery contribution, we felt that nursery-specific age 2 densities provided the most direct proxy for characterising nursery quality in this instance.

Whether these trends are specific only to the fishery in 2015, or are more general, we cannot say at present. However, they suggest either that our density metric was a poor proxy for nursery quality, that nursery quality per se is not of critical importance in this system, that key source populations were missed or inaccurately characterised (see requirement 3, and below), and/or that the environmental and migratory flexibility displayed by herring (Maravelias and Reid 1997; **Paper II**) shrinks the reliance on any particular nursery for recruit supply, an adaptation that may increase the resilience of the stock to local perturbations. We suggest that the answer lies in a combination of these factors – factors that an expansion of the present work over a number of years might disentangle.

Otoliths as management tools

The propensity for conspecifics of differing origins to mix at certain life stages is well known in fishes (e.g. Grabowkski et al. 2012), including herring (Fridriksson and Aasen 1950; Brophy and Danilowicz 2002; Husebø et al. 2005; Johannessen et al. 2009; Geffen et al. 2011), a situation that can pose serious challenges to effective spatial management when data on population origins and mixing rates are few. For example, in Icelandic waters, adult ISS herring commonly mix with the Norwegian spring spawning (NSS) stock during the summer feeding period off the east coast (Óskarsson 2018). Examination of maturity stage is the traditional approach to delineating these two stocks for management purposes. Yet, the method lacks precision, motivating recent refinements in otolith shape analysis that have the potential to improve provenance estimates in the mixed summer fishery (see Libungan and Pálsson 2015; Libungan et al. 2015).

Within fish stocks, otoliths' chemical constituents can offer even greater sensitivity as population markers (e.g. Longmore et al. 2010), and we made use of these here, developing a Bayesian modelling approach to generate estimates of nursery connectivity and contribution of direct relevance for the management and protection of nursery-resident herring populations in Icelandic waters. Our findings point to a tendency for older juveniles to remain within, or very close to the nursery areas they inhabited as one-year olds (see Figure 7), though our data, and inference from other studies (Guðmundsdóttir et al. 2007) also suggest that some straying is possible (see Figure 7a). Sampling limitations precluded a test of retention rates across all nurseries, but if the generality of long-term, nursery-site attachment or straying can be verified, this would act to enhance confidence in using recruitment indices based on either age 1 and/or age 2 abundance as inputs into stock assessment models (see Guðmundsdóttir et al. 2007; ICES 2017, 2018).

As a second key result, we estimated a near-equal contribution from several nurseries to a fished sample of age 3 ISS herring. Whilst our findings are applicable to only a small proportion of the age 3 cohort, the existence of such patterns across the broader population may simplify, yet concurrently complicate management decisions focused on nursery protection with a view to ensuring fishery sustainability. For example, resilience to local perturbations or overexploitation through (currently poorly-quantified) bycatch from commercial shrimp fishing vessels (Thorsteinsson 1992; Jónsdóttir et al. 2017; DNVGL 2018) or natural mortality from whales and other predators (Vikingsson et al. 2014; Samarra and Foote 2015) is increased under such a scenario, making efforts to protect only one or a few key nurseries less critical. Saying this, the collective importance of multiple nurseries makes it harder to obtain the accurate indices of juvenile abundance needed for the assessment models, requiring an expansion of survey effort and among-year consistency in survey coverage, which can be both costly and logistically challenging (e.g. ICES 2018).

Whilst providing an initial guide for management-related discussion, we stress that the scope of our study is somewhat limited; encompassing three years of nursery sampling, and one year of fishery data from a small component of the total age 3 population. Extending data collection over several years, and incorporating other fishery-derived samples across a broader geographic range would allow us to gain deeper insight into the questions we posed, while building confidence in otolith chemistry analysis as a routine tool for management. One key issue is the potential for missing source populations to have influenced our conclusions on mixed stock identity. It is likely that there are sources that we have missed and/or that were not adequately characterised, particularly in the *Nursery retention tests* (see

Guðmundsdóttir et al. 2007), issues that our finite mixture models cannot alleviate. Infinite mixture modelling approaches deal with this explicitly (Neubauer et al. 2013; Loff and Neubauer 2018; Reis-Santos et al. 2018b), and we plan to pursue these in a follow-up paper. Re-running the MSA using these models would provide quantitative corroboration of the number of likely sources, as well as taking uncharacterised sources into account in estimating individual assignment probabilities.

Conclusions

In this paper, we present fundamental data on source-sink dynamics in the ISS herring stock derived from the chemical traits in otoliths, and develop statistical methods that we hope will inspire further investigation into the links among juvenile and adult populations. Though our analysis centred on herring, by incorporating intrinsic effects and explicitly quantifying data- and model-related uncertainties, the Bayesian framework we present offers a quantitative and easily-adaptable template for assessing the scale of connections among putative sources, elucidating nursery-residence patterns, and clarifying the role of nurseries as contributors to harvested populations more generally. With ever-improving understanding of the mechanisms governing otolith chemical trait expression (e.g. Thomas et al. 2017), efforts to refine modelling approaches for these traits that honour this new knowledge will ensure that otoliths reach their full potential in population-delineation studies and fishery-management applications.

Acknowledgements

This work was supported by the Icelandic Association of Herring Fisheries under the grant ‘Rannsóknarsjóður síldarútvegsins 2013’, and by the Norden Top-Level Research Initiative subprogram ‘Effect Studies and Adaptation to Climate Change’, funded through the Nordic Centre for Research on Marine Ecosystems and Resources Under Climate Change (NorMER). We are greatly indebted to Gunnar Jóhannsson and the crew aboard w/w Dröfn RE-35 for their hospitality and help with sample collection, and thank Alan Greig for technical assistance during the LA-ICP-MS analyses. Thanks also to Will Butler, David Eme and John Morrongiello for stimulating discussions regarding the multivariate modelling approach.

References

Alerstam, T., Hedenström, A. and Åkesson. S. 2003. Long-distance migration: evolution and determinants. Oikos 103: 247–260.

Ashford, J., Dinniman, M., Brooks, C., Andrews, A.H., Hofmann, E., Cailliet, G., Jones, C., Ramanna, N. and Gillanders, B. 2012. Does large-scale ocean circulation structure life history connectivity in Antarctic toothfish (*Dissostichus mawsoni*)? Can. J. Fish. Aquat. Sci. 69: 1903–1919.

Beck, M.W., Heck, K.L., Able, K.W., Childers, D.L., Eggleston, D.B., Gillanders, B.M., Halpern, B., Hays, C.G., Hoshino, K., Minello, T.J., Orth, R.J., Sheridan, P.F. and Weinstein M.P. 2001. The identification, conservation, and management of estuarine and marine nurseries for fish and invertebrates. BioScience 51: 633–641.

Botsford, L.W., Hastings, A. and Gaines, S.D. 2001. Dependence of sustainability on the configuration of marine reserves and larval dispersal distance. Ecol. Lett. 4 :144–150.
Brophy, D. and Danilowicz, B.S. 2002. Tracing populations of Atlantic herring (*Clupea harengus* L.) in the Irish and Celtic Seas using otolith microstructure. ICES J. Mar. Sci. 59: 1305–1313.
Bucholtz, R.H., Tomkiewicz, J. and Dalskov, J. 2008. Manual to determine gonadal maturity of herring (*Clupea harengus* L.). DTU Aqua-report 197-08, Charlottenlund: National Institute of Aquatic Resources, Denmark.
Burke, N., Brophy, D. and King, P.A. 2008. Shape analysis of otolith annuli in Atlantic herring (*Clupea harengus*); a new method for tracking fish populations. Fish. Res. 91: 133–143.
Campana, S.E. and Casselman, J.M. 1993. Stock discrimination using otolith shape analysis. Can. J. Fish. Aquat. Sci. 50: 1062–1083.
Cardinale, M., Doering-Arjes, P., Kastowsky, M. and Mosegaard, H. 2004. Effects of sex, stock, and environment on the shape of known-age Atlantic cod (*Gadus morhua*) otoliths. Can. J. Fish. Aquat. Sci. 61: 158–167.
Clausen, L.A.W., Bekkevold, D., Hatfield, E.M.C. and Mosegaard, H. 2007. Application and validation of otolith microstructure as a stock identification method in mixed Atlantic herring (*Clupea harengus*) stocks in the North Sea and western Baltic. ICES J. Mar. Sci. 64: 377–385.
Cowen, R.K., Gawarkiewicz, G., Pineda, J., Thorrold, S.R. and Werner, F.E. 2007 Population connectivity in marine systems: an overview. Oceanography 20: 14–21.
Crook, D.A., Buckle, D.J., Allsop, Q., Baldwin, W., Saunders, T.M., Kyne PM, Woodhead, J.D., Maas, R., Roberts, B. and Douglas, M.M. 2017. Use of otolith chemistry and acoustic telemetry to elucidate migratory contingents in barramundi *Lates calcarifer*. Mar. Freshwater Res. 68: 1554–1566.
DNVGL. 2018. Initial assessment of the ISF Iceland Northern shrimp fishery (inshore and offshore). Final Report for Icelandic Sustainable Fisheries. Reykjavík, Iceland.
Elsdon, T.S. and Gillanders, B.M. 2004. Fish otolith chemistry influenced by exposure to multiple environmental variables. J. Exp. Mar. Biol. Ecol. 313: 269–284.
Fiksen, Ø., Jørgensen, C., Kristiansen, T., Vikebø, F. and Huse, G. 2007. Linking behavioural ecology and oceanography: larval behaviour determines growth, mortality and dispersal. Mar. Ecol. Prog. Ser. 347: 195–205.
Flegal, J., Hughes, J., Vats, D. and Dai, N. 2017. mcmcse: Monte Carlo standard errors for MCMC. R package version 1.3-2. https://cran.r-project.org/web/packages/mcmcse/
Fridriksson, Á. and Aasen, O. 1950. The Norwegian - Icelandic herring tagging experiments, Report No. 1. Fisk. Skr. HavUnders. 9: 1–43.
Garavelli, L., White, J.W., Chollett, I. and Chérubin, L.M. 2018. Population models reveal unexpected patterns of local persistence despite widespread larval dispersal in a highly exploited species. Conserv. Lett. 11: e12567.
Geffen, A.J., Nash, R.D.M. and Dickey-Collas, M. 2011. Characterization of herring populations west of the British Isles: an investigation of mixing based on otolith microchemistry. ICES J. Mar. Sci. 68: 1447–1458.
Gelman, A., Meng, X-L. and Stern, H. 1996. Posterior predictive assessment of model fitness via realized discrepancies. Stat. Sinica 6: 733–807.
Gíslason, S., Arnórsson, S. and Ármannsson, H. 1996. Chemical weathering of basalt in southwest Iceland: effects of runoff, age of rocks and vegetative/glacial cover. Am. J. Sci. 296:837–907.
Grabowski, T.B., Boswell, K.M., McAdam, B.J., Wells, R.J.D. and Marteinsdóttir, G. 2012.

Characterization of Atlantic cod spawning habitat and behavior in Icelandic coastal waters. PLoS One 7: e51321.
Grammer, G., Morrongiello, J., Izzo, C., Hawthorne, P., Middleton, J. and Gillanders, B. 2017. Coupling biogeochemical tracers with fish growth reveals physiological and environmental controls on otolith chemistry. Ecol. Monogr. 87: 487–507.
Grewe, P.M., Feutry, P., Hill, P.L., Gunasekera, R.M., Schaefer, K.M., Itano, D.G., Fuller, D.W., Foster, S.D. and Davies, C.R. 2015. Evidence of discrete yellowfin tuna (*Thunnus albacares*) populations demands rethink of management for this globally important resource. Sci. Rep. 5: 16916.
Grønkjær, P. 2016. Otoliths as individual indicators: a reappraisal of the link between fish physiology and otolith characteristics. Mar. Freshwater Res. 67: 881–888.
Guðmundsdóttir, A., Óskarsson, G.J. and Sveinbjörnsson, S. 2007. Estimating year-class strength of Icelandic summer-spawning herring on the basis of two survey methods. ICES J. Mar. Sci. 64: 1182–1190.
Hadfield, J. 2010. MCMC methods for multi-response generalised linear mixed models: the MCMCglmm R package. J. Stat. Soft. 33: 1–22.
Halfyard, E.A., Webber, D., Del Papa, J., Leadley, T., Kessel, S.T., Colborne, S.F. and Fisk, A.T. 2017. Evaluation of an acoustic telemetry transmitter designed to identify predation events. Methods Ecol. Evol. 8: 1063–1071.
Høie, H., Folkvord, A. and Otterlei, E. 2003. Effect of somatic and otolith growth rate on stable isotopic composition of early juvenile cod (*Gadus morhua* L) otoliths. J. Exp. Mar. Biol. Ecol. 289: 41–58.
Holt, R.E. and Jørgensen, C. 2014. Climate warming causes life-history evolution in a model for Atlantic cod (*Gadus morhua*). Conserv. Physiol. 2: cou050.
Huey. J.A., Crook, D.A., Macdonald, J.I., Schmidt, D.J., Marshall, J.C., Balcombe, S.R., Woods, R.J. and Hughes, J.M. 2014. Is variable connectivity among populations of a continental gobiid fish driven by local adaptation or passive dispersal? Freshwater Biol. 59: 1672–1686.
Huse. G. 2016. A spatial approach to understanding herring population dynamics. Can. J. Fish. Aquat. Sci. 73: 177–188.
Husebø, Å., Slotte, A., Clausen, L.A.W. and Mosegaard, H. 2005. Mixing of populations or year class twinning in Norwegian spring spawning herring? Mar. Freshwater Res. 56: 763–772.
ICES. 2016. Report of the North-Western Working Group (NWWG). 27 April - 4 May 2016, ICES CM 2016/ACOM:08, Copenhagen, Denmark.
ICES. 2017. Report of the North-Western Working Group (NWWG). 27 April - 4 May 2017, ICES CM 2017/ACOM:08, Copenhagen, Denmark.
ICES. 2018. Report of the North-Western Working Group (NWWG). 26 April - 3 May 2018, ICES CM 2018/ACOM:09, Copenhagen, Denmark.
Izzo, C., Reis-Santos, P. and Gillanders, B.M. 2018. Otolith chemistry does not just reflect environmental conditions: a meta-analytic evaluation. Fish. Fish. 19: 441–454.
Jakobsson, J. and Stefánsson, G. 1999. Management of summer-spawning herring off Iceland. ICES J. Mar. Sci. 56: 827–833.
Johannessen, A., Nøttestad, L., Fernö, A., Langard, L. and Skaret, G. 2009. Two components of Northeast Atlantic herring within the same school during spawning: support for the existence of a metapopulation? ICES J. Mar. Sci. 66: 1740–1748.
Jones, C.M., Palmer, M. and Schaffler, J.J. 2017. Beyond Zar: The use and abuse of classification statistics for otolith chemistry. J. Fish Biol. 90: 492–504.
Jónsdóttir, I.G., Bragason, G.S., Brynjólfsson, S.H., Guðlaugsdóttir, A.K. and Skúladóttir,

U. 2017. Yfirlit yfir rækjurannsóknir við Ísland, 1988-2015. Northern shrimp research in Icelandic waters, 1988-2015. Marine and Freshwater Research in Iceland HV-2017-00.
Kalish, J.M. 1989. Otolith microchemistry: validation of the effects of physiology, age and environment on otolith composition. J. Exp. Mar. Biol. Ecol. 132: 151–178.
Korkmaz, S., Goksuluk, D. and Zararsiz, G. 2015. MVN: An R package for assessing multivariate normality. The R Journal 6: 151–162.
Kristmannsdóttir, H., Gíslason, S.R., Snorrason, A., Haraldsson, H., Hauksdóttir, S. and Gunnarsson, A. 2002. Seasonal variation in the chemistry of glacial-fed rivers in Iceland. IAHS-AISH Publication 271: 223–229.
Libungan, L.A., Óskarsson, G.J., Slotte, A., Jacobsen, J.A. and Pálsson, S. 2015. Otolith shape: a population marker for Atlantic herring *Clupea harengus*. J. Fish Biol. 86: 1377–1395.
Libungan, L.A. and Pálsson, S. 2015. ShapeR: An R package to study otolith shape variation among fish populations. PLoS One 10: e0121102.
Loff, J.F. and Neubauer, P. 2018. unmixR: analysis of population structure in R using finite and infinite Bayesian mixture models. R package version 0.4.1. https://github.com/zeloff/unmixR
Logemann, K., Ólafsson, J., Snorrason, Á., Valdimarsson, H. and Marteinsdóttir, G. 2013. The circulation of Icelandic waters – a modelling study. Ocean Sci. 9: 931–955.
Longmore, C., Fogarty, K., Neat, F., Brophy, D., Trueman, C., Milton, A. and Mariani, S. 2010. A comparison of otolith microchemistry and otolith shape analysis for the study of spatial variation in a deep-sea teleost, *Coryphaenoides rupestris*. Environ. Biol. Fish. 89: 591–605.
Louvat, P., Gíslason, S.R. and Allègre, C.J. 2008. Chemical and mechanical erosion rates in Iceland as deduced from river dissolved and solid material. Am. J. Sci. 308: 679–726.
Macdonald, J.I. and Crook, D.A. 2010. Variability in Sr:Ca and Ba:Ca ratios in water and fish otoliths across an estuarine salinity gradient. Mar. Ecol. Prog. Ser. 413: 147–161.
Maravelias, C. and Reid, D. 1997. Identifying the effects of oceanographic features and zooplankton on prespawning herring abundance using generalized additive models. Mar. Ecol. Prog. Ser. 147: 1–9.
Martin, G.B. and Wuenschel, M.J. 2006. Effect of temperature and salinity on otolith element incorporation in juvenile gray snapper *Lutjanus griseus*. Mar. Ecol. Prog. Ser. 324: 229–239.
Melancon, S., Fryer, B.J. and Markham, J.L. 2009. Chemical analysis of endolymph and the growing otolith: fractionation of metals in freshwater fish species. Environ. Toxicol. Chem. 28: 1279–1287.
Mercier, L., Darnaude, A.M., Bruguier, O., Vasconcelos, R.P., Cabral, H.N., Costa, M.J., Lara, M., Jones, D.L. and Mouillot, D. 2011. Selecting statistical models and variable combinations for optimal classification using otolith microchemistry. Ecol. Appl. 21: 1352–1364.
Mirasole, A., Gillanders, B.M., Reis-Santos, P., Grassa, F., Capasso, G., Scopelliti, G., Mazzola, A. and Vizzini, S. 2017. The influence of high pCO_2 on otolith shape, chemical and carbon isotope composition of six coastal fish species in a Mediterranean shallow CO_2 vent. Mar. Biol. 164: 191.
Neubauer, P., Shima, J.S. and Swearer, S.E. 2010. Scale-dependent variability in Forsterygion lapillum hatchling otolith chemistry: implications and solutions for studies of population connectivity. Mar. Ecol. Prog. Ser. 415: 263–274.
Neubauer, P., Shima, J.S. and Swearer, S.E. 2013. Inferring dispersal and migrations from

incomplete geochemical baselines: analysis of population structure using Bayesian infinite mixture models. Methods Ecol. Evol. 4: 836–845.
Niklitschek, E.J. and Darnaude, A.M. 2016. Performance of maximum likelihood mixture models to estimate nursery habitat contributions to fish stocks: a case study on sea bream *Sparus aurata*. PeerJ 4: e2415.
Óskarsson, G.J. 2016. Results of acoustic measurements of Icelandic summer-spawning herring in the winter 2015/2016. Working Document to ICES North Western Working Group, 27 April - 4 May 2016, WD No. 4.
Óskarsson, G.J. 2018. The existence and population connectivity of Icelandic spring-spawning herring over a 50-year collapse period. ICES J. Mar. Sci. 75: 2025–2032.
Óskarsson, G.J. and Reynisson, P. 2015. Leiðangursskýrsla B7-2014: Bergmálsmælingar íslenskrar sumargotssíldar úti fyrir vestur-, suður- og suðausturströnd Íslands á RS Bjarni Sæmundsson, 24. nóv. - 6. des. 2014; Ásamt niðurstöðum D9-2014 og leiðangurs Bolla SH 4. des. 2014. Tekið. Reykjavík.
Óskarsson, G.J., Pálsson, J. and Guðmundsdóttir, A. 2018a. An ichthyophoniasis epizootic in Atlantic herring in marine waters around Iceland. Can. J. Fish. Aquat. Sci. 75: 1106–1116.
Óskarsson, G.J., Ólafsdóttir, S.R., Sigurðsson, Þ. and Valdimarsson, H. 2018b. Observation and quantification of two incidents of mass fish kill of Icelandic summer spawning herring (*Clupea harengus*) in the winter 2012/2013. Fish. Oceanogr. 27: 302–311.
Panfili, J., Darnaude, A.M., Vigliola, L., Jacquart, A., Labonne, M. and Gilles, S. 2015. Experimental evidence of complex relationships between the ambient salinity and the strontium signature of fish otoliths. J. Exp. Mar. Biol. Ecol. 467: 65–70.
Penttila, J. and Dery, L.M. 1988. Age determination methods for northwest Atlantic species. NOAA Tech Rep NMFS-72.
Plummer, M. 2003. JAGS: A Program for Analysis of Bayesian Graphical Models Using Gibbs Sampling. Proceedings of the 3rd International Workshop on Distributed Statistical Computing (DSC 2003), March 20 - 22, Vienna, Austria.
Plummer, M. 2016. rjags: Bayesian graphical models using MCMC. R package version 4-6. https://CRAN.R-project.org/package=rjags.
Plummer, M., Best, N., Cowles, K. and Vines, K. 2006. CODA: convergence diagnosis and output analysis for MCMC. R News 6: 7–11.
R Core Team 2018. R: a language and environment for statistical computing. R Foundation for Statistical Computing, Vienna, Austria.
Reis-Santos, P., Vasconcelos, R.P., Tanner, S.E., Fonseca, V.F., Cabral, H.N. and Gillanders, B.M. 2018a. Extrinsic and intrinsic factors shape the ability of using otolith chemistry to characterize estuarine environmental histories. Marine Environ. Res. 140: 332–341.
Reis-Santos, P., Tanner, S.E., Aboim, M.A., Vasconcelos, R.P., Laroche, J., Charrier, G., Pérez, M., Presa, P., Gillanders, B.M. and Cabral, H.N. 2018b. Reconciling differences in natural tags to infer demographic and genetic connectivity in marine fish populations. Sci. Rep. 8: 1–12.
Rooker, J.R., Secor, D.H., DeMetrio, G., Kaufman, A.J., Ríos, A.B. and Tičina, V. 2008. Evidence of trans-Atlantic movement and natal homing of bluefin tuna from stable isotopes in otoliths. Mar. Ecol. Prog. Ser. 368: 231–239.
Rubin, D. 1976. Inference and missing data. Biometrika 63: 581–592.
da Silva, A.R., Malafaia, G. and Menezes, I.P.P. 2017. biotools: an R function to predict spatial gene diversity via an individual-based approach. Genet. Mol. Res. 16: gmr16029655.

Stanley, R., Bradbury, I., DiBacco, C., Snelgrove, P., Thorrold, S. and Killen, S. 2015. Environmentally mediated trends in otolith composition of juvenile Atlantic cod (*Gadus morhua*). ICES J. Mar. Sci. 72: 2350–2363.

Stock, B. and Semmens, B. 2016a. MixSIAR GUI user manual. Version 3.1: 1–59. https://github.com/brianstock/MixSIAR

Stock, B. and Semmens, B. 2016b. Unifying error structures in commonly used biotracer mixing models. Ecology 97: 2562–2569.

Stock, B.C., Jackson, A.L., Ward, E.J., Parnell, A.C., Phillips, D.L. and Semmens, B.X. 2018. Analyzing mixing systems using a new generation of Bayesian tracer mixing models. PeerJ 6: e5096.

Sturrock, A., Trueman, C., Milton, J., Waring, C., Cooper, M. and Hunter, E. 2014. Physiological influences can outweigh environmental signals in otolith microchemistry research. Mar. Ecol. Prog. Ser. 500: 245–264.

Taillebois, L., Barton, D.P., Crook, D.A., Saunders, T., Taylor, J., Hearnden, M., Saunders, R.J., Newman, S.J., Travers, M.J., Welch, D.J., Greig, A., Dudgeon, C., Maher, S. and Ovenden, J.R. 2017. Strong population structure deduced from genetics, otolith chemistry and parasite abundances explains vulnerability to localized fishery collapse in a large Sciaenid fish, *Protonibea diacanthus*. Evol. Appl. 10: 978–993.

Thomas, O., Ganio, K., Roberts, B. and Swearer, S. 2017. Trace element-protein interactions in endolymph from the inner ear of fish: implications for environmental econstructions using fish otolith chemistry. Metallomics 9:239–249.

Thorsteinsson, G. 1992. The use of square mesh codends in the Icelandic shrimp (*Pandalus borealis*) fishery. Fish. Res. 13: 255–266.

Treml, E.A., Roberts, J.J., Chao, Y., Halpin, P.N., Possingham, H.P. and Riginos, C. 2012. Reproductive output and duration of the pelagic larval stage determine seascape-wide connectivity of marine populations. Integr. Comp. Biol. 52: 525–537.

Valdimarsson, H., Astthorsson, O.S., Palsson, J. 2012. Hydrographic variability in Icelandic waters during recent decades and related changes in distribution of some fish species. ICES J. Mar Sci. 69: 816–825.

Woods, R.J., Macdonald, J.I., Crook, D.A., Schmidt, D.J. and Hughes, J.M. 2010. Contemporary and historical patterns of connectivity among populations of an inland river fish species inferred from genetics and otolith chemistry. Can. J. Fish. Aquat. Sci. 67: 1098–1115.

Wright, P.J., Régnier, T., Gibb, F.M., Augley, J. and Devalla, S. 2018. Assessing the role of ontogenetic movement in maintaining population structure in fish using otolith microchemistry. Ecol. Evol. 8: 7907–7920.

Su, Y.S. and Masanao, Y. 2015. R2jags: Using R to Run 'JAGS'. R package version 0.5-7. https://CRAN.R-project.org/package=R2jags

Table 1. Sampling details for juvenile ISS herring captured during October/November 2013, 2014 and 2015. Shown are the nurseries, and capture sites within them (Site), numbers of fish collected (n), mean standard length (SL) and range (in brackets) of the sample. Numbers of otoliths analysed for Li, Mg, Ca, Mn, Zn, Sr, Ba at the otolith edge (El_{edge}), and in the portion of age 2 otoliths accreted on the nursery grounds one-year earlier (El_{mid}) are presented, in addition to the numbers analysed for $\delta^{13}C$ and $\delta^{18}O$ in whole age 1 otoliths (C/O_{whole}), and at the edge of age 2 otoliths (C/O_{edge}). Samples treated as 'mixed' populations in the mixed stock analyses are highlighted in bold.

Year	Nursery	Site	Age 1				Age 2				
			n	SL (mm)	El_{edge}	C/O_{whole}	n	SL (mm)	El_{edge}	El_{mid}	C/O_{edge}
2013	Öxarfjörður	531	4	76 (69-86)	4	2					
	Ísafjarðardjúp	529	9	82.7 (77-92)	9	7	14	131.9 (129-139)	14	14	7
		D5-102					9	136.1 (126-149)	9	9	7
		D5-110					11	132.7 (125-147)	11	11	3
		D5-115					10	137.4 (130-145)	10	10	7
	Eyjafjörður	530	11	95.6 (87-100)	11	6					
	Breiðafjörður	D1-2					18	107.2 (97-115)	18	16	16
2014	Arnarfjörður	D9-7	14	96.1 (76-118)	14						
		D7-A	20	67.3 (61-73)	20						
		D7-B	8	73.3 (59-97)	8		18	131.1 (113-146)	18	18	5
		D7-C	16	62.2 (57-71)	16						
	Ísafjarðardjúp	D9-6	9	101.0 (81-116)	9		10	139.2 (131-146)	10	**10 ($Ísa_m$)**	7
		D7-92	18	76.1 (63-84)	18						
	Vestmannaeyjar	B7-468					10	117.7 (104-126)	10	10	
	Jökuldjúp north	B7-470					9	123.8 (109-133)	9	8	2
	Jökuldjúp south	B7-471					10	119.9 (114-127)	10	10	2
	Eyjafjörður	D9-4	18	97.7 (77-118)	18						
	Miðfjörður	D7-154	21	89.8 (72-100)	21		20	141.4 (133-150)	20	20	14
	Öxarfjörður	D7-140	22	86.5 (77-99)	22		16	132.4 (120-145)	16	**15 ($Öxar_m$)**	11
	Breiðamerkurdjúp	B7-466					20	126.2 (115-137)	20	19	13
	Skagafjörður	D7-113					20	135.0 (121-147)	20	20	4
2015	Arnarfjörður	D4-14					15	121.9 (104-138)	15	**15 ($Arna_m$)**	15
	Hrútafjörður	D5-18	18	75.3 (69-81)	17	12	15	154.1 (140-173)	15	15	15
	Ísafjarðardjúp	D4-60					15	121.0 (114-125)	15	**15 ($ÍsaD4\text{-}60_m$)**	15
		D4-50					15	132.1 (120-143)	15	**15 ($ÍsaD4\text{-}50_m$)**	15
	Miðfjörður	D5-19	19	78.5 (63-93)	19	15					

Figures

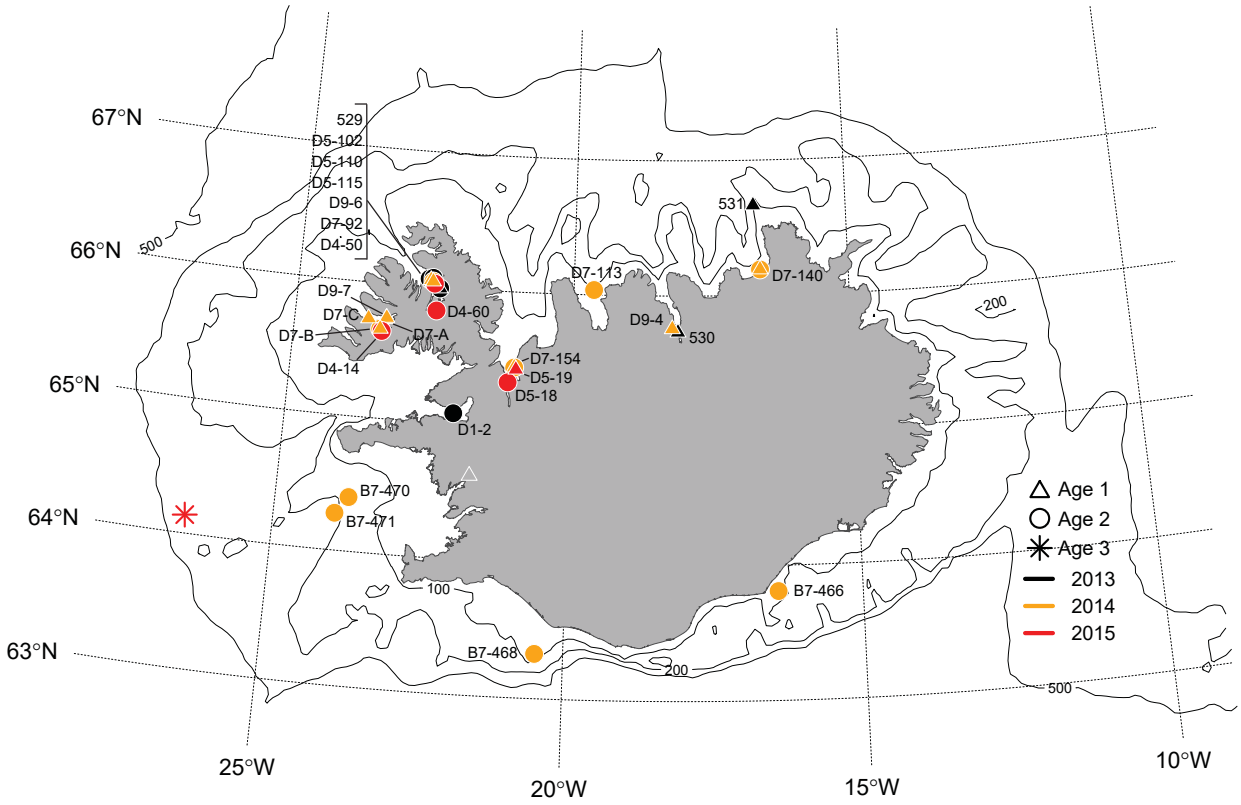

Figure 1. Locations of nursery sites sampled for juvenile ISS herring (i.e. age 1: triangles, age 2: circles) during October / November 2013 (black symbols), 2014 (orange symbols) and 2015 (red symbols) (see Table 1 for site details). The red star denotes the capture location for a sample of age 3 herring (n = 79) caught by the fishery targeting overwintering adults at Kolluáll off Iceland's west coast in November 2015. Nursery sites sampled in different years that overlap exactly in space are offset slightly for clarity. Depth contours (in m – black lines) are overlaid.

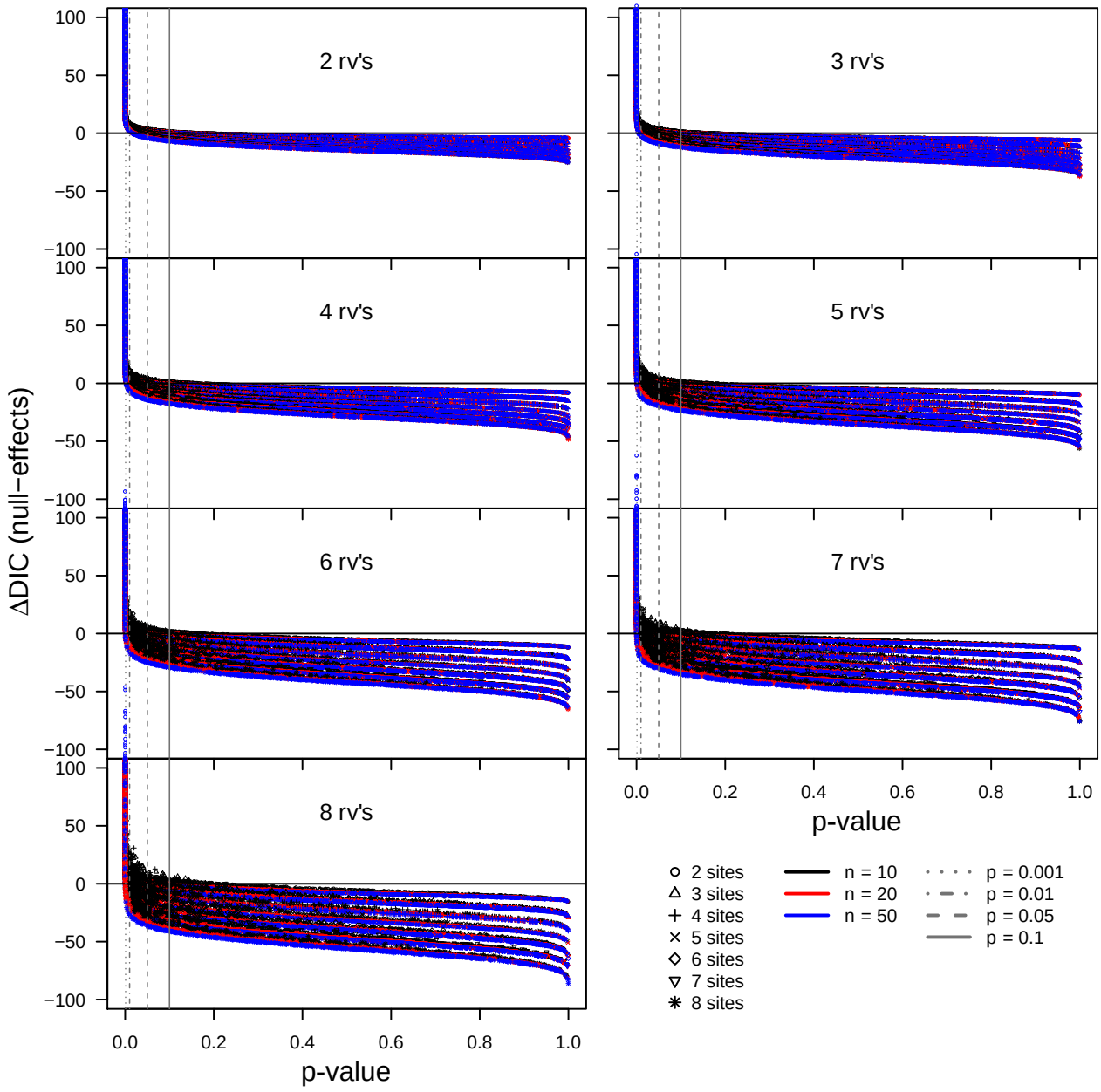

Figure 2. Results from simulations designed to assess the sensitivity of the deviance information criterion (DIC) in detecting differences in otolith chemical signatures among nursery sites. In the plots, each symbol represents a simulated multivariate normal dataset, comprising differing numbers of (1) response variables (rv's) – in our case, reflecting otolith elemental and stable isotopic measurements; (2) nursery sites; and (3) numbers of fish captured per site. For each dataset, we ran a one-way MANOVA and two Bayesian multivariate linear models; one with no site-level effects (i.e. 'null' model), and the other including site-level effects (i.e. 'effects' model). We derived a p-value for the null hypothesis of no multivariate differences among nursery sites from the MANOVA based on Pillai's trace statistic, and plotted this against the difference in DIC values between the Bayesian 'null' and 'effects' models (i.e. ΔDIC (null-effect)).

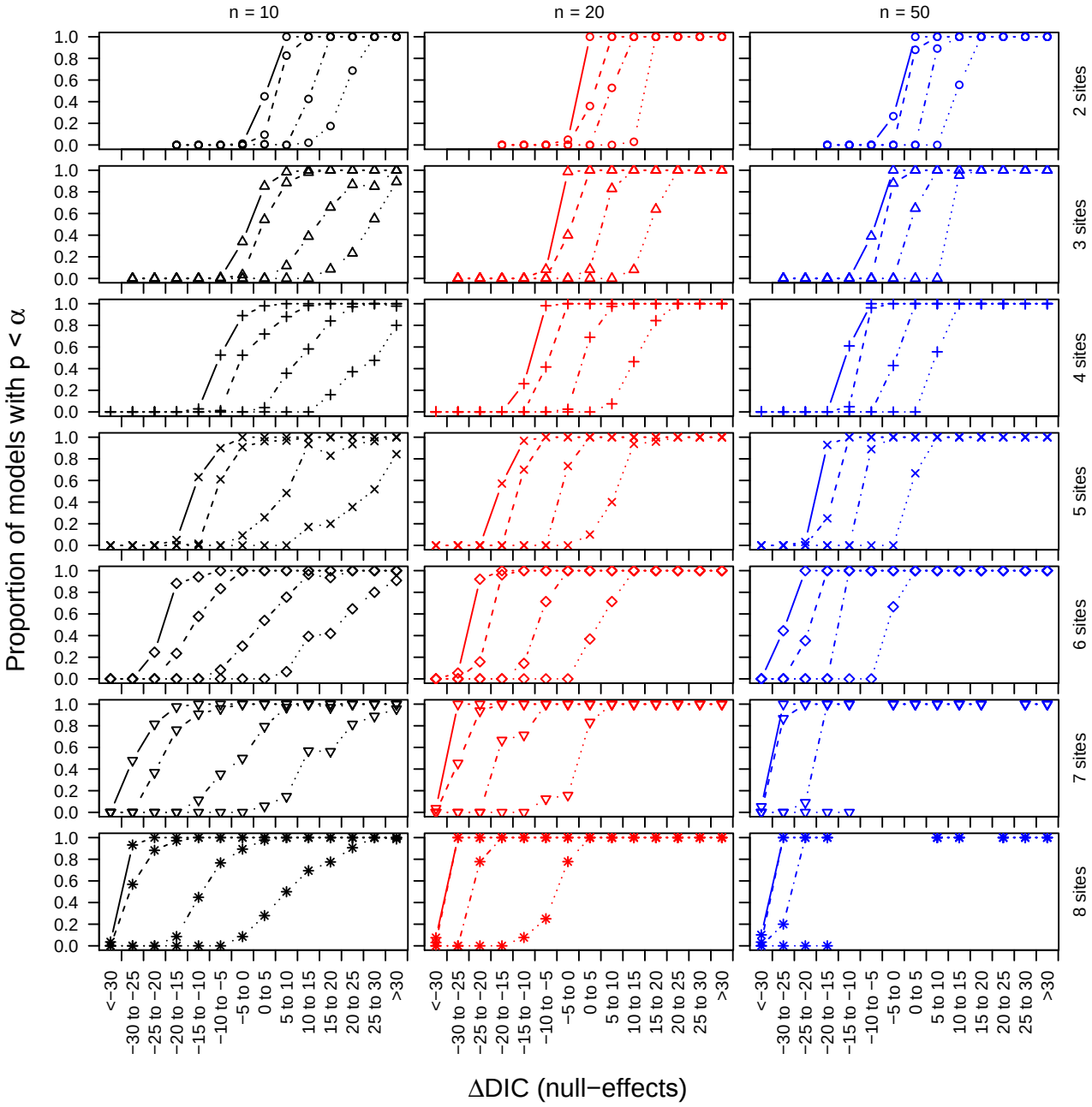

Figure 3. Plots summarizing the simulation output presented in the bottom-left panel of Figure 2 (i.e. results from datasets with 8 rv's). Shown here is the proportion of models for which the p-value (derived from a one-way MANOVA) is < α, where α = 0.1 (solid line), 0.05 (dashed line), 0.01 (dot-dashed line) and 0.001 (dotted line) in relation to the change in DIC values between 'null' and 'effects' models (i.e. ΔDIC (null-effect)).

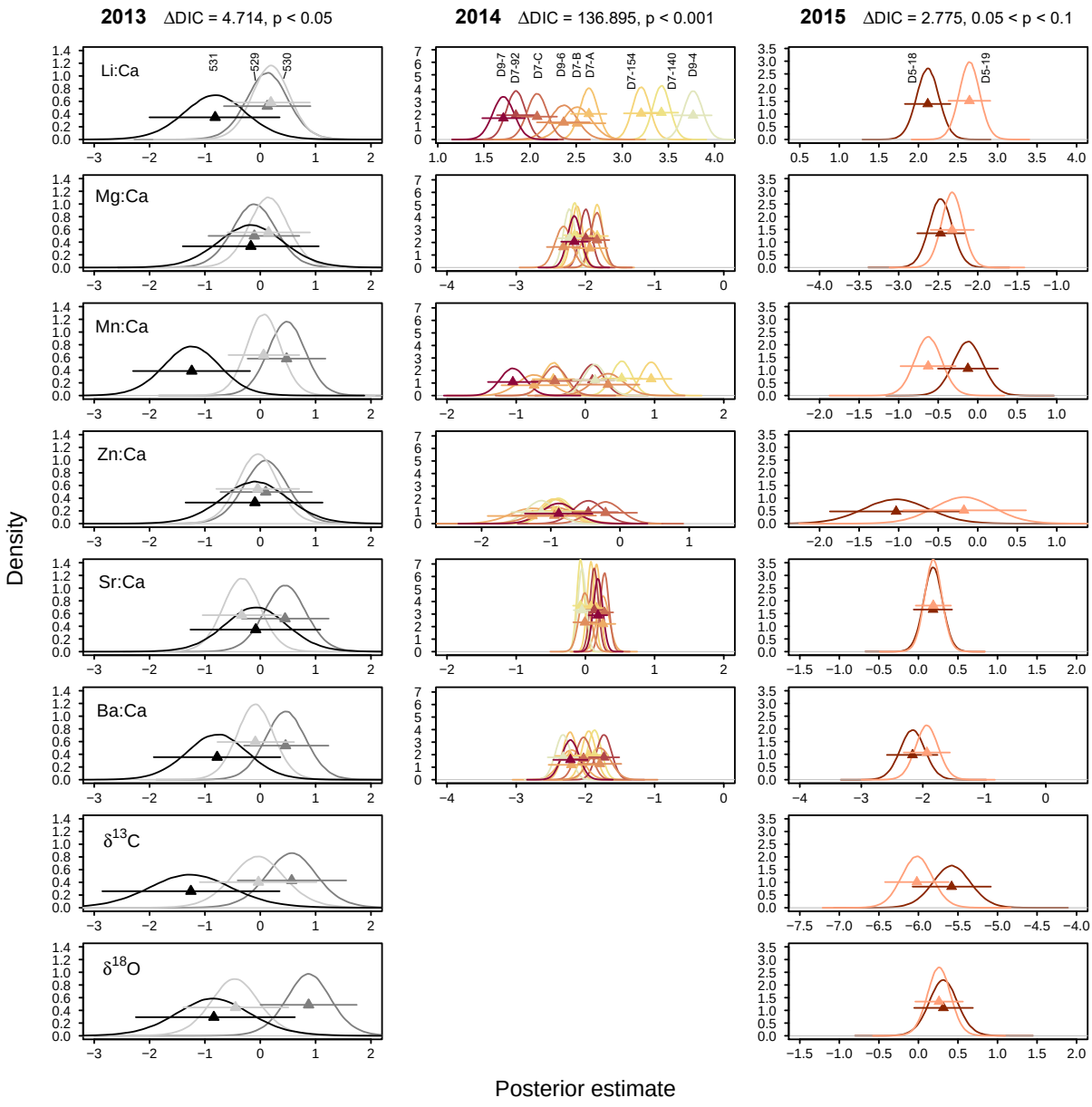

Figure 4. Posterior estimates for age 1 herring, illustrating spatial variation in elemental and isotopic markers among nursery sites sampled in 2013 (left-hand column of plots), 2014 (middle column of plots) and 2015 (right-hand column of plots). Within each sampling year, the posterior densities for each nursery site are presented for each otolith chemical marker included in the model for that year, along with their posterior means (triangles) ± 95% CIs (segments). Data for each site are displayed in a different colour (i.e. 2013: blacks; 2014: oranges; 2015: reds). Means ± 95% CIs are referenced to the x-axis only, and positioned vertically at half of the maximum density value for that site, for clarity. Note that y-axes for all otolith chemical markers within a year (i.e. within each column) are kept consistent, and the ranges of the x-axes are also kept constant. This allows a direct comparison of density shape and magnitude among nursery sites for each otolith chemistry marker within a year. Shown also are the ΔDIC (null-effect) for each year's model, and the associated p-value derived from the smallest sample size tested in our simulation study, i.e. n = 10) (see Figures 2, 3).

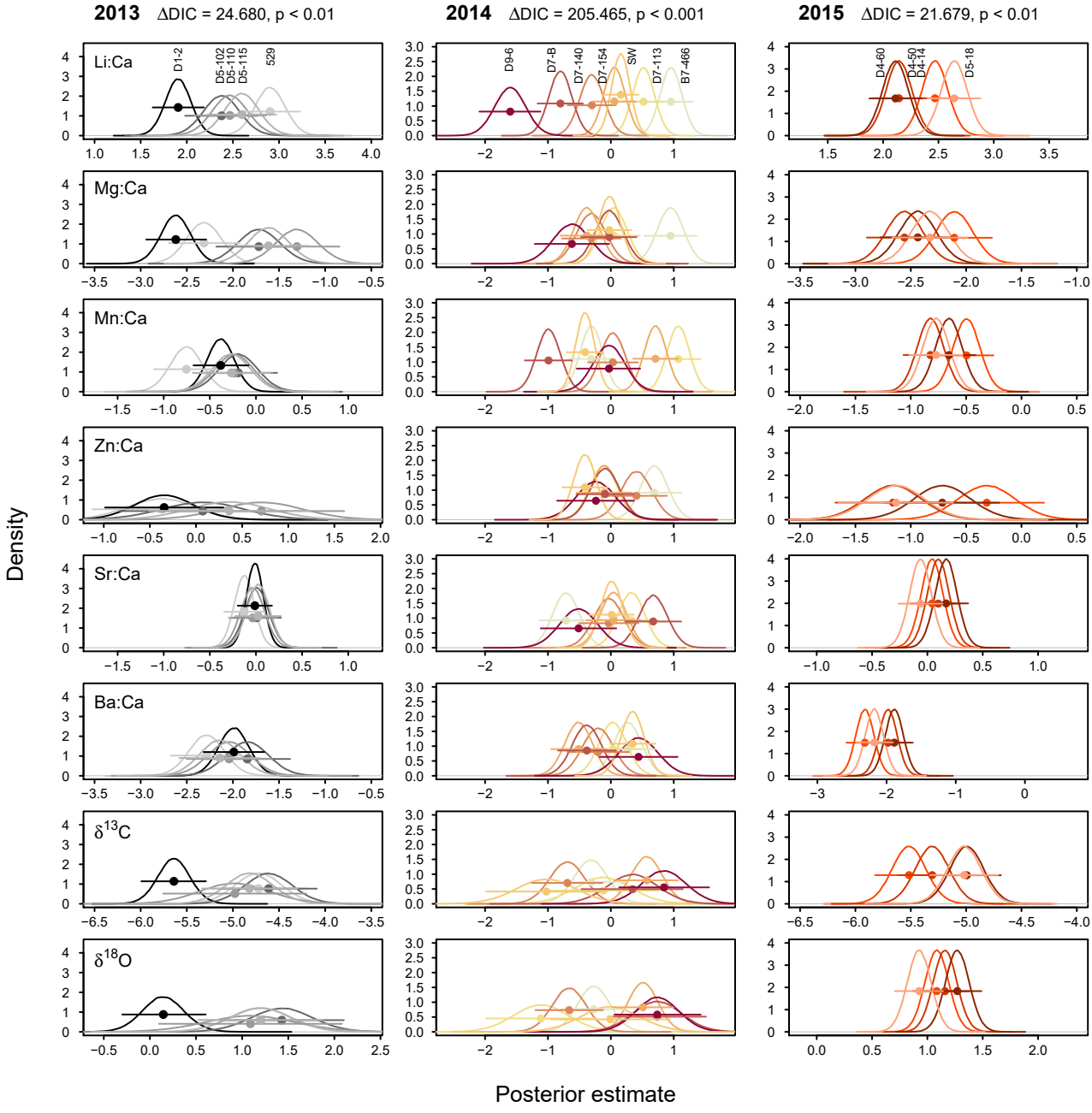

Figure 5. Posterior estimates for age 2 herring, illustrating spatial variation in elemental and isotopic markers among nursery sites sampled in 2013 (left-hand column of plots), 2014 (middle column of plots) and 2015 (right-hand column of plots). Within each sampling year, the posterior densities for each nursery site are presented for each otolith chemical marker included in the model for that year, along with their posterior means (circles) ± 95% CIs (segments). All other information as for Figure 4.

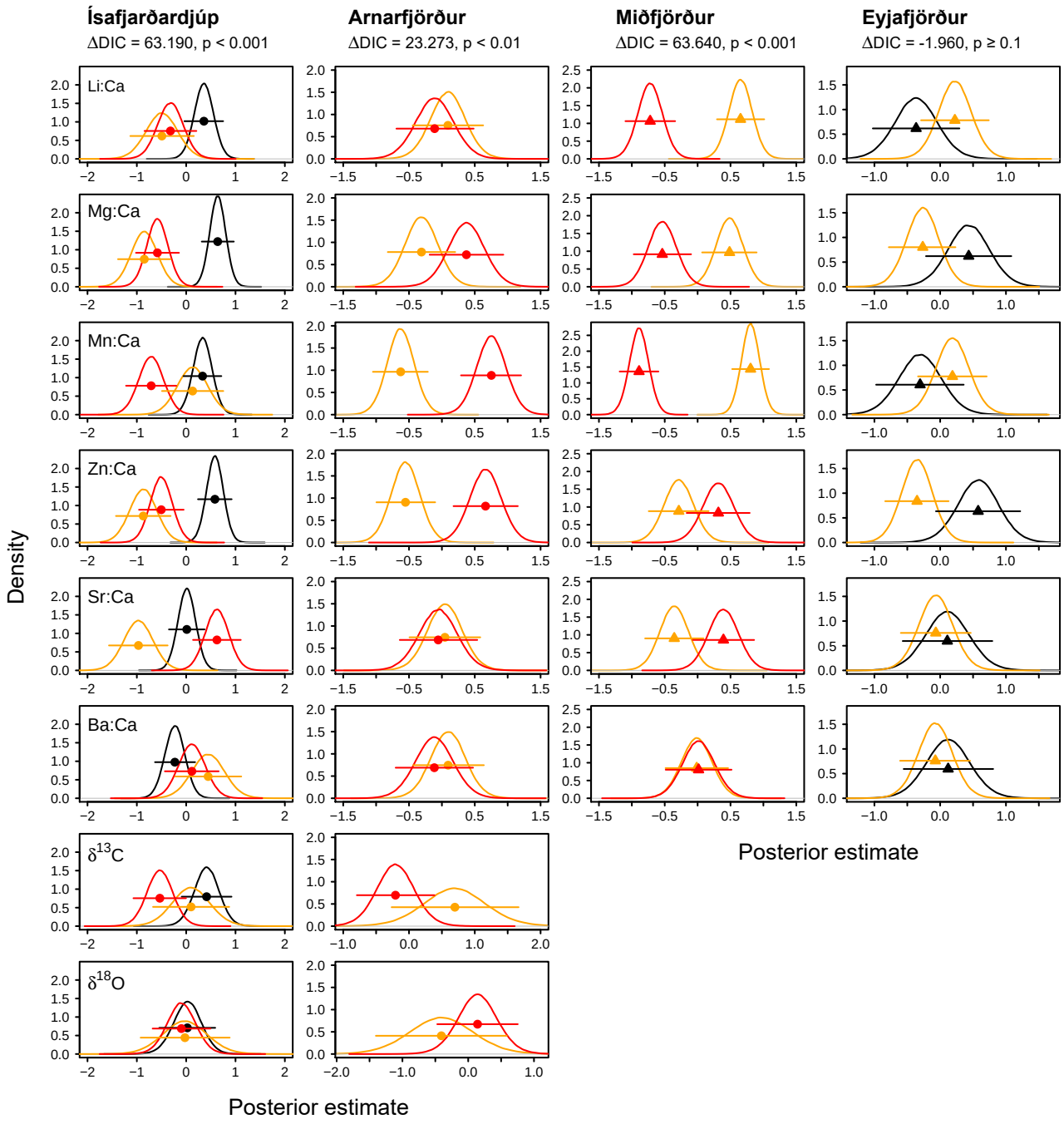

Figure 6. Temporal variation in elemental and isotopic markers at four nursery sites sampled in two (Arnafjörður, Miðfjörður, Eyjafjörður) or three (Ísafjarðardjúp) consecutive years. Within each nursery site, the posterior densities for each year (2013: black lines and symbols; 2014: orange lines and symbols; 2015: red lines and symbols) are presented for each otolith chemical marker included in the model for that site, along with their posterior means (age1: triangles; age 2: circles) ± 95% CIs (segments). Similar to Figure 4, means ± 95% CIs are referenced to the x-axis only, and positioned vertically at half of the maximum density value for that year. Y-axes for all otolith chemical markers within a site (i.e. within each column) are kept consistent, and the ranges of the x-axes are also kept constant. Also shown are the ΔDIC (null-effect) for each site's model, and the associated p-value derived from Figures 2 and 3.

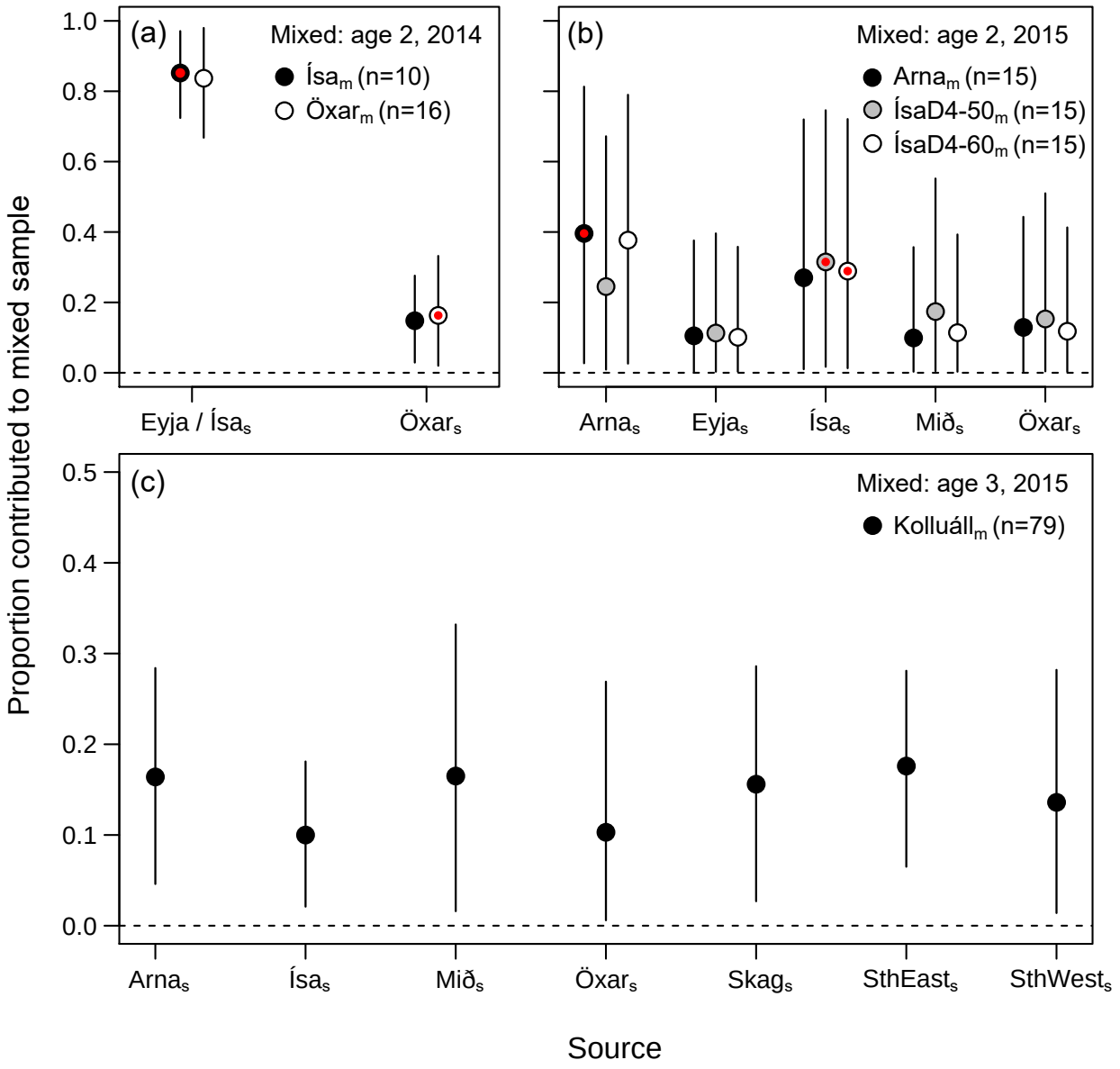

Figure 7. Estimated posterior mean (circles) ± 95 CIs (segments) source contribution to mixed populations of age 2 and age 3 fish as derived from the finite mixture models. Panels (a) and (b) concern the 'Nursery retention tests'. For example, panel (a) displays the proportion of age 2 fish captured in Ísafjarðardjúp (i.e. Ísa$_m$) in 2014 and Öxarfjorður (i.e. Öxar$_m$) in 2014 (i.e. the mixed samples) estimated to have resided in nurseries within Ísafjarðardjúp and Eyjafjörður combined (i.e. Eyja / Ísa$_s$), or in Öxarfjörður (Öxar$_s$) as age 1 fish in 2013 (i.e. the source samples). For each mixed sample in (a) and (b), the red dot highlights the estimated proportion of fish showing nursery-site fidelity between age 1 and age 2. Panel (c) shows results for the mixed sample of age 3 herring captured by the winter fishery at Kolluáll in November 2015, based on seven putative source populations of age 2 fish captured in October/November 2014.

Supplement 1 – Otolith preparation and analysis

Sagittal otolith pairs from all fish were removed under a dissecting microscope, cleaned of adhering tissue, triple-rinsed with Milli-Q – Type 1 Ultrapure water (Merck: www.merckmillipore.com/AU/en) and stored dry in polypropylene microtubes. One sagitta from each fish was selected for measurement of elemental concentrations using laser ablation-inductively coupled plasma-mass spectrometry (LA-ICP-MS). Otoliths were first mounted individually, sulcus downwards, on an acid-washed glass slide in thermoplastic glue (Crystalbond™) and polished them to within 10-15 µm of the primordium using a series of wetted lapping films (9, 5, 3 µm). We then transferred each polished otolith to a master slide, on which otoliths from all capture sites were arranged randomly in Crystalbond™. Master slides were triple-rinsed in Milli-Q – Type 1 Ultrapure water and air-dried overnight in a class 100 laminar flow cabinet at room temperature.

We used a depth-profiling approach to ablate a ~40-µm wide × 11-µm deep disc of otolith material at the dorsal margin of each age 1 and age 2 sample at a position equidistant between the pararostrum and antirostrum. These are termed 'Eledge' samples (see Table 1 main text). Based on daily growth increment widths immediately adjacent to the ablation site, we estimate that this disc reflects otolith material deposited during the final < 2 weeks of life prior to the fish's capture. For age 2 and 3 samples, we used a 40-µm spot size to ablate material accreted in the period one-year prior to the capture date, again at a position equidistant between the pararostrum and antirostrum. These are termed 'Elmid' samples (Table 1 main text), and for each individual are representative of a < 2 week period of nursery residence experienced one-year earlier.

Elemental measurements were made using a Varian 810 quadrupole ICP-MS, coupled to a HelEx (Laurin Technic, and The Australian National University) laser ablation system located at the University of Melbourne, Australia. The HelEx system is built around a Compex 110 (Lambda Physik, Gottingen, Germany) excimer laser. Master slides were placed in the sample cell and the target ablation site on each sample was then digitally plotted using GeoStar v6.14 software (Norris Software: www.norris.org.au). Ablation occurred inside a sealed chamber in an atmosphere of pure He (flow rate: 0.3 l min-1) with the vaporised material transported to the ICP-MS in the Ar carrier gas (flow rate: 1.23 l min-1) via a signal-smoothing manifold. Prior to data acquisition, a pre-ablation step was implemented in which 3 laser pulses were fired (at 78 mJ output energy) at the target sites to remove any surface contaminants. Using the same energy settings, the laser was then pulsed at 5 Hz for 40 s per sample. For each otolith sample, the first 3 s of data in the acquisition sequence were excluded, and the next 15 s retained, encompassing the target disc of otolith material.

Concentrations of seven elements: 7Li, 25Mg, 43Ca, 55Mn, 66Zn, 88Sr and 138Ba were monitored, with 43Ca used as an internal standard. Dwell times were 0.03 s for all elements except Li (0.05 s). Data were processed offline using Iolite version 3.31 (School of Earth Sciences, the University of Melbourne: www.iolite-software.com) (Paton et al. 2011). Subtraction of background ion counts from otolith counts was followed by the normalisation of each element to Ca using a glass reference standard (National Institute of Standards and Technology: NIST 612) which was analysed after every 10th otolith sample. Measurement precision (% relative standard deviation [RSD]) was calculated based on twenty 20-s analyses each of NIST 610 and MACS-3 (United States Geological Survey) reference

standards run concurrently with the otolith samples. Mean RSDs for the NIST 610/MACS-3, respectively, for normalised data, were Li: 0.60/6.23, Mg: 1.21/6·60, Mn: 0.59/3.95, Zn: 1.10/7.92, Sr: 0.34/6.27, Ba 0.34/3.99. Detection limits (DL) were calculated as the mean +3 SD of the background samples. Li, Mg, Mn, Sr and Ba were measured well above DL in the otoliths, but Zn was within 5% of DL in 4.6% of cases. However, given the relatively low RSD for Zn, we elected to include it in our statistical analysis. Elemental data are expressed throughout as molar ratios to Ca (e.g. Li:Ca).

We used the second sagitta from each fish for analysis of stable carbon and oxygen isotope ratios (i.e. $\delta^{13}C$, $\delta^{18}O$). Due to their small size, whole age 1 otoliths were ground, individually, to a fine powder using a mortar and pestle, and between 0.05 and 0.1 mg of the resulting powder transferred to a labelled 0.5 ml polypropylene microtube. The powder samples represent full-lifetime (i.e. ~15-month) records of $\delta^{13}C$ and $\delta^{18}O$ for each age 1 individual, and are expressed as 'C/O_{whole}' samples throughout (Table 1 main text). Age 2 and age 3 otoliths were larger, making sub-sampling possible. These were polished, mounted, cleaned and dried in an identical manner to otoliths prepared for elemental analyses (see above). For the age 2 samples, we used a high-resolution New Wave Research MicroMill system (New Wave Research Inc., Fremont, California, USA) to plot a 200-µm wide × ~25-µm deep drill path along the otolith edge, beginning at the rostrum, and extending along the ventral margin to the postrostrum. The drill speed was set to 5% and scan speed across the sample was 50 µm s-1. Between 0.05 and 0.1 mg of powder was collected per individual, encompassing otolith material deposited during the last ~2 months of the fish's life pre-capture (Clausen et al. 2007). These are termed 'C/O_{edge}' samples (Table 1 main text). In cases where insufficient material was recovered in the first drill pass, we continued drilling along the otolith's dorsal edge from the pararostrum to the antirostrum.

We kept the same drilling parameters for the age 3 otoliths, this time sampling the growth increments laid down one-year prior to capture, i.e. as nursery-resident two-year olds. We milled from the rostral end of the otolith along a path parallel to the ventral margin towards the postrostrum, and collected 0.05 and 0.1 mg of powder per sample, reflecting ~2 months of otolith growth deposited within nursery sites the previous year. These samples are termed 'C/O_{mid}' samples.

Otolith powders were analysed using an automated carbonate preparation device (NuCarb) coupled to a Nu Instruments Perspective dual-inlet stable isotope ratio mass spectrometer in the School of Geography at the University of Melbourne. Three external standards with known $\delta^{13}C$ and $\delta^{18}O$ values (National Bureau of Standards NBS19, NEW1, NEW12) were run concurrently with the otolith samples. The latter two are in-house standards composed of Cararra marble, and calcite, respectively. The isotopic ratios of both these standards have been calibrated against NBS19 and NBS18 using mass spectrometry (Finnegan MAT251 with an automated Kiel device) at the Australian National University. Estimated precision (RSD), based on repeated measurements of NBS19 (n = 5), New1 (n = 18) and New12 (n = 15) across all analysis days was: 3.50, 1.73 and 0.40, respectively for δ13C, and 11.17, 2.43 and 0.53, respectively for $\delta^{18}O$. All stable isotopic measurements are reported relative to the Vienna Pee Dee Belemnite (VPDB) reference standard, and expressed in δ-notation (in ‰).

References

Clausen, L.A.W., Bekkevold, D., Hatfield, E.M.C. and Mosegaard, H. 2007. Application and validation of otolith microstructure as a stock identification method in mixed Atlantic herring (*Clupea harengus*) stocks in the North Sea and western Baltic. ICES J. Mar. Sci. 64: 377–385.

Paton, C., Hellstrom, J., Paul, B. and Hergt, J. 2011. Iolite: Freeware for the visualisation and processing of mass spectrometric. J. Anal. At. Spectrom. 26: 2508–2518.

Supplement 2 - Source contribution, distance and density

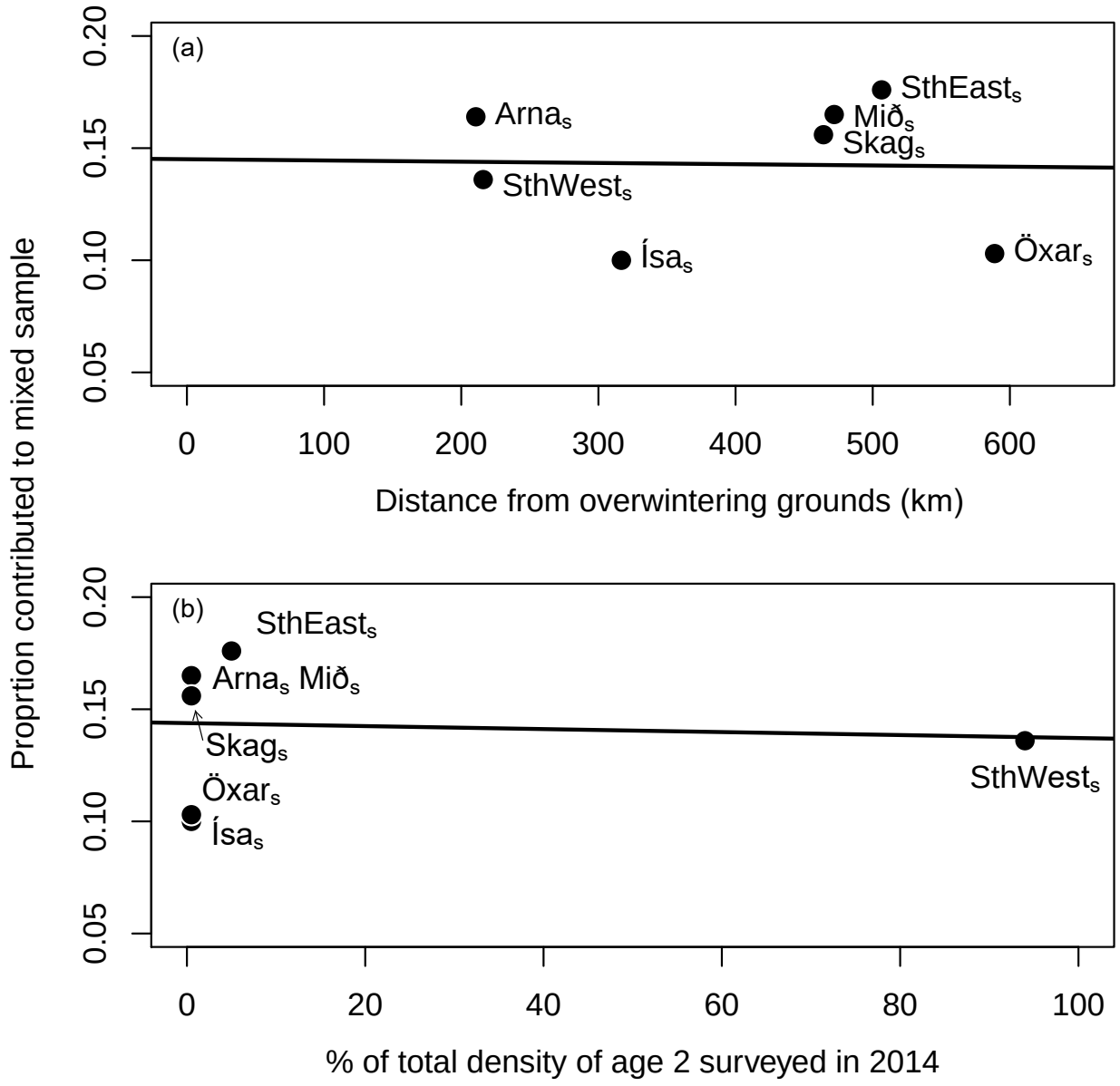

Figure S1. Relationships between the estimated (i.e. posterior mean) contribution of each source population to the mixed sample of age 3 adults captured by the fishery at Kolluáll in November 2015, and (a) the distance from each source to the fishery capture location, and (b) the density of age 2 ISS herring at each source, as estimated from acoustic surveys conducted in November 2014.

Paper V

Otoliths as thermometers: reconstructing temperature histories of fish to predict range shifts under climate change

Jed I. Macdonald

(Manuscript)

Author contributions – Conceived and designed the experiments: JIM; analysed the data: JIM; wrote the manuscript: JIM; reviewed and edited the manuscript: JIM.

Otoliths as thermometers: reconstructing temperature histories of fish to predict range shifts under climate change

Jed I. Macdonald[1,2]

[1]Faculty of Life and Environmental Sciences, University of Iceland, 101 Reykjavík, Iceland
[2]School of BioSciences, The University of Melbourne, Parkville, Victoria 3052, Australia

Abstract

There is growing recognition that intense exploitation of fish populations may reduce their resilience to environmental change, and that fishing and climate can interact to influence the spatial dynamics of harvested species. However, changes in climate alone can be pervasive in rerouting migration paths and reshaping distribution patterns. An empirical means to reconstruct lifetime environmental histories for individual fish would, either alone, or in conjunction with simulation modelling, provide a valuable baseline for predicting how future ocean warming might drive range shifts in commercially-targeted species, and for planning how management strategies should best be adapted. Here, I present a detailed tutorial on the empirical aspect of this equation. Specifically, I measure stable oxygen isotope ($\delta^{18}O$) profiles across otoliths from five adult (i.e. age 6) Icelandic summer spawning (ISS) herring captured off Iceland's east coast to define a contemporary thermal 'niche' and range for these individuals. I then apply this data to make predictions on how adult distribution might shift under projected changes in ocean temperature across the region. Assuming adherence to this niche throughout adult life (a large assumption), I predict that a 1°C increase in water temperature across a region off the northeast Icelandic coast, forecast to undergo warming of up to 2°C by 2046–2065, may create opportunities for poleward expansion in the adult component of the stock, all else being equal. I stress that the results presented here are preliminary, this tutorial serving primarily to illustrate methods to harness otoliths' capacity for forecasting species' responses to future environmental change.

Introduction

Otoliths (fish ear stones) are beautiful structures that have many useful properties for both fish and humans interested in fish. Located in the fish's inner-ear, and composed mainly of aragonite (a form of $CaCO_3$), otoliths play a crucial role in the fish's sensory functioning, balance and hearing. Like trees, otoliths display permanent growth bands that are typically deposited daily, the width of these bands reflecting the growth rate of the fish, and their chemical composition providing an 'environmental diary' of the fish's life. These traits have allowed scientists to accurately determine fish age, to study the consequences of environmental change (e.g. increasing water temperatures) on fish growth and movement, and to reconstruct migration pathways, among several other applications.

Here, I use stable oxygen isotopes (i.e. $\delta^{18}O$, the ratio of O^{18} to O^{16}) measured in otoliths of Icelandic summer spawning (ISS) herring (*Clupea harengus*) to chart their individual temperature histories around Iceland. As the incorporation of $\delta^{18}O$ from water to otolith is mediated by temperature, we can reconstruct the temperatures experienced by the fish provided that the $\delta^{18}O$ values of the water in which they reside are known, or estimate relative temperature change if water $\delta^{18}O$ is uncertain. Given sufficient numbers of samples, some simple equations and assumptions, this information can allow us to estimate the contemporary thermal 'niche' of individuals, or populations, across all life stages.

By making use of projections of how water temperatures may increase under various climate change scenarios, we can then predict if individuals or populations may need to move in the future, and where they might move to. For commercially-important species like Atlantic herring, this type of data is invaluable for developing effective climate change adaptation strategies for fishery management.

Materials and methods

Our dataset 'herring_otolith_data' consists of $\delta^{18}O$ profiles measured across otoliths of five, 6-year old herring, captured offshore of Neskaupstaður on the east coast of Iceland in June 2014 (see Appendix 1 for the full dataset). The first eight rows of the dataset look like this:-

	A	B	C	D	E	F	G	H	I	J
1	capture_site	fish_id	fish_age	date_accret	O_oto.VPBD	SSS	O_water.VSMOW	O_water.VPBD	temp_K	temp_C
2	Nesk	N1-06	0	Dec 2008	2.5	35.006902	0.294141215	-29.69467714	3.56655778	7.23239165
3	Nesk	N1-06	6	Jun 2009	2.5	35.0882609	0.342956547	-29.64732529	3.56519179	7.33981874
4	Nesk	N1-06	12	Dec 2009	2.0	35.1743466	0.394607949	-29.5972224	3.53196067	9.97886064
5	Nesk	N1-06	18	Jun 2010	1.8	35.0876668	0.342600078	-29.64767107	3.52717385	10.3631018
6	Nesk	N1-06	24	Dec 2010	2.1	35.1364087	0.371845232	-29.61930269	3.54331641	9.07147996
7	Nesk	N1-06	30	Jun 2011	2.0	35.0629323	0.32775939	-29.66206684	3.53874526	9.43603747
8	Nesk	N1-06	36	Dec 2011	2.4	35.0432271	0.315936235	-29.67353553	3.56157102	7.6249711

The first four data fields are the site of capture (capture_site), an identifier for each fish (fish_id), the age of that fish in months (fish_age) and the date when the otolith material analysed was accreted (date_accret). The fifth column (O_oto.VPBD) refers to measurements of otolith $\delta^{18}O$ ($\delta^{18}O_{otolith}$) made via secondary ion mass spectrometry (SIMS) on the SHRIMP II instrument at the Australian National University (ANU), Canberra, Australia (see Long et al. 2014 for details on instrumentation). For each otolith, a series of 25-µm diameter SIMS spots were acquired, with spots spaced ~100 µm apart (= 6 months

of fish life), running from the core of the otolith (i.e. the time of hatching) to the dorsal edge (i.e. the time of capture), so incorporating the full life-history of each individual (Figure 1).

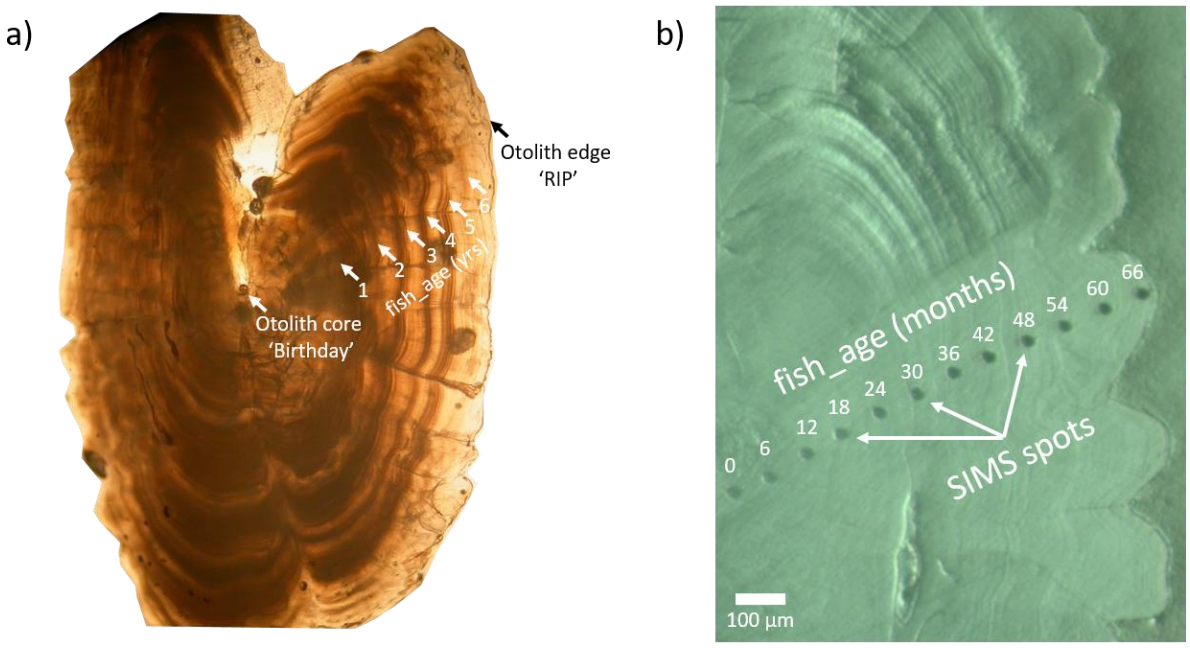

Figure 1. Polished otolith section from a six-year old Atlantic herring viewed under a) transmitted light, showing annual growth increments, and b) reflected light, showing the locations of SIMS spots and the estimated age of the fish (in months) at each SIMS spot.

We can plot the $\delta^{18}O_{otolith}$ life-history profiles for each fish (Figure 2).

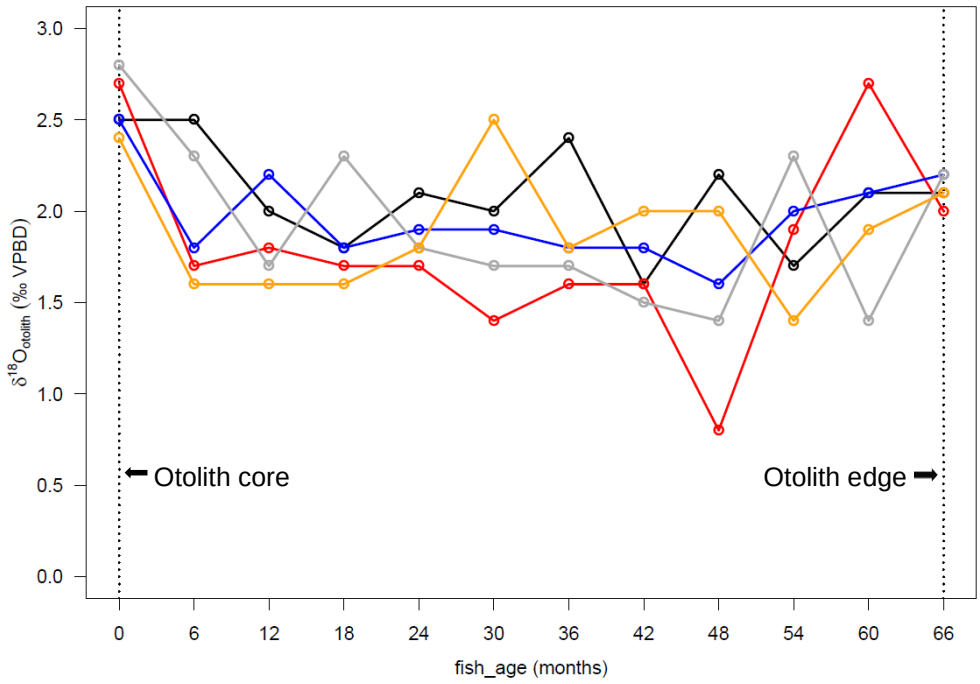

Figure 2. $\delta^{18}O_{otolith}$ life-history profiles for five, 6-year old ISS herring captured off Neskaupstaður in June 2014. Each fish's profile is assigned a different colour.

To convert these profiles into temperature histories we require some more information. First, we need the $\delta^{18}O$ values of the water ($\delta^{18}O_{water}$) in which the fish resides. We often do not have this data, but we can estimate it, by integrating ecological knowledge on the life history of the species and exploiting the general relationship between $\delta^{18}O_{water}$ and salinity:-

$$\delta^{18}O_{water} = a + bS \quad \text{(eq. 1)}$$

where S is the salinity in Practical Salinity Units (PSU).

The a and b coefficients in this relationship vary regionally, but as we know that these herring spend all their adult life in Icelandic waters, we use the following equation developed for Greenland/Iceland/Norwegian seas (LeGrande and Schmidt 2006):-

$$\delta^{18}O_{water} = -20.71 + 0.6S \quad \text{(eq. 2)}$$

Using an ocean model developed for Icelandic waters (CODE – Logemann et al. 2013), we mapped mean sea surface salinity (SSS – data field 6) around Iceland for each 6-month time step associated with the date of otolith accretion at each SIMS spot. We then reduced the extent of the maps to include only the oceanic waters south of Iceland, and finally, converted the resulting SSS maps to $\delta^{18}O_{water}$ maps (O_water.VSMOW – data field 7) (Figure 3).

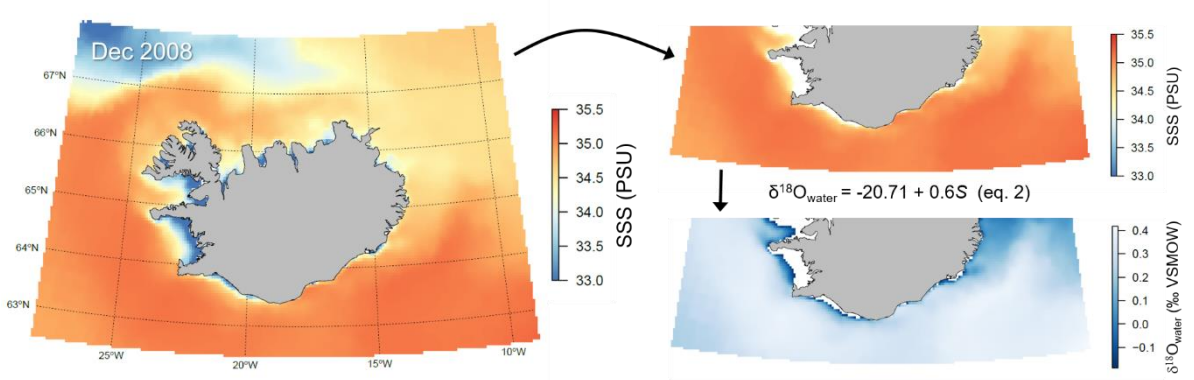

Figure 3. Example of the workflow we used to convert sea surface salinity (SSS) to $\delta^{18}O_{water}$. This example is for December 2008, and we followed this approach for all 6-month time steps. The value we use for SSS (data field 6) and O_water.VSMOW (data field 7) at each 6-month time step is the mean value of all grid cells in the top right and bottom right maps, respectively.

Note that for carbonates such as fish otoliths, $\delta^{18}O$ measurements are typically reported in 'per mil' (‰) relative to the Vienna PeeDee Belemnite standard (VPDB) (see Figure 2). By contrast, $\delta^{18}O_{water}$ measurements are usually reported relative to the Vienna Standard Mean Ocean Water standard (VSMOW), again in 'per mil' (‰) (see Figure 3, bottom right map).

Before we can reconstruct the fish's temperature histories, we must convert our water values from the VSMOW to the VPDB scale. We use the equation of Clark and Fritz (1997):-

$$\delta^{18}O_{water}\,(VPDB) = -29.98 + 0.97002\ \delta^{18}O_{water}\,(VSMOW) \quad \text{(eq. 3)}$$

the results of which are shown in data field 8 (O_water.VPDB).

Results and Discussion

The isotopic partitioning of oxygen between otolith aragonite and ambient water can be described in terms of the isotopic fractionation factor, α, given by:-

$$\alpha = (1000 + \delta^{18}O_{otolith}\,(VPDB)) / (1000 + \delta^{18}O_{water}\,(VPDB)) \quad \text{(eq. 4)}$$

Temperature-dependent fractionation can then be described by the linear relationship:-

$$1000 \ln \alpha = a + bT \quad \text{(eq. 5)}$$

Where a is the intercept and b the slope, both of which are typically empirically derived and may differ by fish species. $T = 1000 / temp_K$, where $temp_K$ denotes the temperature in Kelvin. Here, we use a = -31.14 and b = 17.88, widely-used values determined experimentally by Kim et al. (2007) for fractionation between synthetic aragonite and water. Rearranging eq. 5, we calculate temperature in Kelvin (temp_K – data field 9), then convert to °C (temp_C – data field 10) (eq. 6).

$$T = (1000 \ln \alpha + 31.14) / 17.88$$

$$1000 / temp_K = (1000 \ln \alpha + 31.14) / 17.88$$

$$temp_K = 17880 / (1000 \ln \alpha + 31.14) \text{ (see data field 8)}$$

$$temp_C = temp_K - 273.15 \text{ (see data field 9)} \quad \text{(eq. 6)}$$

We can repeat these calculations at each time step and plot the individual temperature histories (Figure 4).

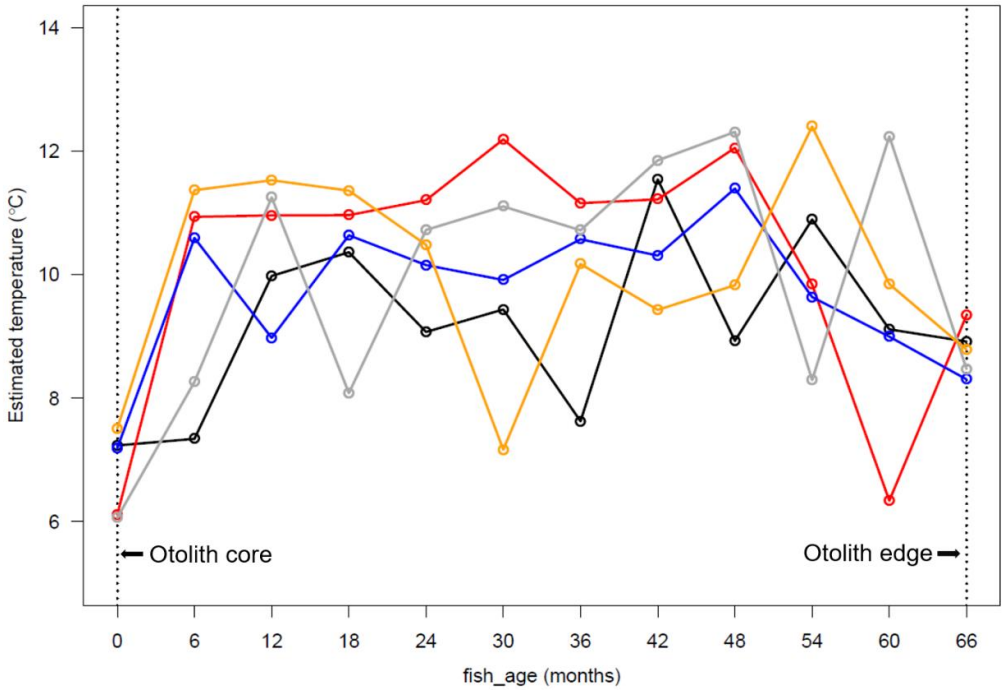

Figure 4. Estimated temperatures (°C) experienced by ISS herring over six years of life. Each fish is assigned a different colour, consistent with Figure 2.

Defining a thermal niche and predicting future distributions

Figure 4 shows some interesting patterns, and we can see that the herring seem to have spent most of their adult lives in waters between 8 and 12°C. We can define this as an approximate, contemporary thermal niche and/or thermal range for adult Icelandic herring (at least for these five fish!), within which they have survived, grown, reproduced, fed and migrated over the six years of their lives.

If we consider this niche as providing strict thermal tolerance limits to the above activities (this is a big assumption), we are then in a position to explore how changing water temperatures predicted under scenarios of ocean warming may act to contract or expand the distributional range of adult Icelandic herring.

For example, here's a plot of annual mean sea surface temperature (SST) around Iceland for 2014 (Figure 5a). By overlaying the 8 to 12°C temperature band (white area in Figure 5b), we can identify the contemporary thermal niche spatially.

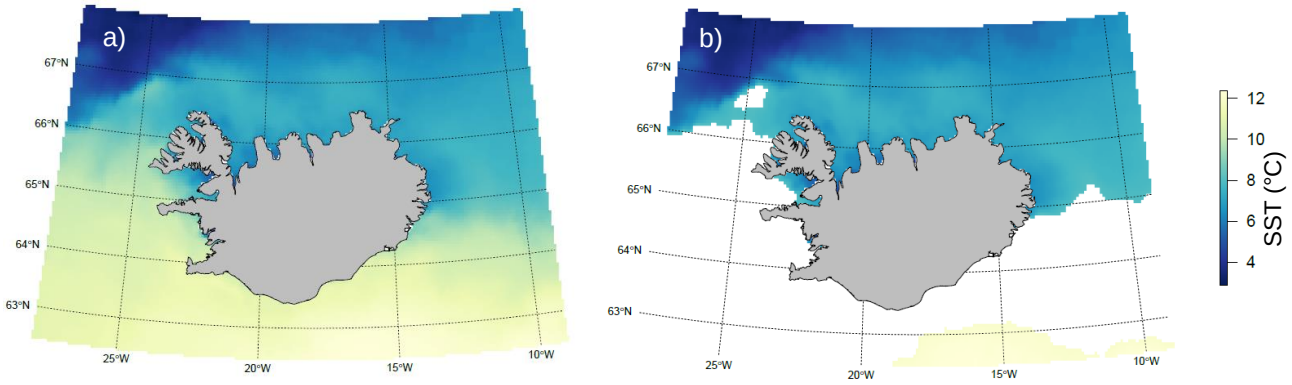

Figure 5. a) Mean annual SST for Icelandic waters in 2014, and b) the same plot with the 8-12°C thermal window identified for adult herring overlaid in white.

Future predictions of SST change in the Northwest Atlantic are regionally variable, with surface waters northeast of Iceland forecast to increase by up to ~2°C by the middle of the century, whilst temperatures to the south of the island remain relatively stable (Figure 6).

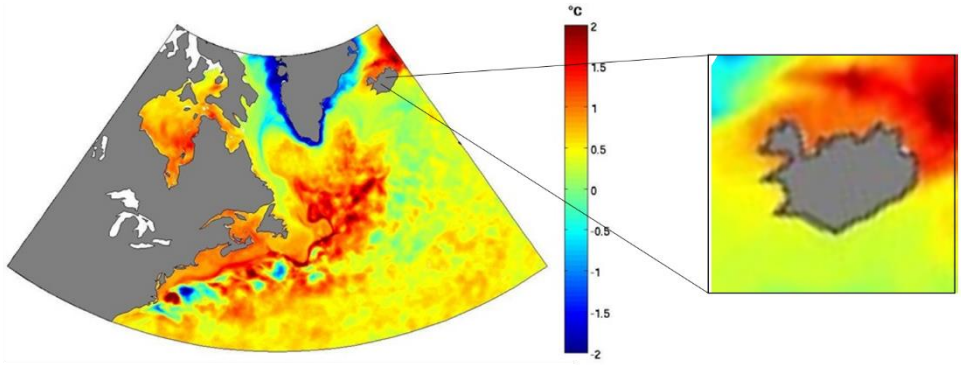

Figure 6. Projected change in SST in Northwest Atlantic waters from the present day to 2046-2065 (source: NOAA 2016).

Given these projections, it seems that adult herring may be a climate change winner; the increase in water temperatures to the northeast potentially opening up opportunities for range expansion, all else being equal.

By simulating even a 1°C increase in SST north of 65°N and east of 20°W, we see that the region within the thermal-niche limits of adult herring expands poleward dramatically (Figure 7).

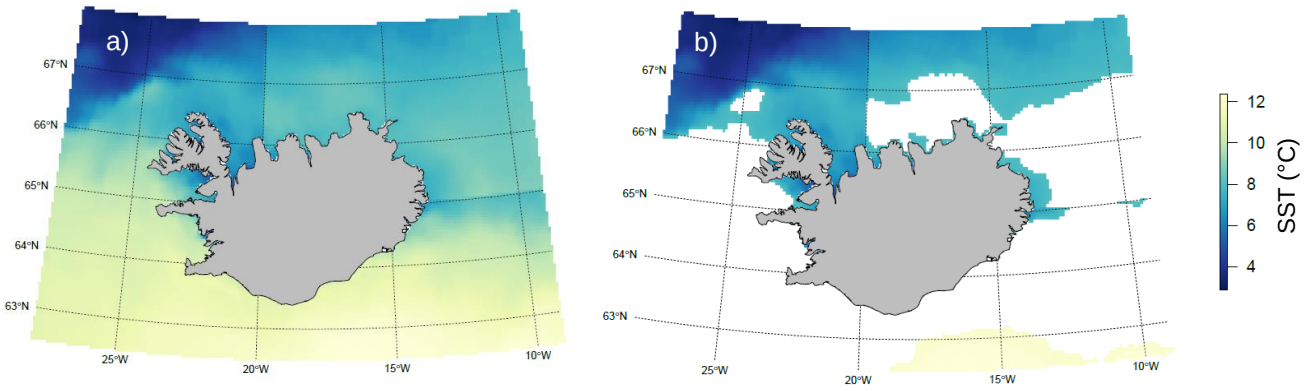

Figure 7. a) An increase of 1°C in SST off the northeast Icelandic coast, as predicted for the middle of this century (see Figure 6), may allow adult herring to expand their range further north, b). As in Figure 6, panel a) shows mean annual SST for Icelandic waters in 2014, and panel b) is the same plot with the 8-12°C thermal window overlaid in white

Whether they are able to colonise these new habitats, choose to do so, or are forced to do so by other external stressors (e.g. fishing pressure, prey scarcity) are questions for a future thesis. However, the approach we outline here, though based on a very small number of samples and some rather large assumptions, does highlight the potential of otoliths' stable isotopic constituents for predicting how species might respond spatially to the rapidly warming oceans of our present and future (see IPCC 2013; Resplandy et al. 2018 and references therein).

Acknowledgements

Funding for this work came from the Icelandic Association of Herring Fisheries under the grant 'Rannsóknarsjóður síldarútvegsins 2013'. Many thanks to Ian Williams at ANU for advice and assistance with the SIMS analysis, and to John Morrongiello (University of Melbourne) and Frazer Thorpe (Gene Technology Access Centre), for the opportunity to prepare and present this tutorial at the 'Using predictive modelling in STEM to solve problems' workshop held in Melbourne in November 2017.

References

Clark, I. and Fritz, P. 1997. Environmental isotopes in hydrogeology. Boca Raton, FL: CRC Press LLC.

IPCC. 2013. Climate Change 2013: The Physical Science Basis. Contribution of Working Group I to the Fifth Assessment Report of the Intergovernmental Panel on Climate Change. *Edited by* T.F. Stocker, D. Qin, G.-K. Plattner, M. Tignor, S.K. Allen, J. Boschung, A. Nauels, Y. Xia, V. Bex and P.M. Midgley. Cambridge University Press, Cambridge, United Kingdom and New York, NY, USA.

Kim, S-T., O'Neil, J.R., Hillaire-Marcel, C. and Mucci, A. 2007. Oxygen isotope fractionation between synthetic aragonite and water: influence of temperature and Mg^{2+} concentration. Geochim. Cosmochim. Acta 71: 4704–4715.

LeGrande, A.N. and Schmidt, G.A. 2006. Global gridded data set of the oxygen isotopic composition in seawater. Geophys. Res. Lett. 33: 12604.

Logemann, K., Ólafsson, J., Snorrason, Á, Valdimarsson, H. and Marteinsdóttir, G. 2013. The circulation of Icelandic waters – a modelling study. Ocean Sci. 9: 931–955.

Long, K., Stern, N., Williams, I.S., Kinsley, L., Wood, R., Sporcic, K., Smith, T., Fallon, S., Kokkonen, H., Moffat, I. and Grün, R. 2014. Fish otolith geochemistry, environmental conditions and human occupation at Lake Mungo, Australia. Quart. Sci. Rev. 88: 82–95.

Resplandy, L., Keeling, R.F., Eddebbar, Y., Brooks, M.K., Wang, R., Bopp, L., Long, M.C., Dunne, J.P., Koeve, W. and Oschlies, A. 2018. Quantification of ocean heat uptake from changes in atmospheric O_2 and CO_2 composition. Nature 563: 105–108.

Appendix 1 - 'herring_otolith_data' dataset

capture_site	fish_id	fish_age	date_accret	O_oto.VPBD	SSS	O_water.VSMOW	O_water.VPBD	temp_K	temp_C
Nesk	N1-06	0	Dec-08	2.5	35.00690202	0.294141215	-29.69467714	3.566557779	7.232391652
Nesk	N1-06	6	Jun-09	2.5	35.08826091	0.342956547	-29.64732529	3.565191794	7.339818743
Nesk	N1-06	12	Dec-09	2	35.17434658	0.394607949	-29.5972224	3.531960669	9.978860641
Nesk	N1-06	18	Jun-10	1.8	35.0876668	0.342600078	-29.64767107	3.527173854	10.36310178
Nesk	N1-06	24	Dec-10	2.1	35.13640872	0.371845232	-29.61930269	3.543316406	9.071479964
Nesk	N1-06	30	Jun-11	2	35.06293232	0.32775939	-29.66206684	3.538745258	9.436037474
Nesk	N1-06	36	Dec-11	2.4	35.04322706	0.315936235	-29.67353553	3.561571019	7.624971103
Nesk	N1-06	42	Jun-12	1.6	35.05753383	0.324520298	-29.66520882	3.512559793	11.54266258
Nesk	N1-06	48	Dec-12	2.2	35.09580647	0.347483883	-29.64293368	3.545118123	8.928047983
Nesk	N1-06	54	Jun-13	1.7	35.05522668	0.323136005	-29.66655161	3.520591392	10.89318723
Nesk	N1-06	60	Dec-13	2.1	35.02725301	0.306351808	-29.68283262	3.54278851	9.113532577
Nesk	N1-06	66	Jun-14	2.1	34.9533651	0.262019058	-29.72583627	3.545267266	8.916181482
Nesk	N5-04	0	Dec-08	2.7	35.00690202	0.294141215	-29.69467714	3.580887174	6.110404298
Nesk	N5-04	6	Jun-09	1.7	35.08826091	0.342956547	-29.64732529	3.520064015	10.93574269
Nesk	N5-04	12	Dec-09	1.8	35.17434658	0.394607949	-29.5972224	3.519757069	10.9605168
Nesk	N5-04	18	Jun-10	1.7	35.0876668	0.342600078	-29.64767107	3.519710893	10.96424413
Nesk	N5-04	24	Dec-10	1.7	35.13640872	0.371845232	-29.61930269	3.516700818	11.20742812
Nesk	N5-04	30	Jun-11	1.4	35.06293232	0.32775939	-29.66206684	3.504567694	12.19189875
Nesk	N5-04	36	Dec-11	1.6	35.04322706	0.315936235	-29.67353553	3.517310536	11.15813538
Nesk	N5-04	42	Jun-12	1.6	35.05753383	0.324520298	-29.66520882	3.516538008	11.22059338
Nesk	N5-04	48	Dec-12	1.5	35.09580647	0.347483883	-29.64293368	3.506262228	12.05399644
Nesk	N5-04	54	Jun-13	1.9	35.05522668	0.323136005	-29.66655161	3.533694262	9.839960619
Nesk	N5-04	60	Dec-13	2.7	35.02725301	0.306351808	-29.68283262	3.577982552	6.337109163
Nesk	N5-04	66	Jun-14	2	34.9533651	0.262019058	-29.72583627	3.539917783	9.342436647
Nesk	N1-11	0	Dec-08	2.5	35.00690202	0.294141215	-29.69467714	3.567118852	7.188290254
Nesk	N1-11	6	Jun-09	1.8	35.08826091	0.342956547	-29.64732529	3.524301181	10.59419456
Nesk	N1-11	12	Dec-09	2.2	35.17434658	0.394607949	-29.5972224	3.544516105	8.975957488
Nesk	N1-11	18	Jun-10	1.8	35.0876668	0.342600078	-29.64767107	3.523752515	10.63837498
Nesk	N1-11	24	Dec-10	1.9	35.13640872	0.371845232	-29.61930269	3.529765293	10.15495569
Nesk	N1-11	30	Jun-11	1.9	35.06293232	0.32775939	-29.66206684	3.532771312	9.913892784
Nesk	N1-11	36	Dec-11	1.8	35.04322706	0.315936235	-29.67353553	3.524564385	10.57300543
Nesk	N1-11	42	Jun-12	1.8	35.05753383	0.324520298	-29.66520882	3.527836355	10.30986017
Nesk	N1-11	48	Dec-12	1.6	35.09580647	0.347483883	-29.64293368	3.514386293	11.39470184
Nesk	N1-11	54	Jun-13	2	35.05522668	0.323136005	-29.66655161	3.536229241	9.637096596
Nesk	N1-11	60	Dec-13	2.1	35.02725301	0.306351808	-29.68283262	3.544271543	8.995424746
Nesk	N1-11	66	Jun-14	2.2	34.9533651	0.262019058	-29.72583627	3.552987748	8.303264403
Nesk	N3-01	0	Dec-08	2.8	35.00690202	0.294141215	-29.69467714	3.581522579	6.060860155
Nesk	N3-01	6	Jun-09	2.3	35.08826091	0.342956547	-29.64732529	3.553502915	8.262460897
Nesk	N3-01	12	Dec-09	1.7	35.17434658	0.394607949	-29.5972224	3.51616194	11.25100797
Nesk	N3-01	18	Jun-10	2.3	35.0876668	0.342600078	-29.64767107	3.555790185	8.081441672
Nesk	N3-01	24	Dec-10	1.8	35.13640872	0.371845232	-29.61930269	3.522681002	10.72469637
Nesk	N3-01	30	Jun-11	1.7	35.06293232	0.32775939	-29.66206684	3.517966492	11.10512362
Nesk	N3-01	36	Dec-11	1.7	35.04322706	0.315936235	-29.67353553	3.522750102	10.71912813
Nesk	N3-01	42	Jun-12	1.5	35.05753383	0.324520298	-29.66520882	3.508750971	11.85170243
Nesk	N3-01	48	Dec-12	1.4	35.09580647	0.347483883	-29.64293368	3.503084023	12.31275039
Nesk	N3-01	54	Jun-13	2.3	35.05522668	0.323136005	-29.66655161	3.553106765	8.293836642
Nesk	N3-01	60	Dec-13	1.4	35.02725301	0.306351808	-29.68283262	3.503965587	12.2409307
Nesk	N3-01	66	Jun-14	2.2	34.9533651	0.262019058	-29.72583627	3.550865619	8.471471308
Nesk	N5-06	0	Dec-08	2.4	35.00690202	0.294141215	-29.69467714	3.563053767	7.50812792
Nesk	N5-06	6	Jun-09	1.6	35.08826091	0.342956547	-29.64732529	3.514707359	11.36870892
Nesk	N5-06	12	Dec-09	1.6	35.17434658	0.394607949	-29.5972224	3.512715009	11.53008293
Nesk	N5-06	18	Jun-10	1.6	35.0876668	0.342600078	-29.64767107	3.514797142	11.3614411
Nesk	N5-06	24	Dec-10	1.8	35.13640872	0.371845232	-29.61930269	3.525691689	10.48228785
Nesk	N5-06	30	Jun-11	2.5	35.06293232	0.32775939	-29.66206684	3.5674283	7.163972953
Nesk	N5-06	36	Dec-11	1.8	35.04322706	0.315936235	-29.67353553	3.529539502	10.17307924
Nesk	N5-06	42	Jun-12	2	35.05753383	0.324520298	-29.66520882	3.538827919	9.42943668
Nesk	N5-06	48	Dec-12	2	35.09580647	0.347483883	-29.64293368	3.533834625	9.82872033
Nesk	N5-06	54	Jun-13	1.4	35.05522668	0.323136005	-29.66655161	3.502004213	12.4007701
Nesk	N5-06	60	Dec-13	1.9	35.02725301	0.306351808	-29.68283262	3.533600077	9.84750343
Nesk	N5-06	66	Jun-14	2.1	34.9533651	0.262019058	-29.72583627	3.546916655	8.785014921

Háskólaprent ehf.